USGS
science for a changing world

Prepared in cooperation with the Air Force Civil Engineer Center

Use of a Numerical Model to Simulate the Hydrologic System and Transport of Contaminants Near Joint Base Cape Cod, Western Cape Cod, Massachusetts

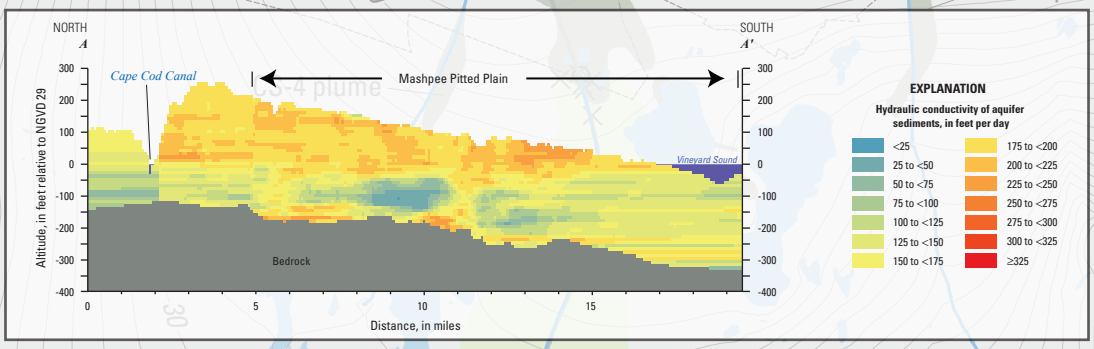

Scientific Investigations Report 2018–5139

U.S. Department of the Interior
U.S. Geological Survey

Cover. Map of plume locations and simulated source areas obtained by reverse particle tracking, Joint Base Cape Cod, Massachusetts. North-south cross section from numerical model showing the distribution of hydraulic conductivity. Images adapted from figures 16 and 44 of this report.

Use of a Numerical Model to Simulate the Hydrologic System and Transport of Contaminants Near Joint Base Cape Cod, Western Cape Cod, Massachusetts

By Donald A. Walter, Timothy D. McCobb, and Michael N. Fienen

Prepared in cooperation with the Air Force Civil Engineer Center

Scientific Investigations Report 2018–5139

U.S. Department of the Interior
U.S. Geological Survey

U.S. Department of the Interior
DAVID BERNHARDT, Secretary

U.S. Geological Survey
James F. Reilly II, Director

U.S. Geological Survey, Reston, Virginia: 2019

For more information on the USGS—the Federal source for science about the Earth, its natural and living resources, natural hazards, and the environment—visit https://www.usgs.gov or call 1–888–ASK–USGS.

For an overview of USGS information products, including maps, imagery, and publications, visit https://store.usgs.gov.

Suggested citation:
Walter, D.A., McCobb, T.D., and Fienen, M.N., 2019, Use of a numerical model to simulate the hydrologic system and transport of contaminants near Joint Base Cape Cod, western Cape Cod, Massachusetts: U.S. Geological Survey Scientific Investigations Report 2018–5139, 98 p., https://doi.org/10.3133/sir20185139.

ISSN 2328-0328 (online)

Acknowledgments

The authors thank the Army National Guard Impact Area Groundwater Study Program for providing well-construction records, delineations of contaminant-plume paths, and access to monitoring wells for water sampling in and near the Camp Edwards training area on Joint Base Cape Cod. The authors also thank Jonathan Davis and Rose Forbes of the Air Force Civil Engineer Center and Benjamin Gregson of the Impact Area Groundwater Study Program for their helpful comments and assistance.

Contents

Figures

Tables

Conversion Factors

U.S. customary units to International System of Units

Multiply	By	To obtain
	Length	
inch (in.)	2.54	centimeter (cm)
foot (ft)	0.3048	meter (m)
mile (mi)	1.609	kilometer (km)
	Area	
acre	0.4047	hectare (ha)
	Flow rate	
foot per day (ft/d)	0.3048	meter per day (m/d)
cubic foot per second (ft^3/s)	0.02832	cubic meter per second (m^3/s)
cubic foot per day (ft^3/d)	0.02832	cubic meter per day (m^3/d)
million gallons per day (Mgal/d)	0.04381	cubic meter per second (m^3/s)
inch per hour (in/h)	0.0254	meter per hour (m/h)
inch per year (in/yr)	25.4	millimeter per year (mm/yr)
	Density	
pound per cubic foot (lb/ft^3)	0.01602	gram per cubic centimeter (g/cm^3)
	Hydraulic conductivity	
foot per day (ft/d)	0.3048	meter per day (m/d)

Datum

Vertical coordinate information is referenced to the National Geodetic Vertical Datum of 1929 (NGVD 29).

Mean sea level in this report is defined as 0 ft (NGVD 29).

Horizontal coordinate information is referenced to the North American Datum of 1983 (NAD 83).

Altitude, as used in this report, refers to distance above the vertical datum.

Supplemental Information

Concentrations of chemical constituents in water are given in micrograms per liter (µg/L).

Abbreviations

AFCEC	Air Force Civil Engineer Center
CFC	chlorofluorocarbon
CIA	Central Impact Area
COV	coefficient of variation
ETR	extraction-treatment-reinjection
FW/SW	freshwater/saltwater
GIS	geographic information system
IAGWSP	Impact Area Groundwater Study Program
JBCC	Joint Base Cape Cod
MassDEP	Massachusetts Department of Environmental Protection
MassGIS	Massachusetts Office of Geographic Information
MEP	Massachusetts Estuaries Project
MMR	Massachusetts Military Reservation
MPP	Mashpee Pitted Plain
NOAA	National Oceanic and Atmospheric Administration
NRCS	Natural Resources Conservation Service
SREF	Streamflow Record Extension Facilitator
SVD	singular value decomposition
SVDA	SVD Assist
SWB	Soil-Water-Balance
USDA	U.S. Department of Agriculture
USGS	U.S. Geological Survey
VOC	volatile organic compound
WWTF	wastewater-treatment facility

Use of a Numerical Model to Simulate the Hydrologic System and Transport of Contaminants Near Joint Base Cape Cod, Western Cape Cod, Massachusetts

By Donald A. Walter, Timothy D. McCobb, and Michael N. Fienen

Abstract

Historical training and operational activities at Joint Base Cape Cod (JBCC) on western Cape Cod, Massachusetts, have resulted in the release of contaminants into an underlying glacial aquifer that is the sole source of water to the surrounding communities. Remedial systems have been installed to contain and remove contamination from the aquifer. Groundwater withdrawals for public supply are expected to increase as the region continues to urbanize. Increases in water-supply withdrawals and wastewater return flow likely will affect the hydrologic system around JBCC and could affect the transport of any contamination that may remain in the aquifer following remediation of contamination from the JBCC. A large amount of diverse data, including water levels, streamflows, water quality, groundwater ages, and lithology, has been collected by U.S. Geological Survey and JBCC personnel and contractors as part of remedial investigations; these data can inform and improve the development and calibration of groundwater models capable of simulating the potential interactions between the residual contamination and groundwater withdrawals for water supply. The U.S. Geological Survey, in cooperation with the Air Force Civil Engineer Center, developed a numerical, steady-state regional model of the Sagamore flow lens on western Cape Cod and evaluated the potential effects of future (2030) groundwater withdrawals on water levels, streamflows, hydraulic gradients, and advective transport near the JBCC. The model and supporting data can have ancillary uses, such as providing boundary conditions to the local-scale models used to design and evaluate remedial systems and facilitating future analyses of the water supplies near the JBCC.

The aquifer consists generally of sandy sediments underlain by impermeable bedrock and is bounded laterally by a freshwater/saltwater interface. The altitude of the bedrock surface was interpolated from borehole data and geophysical measurements. The simulated position of the interface was estimated from a separate two-dimensional model and combined with the measured bedrock surface to define the lower boundary of the coastal aquifer system. The lithology of the aquifer was determined from borehole data and was used to develop a quasi-three-dimensional hydraulic conductivity field; the hydraulic conductivity field was further constrained by a depositional model of the glacial aquifer. The spatial distribution of recharge was determined from climatic and landscape data, and hydrologic boundary conditions were determined from aerial photos and digital elevation model data. These data were incorporated into the three-dimensional, finite-difference groundwater flow model.

Some inputs into the numerical model—aquifer properties, leakances, and recharge—are represented as parameters to facilitate estimation of optimal parameter values in an inverse calibration. A hybrid parameterization scheme, with both zones of piecewise constancy and pilot points, is used to represent hydraulic conductivity; other adjustable parameters include recharge, boundary leakance, and porosity. Water levels and streamflow measurements were compiled from various sources and evaluated to determine the suitability of the measurements for use as observations of steady-state hydrologic conditions. Data regarding the distribution of subsurface contamination and groundwater ages were compiled, evaluated, and used to develop observations of long-term average hydraulic gradients and advective-transport patterns. These observations of steady-state hydrologic conditions were combined with the parameterized groundwater model in an inverse calibration to estimate model parameters that best fit the observations.

Current (2010) and future (2030) conditions were simulated in the model to characterize the groundwater flow system and to determine potential effects of increased groundwater withdrawals on advective-transport patterns at the JBCC. Groundwater flow and advective transport are radially outward from a water-table divide in the northern part of the JBCC; flow diverges from the divide toward all points of the compass. Most groundwater flow and contaminant transport occur in shallow parts of the aquifer. On average, about one-half of the groundwater flux occurs in the shallowest 20 percent of the saturated thickness; shallow flow is even more predominant near streams and lakes. Projected (2030) increases in groundwater withdrawals decrease water levels by a maximum of about 1.2 feet in the northern part of the JBCC; drawdowns exceeding 1 foot generally are limited to areas near the largest increases in withdrawals, such as in the northern part of the JBCC, near Long Pond in Falmouth, and in eastern Barnstable. Streamflow decreases average about 6 percent; the largest

decreases are in areas with the largest drawdowns. Changes in hydraulic-gradient directions at the water table exceed 1 degree in about 13 percent of the aquifer, generally near groundwater divides where gradient magnitudes are small and near large groundwater withdrawals. Predictions of advective transport from randomly selected locations at the water table are similar for current (2010) and future (2030) groundwater withdrawals. The results indicate that projected increases in groundwater withdrawals affect water levels and streamflows, but effects on hydraulic gradients and advective transport at the JBCC likely are small.

Several underlying assumptions inherent in the model, including observations and weights used in the calibration, representation of local-scale heterogeneity, and simulation of the freshwater/saltwater interface, could affect model calibration and predictions; these assumptions were evaluated with alternative models and alternative inverse calibrations. The preferred calibrated version of the model (the JBCC regional model) uses water levels, streamflows, plumes, and groundwater ages as observations for the calibration; plumes are good indicators of long-term average hydraulic gradients and advective transport and are assigned the largest weights. Eight alternative calibrations were performed in which different, but reasonable, observations and weights were used. In some cases, the fit to individual types improved with increased weights on those observation types; however, the preferred calibrated model had the best overall fit to the observations, as indicated by absolute mean residuals. The preferred calibrated model had a better fit to plume observations than any of the eight alternative calibrations, including those with larger weights on the plume observations.

Fine-grained silty sediments occur in many parts of the aquifer, and silt lenses can locally affect hydraulic gradients. The extents and hydraulic properties of the silt lenses generally are unknown, and they are represented implicitly in the regional model as contributors to average hydraulic conductivity. A set of alternative models in which silts were represented with different correlation distances and hydraulic conductivities indicated that explicitly representing silt lenses could affect model calibration, as indicated by increases in the absolute mean residuals relative to those from the preferred calibrated model; the residuals increased with increasing correlation distance and decreasing hydraulic conductivity. However, comparison of advective-transport predictions, which generally were similar for different silt realizations and the preferred calibrated model, indicated that the implicit representation of local-scale heterogeneity may be sufficient at the regional scale and that the preferred calibrated model adequately represents regional-scale hydraulic gradients. For the coastal boundary, as represented in the preferred calibrated model, a specified coastal leakance and associated freshwater/saltwater interface position were assumed and were not adjusted during the calibration. Two alternative models representing silty and sandy seabeds and their associated interface positions were developed to test the importance of the assumed coastal-boundary condition. Absolute mean residuals generally were similar for the two alternative models and the preferred calibrated model, indicating that the leakance of the seabed likely would not greatly affect model calibration. Coastal leakances would affect the balance between discharge to coastal waters and streams, and the two alternative models resulted in different predictions of streamflow—streamflows increase with smaller (silty) seabed leakances. However, predictions of advective transport, particularly near the JBCC, generally were similar between the alternative and preferred calibrated models, indicating that the seabed leakance and associated interface position at the coastal boundary does not affect simulations of advective transport in inland parts of the aquifer.

Introduction

Training and operational activities at Joint Base Cape Cod (JBCC), a multiuse military facility located on western Cape Cod, Massachusetts (fig. 1), have resulted in the release of anthropogenic contaminants into an underlying sand and gravel aquifer that is the sole source of water to the surrounding communities. The JBCC includes live-fire Army National Guard training grounds in the central and northern part of the facility, and the Otis Air National Guard Base in the southern part of the facility (fig. 2*A*). Starting in the 1980s, the Army National Guard, the Air National Guard, and the U.S. Air Force conducted numerous investigations to map the extent of groundwater contamination at the site, determine potential adverse effects to the region's water resources, and design and implement remediation of contaminant plumes determined to be potential threats to water supplies.

These investigations included the collection and analysis of water samples, characterization of the aquifer sediments, evaluation of hydrologic conditions, and development of numerical models to simulate the transport of contaminants from potential surface sources to wells and ecological receptors. Numerical models also were used in the design and evaluation of remediation systems. These models, which incorporate local-scale chemical and geologic information, require boundary conditions from a regional-scale model to ensure that analyses are consistent and reflect the regional flow system as well as local hydrogeologic conditions.

The U.S. Geological Survey (USGS) has developed and maintained regional-scale models of the western Cape Cod aquifer system as part of ongoing technical assistance to the U.S. Army, National Guard Bureau, and U.S. Air Force (Masterson and Barlow, 1997; Masterson and others, 1997b; Walter and Masterson, 2003). Since the most recent (2002) update of the regional model of western Cape Cod (Walter and Whealan, 2005), extensive data have been collected regarding the lithology and hydrology of the aquifer, as well as regional groundwater flow patterns, as indicated by mapped contaminant plumes and groundwater ages. In 2010, the USGS, in cooperation with the Air Force Civil Engineer Center (AFCEC),

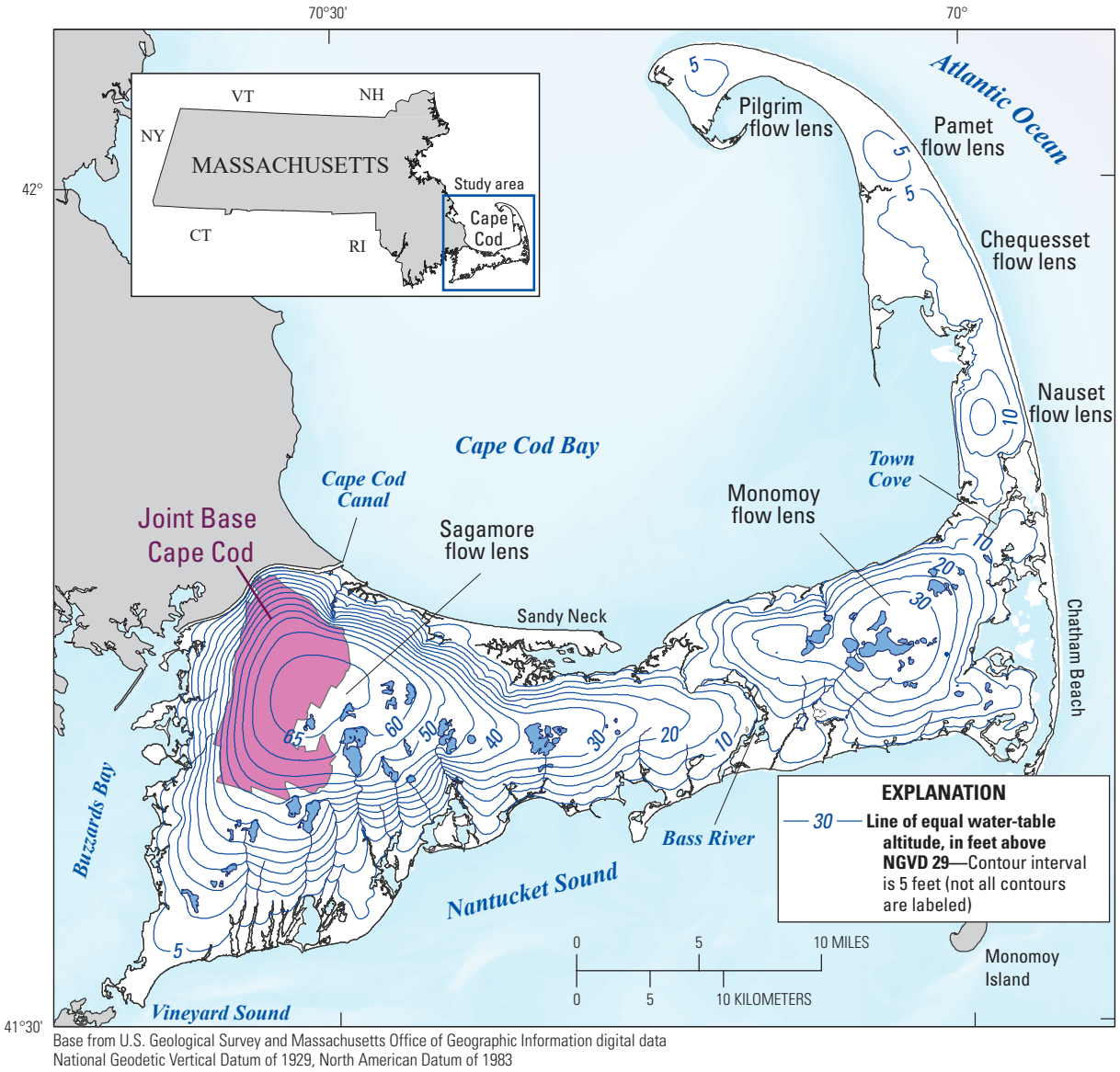

Figure 1. Location of Joint Base Cape Cod and study area on western Cape Cod, Massachusetts. Modified from Walter and others (2016). NGVD 29, National Geodetic Vertical Datum of 1929.

began an effort to update the regional model of western Cape Cod, with particular emphasis in the area around the JBCC, with recent (since and including 2003) data collected as part of ongoing remedial investigations. The purpose of the updated model is to provide a regional-scale tool to ensure (1) that local-scale models used in the design and evaluation of remedial systems are linked to a regional model that is, in turn, informed by the most recent hydrologic and lithologic data and (2) that, as local communities address their growing need for potable water, an updated regional model is available to evaluate the effects of contaminants emanating from the JBCC on the water resources of western Cape Cod, as well as the effects of increased water-supply withdrawals on the hydrologic system.

The population of Cape Cod more than doubled between 1970 and 2010 (Cape Cod Commission, written commun., March 12, 2012), and demand for potable water by the four communities surrounding the JBCC is expected to increase over the next two decades with additional development and population growth. Future (2030) pumping is projected to increase by about 3 million gallons per day (Mgal/d) or about 38 percent over current (2010) withdrawals (Massachusetts Department of Conservation and Recreation, written commun., April 2011). The increase in water-supply withdrawals and the redistribution of wastewater return flow likely will affect the hydrologic system around the JBCC; possible effects include changes in the water-table altitude, streamflows, and hydraulic gradients. Changes in hydraulic gradients are of

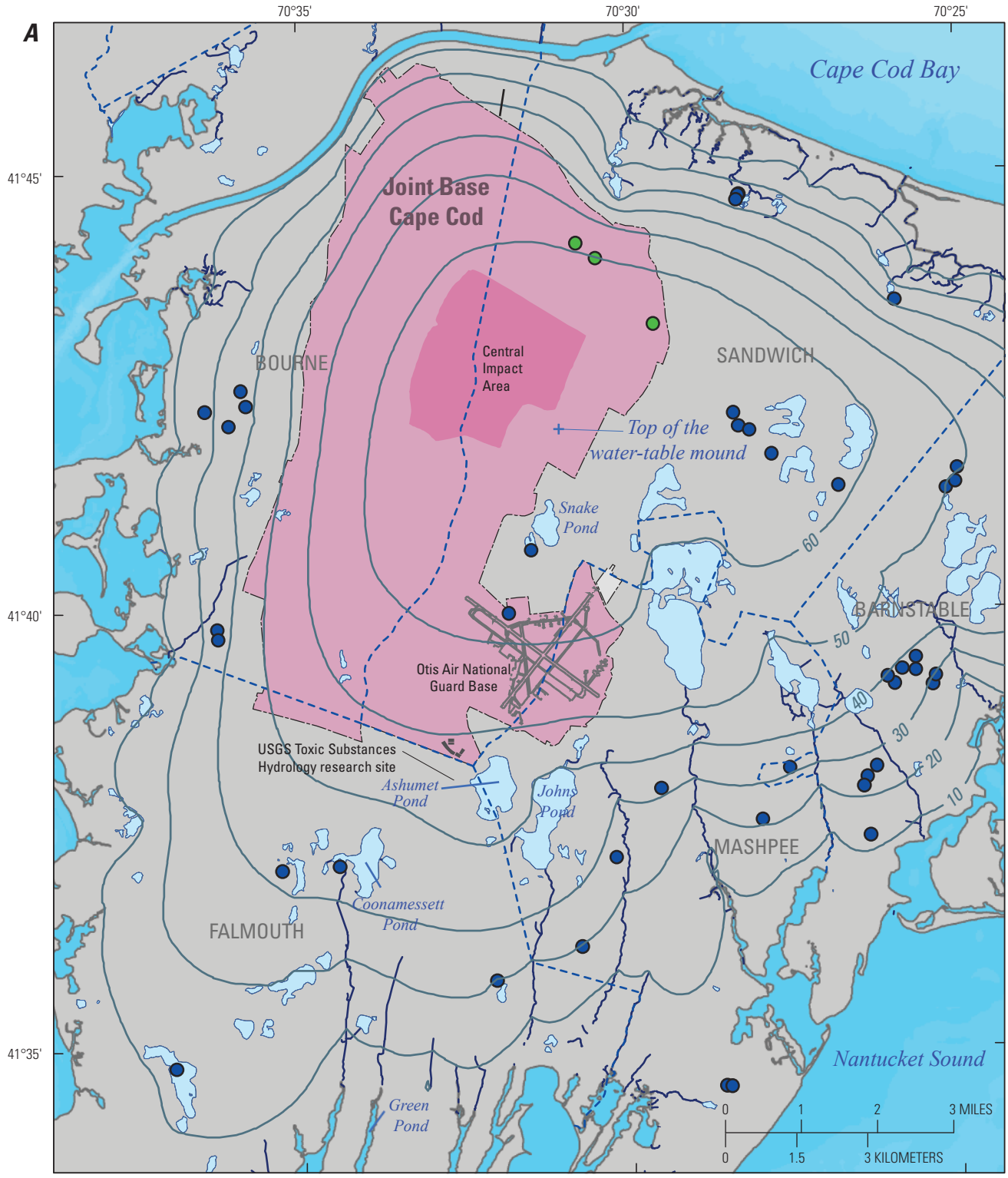

Base from U.S. Geological Survey and Massachusetts Office of Geographic Information digital data
National Geodetic Vertical Datum of 1929, North American Datum of 1983

EXPLANATION

10 — **Line of equal water-table altitude, in feet above NGVD 29**—Interval is 10 feet

Public-supply well—Pumped in 2010

Upper Cape Cooperative well—Pumped in 2010

Figure 2. *A*, The water table and public-supply wells in and near Joint Base Cape Cod, western Cape Cod, Massachusetts. NGVD 29, National Geodetic Vertical Datum of 1929.

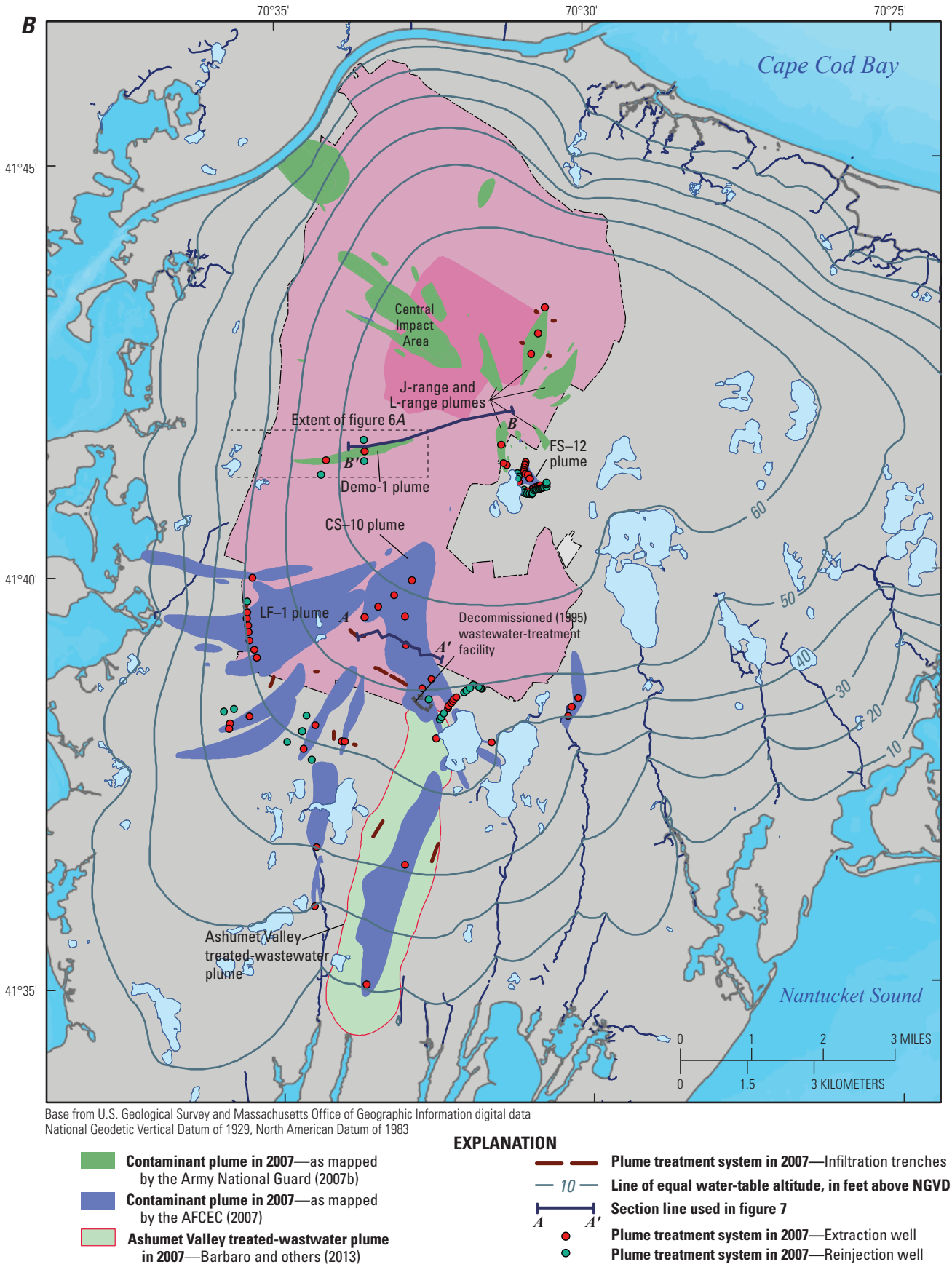

Figure 2. *B*, The water table, contaminant plumes, and remedial infrastructure in and near Joint Base Cape Cod, western Cape Cod, Massachusetts. AFCEC, Air Force Civil Engineer Center; NGVD 29, National Geodetic Vertical Datum of 1929; USGS, U.S. Geological Survey.

particular interest because they could affect the directions of advective transport of residual contamination emanating from the JBCC. A newly updated model incorporating future (2030) pumping stresses can be used to evaluate the effect of future water-supply withdrawals on the regional hydrologic system of western Cape Cod and hydraulic gradients within and near the JBCC.

Purpose and Scope

This report describes use of a numerical model to simulate the hydrologic system and transport of contaminants near JBCC. The report discusses (1) the compilation and analysis of data relevant to the hydrologic system of western Cape Cod and the transport of contaminants near the JBCC; (2) the use of those data to develop and calibrate a new regional groundwater flow model of the Sagamore flow lens (a hydraulically distinct groundwater flow system within the Cape Cod aquifer), with particular emphasis on the area around the JBCC (fig. 1); (3) the use of the model to characterize current (2010) hydrologic conditions and to evaluate the potential effects of future (2030) water-supply withdrawals and return flow on the hydrologic system; and (4) limitations and technical considerations relevant to the use of the calibrated model to make predictions of advective transport from sources on the JBCC.

Four general types of datasets are discussed, including (1) water levels and streamflows, (2) climate, land use, and water use, (3) lithology and bedrock, and (4) advective transport of contaminants from the JBCC, including plume extents and groundwater ages. Analyses of the data include the use of climate and spatial data to estimate recharge rates, the development of initial hydraulic conductivity fields from lithologic data, the use of time-varying well and streamflow data to estimate steady-state hydrologic conditions, and the use of mapped plumes and groundwater ages to estimate hydraulic gradients.

The development and calibration of the new regional groundwater flow model of the Sagamore flow lens is presented, including discussions of the underlying conceptualization and how it informs representation of model discretization, boundaries, and parameterization. The use of an existing model to simulate the dynamic position of the freshwater/saltwater interface in the Sagamore and Monomoy flow lenses (western and central Cape Cod) is also discussed, as is the incorporation of results from the existing freshwater/saltwater interface model into the new regional groundwater flow model of the Sagamore flow lens. The derivation of model-calibration targets from assembled hydrologic and tracer data is discussed, as is the use of inverse-calibration methods to estimate values of model parameters. The report includes a discussion of model fit to observed values and the sensitivity of simulated equivalents to model parameters.

The report also discusses the groundwater system as simulated by the new regional model, including gradient directions and magnitudes, groundwater fluxes, and ages of groundwater for current (2010) conditions. The potential effects of future (2030) pumping on water-table altitudes, streamflows, and hydraulic gradients, and on predictions of advective transport, are presented.

Factors affecting model calibration and considerations relevant to the use of the new regional model to predict advective transport are included in the report. Factors affecting model calibration include different observation types and the relative weighting of those observations in an inverse calibration and alternative representations of local-scale heterogeneity and the freshwater/saltwater interface. The effect those factors have on model predictions also is discussed.

Site History

The JBCC encompasses about 22,000 acres and was formerly known as the Massachusetts Military Reservation (MMR); military activity at the facility began as early as 1911. Several military branches have operated installations at the facility, including the U.S. Air Force, U.S. Army, Air and Army National Guards, and U.S. Coast Guard. The two largest installations are the Otis Air National Guard Base in the southern part of the JBCC and an impact area for the Army National Guard live-fire training facility in the central and northern part of the JBCC (fig. 2*A*). Additionally, the U.S. Coast Guard operates an air station at the JBCC.

The former Otis Air Force Base operated from 1948 until 1973, after which operations were transferred to the Air National Guard. Contamination was first observed in the late 1970s near the former site of the MMR wastewater-treatment facility (WWTF), along the southern boundary of the JBCC (fig. 2*B*). The area around the facility has been used since 1983 as a USGS Toxic Substances Hydrology research site. The JBCC Installation Restoration Program was initiated in 1986 to characterize groundwater contamination within and near the Otis Air National Guard Base and to determine potential effects of the contamination on the region's water resources. Numerous contaminant plumes and potential source areas have been characterized since the inception of the Installation Restoration Program (AFCEC, 2007). Source areas include those associated with normal operations, such as the landfill and WWTF, as well as training activities, chemical and aviation fuel spills, and fuel-pipeline leaks. Contaminants of most concern include (1) volatile organic compounds (VOCs), (2) contaminants associated with aviation fuel (BTEX compounds—benzene, xylene, ethylbenzene, and toluene—and fuel additives such as ethylene dibromide), and (3) nutrients (phosphorus and nitrogen) associated with the former site of the JBCC WWTF. Some plumes are associated with well-known sources, such as the plumes emanating from the former site of the landfill (LF–1 plume) and WWTF (Ashumet Valley plume), whereas plumes emanating from some fuel or chemical spills, such as CS–10 (fig. 2*B*), have source locations and histories that are less well known.

The largest installation at the JBCC is the Army National Guard training facility known as Camp Edwards, which encompasses about 14,000 largely undeveloped acres in the central and northern part of the JBCC. The site was operated by the U.S. Army until 1974, after which it became an Army National Guard training facility. The northern part of the installation includes an area known as the Central Impact Area (CIA) (fig. 2*B*) where live-fire artillery training has been conducted since the 1930s. The installation also includes several ranges used historically for mortar, rocket, and small-arms training, as well as several locations used for the disposal of munitions. In the mid-1990s, parts of Camp Edwards were considered as an auxiliary source of potable water to replace any loss of water supplies owing to contamination emanating from sources elsewhere on the MMR. The Impact Area Groundwater Study Program (IAGWSP) was initiated in 1997 to characterize subsurface contamination at the facility and the suitability of the area for water-supply development. Several potential source areas and contaminant plumes in the underlying aquifer have been identified since the inception of the IAGWSP (Army National Guard, 2007b). The contaminants of most concern at the site are explosives (RDX) and perchlorate. Primary source areas include (1) the CIA, (2) the J ranges, and (3) Demolition Area 1 (Demo-1) (fig. 2*B*). RDX has been introduced into the aquifer underlying the CIA by residues from ordnance explosions or partially exploded ordnance. Small, individual sources within the CIA are spatially distributed and essentially represent a nonpoint contaminant source. From the mid-1930s until the late 1990s, the J ranges were the site of live-fire mortar, rocket, and small-arms training and the disposal of ordnance and explosives as part of defense contractor testing. Demo-1 was the site of demolition training and ordnance disposal from the 1970s until the 1990s. The IAGWSP identified several areas suitable for water-supply development within the northern part of the JBCC, and three water-supply wells were installed during 2001–2 (fig. 2*A*) to augment water supplies for the four communities surrounding the JBCC; the wells, which are managed by the Upper Cape Regional Water Supply Cooperative, are referred to in this report as the Upper Cape Cooperative wells (fig. 2*A*). In 2010, about 1.3 Mgal/d of water was being pumped from the wells annually, most of which was used by communities to the south of the JBCC (Upper Cape Regional Water Supply Cooperative, 2015). For the purposes of this report, the current condition refers to pumping and return flow in 2010.

The JBCC is underlain by a permeable sand and gravel aquifer and, in some instances, plumes of contaminated groundwater have migrated several miles downgradient from source areas (fig. 2*B*). The JBCC includes parts of four towns: Falmouth, Mashpee, Sandwich, and Bourne (fig. 2*A*). These towns rely on groundwater as their sole source of water, and several public-supply wells are potentially downgradient from contaminant sources and plumes emanating from the JBCC (fig. 2*B*). To better protect the region's water resources, remedial systems have been installed within or downgradient from several contaminant plumes at the JBCC (fig. 2*B*). The systems, generally referred to as "extraction-treatment-reinjection" (ETR) systems, extract and treat contaminated water and reintroduce the water into the aquifer through reinjection wells or infiltration trenches or as surface-water discharges. In 2012, contaminated groundwater was being extracted from 140 wells; the treated water was reintroduced into the aquifer through 61 reinjection wells and 19 infiltration trenches (Army National Guard, 2013) (fig. 2*B*). It is estimated that the systems typically will operate for about 20 years. Following cessation of the ETR systems, it is possible that some residual contamination may remain in the aquifer.

Hydrogeology

Cape Cod is underlain by unconsolidated sediments that generally are highly permeable and nearly 1,000 feet (ft) thick in some areas. The region receives substantial rainfall, and the unconsolidated sediments compose the sole source of potable water for the region's communities. The Cape Cod aquifer system consists of six separate flow lenses: Sagamore, Monomoy, Nauset, Chequesset, Pamet, and Pilgrim (fig. 1). Each flow lens represents a distinct aquifer system that is hydraulically separate from adjacent flow lenses. The JBCC is on the western part of the Sagamore flow lens—the largest and westernmost of the flow lenses (fig. 1). The geologic history and hydrology of Cape Cod have been documented in numerous publications, including LeBlanc and others (1986), Oldale (1992), Uchupi and others (1996), and Masterson and others (1997a).

Geologic Setting

The glacial sediments, which consist of gravel, sand, silt, and clay and are underlain by crystalline bedrock, were deposited 15,000–16,000 years ago within and near the margins of retreating continental ice sheets (Oldale and Barlow, 1986; Uchupi and others, 1996). The altitude of the bedrock surface underlying the glacial sediments ranges from about 50 ft below the National Geodetic Vertical Datum of 1929 (NGVD 29) near the Cape Cod Canal to more than 900 ft below NGVD 29 beneath the outer part of Cape Cod; the bedrock surface beneath the JBCC varies from about −125 to −250 ft NGVD 29 (Fairchild and others, 2013). The surficial geology of Cape Cod is characterized by broad, gently sloping outwash plains and hummocky terrain associated with glacial moraines and ice-contact deposits. Outwash sediments, which compose most of the glacial sediments underlying Cape Cod, were deposited in fluvial and lacustrine depositional environments associated with proglacial lake deltas analogous to those seen in present-day fluvial deltas (Oldale, 1992). Moraines were deposited in low-energy environments at the margins of the ice sheets and generally are finer grained and less sorted than are outwash sediments; ice-contact deposits were deposited within high-energy fluvial environments beneath and inside the ice sheets and generally are coarser grained than

are the outwash deposits. The largest outwash plain on the Sagamore flow lens is the Mashpee Pitted Plain (MPP), which underlies most of the JBCC. The MPP is bounded to the east by the Barnstable Plain and to the west and north by the Buzzards Bay and Sandwich Moraines (fig. 3).

Outwash sediments underlying the Mashpee outwash plain generally become finer grained with depth and to the south (fig. 3*B*) and with increasing distance from the sediment source near the present-day Cape Cod Canal. These deposits are broadly divided into three depositional units: coarse-grained sand and gravel deposited in meltwater streams (topset beds), fine to medium sands deposited in nearshore lacustrine environments (foreset beds), and fine sand and silt deposited in offshore lacustrine environments (bottomset beds) (Masterson and others, 1997a). Geologic contacts generally are absent laterally within depositional units, and grain size trends are gradational. Sediments underlying the northern part of the MPP, near the sediment source, generally consist of coarse-grained, sandy sediments that extend to near bedrock (fig. 4*A*). In the central and southern part of the MPP, the grain size generally is finer, with interbedded lenses of fine sand (figs. 4*B*–*C*). Numerous collapse structures are within the outwash plain, beneath kettle holes; these structures were formed by the melting of buried blocks of remnant glacial ice and the subsequent collapse of the overlying sediments.

Grain size can be observed in lithologic logs (Masterson and others, 1997a); however, local-scale heterogeneities are common throughout the aquifer, including lenses of finer grained, silty sediments within generally coarse-grained sediments (figs. 4*A*–*E*). Two types of silty deposits are present in the aquifer: "basal" silts and "hanging" silts. Basal silts are present in deeper parts of the aquifer, generally are thicker and extend to bedrock, and represent deposition in lacustrine environments that generally reflect the regional depositional model (fig. 3*B*) (Masterson and others, 1997a). Hanging silts generally are thinner, are present within coarser grained sediment in shallower parts of the aquifer, and may represent deposition locally within fluvial environments.

Hydrologic Setting

The unconsolidated glacial sediments underlying Cape Cod compose an unconfined aquifer system that is bounded below by relatively impermeable bedrock, above by the water table, and laterally by saltwater—Cape Cod Bay to the northeast, Cape Cod Canal to the northwest, Buzzards Bay to the west, and Nantucket Sound to the south. The Sagamore flow lens on central and western Cape Cod is the largest and westernmost of the six hydraulically distinct freshwater lenses that underlie Cape Cod (fig. 1); the flow lens is hydraulically separated at its northwestern extent from mainland Massachusetts by the Cape Cod Canal and from the adjacent Monomoy flow lens at its eastern extent by the Bass River. Recharge from precipitation is the sole source of water to the aquifer system. About 45 inches of precipitation falls annually on Cape Cod; slightly more than one-half of the precipitation recharges the aquifer across the water table (LeBlanc and others, 1986); the remainder is lost to evapotranspiration. Surface runoff is negligible owing to the sandy soils and low topographic relief of the area.

Water-table altitudes exceed 65 ft above NGVD 29 in the northwestern part of the Sagamore flow lens (fig. 5*A*). Groundwater flows from regional groundwater divides towards natural discharge locations at streams, coastal estuaries, and the ocean (fig. 5*A*). On western Cape Cod, the groundwater flows radially outward from a regional water-table divide in the northwestern part of the Sagamore flow lens, beneath the northern part of the JBCC (fig. 5*A*). Most groundwater flows through shallow sediments and discharges to streams and estuaries; groundwater recharging the aquifer near groundwater divides flows deeper in the aquifer and discharges to the ocean (fig. 5*B*). Most groundwater discharge (about two thirds of the total) discharges into saltwater bodies. About 25 percent of groundwater is discharged into freshwater streams and wetlands, and a small amount (less than 10 percent) is removed from the system for water supply (Walter and Whealan, 2005).

Water-table contours and groundwater flow patterns are strongly affected locally by ponds and streams. Kettle-hole ponds, which are in hydraulic connection with the aquifer, focus groundwater flow. Groundwater flow paths converge in areas upgradient of the ponds, where groundwater discharges into the ponds, and diverge in downgradient areas, where pond water recharges the aquifer (fig. 5*C*). The degree to which ponds interact with the surrounding aquifer is, to an extent, a function of pond-bottom sediments. Some ponds have surface-water outlets that drain into freshwater streams. Streams generally are areas of groundwater discharge (gaining streams) and receive water from the aquifer. Some stream reaches may lose water to the aquifer (losing streams), particularly in areas downgradient from pond outflows; however, these generally are limited in extent.

About 7 percent of the water recharging the Cape Cod aquifer system is removed for water supply (Walter and Whealan, 2005). Most of this water is returned to the system as wastewater return flow, either as dispersed septic-system return flow or as point discharges to the aquifer at WWTFs. Although most of the water withdrawn for public supply is returned to the aquifer, the water is usually recharged in areas away from the withdrawals, particularly in areas served by public water supply. Large-capacity public-supply wells decrease groundwater levels and can affect natural resources by drying vernal pools, drawing down ponds, and decreasing streamflows by changing hydraulic gradients and either intercepting groundwater that would have discharged to a stream or receiving water through direct infiltration from a pond or stream. Water-table altitudes and streamflows can increase locally in the vicinity of large wastewater-disposal facilities. In addition, pumping and redistribution of return flow can affect hydraulic gradients in the aquifer and could affect the advective transport of contaminants.

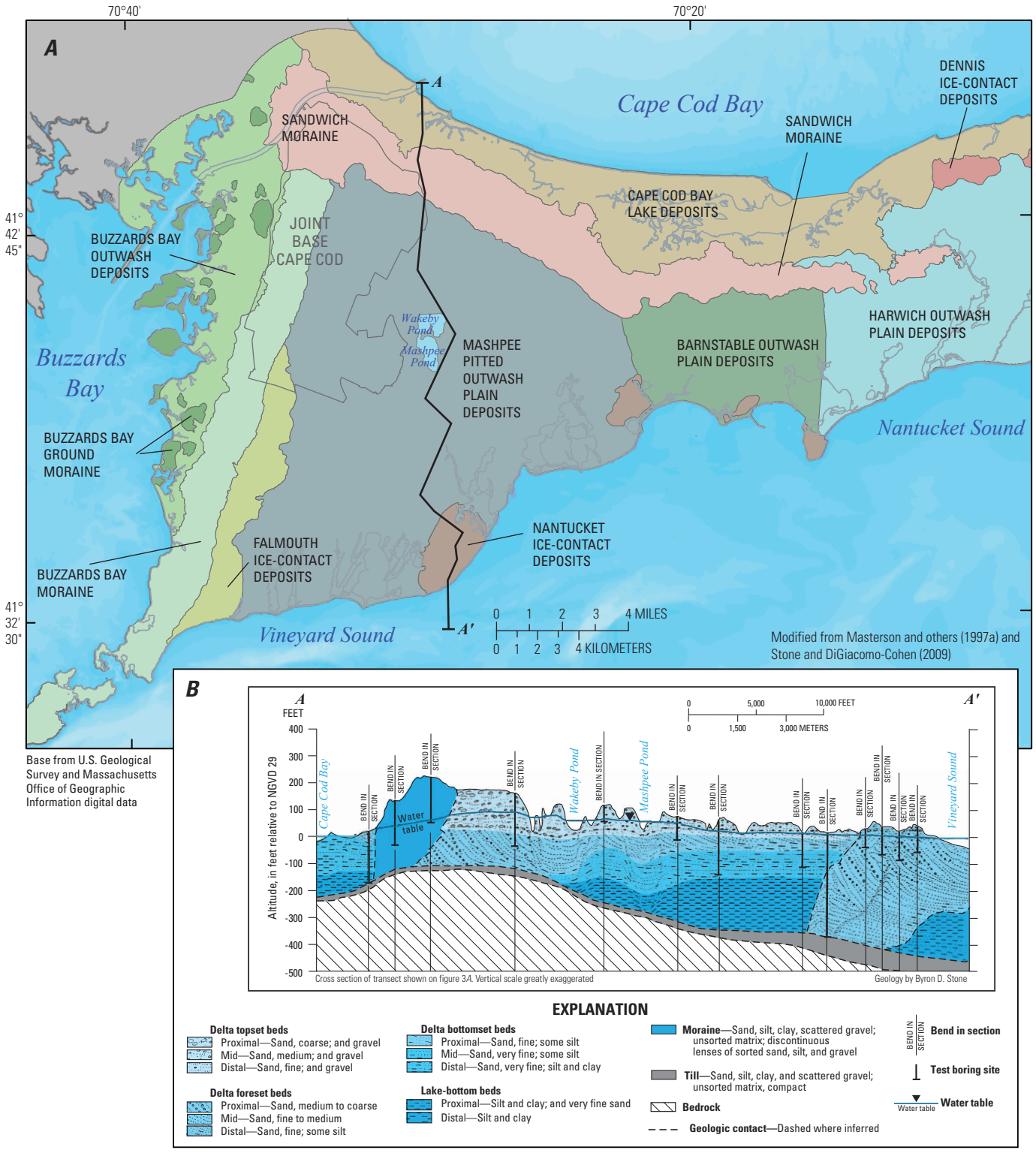

Figure 3. *A*, Surficial geologic units, and *B*, geologic section (*A*–*A*′) extending north-south through the Mashpee Pitted Plain, western Cape Cod, Massachusetts. Figure 3*B* modified from Masterson and others (1997a). NGVD 29, National Geodetic Vertical Datum of 1929.

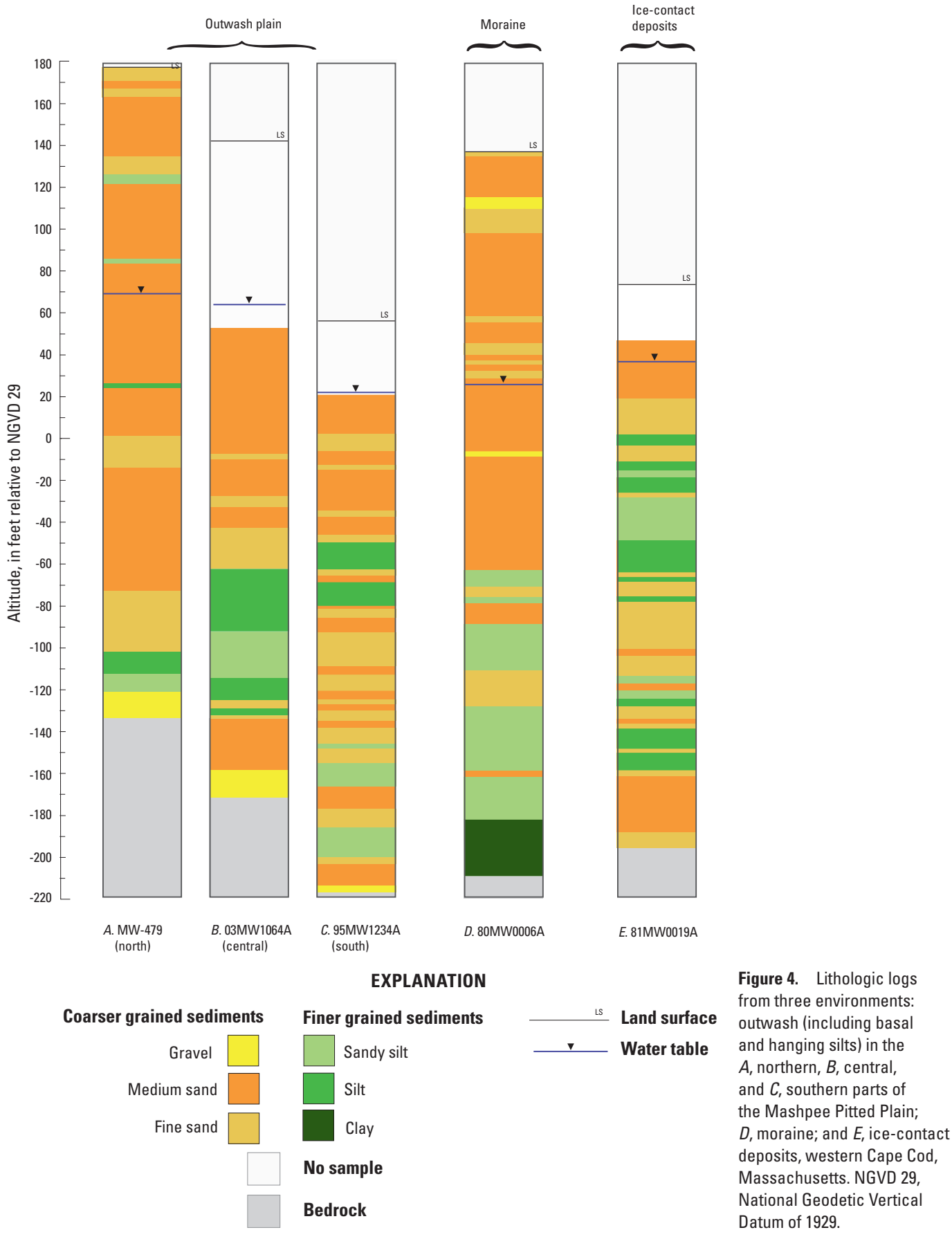

Figure 4. Lithologic logs from three environments: outwash (including basal and hanging silts) in the *A*, northern, *B*, central, and *C*, southern parts of the Mashpee Pitted Plain; *D*, moraine; and *E*, ice-contact deposits, western Cape Cod, Massachusetts. NGVD 29, National Geodetic Vertical Datum of 1929.

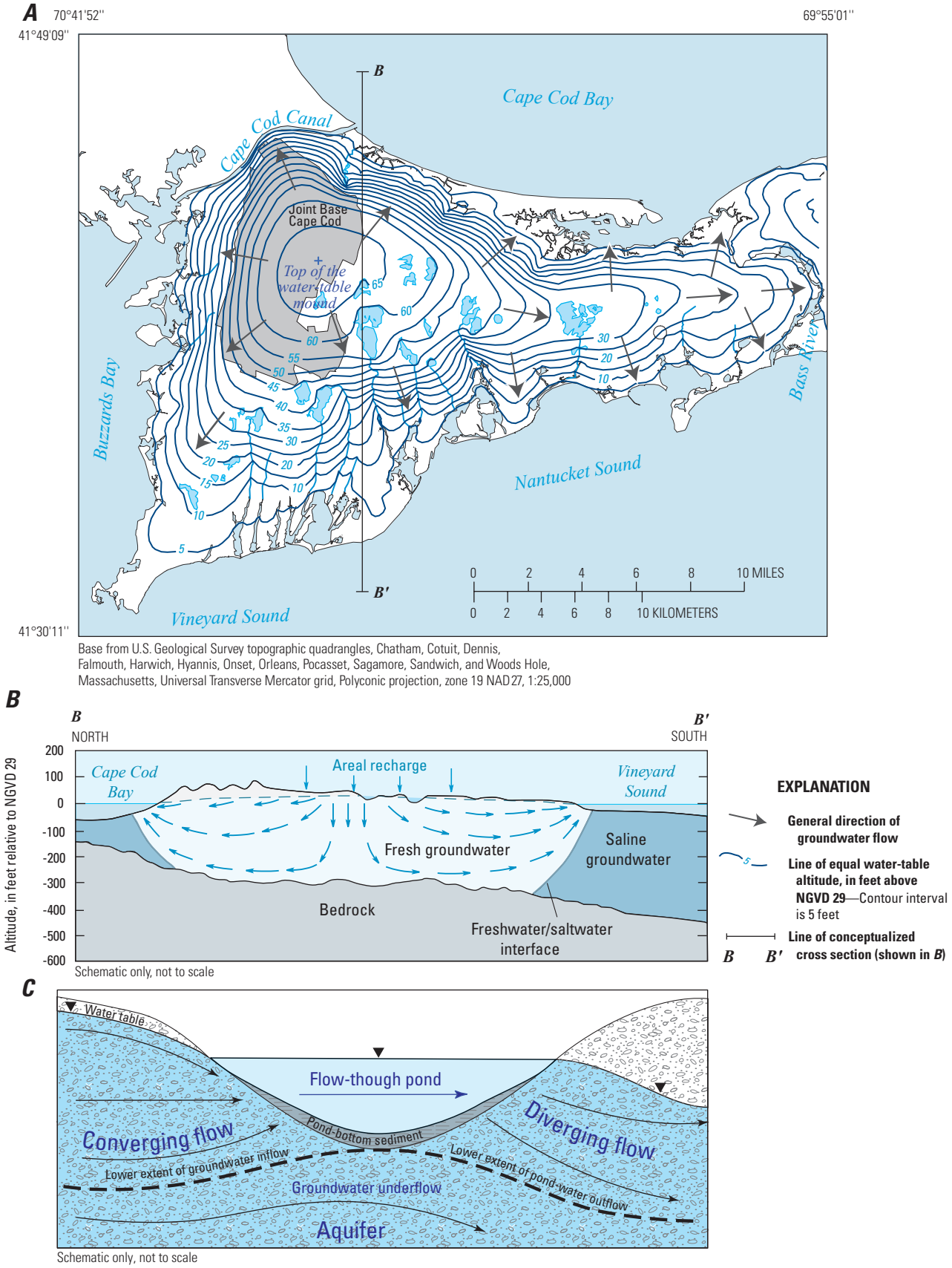

Figure 5. *A*, Water-table altitude and groundwater flow directions; *B*, generalized north-south hydrologic section showing vertical flow paths on western Cape Cod, Massachusetts; and *C*, generalized groundwater flow patterns near a flow-through pond. Figures *A* and *B* modified from Walter and Whealan (2005); figure *C* modified from Winter and others (1998). NAD27, North American Datum of 1927; NGVD 29, National Geodetic Vertical Datum of 1929.

Contaminant Transport

Advective transport refers to the movement of a solute with the rate of average groundwater velocity and is the dominant component of transport for conservative solutes in the Cape Cod aquifer owing to high recharge rates and the permeable aquifer sediments (LeBlanc, 1984). Groundwater velocities of more than 1.5 feet per day (ft/d) have been measured at the USGS Toxic Substances Hydrology research site near the former WWTF along the southern boundary of the JBCC (fig. 2*B*) (LeBlanc and others, 1991). The rate of advective transport in the aquifer is related to the location of a source area relative to regional groundwater divides and discharge locations; near divides, where horizontal gradients are small and downward components are substantial, groundwater flow is more vertical and slower than flow recharged farther from divides, where horizontal flow predominates (fig. 5*B*) (Walter and Masterson, 2003; Walter and others, 2004). Traveltime, defined as the total time required for water to move from a recharge location at the water table to a natural discharge location, is greatest for groundwater flow that originates near regional groundwater divides and ranges from essentially zero (adjacent to discharge boundaries) to hundreds of years (near groundwater divides). Most areas of western Cape Cod have traveltimes of 20 years or less (Walter and others, 2004).

Generally permeable, sandy sediments and high recharge rates make the Cape Cod aquifer susceptible to groundwater contamination, and several plumes of contaminated groundwater have migrated downgradient from sources on the JBCC (fig. 2*B*). A plume of sewage-contaminated groundwater emanating from the former site of the JBCC WWTF has been transported, primarily by advection, more than 7 miles downgradient from the source (Barbaro and others, 2013). Contaminant plumes, including VOCs emanating from the sources in the southern part of the JBCC, and RDX and perchlorate emanating from the Army National Guard training facility, have been transported as far as 5 miles downgradient from source areas (fig. 2*B*).

Advection is the principal component of transport in the aquifer; therefore, the shape and extent of a contaminant plume is a function of regional horizontal and vertical hydraulic gradients. In the northern part of the JBCC, which is underlain by a radial groundwater divide, plumes emanating from sources located in close proximity are transported in different directions and form a radial pattern of contaminant transport (fig. 2*B*). Contaminant plumes follow the regional hydraulic gradient, orthogonal to water-table contours, towards discharge locations (streams and coastal waters) or towards ponds (fig. 2*B*). Groundwater flux in an unconfined aquifer decreases with depth in the aquifer, and, as a result, most plumes generally are within shallower parts of the aquifer, where most groundwater flow occurs. As an example, the Demo-1 plume, which contains perchlorate and emanates from a former ordnance-training area, has migrated nearly 2 miles downgradient since training began at the site in the late 1970s (figs. 2*A* and 6*A*); the plume is present within the upper half of the aquifer along the length of the plume. The presence of fine-grained sediments at depth further shifts groundwater flow and advective transport into shallower parts of the aquifer.

Local-scale heterogeneities, such as silt lenses within the sandy aquifer sediments, can locally affect hydraulic gradients and the distribution of contaminants in the aquifer. The downgradient part of the Demo-1 plume may locally be affected by silt lenses within the sandy aquifer sediments. Contamination is present above the silts but, as defined by existing wells, not below an altitude where contamination is present upgradient in the absence of any silt lenses (fig. 6*B*). The distribution of VOCs in some parts of the CS–10 plume is correlated with silt lenses, suggesting that heterogeneity may affect advective transport of contamination in the aquifer and the plume may emanate from numerous source areas (fig. 7*A*). Local-scale heterogeneity also may affect groundwater ages (fig. 7*B*). The vertical location of peak concentrations of tritium is a general indicator of the altitude of water recharged into the aquifer in 1963, corresponding to peak atmospheric concentrations of the isotope. Tritium peaks generally are at a similar altitude in an aquifer, assuming homogenous sediments and a similar bedrock altitude (Vogel, 1967). Tritium peaks from sampled borings in the JBCC have a wide range of altitudes, as exemplified in three borings from the northern part of the JBCC (fig. 7*B*). Tritium peaks can occur much shallower in the aquifer than would be expected, assuming average recharge rates and saturated thickness, often in association with lenses of fine sand and silt.

Natural recharge rates vary over seasonal and multiyear time scales, and, as a result, streamflow, water levels, and hydraulic gradients in the aquifer change over time. Water levels near the northern part of the JBCC can vary by as much 10 ft between extremely wet and dry years (Walter and Whealan, 2005). The location of regional groundwater divides and hydraulic gradients also can change substantially over time (Walter and Masterson, 2003). However, time-varying recharge and hydraulic gradients likely do not greatly affect advective-transport patterns owing to the longer, decadal time-scales of advective transport as compared to the smaller time scales over which hydrologic conditions vary (Walter and Masterson, 2003). As a result, the advective transport of contaminants generally can be simulated as a steady-state process. However, time-varying gradients may, along with some transverse dispersion, cause plumes to be wider than steady-state gradients would indicate. The maximum observed width of the Demo-1 plume exceeds that of the source area by a factor of more than three (Army National Guard, 2009) (fig. 6*C*).

Several processes other than advection can affect the transport of contaminants from sources at land surface, beginning with transport through the unsaturated zone. The thickness of the unsaturated zone beneath possible source areas at the JBCC ranges from less than 20 ft in the southern part to more than 100 ft beneath the northern part of the installation. The effect of the unsaturated zone is to delay the arrival of contaminants at the water table. An unsaturated zone thickness of 112 ft results in a transport time of about 2.4 years,

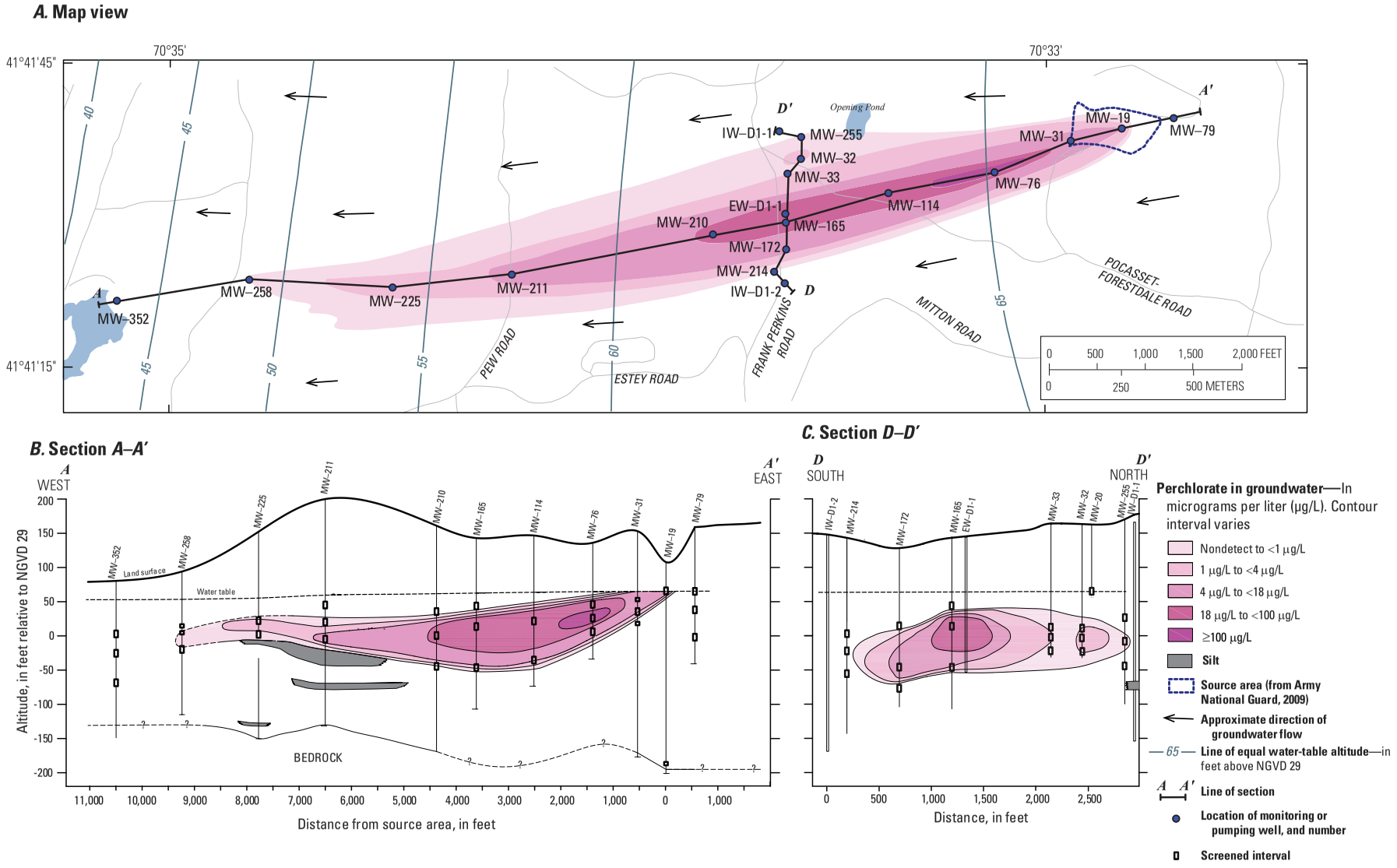

Figure 6. *A*, The concentration of perchlorate in the Demolition Area 1 (Demo-1) contaminant plume and source area, *B*, longitudinal section (*A*–*A*′) of the Demo-1 plume, and *C*, transverse section (*C*–*C*′) of the Demo-1 plume, western Cape Cod, Massachusetts. Figure 6*A* modified from Army National Guard (2005). Location of figure 6*A* is shown on figure 2*B*. NGVD 29, National Geodetic Vertical Datum of 1929.

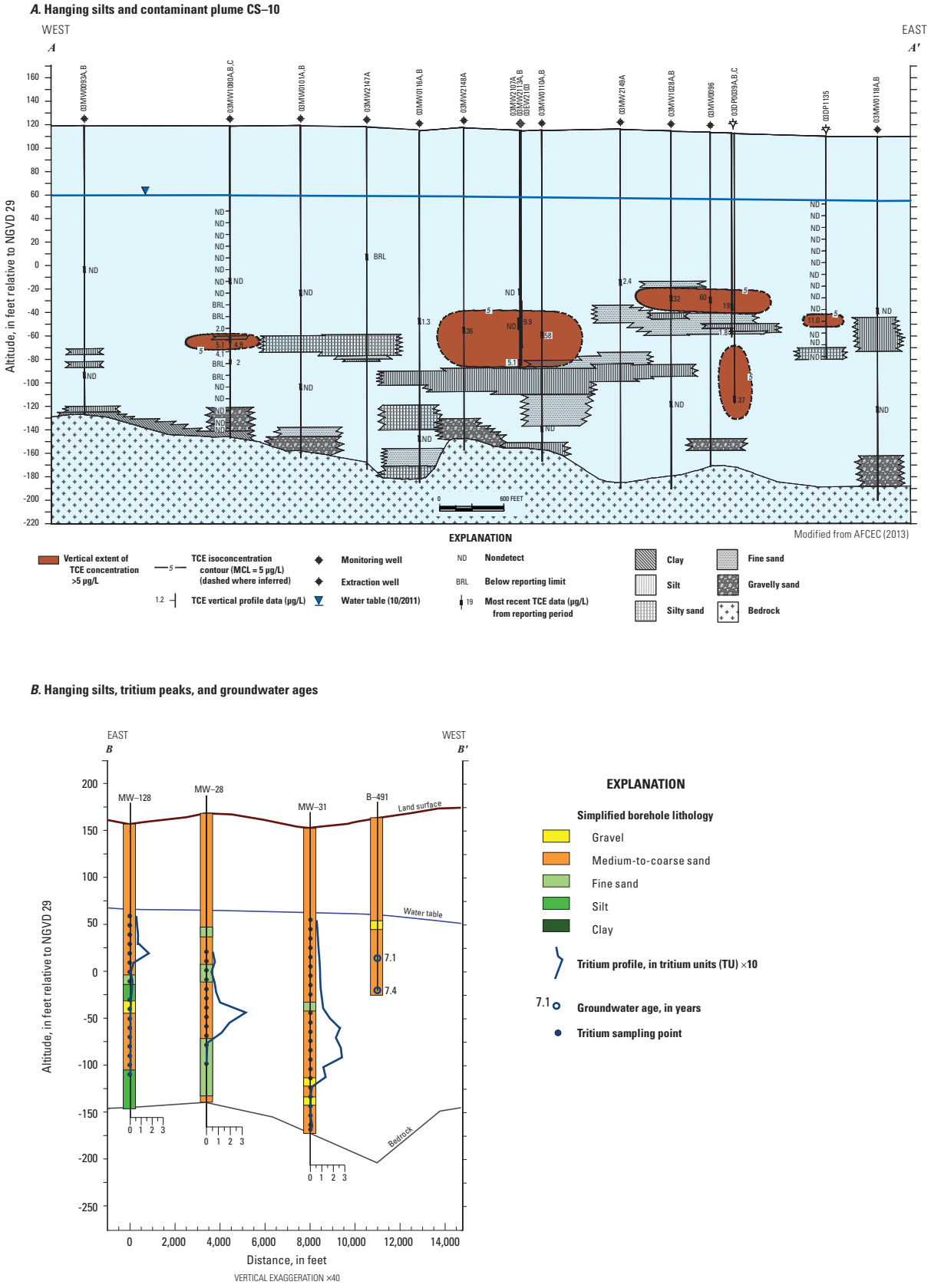

Figure 7. *A*, Hanging silts and a contaminant plume (*A*–*A*′) and *B*, hanging silts, tritium peaks, and groundwater ages (*B*–*B*′), western Cape Cod, Massachusetts. Section locations are shown on figure 2*B*. AFCEC, Air Force Civil Engineer Center; MCL, maximum contaminant level; NGVD 29, National Geodetic Vertical Datum of 1929; TCE, trichloroethylene; µg/L, microgram per liter.

assuming average recharge rates and hydraulic parameters typical of Cape Cod sediments (Jeff Barbaro, USGS, written commun., 2010). Dispersion, which refers to the spreading of solute mass arising from aquifer heterogeneity, occurs in all porous sediments and is scale dependent. Longitudinal dispersion refers to a spreading of mass in the direction of groundwater flow. It is the largest component of dispersion in the Cape Cod aquifer system and results in a spreading of mass near the leading edges of plumes (figs. 6*A–B*). Longitudinal dispersion results in smaller traveltimes for low initial contaminant concentrations to a receptor, though not for the final, elevated steady-state concentrations (Walter, 2008). Transverse and vertical components of dispersion refer to spreading of mass orthogonal to groundwater flow directions and typically are much less than longitudinal dispersion (fig. 6*C*).

Attenuation through chemical and biological processes can slow the movement of a contaminant or decrease its concentrations. Groundwater in the Cape Cod aquifer generally is oxic with low organic carbon content (LeBlanc, 1984), and attenuation of contaminants of concern at the JBCC generally is limited. Interactions with aquifer sediments, such as sorption, can slow the movement of some organic compounds, including VOCs and RDX. Whereas BTEX compounds degrade under conditions prevalent in the Cape Cod aquifer system, associated fuel additives, such as ethylene dibromide (EDB), are stable compounds that persist in the environment and can be transported conservatively in the aquifer. Nitrogen and phosphorus are contaminants of concern in sewage-contaminated groundwater near the former WWTF. Nitrogen, which adversely affects estuarine ecosystems, can be naturally attenuated by denitrification in reducing environments, though those conditions are limited in the Cape Cod aquifer (Barbaro and others, 2013). Phosphorus, which can adversely affect freshwater ecosystems, is strongly sorbed to aquifer sediments and moves slowly in the aquifer (Walter and others, 1996), though phosphorus is discharging into Ashumet Pond, which is downgradient from the former WWTF.

Data Compilation and Analysis

A variety of data—hydrologic, climatic, lithologic, chemical, and water-use—were compiled and analyzed for use as model inputs and to provide observation data to calibrate the model (table 1). Climatic and land-use data were used to estimate the spatial distribution of recharge by using the Soil-Water-Balance (SWB) model (Westenbroek and others, 2010). Observed positions of the freshwater/saltwater interface at 19 locations were used, in combination with a numerical model, to estimate the regional interface position, and passive seismic and borehole data were used to determine the altitude of the bedrock surface. The observed bedrock altitude and simulated interface position were used in combination to determine the subsurface geometry of the aquifer. Lithologic data from more than 950 boreholes were used to characterize spatial patterns of horizontal and vertical hydraulic

Table 1. Summary of data types assembled for use as observations in calibrating the numerical groundwater model of the Sagamore flow lens, western Cape Cod, Massachusetts.

[^{3}He/^{3}H, helium-3/tritium ratio; CFC, chlorofluorocarbon]

Data type	Data description	Number of observation sites identified	Number of observation sites used for calibration	Sources[1]
Hydraulic head—wells	Monitoring well water level	5,517	535	1, 2, 4, 5
Hydraulic head—ponds	Pond stage site	109	12	1, 2, 3, 4, 5
Streamflow	Streamflow measurement site	80	29	1, 4, 6
Plume path	Plume transect and corresponding source location	31	31	1, 4, 5
Age—^{3}He/^{3}H	Groundwater age	93	93	1
Age—CFC	Groundwater age	15	15	1
Age—tritium peak	Groundwater age calculated from tritium peak position	24	24	1
Mound position	Estimated position of regional water-table mound	1	1	1, 5
Ashumet pond hinge	Estimated position along shoreline of zero vertical gradient	1	1	1

[1]Sources:

1. U.S. Geological Survey (2018a, b, c)
2. Cape Cod Commission (2018)
3. Association to Preserve Cape Cod (2018)
4. U.S. Air Force Civil Engineer Center (AFCEC) Installation Restoration Program (AFCEC, 1996, 2000, 2001, 2003, 2007, 2013)
5. U.S. Army National Guard (ARNG) Impact Area Groundwater Study Program (ARNG, 2005, 2007a, b, 2009, 2010a, b)
6. Massachusetts Estuaries Project (2018)

conductivity and to determine initial parameter values for model calibration. Water-level and streamflow data were compiled and evaluated for use as observations in model calibration. Indicators of advective flow—contaminant plume paths and groundwater ages—also were compiled and evaluated for use as observations of long-term average hydraulic gradients.

Hydrologic Data

Calibration of a steady-state numerical model requires observations that generally are representative of long-term average hydrologic conditions. Water-level observations, including surface-water stages, were compiled from many sources, including the USGS (https://waterdata.usgs.gov), the Cape Cod Commission, the Association to Preserve Cape Cod, local water suppliers, the Air Force Civil Engineer Center (AFCEC), and the Army National Guard. A total of 5,626 water-level measurements (monitoring wells and ponds) were compiled from the various sources (fig. 8); most of the monitoring wells are located in or near the JBCC and generally near mapped contaminant plumes. The altitudes of the well screens vary, and the screen altitudes represent most vertical parts of the aquifer. Kettle-hole ponds on Cape Cod are surface expressions of the water table, and water levels have been measured at 109 surface-water bodies on western Cape Cod by using leveling methods and staff and siphon gages (table 1).

The period of record for each water-level site was evaluated to determine the degree to which the data represent a long-term average hydrologic condition. Thirty-eight wells have monthly or continuous measurements that extend back more than 30 years; three of those have regular measurements that extend back more than 50 years. A total of 2,478 sites have intermittent measurements that extend back more than 10 years (referred to as "partial-record sites"); 1,263 of these sites were measured only once. Water-level measurements for each partial-record were compared to measurements at the 29 long-term index wells measured monthly by the Cape Cod Commission (periods of record greater than 30 years) during the same period of record. The partial-record well and its mean water level were included as a calibration target if the partial period occurred during near average conditions at the long-term wells. The water level was considered near average if, during the period of the partial record, the averaged water levels during the same period at the 29 long-term wells were within 20 percent of one standard deviation of their averaged long-term mean. As an example, figure 9*A* shows a hydrograph for long-term well MA–SDW 253 and partial-record well 27MW0023A (fig. 8); the mean water level is 55.52 ft for the partial period of record (1998–2008). The full-record mean water level for well MA–SDW 253 is 61.29 ft with a standard deviation of 1.90 ft. The mean water level in the long-term well during the partial period of record of well 27MW0023A (1998–2008) is 61.05 ft, which differs from the full-record mean by 0.24 ft, or about 12.6 percent of one standard deviation. Considering all 29 long-term wells, the mean for that period of record is, on average, within 14.9 percent of one standard deviation. The mean water level at site 27MW0023A, therefore, is considered near average and is included as a calibration target. A similar process was used to identify 510 partial-record wells and 10 ponds that were suitable for use as steady-state water-level observations, in addition to the 29 long-term wells.

Streams on Cape Cod generally are gaining streams, and about 40 percent of groundwater discharge on the Sagamore flow lens is into streams (Walter and Whealan, 2005). Most large streams on western Cape Cod are in the southern part of the flow lens, draining the MPP. Sources of streamflow-measurement data include the USGS, the Massachusetts Department of Environmental Protection (MassDEP) Massachusetts Estuaries Project (MEP), and the JBCC. The largest stream on western Cape Cod, the Quashnet River, has been continuously measured since 1988 (USGS site number 011058837) (fig. 8; USGS, 2017; https://waterdata.usgs.gov/ma/nwis/sw). Precipitation records from National Oceanic and Atmospheric Administration (NOAA) weather station Hyannis (Barnstable Municipal Airport [KHYA]) (NOAA National Climatic Data Center, 2012) compared with records from long-term well MA–SDW 253 and the Quashnet River site show that water levels and streamflows respond proportionally to increases and decreases in precipitation (fig. 10). The annual mean streamflows at the Quashnet River range from 11.0 to 25.3 cubic feet per second (ft^3/s). The Backus River, Coonamessett River, and Mill Creek (fig. 8) have previously been measured frequently or continuously over 1- to 2-year periods. Measurements of streamflow also have been made at an additional 76 partial-record sites on western Cape Cod, including 13 sites which have been measured more than five times.

The suitability of mean partial-record streamflows for use as observations of steady-state conditions was determined by comparison to the long-term record at the Quashnet River, which has a mean of 17.41 ft^3/s and a standard deviation of 5.7 ft^3/s (fig. 9*B*). The mean streamflow at a partial-record site was assumed to be reasonable as a steady-state calibration target if the mean streamflow at the Quashnet River during the partial-record period differed by less than 30 percent of the standard deviation (about 1.7 ft^3/s) from the long-term mean. Mean partial-record streamflows from 29 sites were assumed to be suitable as observations of near-average hydrologic conditions. Many of the measurements were made as part of synoptic measurements in May 2002, when hydrologic conditions were determined to be near average (Walter and Whealan, 2005). In addition, average long-term streamflows for sites with more than five nonzero measurements were estimated by correlating the partial records to the full period of record for the Quashnet River. The Streamflow Record Extension Facilitator (SREF) program (Granato, 2009) was used to extend limited data from 10 partial-record sites, including Backus River, Coonamessett River, and Mill Creek. The SREF program implements the maintenance of variance extension methods (MOVE.1 and MOVE.3) described by Hirsch (1982) and Vogel and Stedinger (1985).

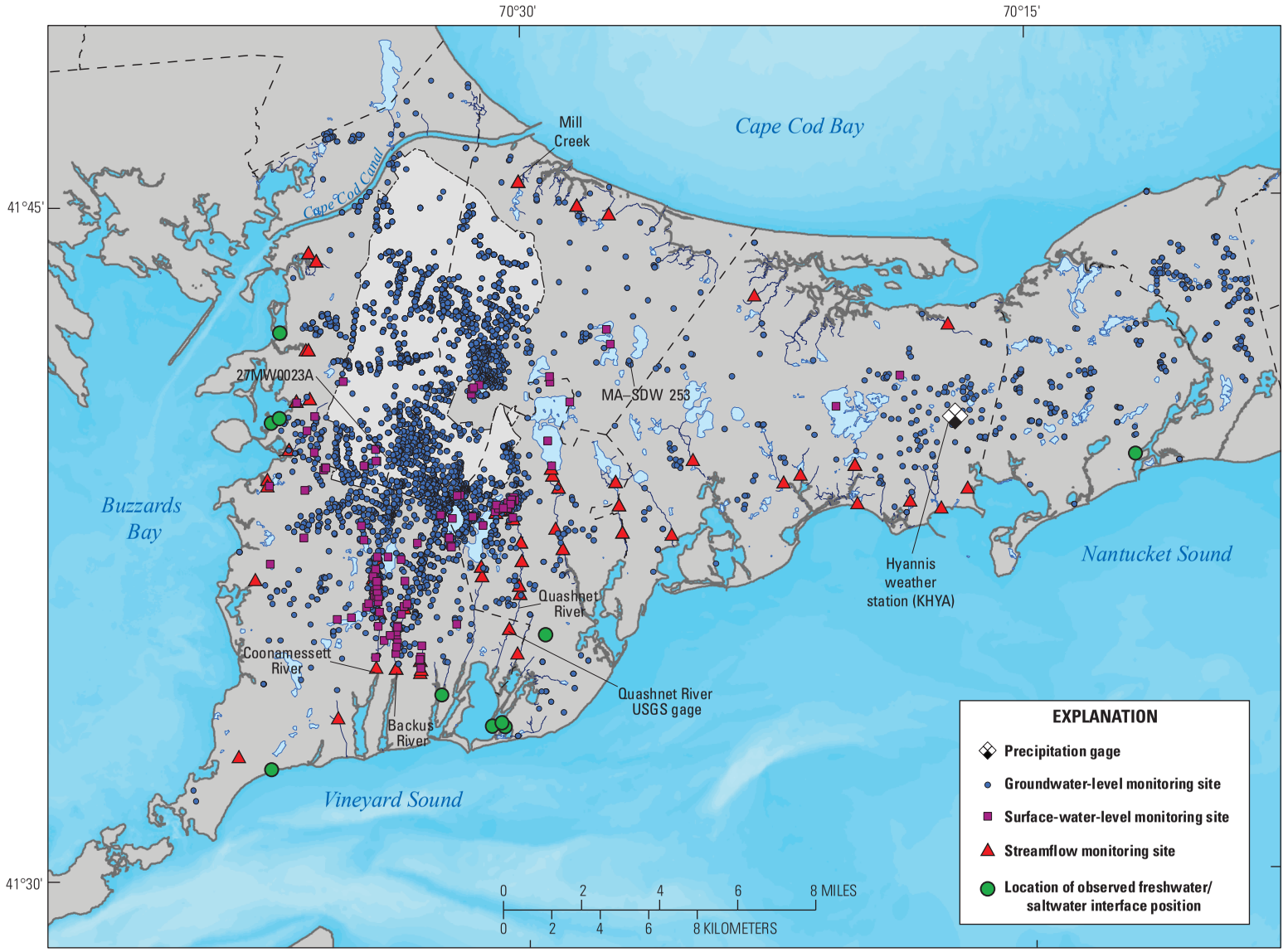

Base from U.S. Geological Survey and
Massachusetts Office of Geographic Information digital data
National Geodetic Vertical Datum of 1929, North American Datum of 1983

Figure 8. Locations of the Hyannis weather station (Barnstable Municipal Airport [KHYA]) precipitation gage, groundwater wells, surface-water sites, and observed freshwater/saltwater interface positions on western Cape Cod, Massachusetts. USGS, U.S. Geological Survey.

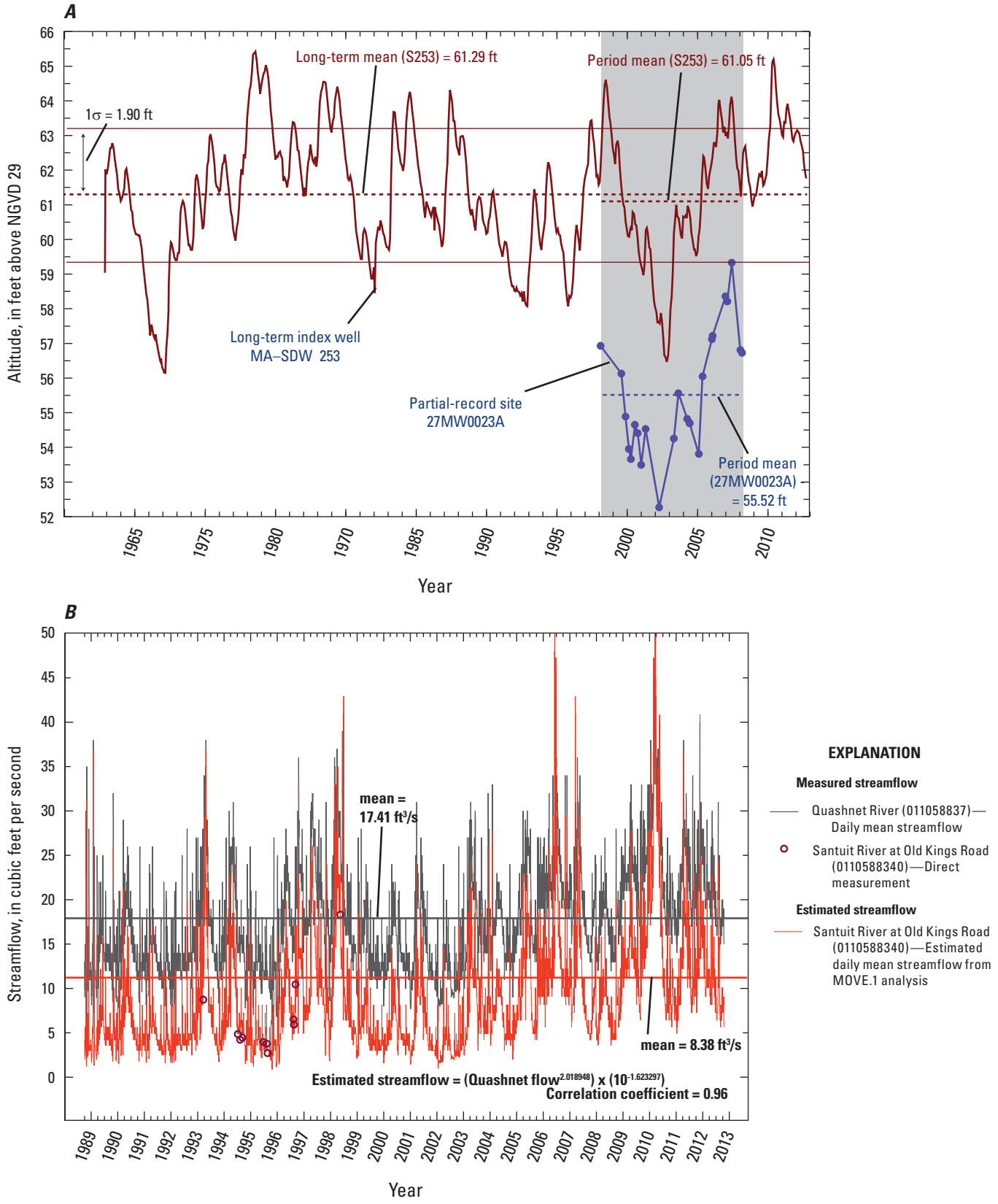

Figure 9. *A*, Overlap of long-term well (MA–SDW 253) (1962–2012) and partial-record well (27MW0023A), and *B*, maintenance of variance extension, type 1 (MOVE.1) analysis (Hirsch, 1982) for partial-record streamflow site (Santuit River at Old Kings Highway), 1988–2012, western Cape Cod, Massachusetts. Modified from Walter and others (2016). ft, foot; ft^3/s, cubic foot per second; NGVD 29, National Geodetic Vertical Datum of 1929.

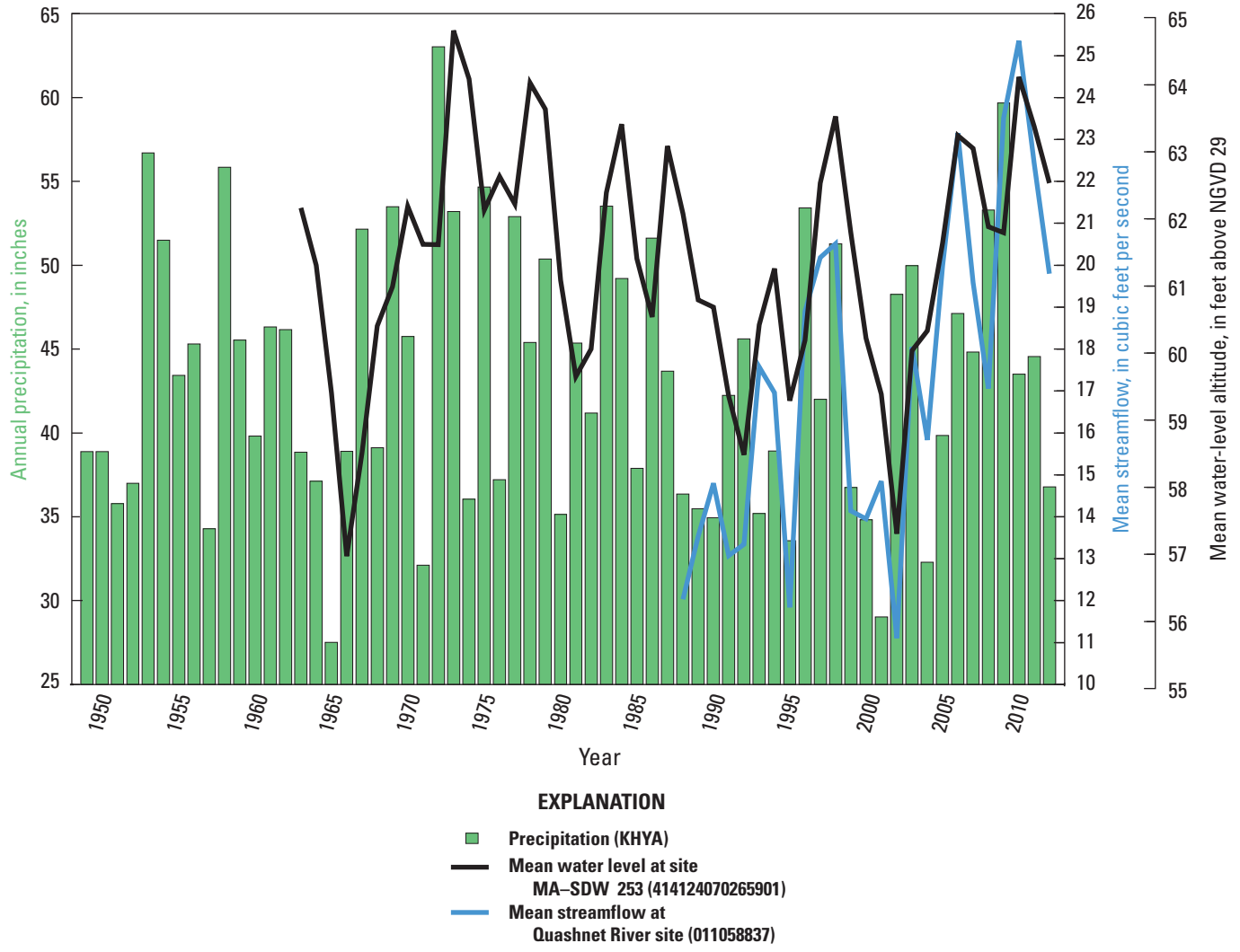

Figure 10. Precipitation from Hyannis weather station (Barnstable Municipal Airport [KHYA]) and hydrographs for a long-term well (MA–SDW 253) and continuous-record streamflow site (Quashnet River), 1949–2012, western Cape Cod, Massachusetts. Modified from Walter and others (2016). NGVD 29, National Geodetic Vertical Datum of 1929.

Climate and Land-Use Data

Cape Cod has a continental climate typified by warm, often humid summers and cold winters (Peel and others, 2007). The climate is moderated by the proximity to ocean waters, as compared to interior parts of the northeastern United States. Precipitation, which is the sole source of water to the Cape Cod aquifer system, generally is evenly dispersed throughout the year and declines slightly, on average, during the summer months. Precipitation at the NOAA weather station in Hyannis, Mass., on the eastern side of the study area, averaged 43.4 inches per year (in/yr) (figs. 8 and 10) between 1949 and 2012. About half of the precipitation recharges the aquifer at the water table; the remainder is lost to evapotranspiration. Natural recharge on Cape Cod has been estimated by using several methods, including groundwater model calibration, water balance approaches using various methods to estimate evapotranspiration, and age dating techniques (LeBlanc and others, 1986; Barlow and Hess, 1993; Solomon and others, 1995; Masterson and others, 1997b; Massey and others, 2006). These estimates, over varying timescales and locations, range greatly from 16.0 to 45.2 in/yr.

Aquifer recharge is a function of climatic conditions (precipitation, temperature) and landscape characteristics (vegetation, soil properties, land use), and variations in these factors affect the rates and distribution of recharge. The amount of precipitation and evapotranspiration and the ability of the soils to absorb and store water are important components in estimating recharge. The SWB model accounts for processes that occur as water moves through unsaturated soils and sediments to the water table and is based on a modified version of the Thornthwaite-Mather approach (Thornthwaite and Mather,

1957). The method incorporates land slope, soil properties, and climatic data, and it produces a spatially distributed recharge grid (Westenbroek and others, 2010). The computer code uses commonly available geographic information system (GIS) data layers in combination with tabular climatological data to produce gridded recharge data that can be imported into the groundwater models.

Tabular data compiled for this study include daily precipitation and temperature values at the Hyannis, Mass., weather station for the period between 1949 and 2012 (NOAA National Climatic Data Center, 2012). Distribution of land use for Cape Cod, as gridded GIS data, was accessed at the Massachusetts Office of Geographic Information (MassGIS) website (MassGIS, 2012b). The 2005 land-use data layer is classified into 13 descriptions for Cape Cod; the dominant land uses are residential and forested (fig. 11*A*). The U.S. Department of Agriculture (USDA) Natural Resources Conservation Service (NRCS) has classified hydrologic soil groups by the ability of water to enter and pass through the soil, an important characteristic of each soil group (USDA NRCS, 2012). These classifications range from high infiltration/low runoff (greater than 0.30 inch per hour [in/hr]) to very slow infiltration/high runoff (less than 0.05 in/hr). In the study area, the Buzzards Bay and Sandwich Moraines are classified as high infiltration/low runoff, whereas infiltration in the central part of the MPP is more moderate (fig. 11*B*). Industrialized areas and wetland areas have slow to very slow infiltration and high runoff rates. The SWB model also uses available water capacity, a measure of water held in soil that is available for use by plants (USDA, 1998), reported as inches of water per foot of soil thickness. The available water capacity on western Cape Cod, compiled as gridded data from the USDA NRCS, ranges from about 4 inches per foot of soil thickness in coastal wetlands to less than 1 inch per foot of soil thickness in forested parts of the Buzzards Bay Moraines. The SWB model, as applied in this study, calculates recharge as

$$\text{Recharge} = \textit{precip} - \textit{interception} - \textit{runoff} - \textit{actual evapotranspiration}\ (\textit{ET}), \quad (1)$$

where

precip is precipitation,

interception is amount of rainfall trapped and used by vegetation and evaporated or transpired from plant surfaces,

runoff is surface runoff calculated from NRCS curve number rainfall-runoff relation (Cronshey and others, 1986), and

actual ET is evaporation and plant transpiration.

The SWB model was used to estimate annual average conditions for the period between 1949 and 2012. Results of the simulations indicate the mean recharge rate throughout the study area is about 19.3 in/yr and varies from 0 in/yr over surface-water bodies and large impermeable surfaces (such as the JBCC runways) to more than 23 in/yr over the moraine areas and southern parts of the outwash plains (fig. 12). The SWB-estimated recharge values generally were lower than previous recharge estimates for the study area, although the SWB model provides spatial variability that can be scaled to expected mean values. Note that the recharge rate of 0 in/yr is a result of the SWB methodology and that the recharge rate into surface waters used in the analysis is 16 in/yr, generally representing the difference between precipitation and pan evaporation.

Lithologic Data

Lithologic data were compiled from various sources (fig. 13), including Federal and State agencies, water suppliers, drillers, landowners, and private consultants, for 973 boreholes (USGS, 2019; MassDEP, 2019; AFCEC, 2019; Army National Guard, 2019). Most of the boreholes were drilled as part of contaminant-plume remedial activities at the JBCC. Sediment samples were collected by using split spoon sampling with an auger rig, rotary air methods (Barber rig), and continuous coring with sonic techniques and were used to develop lithologic logs of the aquifer at each site. The quality and detail of the lithologic logs vary on the basis of the method of collection and the geologist interpreting the sediment samples. The unconsolidated glacial sediments on Cape Cod are underlain by crystalline bedrock that is substantially less permeable than the glacial sediments. The depth and morphology of the bedrock surface recently was mapped by using the boreholes in combination with measurements of bedrock depth obtained by using ambient-noise seismic techniques (Fairchild and others, 2013). The general eastern extent of this recently mapped surface is near the boundary between the MPP and the Barnstable Plain deposits; the bedrock surface to the east of this area was previously mapped by Stone (Bryon Stone, USGS, written commun., 1997) from boreholes and seismic methods. The two surfaces were merged together to create a seamless bedrock surface. In general, the undulating bedrock surface slopes downward from the northwest to the south-southeast. The altitude of the bedrock surface in the study area ranges from about 50 ft below NGVD 29 in the area of the Cape Cod Canal to about 525 ft below NGVD 29 on the easternmost boundary of the study area, underlying the Harwich Outwash Plain deposits (fig. 13).

The glacial sediments consist of moraine, ice-contact, lacustrine, and outwash deposits; the latter are broadly divided in three depositional units—topset, foreset, and bottomset beds—that generally fine with depth and with increasing distance to the south (Oldale, 1992; Masterson and others, 1997a). About half of the 973 boreholes used were drilled to bedrock. The distribution of grain size, as observed in the lithologic logs, generally reflects the depositional model. Most of the sediment samples were collected in the central part of the MPP and indicate fine to medium sands, with silty deposits observed in lenses of varying thickness. Basal and hanging silts with thicknesses greater than 5 ft were observed in about

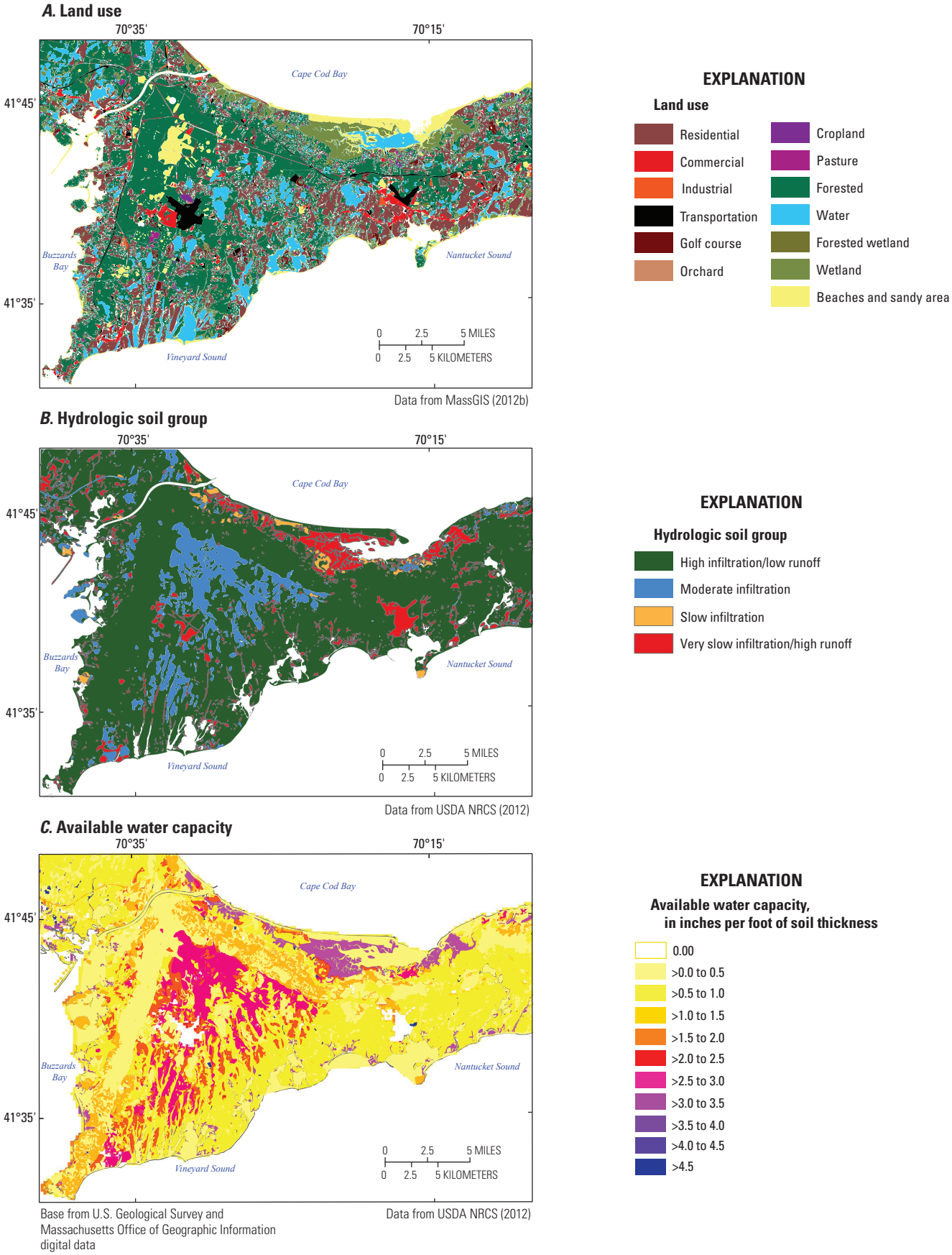

Figure 11. The distribution of Soil-Water-Balance model input variables, including *A*, land use, *B*, hydrologic soil group, and *C*, available water capacity, western Cape Cod, Massachusetts. MassGIS, Massachusetts Office of Geographic Information; USDA NRCS, U.S. Department of Agriculture Natural Resources Conservation Service.

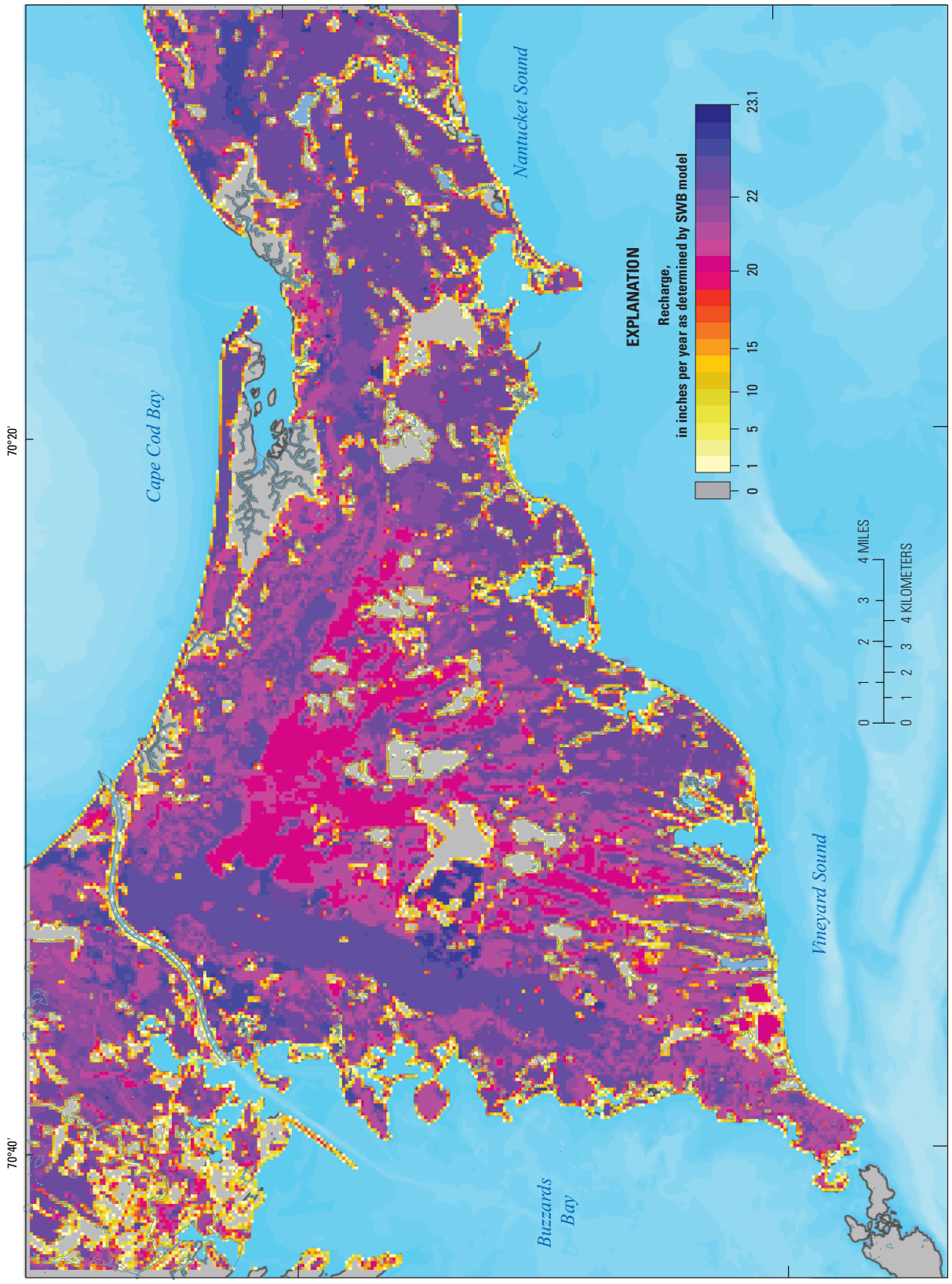

Figure 12. Estimated recharge from the Soil-Water-Balance (SWB) modeling approach for western Cape Cod, Massachusetts.

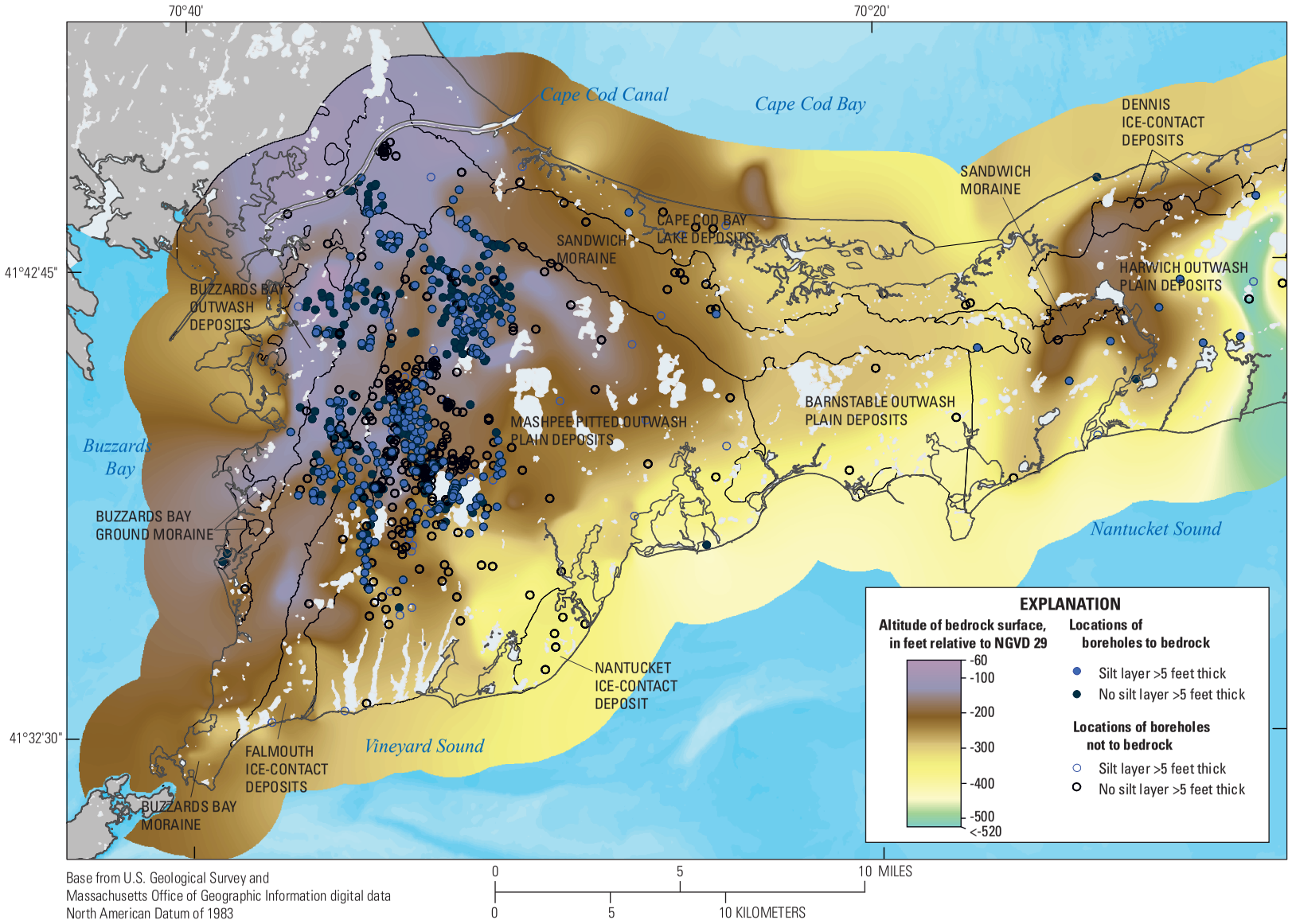

Figure 13. Bedrock surface, locations of deep boreholes, locations of silt layers greater than 5 feet thick, and surficial geologic units, western Cape Cod, Massachusetts. NGVD 29, National Geodetic Vertical Datum of 1929.

one-third of the boreholes. The presence of these finer grained sediments can affect flow patterns and contaminant transport through the aquifer, as discussed previously in the "Contaminant Transport" section.

Individual logs were processed by grouping the sediments into eight general lithologic categories—gravel, sand and gravel, coarse sand, medium sand, fine sand, silty sand, silt, and clay—to facilitate incorporation of the complex and variable lithologic data into a groundwater flow model. Sediment types were grouped by Unified Soil Classification System classes (American Society for Testing and Materials, 1985) where possible; each classified sediment type was assigned general horizontal and vertical hydraulic conductivity values, as described in figure 14, based on previous aquifer tests and values used previously in numerical models of the aquifer (Masterson and others, 1997b). Thickness-weighted hydraulic conductivity values were calculated within regular 10-ft layers extending from land surface (a maximum of 290 ft above NGVD 29) to bedrock (a minimum of −440 ft relative to NGVD 29) at each borehole. Horizontal hydraulic conductivities were calculated as arithmetic means over each 10-ft interval; vertical hydraulic conductivities were calculated as geometric means (fig. 14).

Kriging, a geostatistical method of interpolation, was used to interpolate hydraulic conductivities (horizontal and vertical) between point values representing individual logs for each 10-ft layer. Interpolated hydraulic conductivity fields were developed separately for each major surficial unit (Stone and DiGiacomo-Cohen, 2009). Ordinary kriging using an exponential model was used to predict unknown values on the basis of the given relation with neighboring known values (Oliver and Webster, 1990). Optimized kriging parameters—nugget, range, partial sill, lag size—were determined by using the ArcGIS Spatial Analyst extension (Esri, 2014). The process produced 600 variograms (75 vertical intervals and 8 surficial units) for horizontal and vertical conductivity fields (fig. 15). Each variogram relates a correlation distance and semivariance [$0.5 \times (\textit{mean difference})^2$] between two data points and predicts values for intermediate points. Kriged (predicted) values for each surficial unit within each horizontal, constant-thickness (10-ft) layer were merged into a continuous regular grid of hydraulic conductivity values for the entire model domain. As an example, the kriged field for an altitude between −40 and −50 ft (NGVD 29) is fairly uniform, with values ranging predominantly between 50 and 200 feet per day (ft/d; fig. 15). Individual data points dominate the kriging process in areas with limited data, such as regions with generally coarse sediments in the southern part of the Buzzards Bay outwash plain and moraine and regions with generally fine sediments to the east in the Barnstable and Harwich outwash plains. The kriged hydraulic conductivity values vary greatly in areas with denser data, such as the MPP. Kriging generally preserves the heterogeneity defined by closely spaced boreholes, but generally produces smoother hydraulic-conductivity fields in areas with sparser data.

The vertically stacked grids of hydraulic conductivity values, truncated by land surface and the bedrock surface, provided the initial rendering of aquifer hydraulic conductivities supported by the lithologic logs (fig. 16). Spatial patterns in the quasi-three-dimensional hydraulic conductivity field generally preserve major aspects of the deposition model of western Cape Cod (Masterson and others, 1997a). Coarse sediments (hydraulic conductivity of 200 to 325 ft/d) generally are prevalent above sea level (0 ft, NGVD 29), corresponding to the prevalence of fluvial outwash deposits. The western part of the MPP, including the JBCC, generally is underlain by fine sand and silt (less than 50 ft/d) that represent glaciolacustrine deposits.

Tracers of Advective Transport

Contaminant plumes and groundwater ages are indicators of long-term average hydraulic gradients and advective flow patterns, and data regarding contaminant distribution and groundwater ages were compiled and evaluated for use as steady-state calibration targets. Several plumes, migrating from source areas on the JBCC, have been delineated as part of ongoing remedial investigations. Sources of mapped contaminant plumes include a former landfill, a decommissioned wastewater-treatment facility, chemical and fuel spills, and sources related to range activities (fig. 2*B*). Each plume was rated as a calibration target on the basis of the existence of a known source area and the availability of a well-defined geochemical section orthogonal to regional hydraulic gradients with points adequate to define the plume boundary. Information pertaining to each plume and its delineation was obtained from remedial investigations and scientific reports by AFCEC, Army National Guard, and the USGS (AFCEC, 1996, 2000, 2001, 2003; Army National Guard, 2005, 2007a, 2010a, b; Barbaro and others, 2013). Plume delineations generally between about 1995 and 2005 were used to avoid the potential effects of current (2010) pump and treat systems on contaminant distributions.

Thirty-one pairs of sources and plume sections were selected from 15 contaminant plumes (fig. 17*A*) for use as steady-state calibration targets. The observation point in each plume section, generally representing the center of mass, is defined as the estimated center of the area of detection for the contaminant of concern. These were determined by inspection of transverse sections of chemical data and are, to a degree, subjective. The horizontal and vertical position did not correspond to the position of highest concentration at the time of sampling for most cases. As an example, the center point of contamination for section *A–A′* through the Demo-1 plume (figs. 17*A* and *B*) is about 200 ft to the north of and 20 ft deeper than the center of the contoured area of highest concentration (>18 parts per billion of perchlorate in 2005). This position in the aquifer represents a reasonable point of interception of water recharging the water table beneath the Demo-1 source area under long-term average conditions.

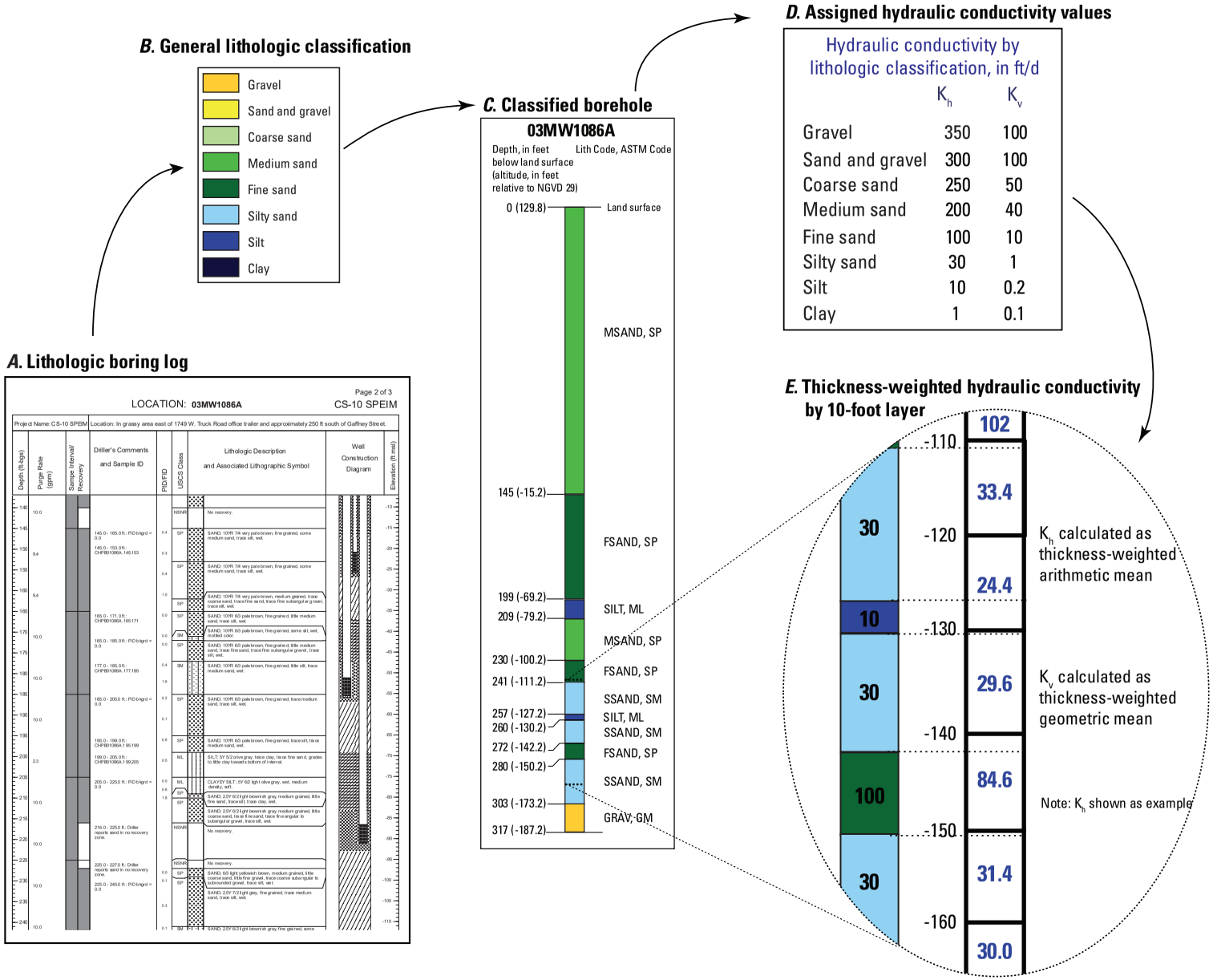

Figure 14. Schematic diagram illustrating lithologic data processing. NGVD 29, National Geodetic Vertical Datum of 1929. ASTM, American Society for Testing and Materials; ft/d, foot per day; K_h and K_v, horizontal and vertical hydraulic conductivity.

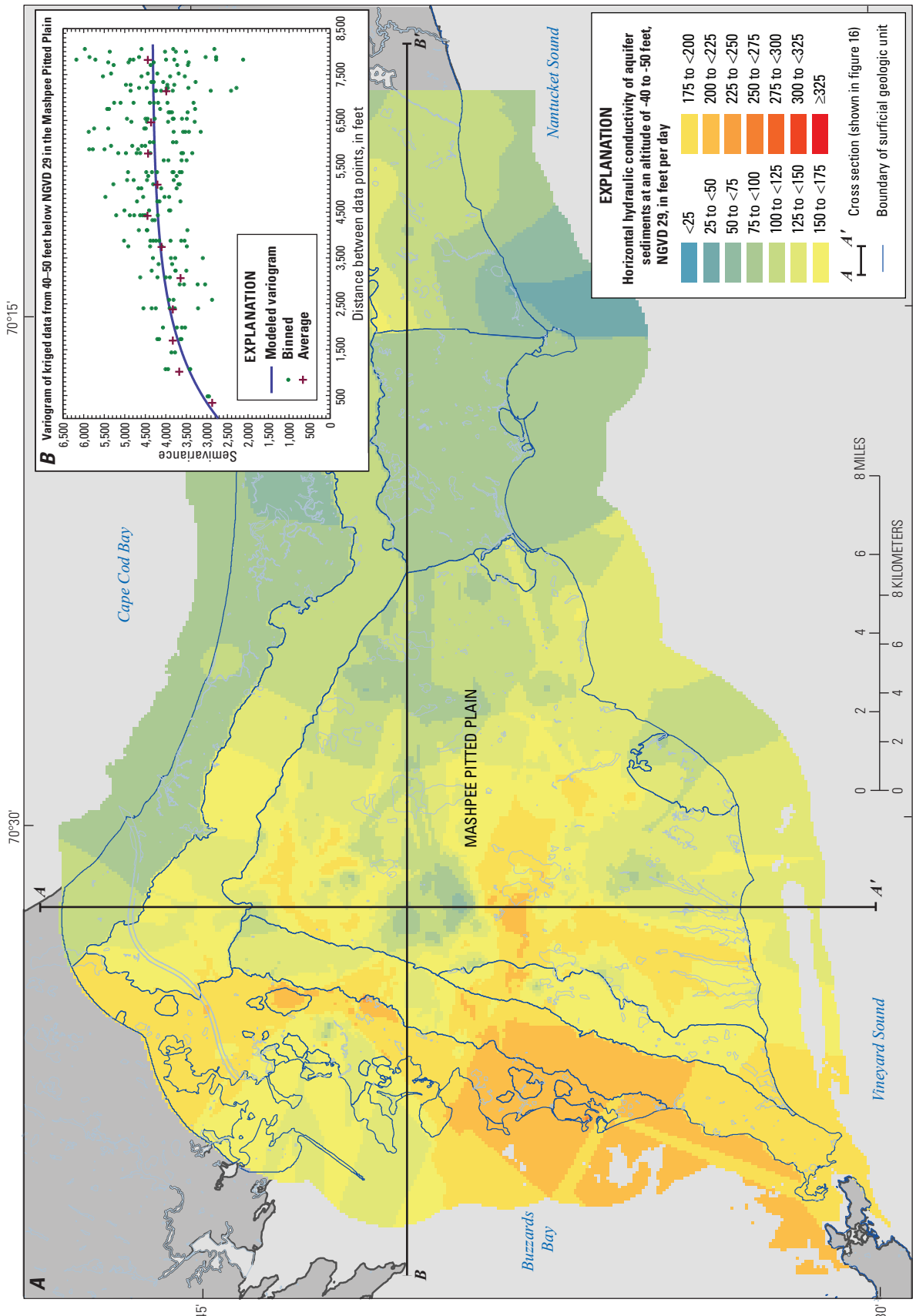

Figure 15. *A*, Distribution of horizontal hydraulic conductivity at an altitude between –40 and –50 feet as determined by kriging of lithologic data and *B*, variogram of corresponding data points in the Mashpee Pitted Plain, Cape Cod, Massachusetts. NGVD 29, National Geodetic Vertical Datum of 1929.

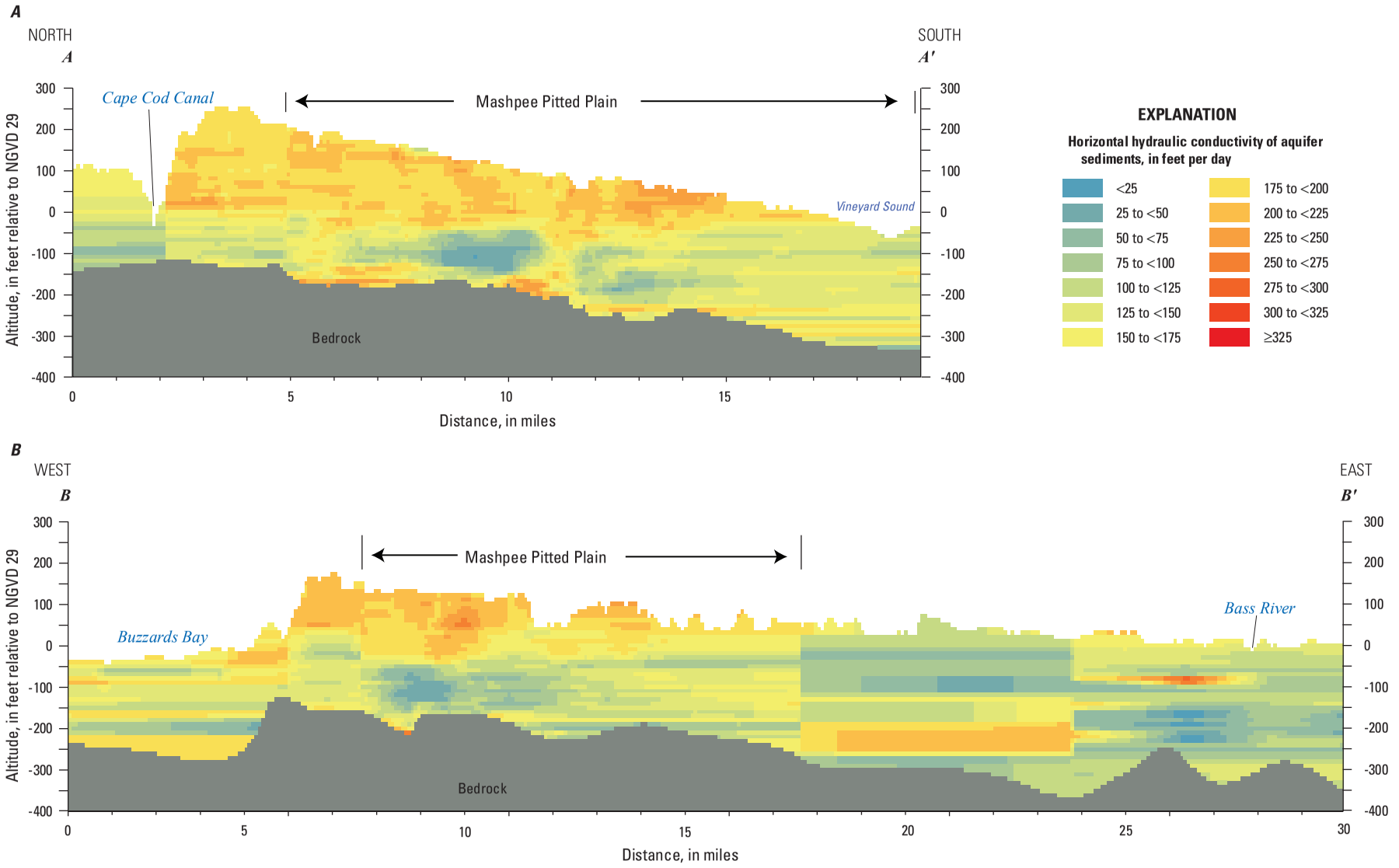

Figure 16. The distribution of horizontal hydraulic conductivity as determined by kriging of lithologic data, western Cape Cod, Massachusetts. *A*, north-south cross section *A*–*A*′. *B*, east-west cross section *B*–*B*′. Section locations are shown on figure 15. NGVD 29, National Geodetic Vertical Datum of 1929.

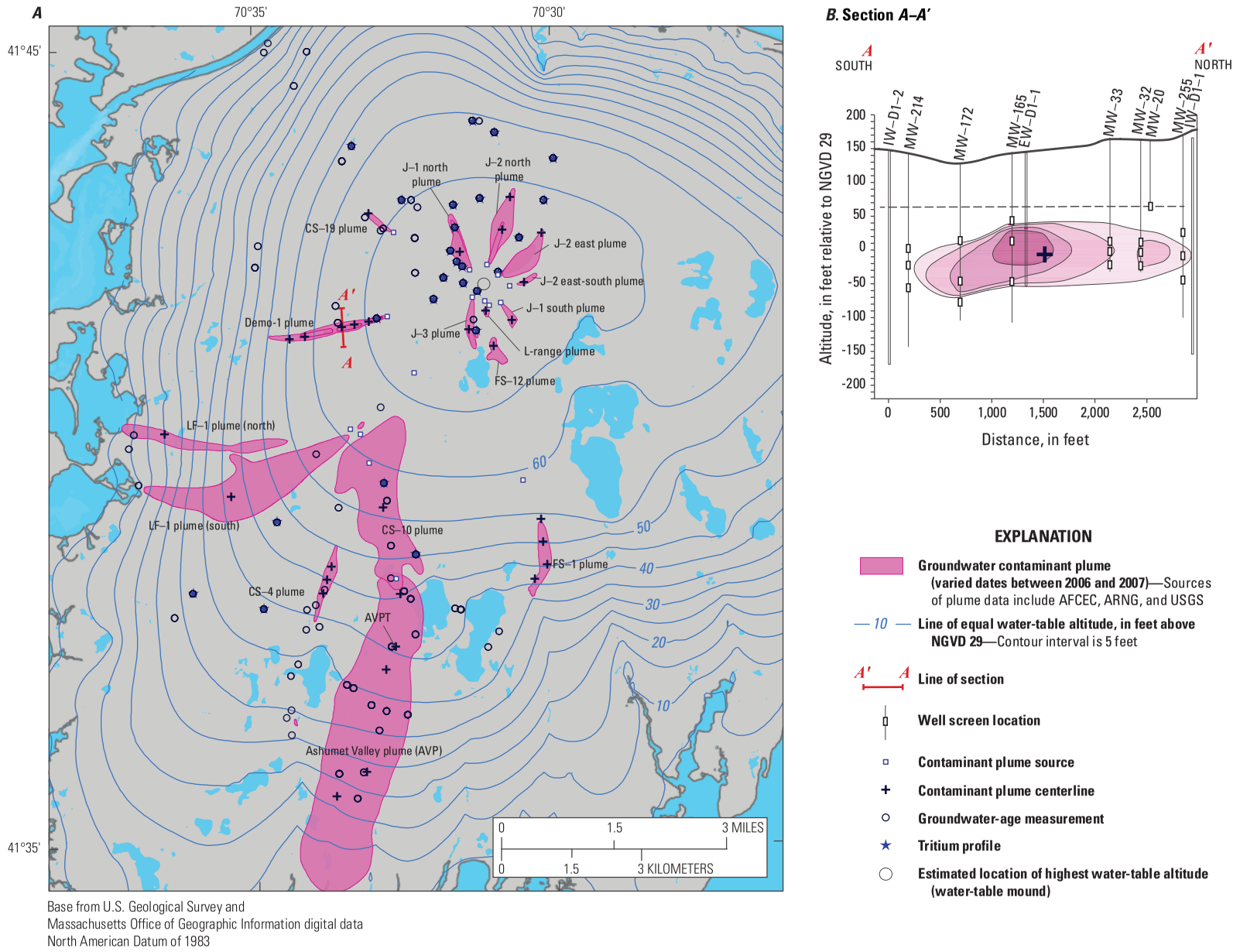

Base from U.S. Geological Survey and
Massachusetts Office of Geographic Information digital data
North American Datum of 1983

Figure 17. *A*, Selected Joint Base Cape Cod plumes, plume center points and observed source areas, the top of the water-table mound, and groundwater-age sampling sites and *B*, an example of a transverse section, western Cape Cod, Massachusetts (AFCEC, 1996, 2000, 2001, 2003; Army National Guard, 2005, 2007a, 2010a, b; Barbaro and others, 2013). AFCEC, Air Force Civil Engineer Center; ARNG, Army National Guard; AVPT, Ashumet Valley Plume calibration observation point; NGVD 29, National Geodetic Vertical Datum of 1929; USGS, U.S. Geological Survey.

Multiple observations along a presumed flow path emanating from the same source were determined for 6 of the 15 selected plumes. The choice of a position is, to a degree, subjective and based on a decision about the preferred location of a predicted particle path.

The age of groundwater recharged within the previous 50 years, as estimated from environmental tracers, yields insight into recharge rates and long-term hydraulic gradients and can provide steady-state calibration targets for groundwater flow models. Tracers applicable to young groundwater include tritium (^{3}H), helium-3 (^{3}He), and chlorofluorocarbons (CFCs). A total of 376 tritium samples were collected at 24 profile locations between August 1998 and October 2005, and 93 helium-3/tritium ratios (^{3}He/^{3}H) were determined from samples collected between June 1994 and July 2004. Fifteen samples were analyzed for CFCs (fig. 17*A*). The apparent ages and traveltimes derived from peak tritium concentrations generally indicate that groundwater age increases with depth in the system and that trends are linear near the water table and nonlinear with increasing depth. Variations in age gradients occur in discharge and recharge zones around kettle-hole ponds, near streams, and near the coast and in areas of hydrologic stresses, such as water-supply pumping and wastewater return flow. Apparent groundwater ages determined by both ^{3}He/^{3}H and CFC methods ranged between 0.1 and 41 years for samples collected at different vertical positions throughout the aquifer. Of the 108 measurements of apparent groundwater age, 91 were collected at a depth within 100 ft of the water table; of those, 39 were collected at a depth within 50 ft of the water table. Sixteen of the remaining 17 samples were collected in the deepest quarter of the saturated thickness.

Tritium measurements, in profile, provide the general altitude of water that entered the unsaturated zone during the period of highest atmospheric concentration, in about 1963 (Plummer and others, 1993). The traveltime associated with an individual tritium peak was calculated as the difference in time between 1963 and the sample date and then further reduced by an estimated traveltime through the unsaturated zone. Traveltime through the unsaturated zone is dependent on the unsaturated zone thickness, the moisture content, and the porosity of the sediments. The recharge location and unsaturated zone thickness were estimated by using the groundwater flow model by Walter and Whealan (2005). Estimated unsaturated zone traveltimes for the 24 Cape Cod samples ranged from 2.6 to 6.5 years. The altitude of the tritium peak in the 24 boreholes varied as much as 128 ft, with an average depth below the water table of 104.3 ft, reflecting the heterogeneous nature of the sediments and the local effects of fine sands and silt layers on hydraulic gradients. Information on tritium profile locations and concentrations are available in Walter and others (2019) and USGS (2019).

Groundwater-age dating refers to the dating of a chemical substance that is dissolved in the groundwater and not of the water itself (Plummer and others, 1993); different types of mixing models exist for dating groundwater. Apparent ages determined for samples on Cape Cod represent apparent piston-flow ages, and the simplifying assumption of a piston-flow model can cause difficulties where old and young waters are mixed. The representation of groundwater age by a single value and date does not account for these physical mixing processes (Varni and Carrera, 1998; Weissmann and others, 2002). Another consideration is that samples collected over screened intervals spanning from 2 to 10 ft in length could inherently result in mixing of sampled water in the screened zone, including possible mixing of old and young waters. These limitations and uncertainties need to be accounted for when comparing observed ages to simulated traveltimes.

Water Use

About 7 percent of water recharging the aquifer system of western Cape Cod is withdrawn for water supply (Walter and Whealan, 2005). Current (2010) groundwater withdrawals from public-supply wells and future withdrawals by town, based on projected demand, were compiled as part of a National Resources Damage Assessment project investigating water availability on western Cape Cod (Upper Cape Regional Water Supply Cooperative, 2015). The source of the data was the Massachusetts Department of Conservation and Recreation. Currently (2010), about 19.7 Mgal/d of water is withdrawn from the aquifer from 85 wells (fig. 18*A*). The largest withdrawal is from Long Pond in Falmouth, the region's only surface-water withdrawal. The largest groundwater withdrawals by town are in Barnstable, to the east of the JBCC; the largest withdrawal near the JBCC, by town, is in Falmouth (fig. 19). Projections of future (2030) water-supply demand indicate about a 6.5 Mgal/d (or about a 31 percent) increase for the Sagamore flow lens (fig. 1) between 2010 and 2030; the smallest and largest increases are about 13 and 56 percent in Yarmouth and Mashpee, respectively (fig. 19). Currently (2010), about 0.5 Mgal/d, or about 2 percent of the total withdrawal, is withdrawn by about 1,730 private wells in the Sagamore flow lens. The total volume of water withdrawn from private wells is less than 5 percent in all of the towns neighboring the JBCC, and generally the pumped water is returned to the aquifer on site so that effects on the hydrologic system are negligible. The three Upper Cape Cooperative wells (fig. 18*A*) are an auxiliary source of water to the four towns surrounding the JBCC (Bourne, Falmouth, Mashpee, and Sandwich) and were installed to offset any possible damage to the region's water resources. About 1.3 Mgal/d of water was pumped from the wells in 2010; however, no projections for future pumping are available. It is assumed that future pumping rates from the wells will be proportional to overall regional demand, as defined by the 2030 projections for the four towns.

About 85 percent of pumped water is returned to the aquifer as wastewater return flow. The distribution of return flow is determined from parcel-scale water-use data (Thomas Cambareri, Cape Cod Commission, written commun., 2012). The dataset was assembled from water-use data and tax assessor maps as part of the MEP; water use for each individual

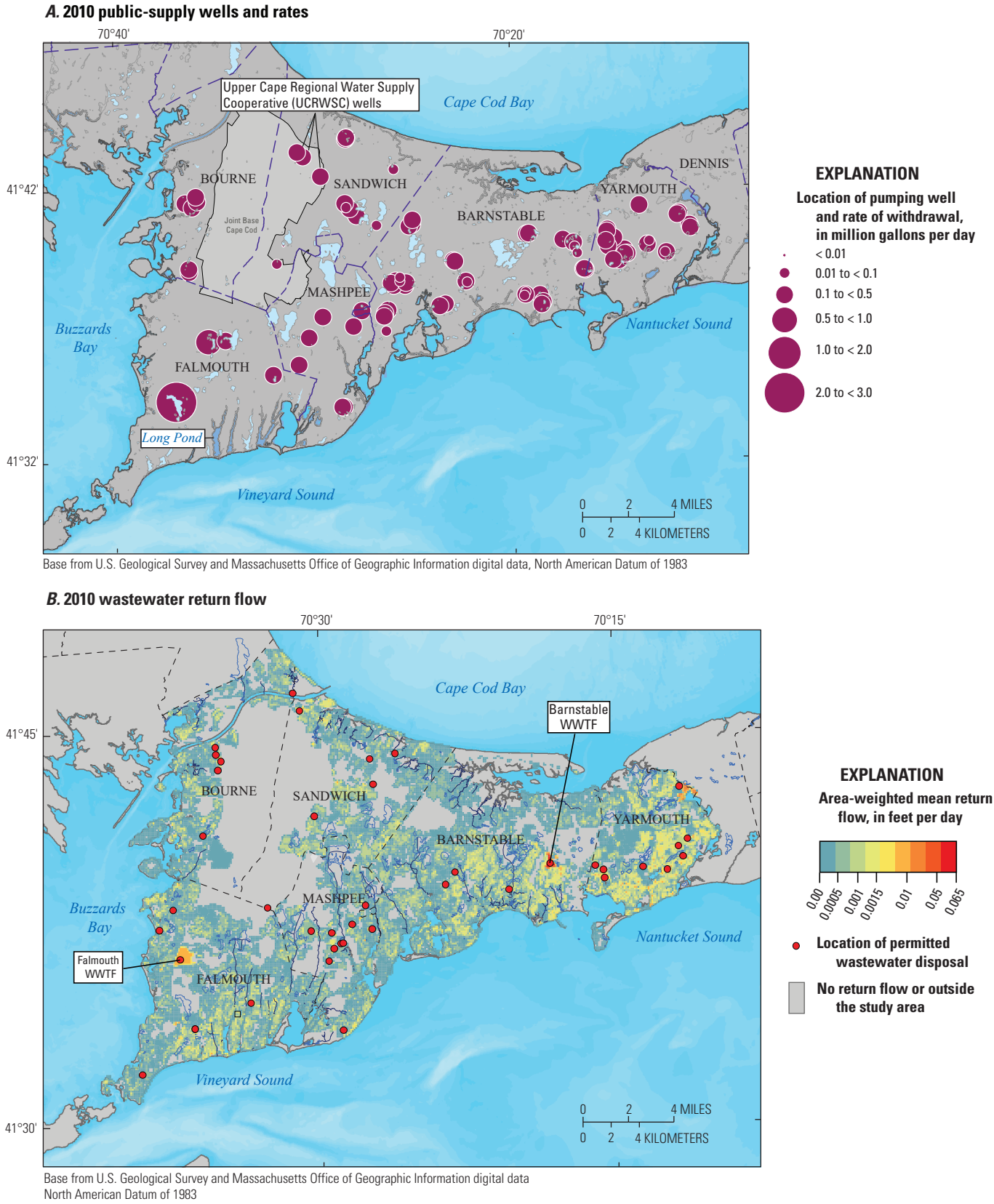

Figure 18. *A*, Public-supply wells with 2010 pumping rates and, *B*, 2010 wastewater return flow, western Cape Cod, Massachusetts. WWTF, Wastewater-treatment facility.

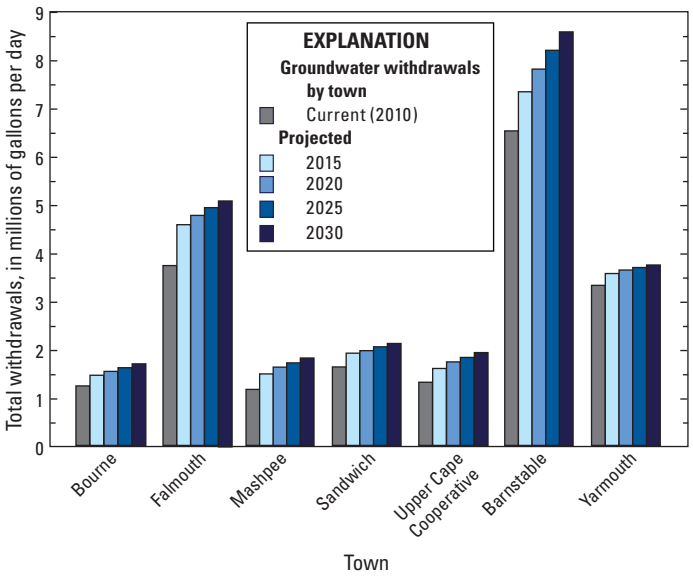

Figure 19. Pumping from public-supply wells for 2010 and projected for 2015–30, by town, western Cape Cod, Massachusetts.

parcel is used by the MEP to estimate nitrogen loads to estuaries and was previously used by the USGS in the simulation of nitrogen transport in the aquifer (Walter, 2013). The rate of return flow is a function of residential housing density and is largest in populated areas of Barnstable, Yarmouth, and Falmouth (fig. 18*B*). Wastewater also is returned to the aquifer at 41 WWTFs on the Sagamore flow lens. The largest WWTF is in Barnstable, where about 1.7 Mgal/d of treated wastewater is discharged into the aquifer (fig. 18*B*). The largest WWTF near the JBCC is in Falmouth; about 0.45 Mgal/d of wastewater was discharged at the site in 2010.

Numerical Model Development

A steady-state numerical groundwater flow model of the Sagamore flow lens was developed that incorporates the large amount of diverse data collected as part of remedial investigations at the JBCC. The model was designed to allow for an analysis of the effects of anthropogenic stresses—pumping and return flow—on water levels, streamflows, and hydraulic gradients and to evaluate, if needed, the potential effect on future water supplies of residual contamination remaining in the aquifer following contaminant remediation at the site. In the development of the model, the finite-difference modeling program MODFLOW–2005 (Harbaugh, 2005) was used to simulate the aquifer system of the Sagamore flow lens. Finite-difference models represent an aquifer system as discrete, interconnected blocks (or cells) of aquifer with intrinsic properties and boundary conditions representing surface-water features, wells, or recharge. The model output includes, for each model cell, head in the cell and flow terms between the cell and all neighboring cells. This information can be used to evaluate the effects of changing stresses on water levels, streamflows, and hydraulic gradients and, when used with the particle-tracking program MODPATH (Pollock, 1994), can represent the advective transport of conservative solutes in an aquifer.

The model design incorporates data collected in and around the JBCC as part of remedial investigations and ongoing USGS investigations into the hydrology of western Cape Cod. Lithologic logs were used to develop initial hydraulic conductivity fields. Measurements of bedrock altitudes (described in the "Lithologic Data" section) and modeling of the freshwater/saltwater interface were used to refine the geometry of the aquifer system. A highly parameterized calibration approach, wherein gradational hydraulic fields can be estimated by using pilot points (Doherty, 2003), was used to calibrate the model to a diverse set of observations, including water levels, streamflows, groundwater ages, and advective-transport observations from mapped contaminant plumes on the JBCC.

Input and output files for the regional groundwater flow model are available in a USGS data release (Walter and others, 2019).

Numerical Model Design

Two numerical models were used in this analysis: (1) an existing two-dimensional (one layer) model (referred to here as the "freshwater/saltwater (FW/SW) interface model") capable of simulating the position of the freshwater/saltwater interface on western and central Cape Cod and (2) a new steady-state, three-dimensional (32 layers) model (referred to here as the "JBCC regional model") that incorporates the simulated interface position and is capable of representing hydrologic conditions on the Sagamore flow lens and advective transport in and near the JBCC. The FW/SW interface model was used to define the subsurface extent of the aquifer as simulated in the JBCC regional model. Regional models have been previously developed for several coastal aquifers in southeastern Massachusetts, including separate models of the Sagamore and Monomoy flow lenses on Cape Cod (Walter and Whealan, 2005), a single model of the four other Cape Cod flow lenses (Lower Cape Cod aquifer) (Masterson, 2004), and a model of the Plymouth-Carver aquifer on the mainland adjacent to Cape Cod (Masterson and others, 2009) (fig. 20). The extents of the models used in this analysis include parts of all four existing regional models, and those models provide information relevant to development of the steady-state, three-dimensional JBCC regional model, including aquifer properties, reasonable approximations of current water-table altitudes, and the geometry of hydrologic boundaries.

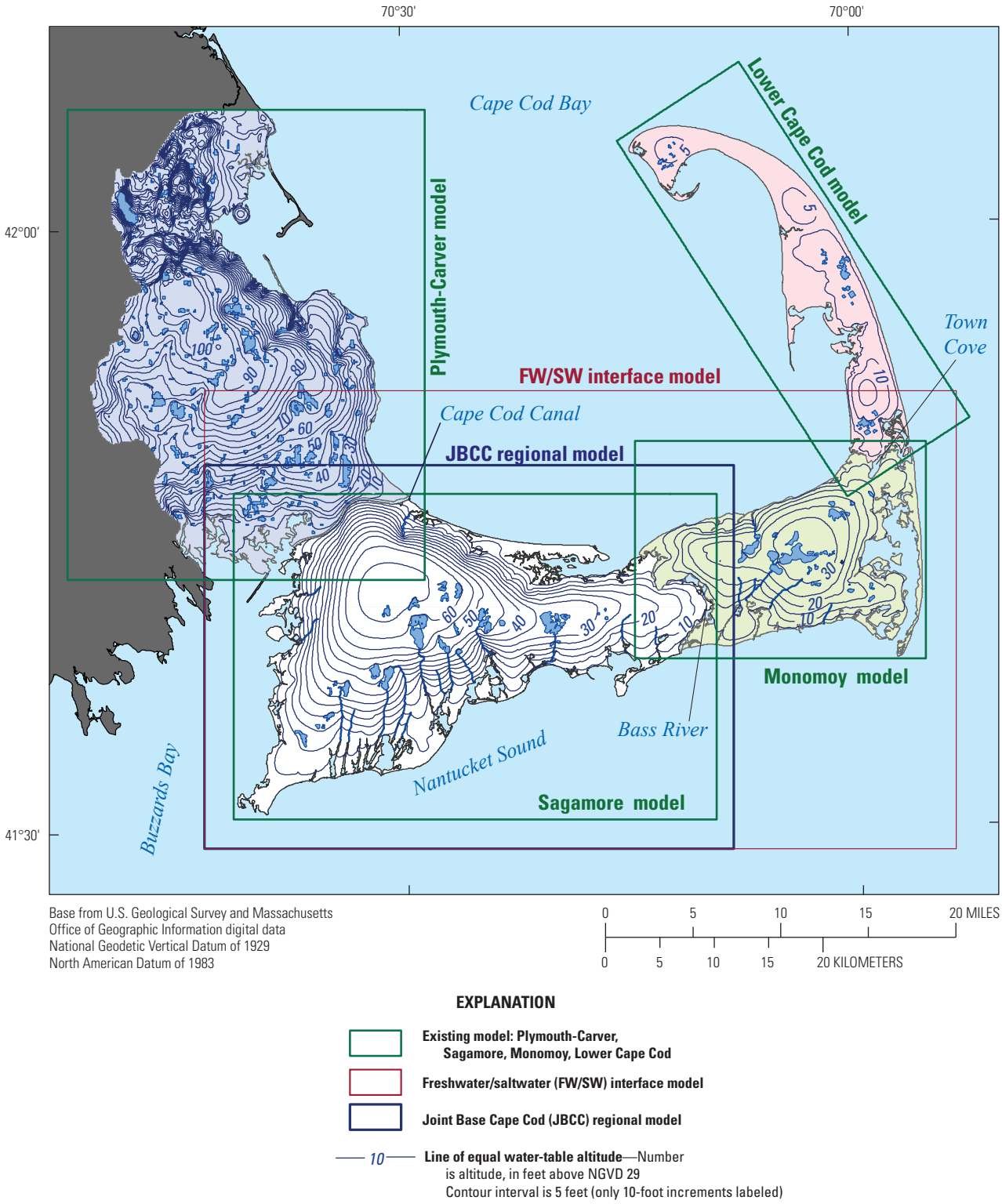

Figure 20. Previously developed regional models of southeastern Massachusetts (Plymouth-Carver to Lower Cape) and extents of the existing two-dimensional freshwater/saltwater (FW/SW) interface model and newly developed three-dimensional Joint Base Cape Cod (JBCC) regional model grids, southeastern Massachusetts. Modified from Walter and others (2016). NGVD 29, National Geodetic Vertical Datum of 1929.

Simulation of the Freshwater/Saltwater Interface

Most groundwater in the Cape Cod aquifer system discharges to estuaries and coastal waters, and the groundwater system is bounded laterally by a dynamic freshwater/saltwater interface. The position of the interface represents a balance between fresh groundwater flow and denser saltwater that is, in part, a function of leakances at coastal boundaries. The position of the interface could affect the distribution of groundwater discharge and regional hydraulic gradients and may affect the advective transport of contaminants from sources on the JBCC to coastal discharge locations. The most recent models of the Sagamore and Monomoy flow lenses assume an arbitrarily assigned steep, offshore interface (Walter and Whealan, 2005). The freshwater/saltwater interface was simulated by use of the existing two-dimensional FW/SW interface model developed as part of an investigation of the potential effects of sea-level rise on the Cape Cod aquifer system (Walter and others, 2016). The FW/SW interface model incorporates both the Sagamore and Monomoy flow lenses and extends beyond the Cape Cod Canal to the west and beyond Town Cove to the east; these two coastal waters are the western and eastern extents of the combined aquifer system (fig. 20). The model grid consists of one layer, 1,384 rows, and 2,272 columns, with a uniform horizontal discretization of 100 ft. Hydraulic conductivity and recharge were derived from the four existing calibrated regional models, parts of which are encompassed by the FW/SW interface model. The hydraulic conductivities of cells in the model are equivalent to the thickness-averaged hydraulic conductivities of the corresponding layers in the existing three-dimensional regional models, resulting in an equivalent transmissivity. Recharge, pumping, and return-flow stresses also were derived from values in the corresponding calibrated regional models (Walter and others, 2016).

The bottom of the FW/SW interface model is a continuous bedrock surface interpolated from data collected near the JBCC (Fairchild and others, 2013) and, to the east, a bedrock surface previously used in regional models of the Sagamore and Monomoy flow lenses (Walter and Whealan, 2005). The top of the model is land surface derived from 10-meter digital elevation model data. The finer horizontal discretization of the FW/SW interface model (100 ft as compared to 400 ft for the existing regional models) allows for a more detailed representation of freshwater and saltwater surface-water boundaries (fig. 21). Estuaries, coastal waters, and streams are represented as head-dependent flux boundaries: estuaries and coastal waters by use of the General Head Boundary package; and streams, salt marshes, and surface-drained wetlands by use of the Drain package (McDonald and Harbaugh, 1988).

Coastal-water boundaries were extended seaward well beyond the likely discharge of freshwater so that the position of the freshwater/saltwater interface and the seaward extent of freshwater discharge could be determined numerically. The position of the freshwater/saltwater interface was calculated by using the SWI2 package (Bakker and others, 2013). The software program calculates transient interface positions between two or more aqueous solutions with different densities by solving continuity of flow equations for each fluid along the interface; the numerical solution of a vertical interface position is coupled with the solution of the groundwater flow equation by MODFLOW for each time step. The freshwater/saltwater interface on Cape Cod is assumed on the basis of observed profiles to be sharp (LeBlanc and others, 1986); therefore, two solution densities were specified—freshwater and saltwater—and one interface position was calculated. Salty groundwater is assumed to have a density of 1.025 grams per cubic centimeter; the initial interface position was determined from simulated water-table altitudes by using a simple Ghyben-Herzberg relation, in which the depth to salty groundwater below sea level (0 ft, NGVD 29) is assumed to be 40 times the water-table altitude. The total simulation time was 100 years: 36,500 time steps with a uniform length of one day. A detailed discussion of the model and the use of SWI2 to simulate the interface position are presented in Bakker and others (2013).

Fresh groundwater is underlain by bedrock in most areas of western Cape Cod (fig. 22) owing to the high recharge rates, shallow bedrock (−100 to −300 ft), and high water-table altitudes (>60 ft). Fresh groundwater is underlain by salty groundwater in some areas near the coast, particularly along the shore of Nantucket Sound where the complex coastal morphology and the discharge of groundwater into several streams results in the presence of salty groundwater as much as 3 miles inland from the coast (fig. 21). Fresh groundwater extends to bedrock in most areas of central and western Cape Cod with regional interfaces near Cape Cod Bay, Buzzards Bay, Nantucket Sound, and the Atlantic Ocean (figs. 22*A*–*C*) and local interfaces near some estuaries, such as the Bass River (fig. 21) and Waquoit Bay (fig. 22*B*). The freshwater aquifer is underlain by bedrock beneath all of the JBCC (fig. 21).

The position of the interface is sensitive to leakances at coastal boundaries, which is a parameter that is not well known and can be difficult to estimate during model calibration. The interface would be shallower and extend farther inland if leakances at the coastal boundaries were higher because groundwater discharge in coastal areas would be higher. The sensitivity of the interface position to coastal leakance was determined over a large range of coastal leakances (two orders of magnitude: 0.2–20 ft/d), representing values generally corresponding to silty and sandy end members. Observed interface positions at 17 locations (fig. 21) were assembled from historical data (LeBlanc and others, 1986), data from previous water-supply reconnaissance (Sandwich Water Department, written commun., 2006), and data collected as part of ongoing USGS activities near the JBCC (Denis LeBlanc, USGS, written commun., 2013) and used to determine the simulated interface position that best matched observed positions. The results show that low leakances tend to predict an interface position deeper than the observed depth, and high leakances predict a shallower-than-observed interface position (fig. 23). The mean depth (expressed as an altitude) residual ranged from −34.6 ft (indicating an overprediction of depth) for a leakance of 0.2 ft/d to 51.3 ft (indicating an

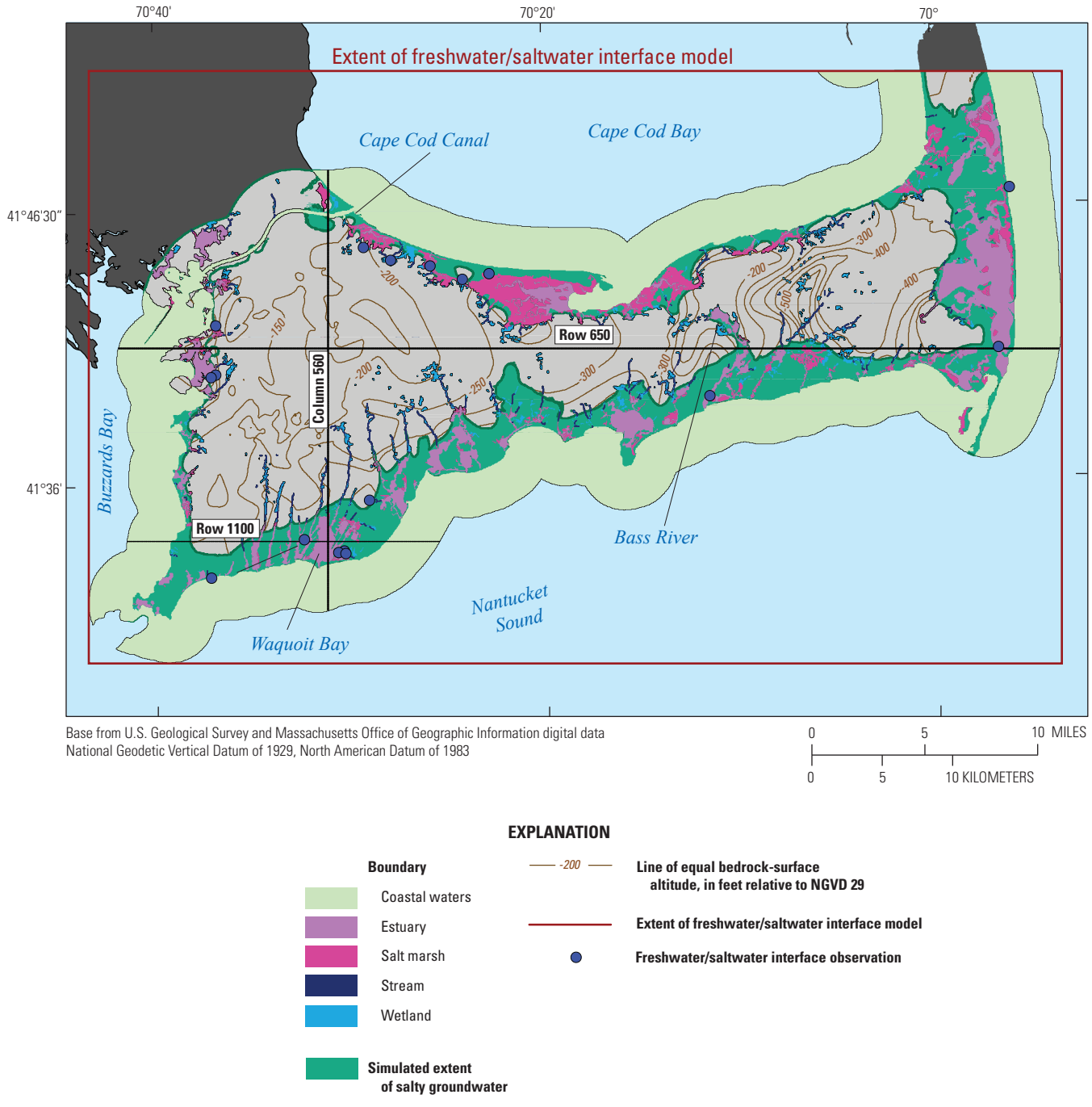

Figure 21. Hydrologic boundaries for the freshwater/saltwater interface model, bedrock altitudes, locations of observed interface positions, and the landward extent of salty groundwater, Cape Cod, Massachusetts. Modified from Walter and others (2016). NGVD 29, National Geodetic Vertical Datum of 1929.

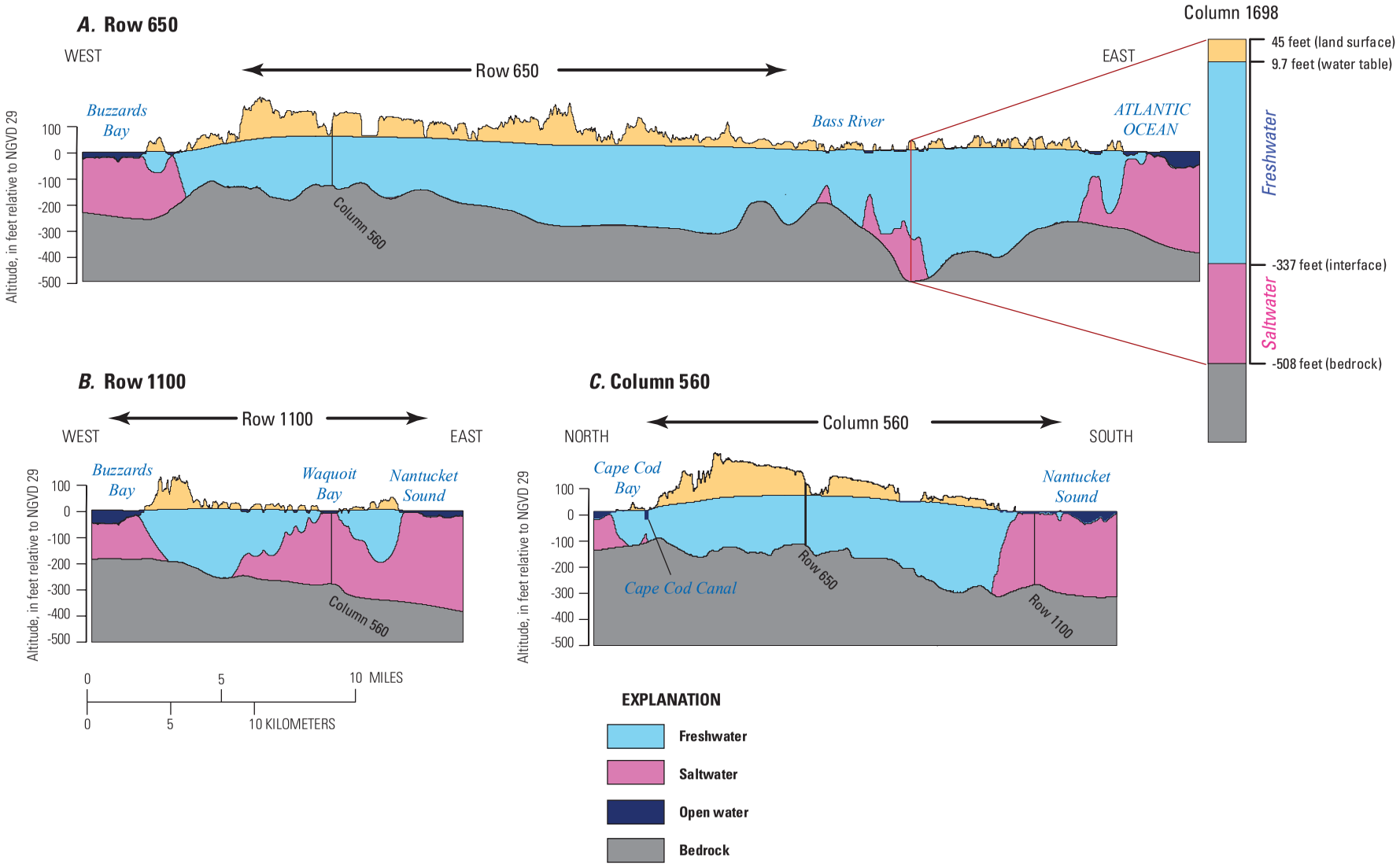

Figure 22. Location of the freshwater/saltwater interface position along, *A* and *B*, east-west and *C*, north-south cross sections, Cape Cod, Massachusetts. Modified from Walter and others (2016). Section locations are shown on figure 21. NGVD 29, National Geodetic Vertical Datum of 1929.

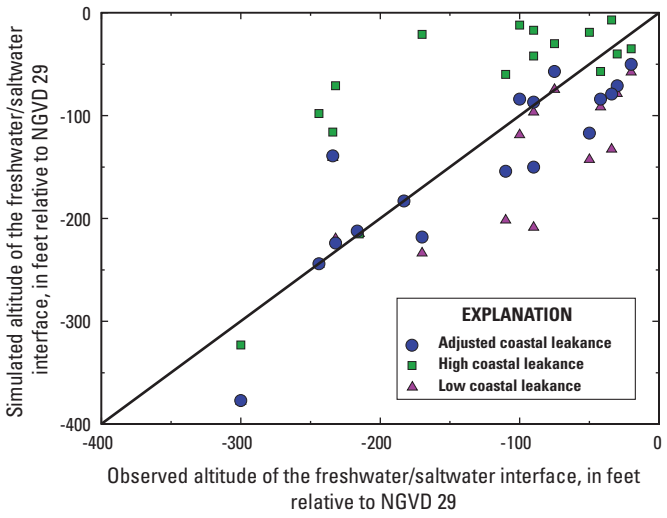

Figure 23. Differences between simulated and observed freshwater/saltwater interface positions at 17 selected locations for a range of coastal leakances, Cape Cod, Massachusetts. NGVD 29, National Geodetic Vertical Datum of 1929.

underprediction of depth) for a leakance of 20 ft/d. The lowest mean residual was −18.2 ft for a simulated leakance of 0.4 ft/d, which is consistent with the silty sediments observed in many estuaries. It is assumed that the interface position reasonably matches field observations, although this analysis represents a trial-and-error approach and not a true best-fit calibration. Note that the interface has a simple monotonic shape (fig. 22) and that local inversions, such as might be caused by local-scale heterogeneities, could not be included in this analysis because the aquifer is simulated as a single layer. However, it also is assumed that these local conditions, if they exist, do not appreciably affect the advective transport of contaminants farther inland near the JBCC.

Model Grid and Hydraulic Boundaries

The new three-dimensional model of the Sagamore flow lens (the JBCC regional model), with an emphasis on the area in and around the JBCC, uses MODFLOW–2005 (Harbaugh, 2005) to simulate the groundwater flow system. The finite-differences grid extends to the northwest of the Cape Cod Canal and to the east of the Bass River (figs. 20, 22*A*) and consists of 290 rows and 400 columns with a uniform horizontal discretization of 400 ft. The grid is coincident with the grids of existing regional models of the Sagamore and Monomoy flow lenses and the FW/SW interface model (fig. 20). There are 51,521 active cells in the top layer of the model (out of a total of 116,000) (fig. 24*A*).

The model has 32 layers of varying thicknesses and bottom altitudes. The top of the model is a surface derived from simulated heads extracted from existing regional models of the Sagamore and Monomoy models on Cape Cod and the Plymouth-Carver aquifer (fig. 20) and the altitude of land-surface or bathymetry at surface-water boundaries (fig. 24*A*). The bottom of layer 1 in each cell was initially specified to have an altitude of 10 ft less than the top of the model (fig. 24*B*). The use of both simulated heads and land surface or bathymetry can lead to offset layers in areas with steep hydraulic gradients near surface-water bodies. A smoothing algorithm was used to minimize large changes in model layer altitudes near surface-water bodies, whereby cell bottoms were iteratively lowered until there was at least a 50-percent overlap vertically between all neighboring cells. The bottom of layers 2 through 25 were then equally divided between the adjusted bottom of layer 1 and an altitude of −200 ft (NGVD 29). Layers 26 through 30 were equally subdivided between −200 and −300 ft (NGVD 29) with a constant thickness of 20 ft. Layers 31 and 32 were assigned bottom altitudes of −370 and −450 ft, respectively. Following definition of layer bottoms, the active model grid was truncated from below by a composite surface representing the top of bedrock and the position of the freshwater/saltwater interface (fig. 24*B*). Cells in layer 1 with thicknesses of less than 5 ft following truncation by the freshwater/saltwater interface were specified as inactive to remove stranded offshore cells. The average thicknesses of the top 25 layers, after truncation, were less than 10 ft; layers 26 through 30 had average thicknesses between 16 and 18 ft; and layers 31 and 32 had average thicknesses of 27 and 14 ft respectively. Active cells below layer 1 ranged from 50,558 in layer 2 to 331 in layer 32, which is truncated by bedrock throughout the Sagamore flow lens.

Surface-water features are represented as head-dependent flux boundaries. The locations of these features were determined by using aerial photos and digitized hydrography. Coastal water bodies, including estuaries and open coastal waters, are represented by using the General Head Boundary package (McDonald and Harbaugh, 1988); salt marshes and fresh surface waters, which include streams, wetlands connected to streams, and pond outlets, are represented by using the Drain package (fig. 24*A*). Boundary altitudes in saltwater boundaries were determined by using freshwater-equivalent heads determined from bathymetry data and, where available, tidal altitudes obtained from the MEP (2019). The locations and types of hydraulic boundaries were determined by using 30-cm-resolution aerial photos obtained from MassGIS (2012a). Boundary altitudes in fresh surface waters were estimated from 10-meter digital elevation model data (MassGIS, 2012b); the estimated altitude of the surface-water boundary is the top of the model. Ponds, which are hydraulically important in the Cape Cod aquifer system, are represented as areas with an essentially infinite horizontal and vertical hydraulic conductivity of 100,000 and 10,000 ft/d, respectively. This method allows the ponds to respond to changes in hydraulic stresses and reasonably creates the hydraulic gradients observed upgradient and downgradient from ponds, which are flow-through features. Some ponds drain through surface-water outlets to streams. These pond outlets are represented as drains within the pond that have an essentially infinite leakance term and an altitude corresponding to the pond-surface

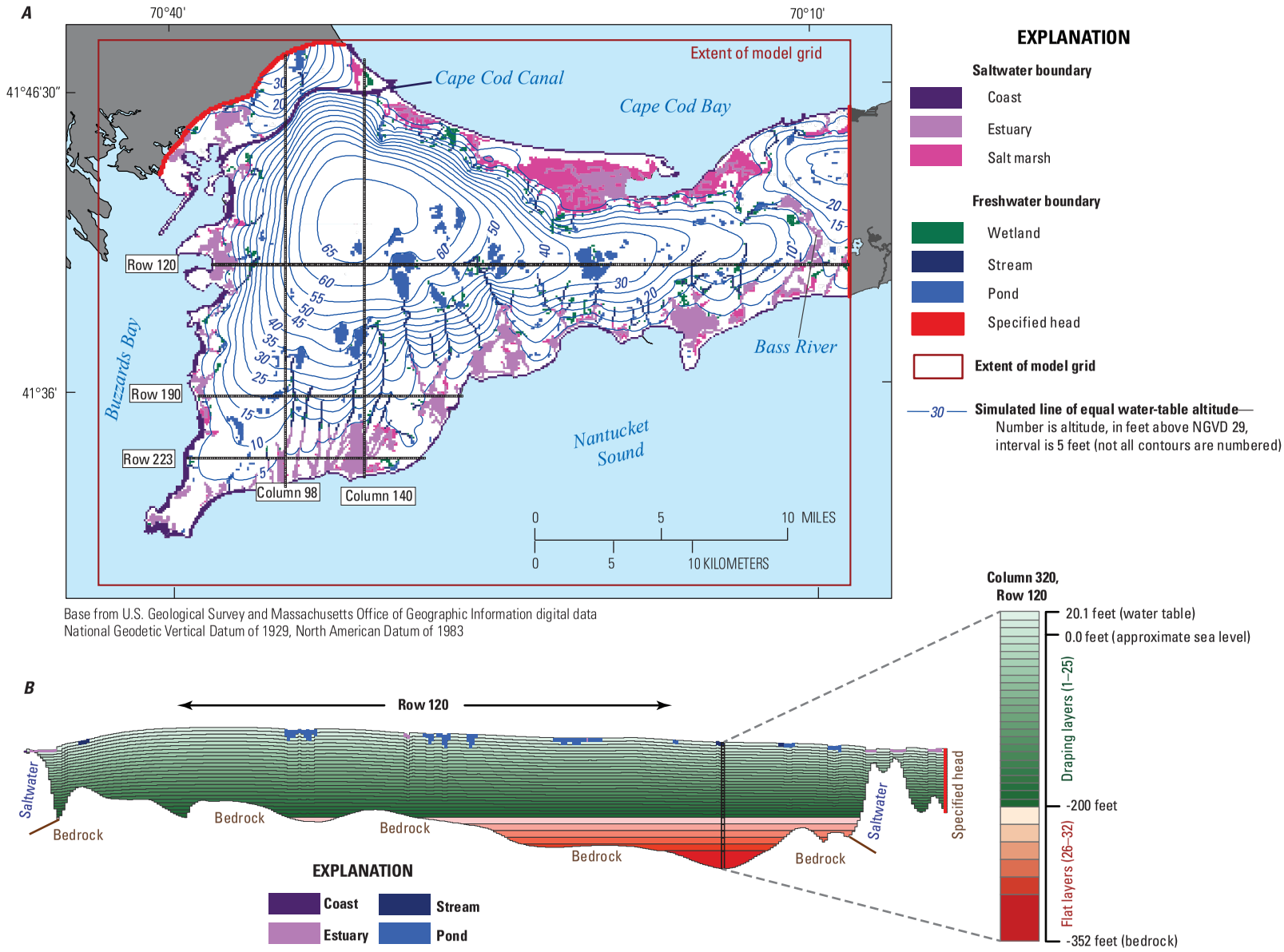

Figure 24. *A*, The Joint Base Cape Cod (JBCC) regional model grid with hydraulic boundaries and simulated water table from previously developed models of southeastern Massachusetts and *B*, east-west section showing vertical layering of regional model grid. NGVD 29, National Geodetic Vertical Datum of 1929.

altitude. This method effectively allows flow to change with changing pond levels and can simulate the cessation of flow during drought conditions (Walter and Whealan, 2005). Note that little is known about many pond outlets, which generally are man-made features, and some are managed to control water levels or to flood cranberry bogs.

Aquifer Properties

Hydraulic conductivity was estimated from lithologic logs for a series of 75 stacked grids from land surface to the bedrock surface, each with a uniform bottom altitude and thickness of 10 ft. Most lithologic logs were collected as part of remedial investigations at the JBCC; these logs generally are based on continuous split-spoon and sonic-rig cores. Some logs, such as those collected as part of water-supply development, are based on driller's logs and may provide less detail than those based on core samples. As discussed in the "Lithologic Data" section, kriging was used to interpolate hydraulic conductivity fields for each 10-ft layer from individual logs. Separate kriged hydraulic conductivity fields were developed for major surficial units recently mapped for the Pocasset, Falmouth, Sandwich, Cotuit, Hyannis, and Dennis USGS Quadrangles (Stone and DiGiacomo-Cohen, 2009); the separate data fields were merged into a single gridded hydraulic conductivity field coincident with the finite-difference model grid.

Model layers 1 through 25 had similar thicknesses (about 10 ft), as the hydraulic conductivity data grids and the horizontal grids of hydraulic conductivity were mapped to the vertically deformed model grid by assigning to each model cell the hydraulic conductivity value from the hydraulic conductivity data grid with the altitude nearest to that of the center of the model cell. Model layers 26 through 30 were thicker and could include two or more data grids; the model cell was assigned the thickness-weighted mean of the values from individual data layers within each model layer. The mapped hydraulic conductivity values at cells containing a pilot-point parameter were used to determine the initial values of those parameters. The highest horizontal hydraulic conductivity values (greater than 200 ft/d) in layer 7, which corresponds to an altitude of about −35 ft (NGVD 29), generally occur in the southern and central parts of the JBCC (figs. 1, 25*A*): a similar trend was seen in the kriged data (fig. 15). Horizontal hydraulic conductivity in layer 7 ranges from about 30 to about 225 ft/d, whereas vertical hydraulic conductivity ranges from about 1 to about 50 ft/d (fig. 25*B*). Pond bathymetry is used to determine those model cells that represent ponds, which are simulated as areas with an essentially infinite horizontal and vertical hydraulic conductivity of 100,000 and 10,000 ft/d, respectively.

The hydraulic conductivity values (horizontal and vertical) for the 32 model layers, excluding pond cells, were further simplified by averaging values for individual model layers within four vertical groups: layers 1–4, layers 5–9, layers 10–21, and layers 22–32 (fig. 26). This simplification was necessary to facilitate a highly parameterized calibration approach that uses pilot points. Horizontal and vertical hydraulic conductivities generally decrease with depth (figs. 26*A* and *B*). Horizontal hydraulic conductivity in the model decreases from about 300 ft/d in the top vertical group to about 10 ft in the lowest group and vertical hydraulic conductivity from about 70 ft/d near the top of the aquifer to about 1 ft/d at depth. This pattern in hydraulic conductivity, analogous to spatial trends in grain size, is consistent with the general depositional model of western Cape Cod (Masterson and others, 1997a).

Hydraulic Stresses

Areal recharge from precipitation is the sole source of water to the Cape Cod aquifer system; about half of the precipitation recharges the aquifer (LeBlanc and others, 1986). Recharge is represented as a specified-flux boundary at the water table by use of the Recharge package (McDonald and Harbaugh, 1988). The spatial variability of recharge on western Cape Cod, as a function of land use and soil characteristics, was calculated by using the SWB model (fig. 12). The resultant mean value of 19.3 in/yr likely is lower than actual rates based on observations of streamflow, water levels, and plume transport and on previous modeling of this and other aquifer systems in southern New England (Masterson and others, 1997b; DeSimone and others, 2002; Walter and Whealan, 2005; Masterson and others, 2007). Natural recharge onto aquifer sediments is represented as a single parameter value applied to an array of multipliers that represent the spatial variability of natural recharge (fig. 27*A*); this approach can both represent recharge rates that likely are more reasonable (higher) for the Cape Cod system and preserve the predicted spatial variability arising from land-use and soil characteristics. Multipliers were determined by normalizing the recharge predicted from SWB in each cell to the mean of all aquifer cells in the top model layer. Multipliers range from about 0.1 to about 1.3 (fig. 27*B*) and have a mean value of 1.

Groundwater withdrawals from public-supply wells and Long Pond, the region's only surface-water drinking-water source, are represented as specified flux boundaries in the model cell containing the well by use of the Well package (McDonald and Harbaugh, 1988). Annually averaged rates are simulated; one regional model cell contains more than one well, in which case all pumping rates within the cell are summed and simulated as a single withdrawal at the center of the model cell. The 85 wells (fig. 28*A*) were represented in 84 cells within the regional model. Current (2010) pumping rates were obtained from data collected as part of the National Resources Damage Assessment project discussed in the "Water Use" section. Future (2030) pumping rates were estimated from projected demand increases (fig. 19) for each town by distributing the total increase within a town to individual wells on the basis of their proportion of the town's total pumping in 2010.

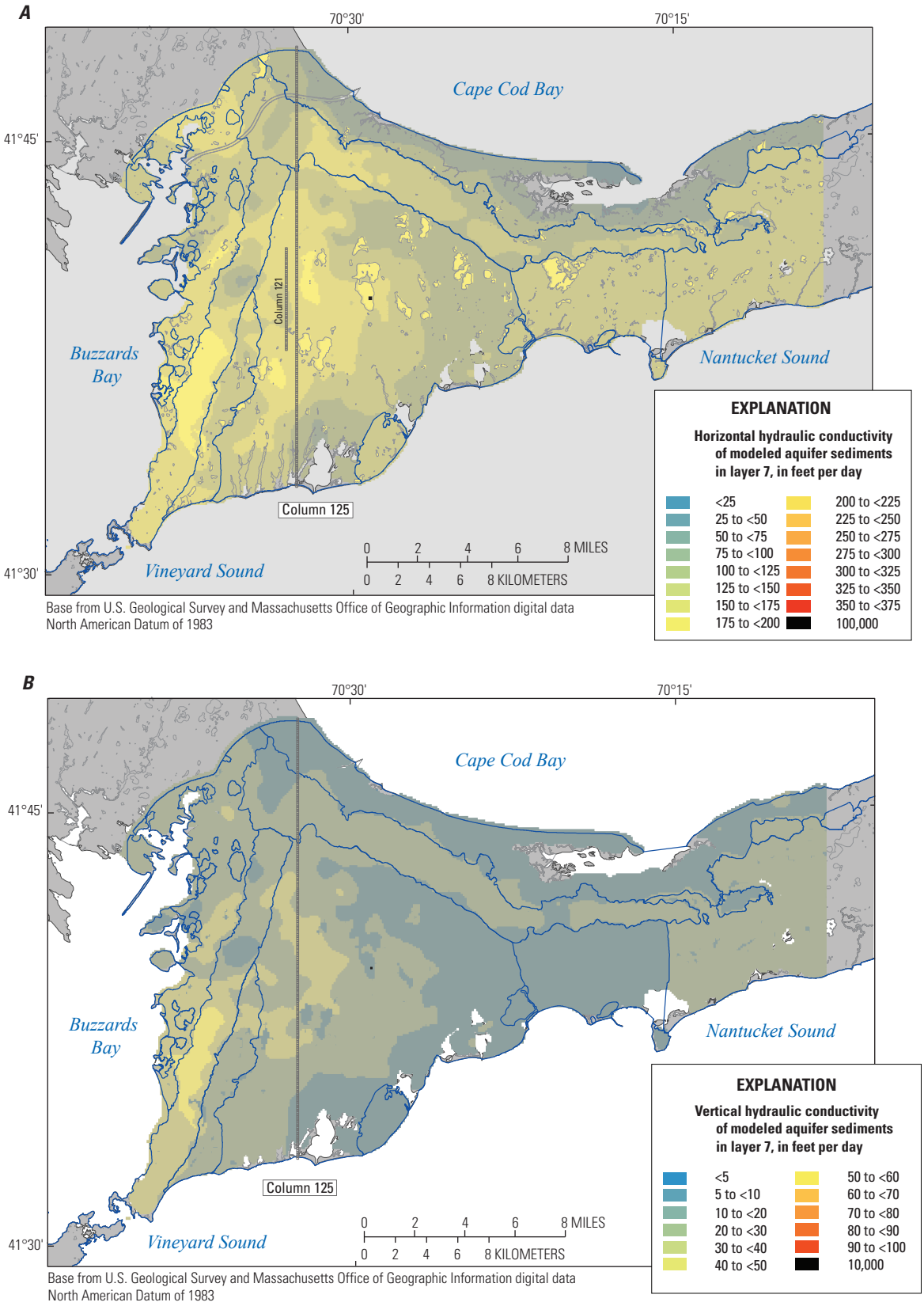

Figure 25. Distribution of initial *A*, horizontal and *B*, vertical hydraulic conductivity fields for layer 7 of the regional groundwater flow model, western Cape Cod, Massachusetts. The altitude of layer 7 is about –35 ft (National Geodetic Vertical Datum of 1929).

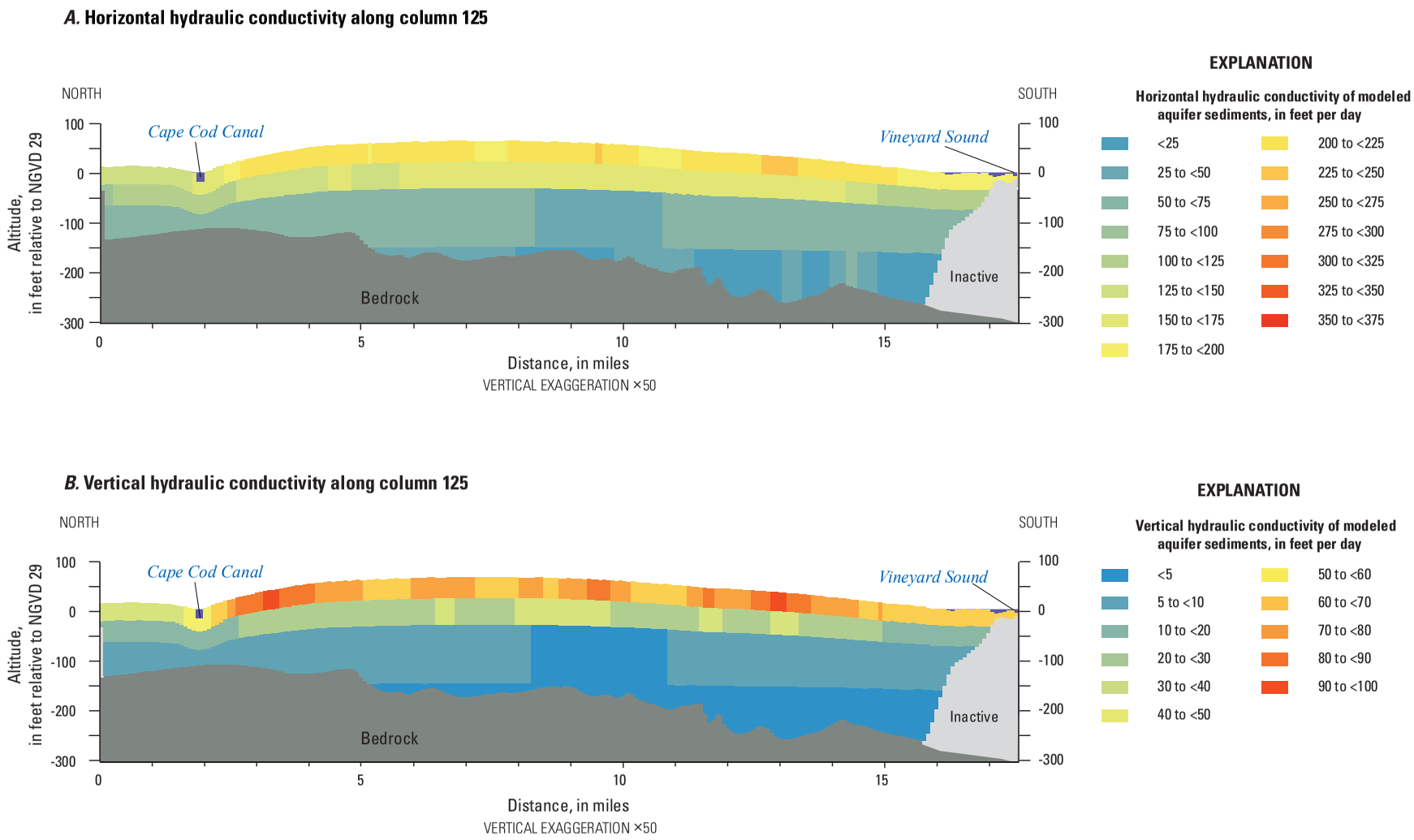

Figure 26. Initial modeled *A*, horizontal and *B*, vertical hydraulic conductivity in four vertical groups of individual model layers (layers 1–4, layers 5–9, layers 10–21, and layers 22–32) along a north-south section through the Mashpee Pitted Plain, western Cape Cod, Massachusetts. Section location is shown on figure 25. NGVD 29, National Geodetic Vertical Datum of 1929.

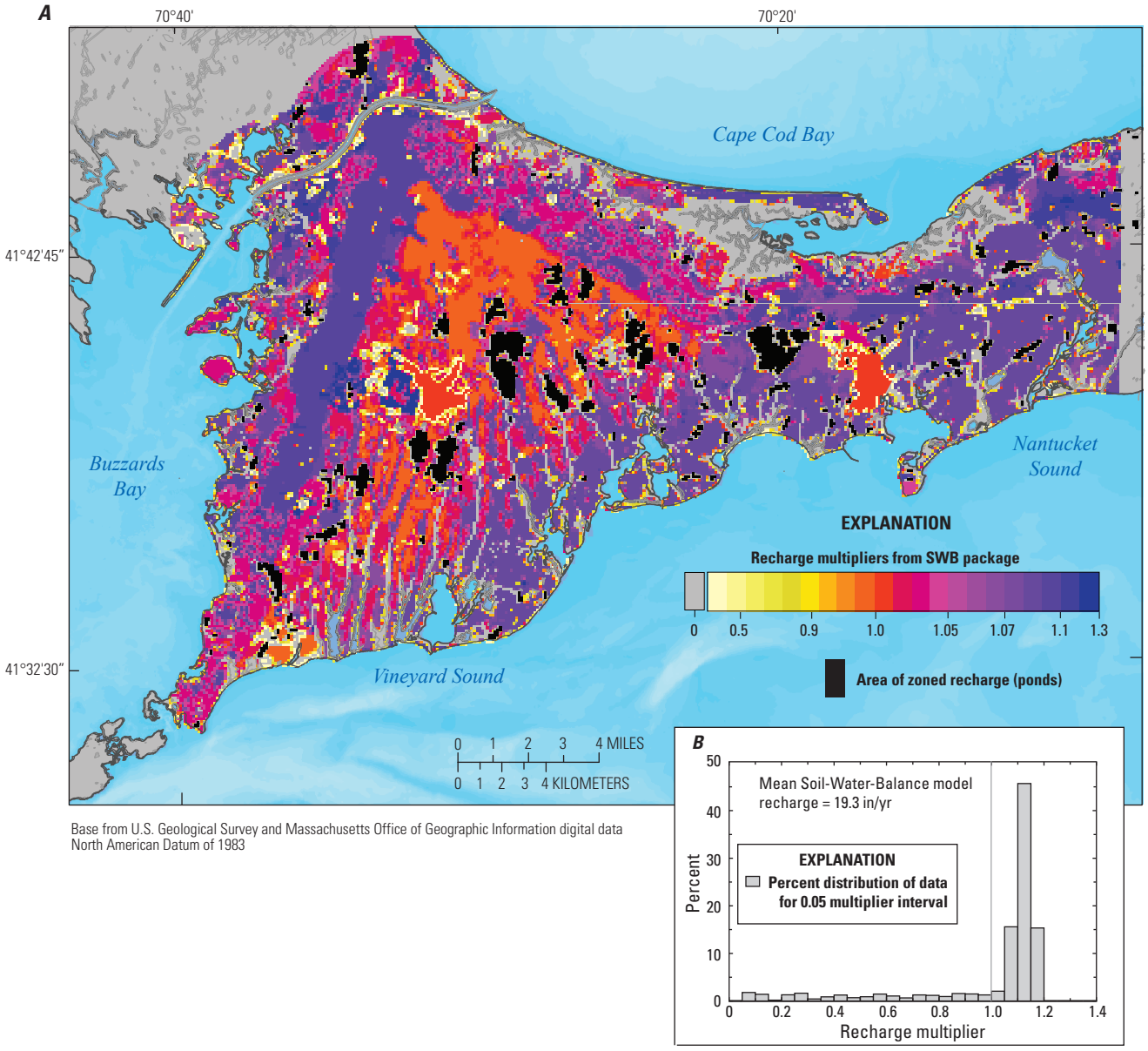

Figure 27. *A*, Modeled recharge multipliers for western Cape Cod, Massachusetts, and *B*, a histogram of multiplier values. in/yr, inch per year; SWB, Soil-Water-Balance.

Wastewater return flows at the 41 current (2010) wastewater-disposal locations (operating WWTFs) (fig. 28*A*) were simulated as areas of enhanced recharge by uniformly distributing the volumetric rate of flow over the total area of regional model cells that encompass the disposal infrastructure. Future (2030) wastewater return flow was determined by increasing flow proportionally to the projected increases in water demand for each town (fig. 19). Wastewater disposal at onsite septic systems is the largest component of wastewater return flow in most areas of Cape Cod, and detailed data are available on the distribution of this return flow from parcel-scale water-use data (MEP, 2019; Walter, 2013). A GIS was used to convert the spatial distribution of water use, after removing 15 percent to consumptive loss, into a form suitable for input as return flow into the groundwater model. The process consists of three steps: (1) converting the vector data to a data raster coincident with the model grid, (2) calculating the area-weighted mean return flow within each raster cell, and (3) mapping the rasterized data to the model grid so values are in model coordinates (fig. 28*C*). A data raster, as used in this report, refers to the spatial representation of vector data as values in a continuous grid of square cells. The result is a raster of area-weighted mean return-flow rates that is coincident with the model grid (fig. 28*A*). The area-weighted mean for each raster cell is overlaid onto the model grid and, along with model cells representing return flow at wastewater-disposal locations, converted into model coordinates for input into the model as areas of enhanced recharge by using the Recharge Package (McDonald and Harbaugh, 1988).

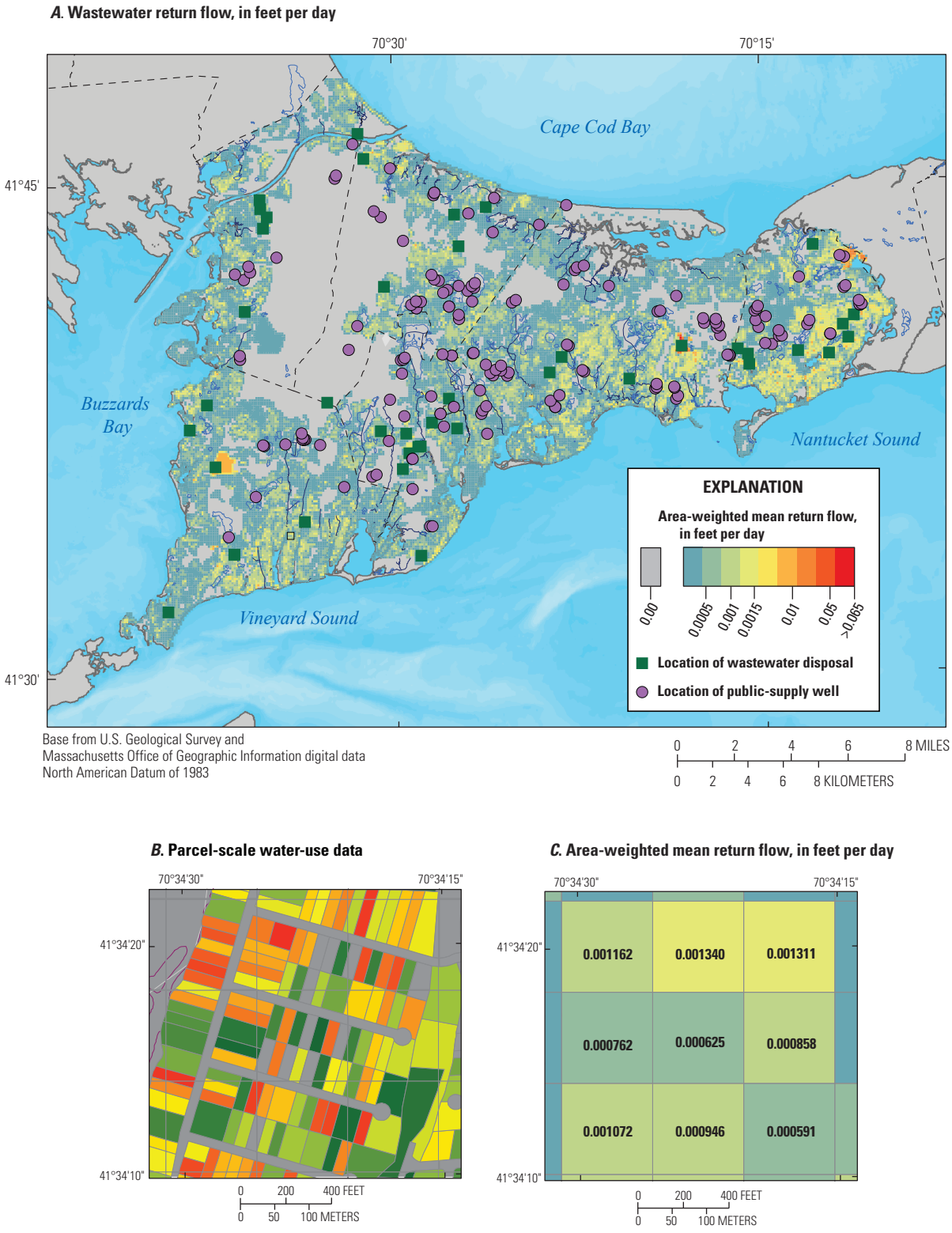

Figure 28. *A*, Public-supply wells, wastewater-disposal locations, and calculated wastewater return flow, western Cape Cod, Massachusetts, with inset of area of detail showing *B*, parcel-scale water-use vector data and *C*, area-weighted mean return flow raster data. Wastewater return flow calculated from parcel-scale water-use data and wastewater treatment facility discharge, rasterized to model grid.

Model Calibration

The JBCC regional model (fig. 20) was calibrated by adjusting model input parameters to match observed water levels, streamflows, indicators of advective transport, and hydraulic gradients. Previous models of the region used a trial-and-error approach whereby parameters were manually adjusted until an acceptable fit to observed data was achieved (Masterson and Barlow, 1997; Masterson and others, 1997b; Walter and Whealan, 2005). This approach can be used to produce calibrated models that reasonably match observed hydrologic conditions; however, the resulting parameters are highly nonunique, and the match to observed conditions does not represent a statistical best fit. Inverse-calibration methods, as used in this analysis, use nonlinear regression to estimate parameters that best fit observed hydrologic conditions and were previously used on the Sagamore flow lens to improve model calibration (Walter and LeBlanc, 2008).

Inverse-calibration methods determine the model parameters that best fit a given set of observations by using an iterative form of Gauss-Levenberg-Marquardt nonlinear regression to minimize an objective function (Levenberg, 1944; Marquardt, 1963). The objective function formulates the weighted fit between observations and simulated equivalents and can include prior information on aquifer characteristics. Two sets of tasks are required to utilize inverse methods in model calibration: (1) the definition of model parameters that can be adjusted between regression iterations and (2) the conversion of observations to a form for which simulated equivalents can be computed from the model. In this analysis, the inverse-modeling software package PEST (Doherty, 2010) was used to calibrate the JBCC regional model of the Sagamore flow lens. The software package allows for the use of highly parameterized model inputs and has a large degree of flexibility in defining observations as derived quantities.

The calibration period generally is consistent with hydrologic data, pumping stresses, and return flow for the period 1995–2000; this period generally predates the initiation of large-scale plume remediation at the JBCC. The use of the 1995–2000 hydraulic stresses was determined to be consistent with stresses under which the contaminant plumes developed. Therefore, the inclusion of highly weighted plume observations for calibration to advective-transport patterns made it necessary to use hydraulic stresses for the period 1995–2000. Note that the pumping rates used for model calibration differ from stresses used in the analysis of the effects of pumping on hydraulic gradients and advective transport in the aquifer, which use current (2010) and projected (2030) pumping rates described in the "Water Use" section. The pumping and return-flow stresses, which are the same as those used in a previous calibration of a regional model of western Cape Cod, were determined from average rates for the period 1995–2000 (Walter and Whealan, 2005). Pumping by town was similar for those stresses and current (2010) stresses compiled as part of this effort. One important difference is the operation of the Upper Cape Cooperative wells in the northern part of the JBCC since 2003 (fig. 2); 1.3 Mgal/d of water was withdrawn from the wells in 2010. The wells are near the top of the water-table divide where gradients generally are small, and pumping of the wells affects water levels and hydraulic gradients in the northern part of the JBCC (Walter and Whealan, 2005).

Model Parameterization

The model inputs were expressed as parameters for use in the inverse calibration to observed hydrologic conditions. A total of 4,568 parameters were used to represent model inputs. Three types of model parameters were included in the inverse calibration: recharge, boundary leakances, and hydraulic conductivity (horizontal and vertical) represented by zones and pilot points. The complexity of the parameterization scheme is a function of the location of observations and the intended model predictions.

Recharge and Leakance Parameters

Natural recharge is represented by two parameters: recharge to aquifer sediments and recharge to pond surfaces. Pond recharge is specified as 16 in/yr, representing the difference between precipitation and pan evaporation for Cape Cod (Walter and Whealan, 2005); no recharge is specified for streams and wetlands. Recharge to aquifer sediments is the only recharge parameter included in the inverse-calibration regression. Multipliers of recharge, derived by normalizing values in individual cells—computed by using the SWB model—to the average value of 19.3 in/yr, are used to spatially distribute recharge on the basis of land use and soil characteristics. The parameter value applied to the multipliers, which represents the average recharge rate, was initially adjusted from 19.3 to 27.25 in/yr to better reflect effective recharge rates for the Cape Cod aquifer on the basis of prior information. This adjusted parameter value was allowed to change during the regression. Upper and lower constraints of 30 and 20 in/yr, respectively, were imposed on the parameter value. In addition, wastewater return flow in each of the seven Cape Cod towns within the model domain is represented as a separate recharge parameter and is spatially distributed by using multipliers derived from parcel-scale water-use data (fig. 28).

Leakances at boundaries refer to the vertical resistance to flow within surface-water bottom sediments and are a function of the vertical hydraulic conductivity and the thickness of the bottom sediments. The thickness of stream, wetland, and pond sediments was assumed to be 10 ft. The vertical hydraulic conductivities of sediments underlying streams and wetlands, represented as drains in the regional model (fig. 24), are represented as parameters that were adjusted during calibration. The vertical hydraulic conductivity of bottom sediments in both freshwater and saltwater wetlands was specified as 0.1 ft/d, consistent with previous calibrated models of the Cape Cod aquifer system (Walter and Whealan, 2005). The vertical hydraulic conductivity of stream-bottom sediments was allowed to change as part of the inverse-calibration

regression to best match observed conditions. The initial vertical hydraulic conductivity was specified as 1 ft/d, consistent with previously calibrated models of the system.

Coastal boundaries—open coastal waters and inland estuaries—are represented as general-head boundaries in the JBCC regional model (fig. 24). The vertical hydraulic conductivities of coastal-bottom sediments were specified as 0.4 ft/d in open coastal waters and 0.2 ft/d in estuaries; these values represent a twofold increase over values used in previously calibrated models. The values were used because they produce a freshwater/saltwater interface position that best matches observations, as determined by using the interface model (fig. 23). The vertical hydraulic conductivity of coastal-bottom sediments was not allowed to vary during the inverse-calibration regression owing to the correlation between coastal leakances and the position of the interface, which was represented in the groundwater flow model as a static no-flow boundary that was consistent with the specified leakances (fig. 24). The importance of coastal leakances in model calibration and predictions was evaluated by a sensitivity analysis.

Leakances at the bottoms of kettle-hole ponds, which are flow-through features that focus groundwater flow in upgradient areas and disperse flow in downgradient areas, can locally affect horizontal and vertical gradients (Walter and others, 2002). The horizontal leakance was implicitly represented by using the Horizontal-Flow Barrier Package (Hsieh and Freckleton, 1993), which allows for a specified resistance to flow between adjacent model cells; the barriers were specified between any cells that represent a pond and adjacent cells that represent aquifer material. The initial pond-bottom leakance was determined assuming a horizontal hydraulic conductivity of 100 ft/d and a thickness of 10 ft for pond-bottom sediments; the parameter value was allowed to change during the inverse-calibration regression. The vertical resistance to flow into the pond can be represented by the vertical hydraulic conductivity of the aquifer sediments in the layer underlying a pond. Aquifer sediments underlying ponds are defined as a separate parameter representing collapse structures where coarse sediments extend deeper into the aquifer than surrounding areas. The sensitivity of simulated hydrologic conditions to pond-bottom sediments was evaluated with sensitivity analyses.

Hydraulic Conductivity

Previous inverse calibration of a model of the Cape Cod aquifer (Walter and LeBlanc, 2008) used a zoned parameterization scheme in which regions representing broad geologic knowledge were defined as areas of piecewise constancy, represented by a single parameter. Parameter complexity using zones and Gauss-Levenberg-Marquardt nonlinear regression generally is limited by the need for a given problem to be invertible for a solution to be achieved. Overly complex parameterization schemes can result in highly correlated or insensitive parameters that can limit the ability to achieve a reasonable solution or an acceptable fit to observations. The use of pilot points allows parameters to be represented as discrete points and regions between each pilot-point parameter to be defined by kriging using the estimated values at the points. This approach, when combined with singular value decomposition (SVD) (Doherty and Hunt, 2010), can allow for complex and gradational hydraulic conductivity fields and often an improved fit to observations. The method also allows for the use of regularization to balance prior information on hydraulic conductivity with fit to observations, which allows for the preservation of geologic knowledge and can minimize overfitting to observations that can arise in highly parameterized models.

The hydraulic conductivities of aquifer sediments, both horizontal and vertical, are represented in the regional model by a combination of zones and pilot points. Pilot points are used where observations are most abundant and predictions are of greatest value. Single-parameter zones are used in areas with fewer observations and where predictions are of lesser value. Note that this parameterization scheme reflects the objective specific to this analysis—the prediction of hydraulic gradients and advective transport near the JBCC. The aquifer system was zoned by using updated and digitized geologic quadrangles for western Cape Cod (Stone and DiGiacomo-Cohen, 2009) (fig. 29*A*); these zones were used to group and correlate the pilot-point parameters within these depositional units. It is assumed that this broad zonation represents a reasonable limit regarding subdivision of the aquifer; no arbitrary zones were defined within surficial geology zones to minimize bias.

The pilot-point network consists of 643 pairs of horizontal and vertical hydraulic conductivity parameters within six aquifer zones (fig. 29*A*): the Mashpee Pitted and Buzzards Bay outwash plains, the Sandwich and Buzzards Bay Moraines, the Falmouth ice-contact deposits, and the Cape Cod lake deposits (fig. 29*A*). Only pilot points within a zone were used to generate, by kriging, the hydraulic conductivity fields within that zone. The pilot points were applied to four separate vertical groups: group 1 (layers 1–4), group 2 (layers 5–9), group 3 (layers 10–20), and group 4 (layers 21–32) (fig. 29*B*). The mean bottom altitudes of groups 1, 2, 3, and 4 are −31, −71, −160, and −450 ft (NGVD 29), respectively. The number of pilot points decreases with depth as the lateral extent of the zones decreases. There are 643, 618, 597, and 409 pairs of pilot-point parameters in groups 1, 2, 3, and 4, respectively, and a total of 4,534 separate pilot-point parameters. Only the top layer of each vertical group has defined pilot points. Following estimation of parameter values at a pilot point, the parameter field was interpolated by kriging for the top layer of each group; the resultant fields were then copied into the lower layers of each group prior to input into the model. This simplification was possible owing to the monotonic decrease in lateral extent of the aquifer with depth as defined by the bedrock and the freshwater/saltwater interface surfaces (fig. 29*B*).

Initial values of hydraulic conductivity were obtained from the hydraulic conductivity fields derived from lithologic logs (fig. 15) and mapped to the model grid (fig. 25). The thickness-weighted mean horizontal hydraulic conductivity

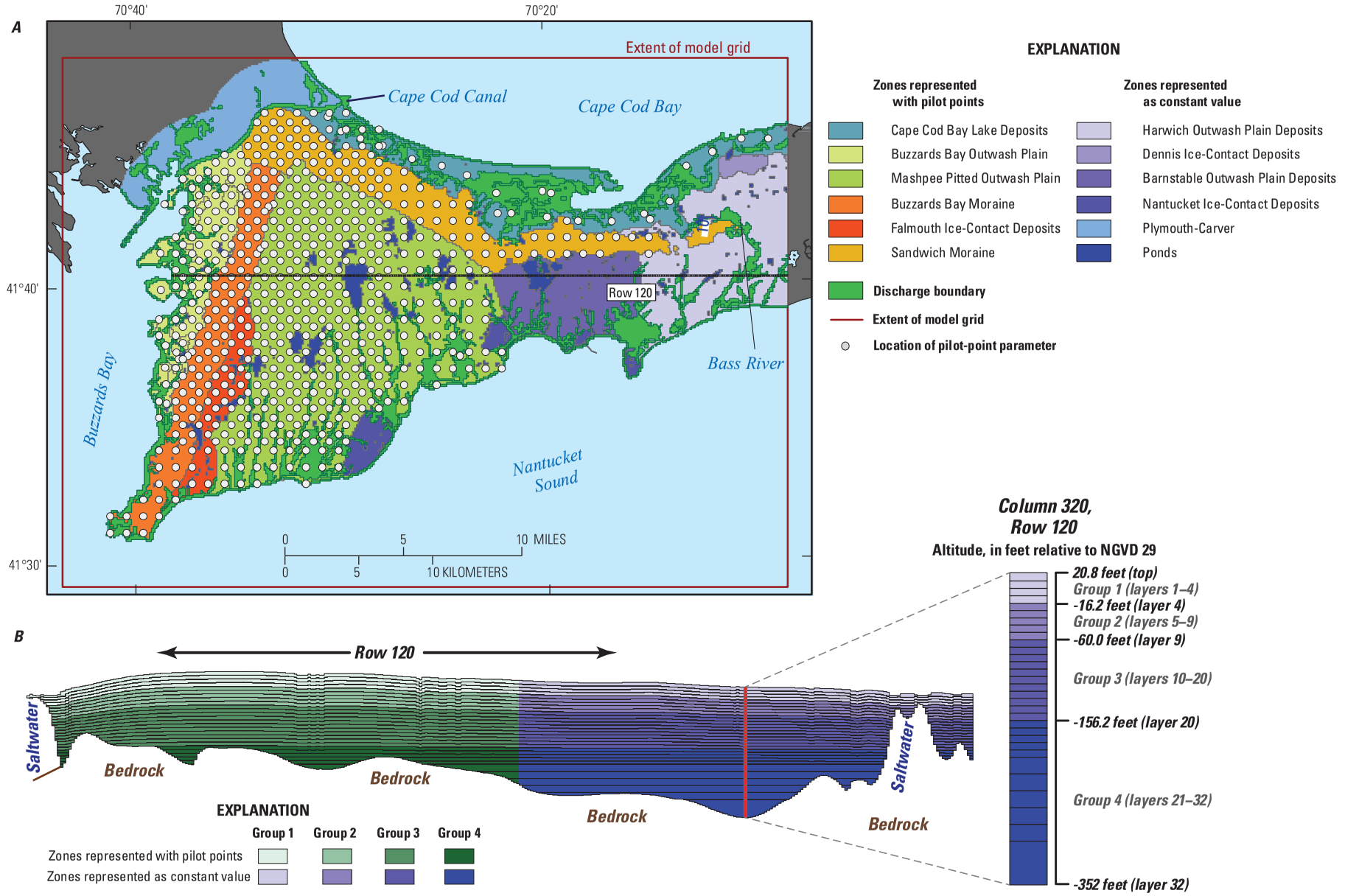

Figure 29. *A*, Aquifer zones (from surficial geology) and pilot-point network, western Cape Cod, Massachusetts, and *B*, section of model grid showing four-layer vertical zonation. Modified from Walter and others (2016). NGVD 29, National Geodetic Vertical Datum of 1929.

of the layers for the row and column containing each pilot-point parameter was assigned as the initial value of hydraulic conductivity; geometric means were used for vertical hydraulic conductivity; the process was done for each of the four vertical parameter groups. The initial mean horizontal hydraulic conductivities of vertical groups 1, 2, 3, and 4 were about 184, 162, 138, and 141 ft/d, respectively, and the mean vertical hydraulic conductivities were about 36, 30, 24, and 28 ft/d, respectively (fig. 30). These values, particularly for groups 3 and 4, which are deeper in the aquifer, were substantially higher than values consistent with the depositional model of western Cape Cod (Masterson and others, 1997a) and values from previously calibrated models of the system (Masterson and others, 1997b; Walter and Whealan, 2005). Initial model runs using the derived fields, as mapped to the model grid, resulted in a maximum simulated water-table altitude that was about 20 ft below the observed maximum altitude of about 70 ft, indicating that the derived fields may be an overestimate of actual aquifer transmissivity. These higher transmissivities could result in model cells, with associated observations of water-table altitude, that go dry, which would preclude the ability to inversely calibrate the model.

The four-step process by which lithologic logs were used to derive hydraulic conductivity fields from lithologic data (fig. 14) leads to some degree of undefinable error in the derived fields, and the paucity of data at depth could lead to spatial bias, particularly in deeper parts of the aquifer. To counter the effects of error and bias in parameters, additional prior information regarding aquifer characteristics was obtained from several sources (including the depositional model of western Cape Cod, hydraulic conductivity values from previously calibrated models, and the location of water-supply wells) and was used to rationally adjust initial

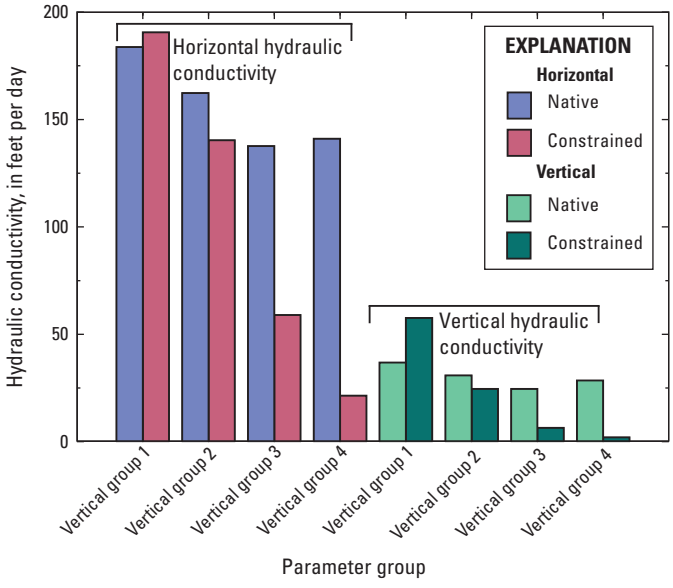

Figure 30. Native and constrained initial horizontal and vertical hydraulic conductivity values for four vertical parameter groups.

hydraulic conductivity values. The depositional model of the Mashpee Pitted Plain as a proglacial lacustrine delta indicates that sediments fine with depth and to the south with increasing distance from the sediment source (fig. 3*B*) (Masterson and others, 1997a); a previously calibrated model of the Sagamore flow lens, using those grain-size trends and including information from aquifer tests, matched observed hydrologic conditions well (Walter and Whealan, 2005).

The hydraulic conductivity fields from the Walter and Whealan (2005) model were mapped to the new model grid and used to estimate a second set of initial hydraulic conductivity values for the pilot-point parameters. For each vertical group of parameters, the ratio of the mean of this second set of values, referred to as "constrained values," to the mean estimated from the lithologic logs, referred to as "native values" and derived from the logs, was used to normalize the initial hydraulic conductivity values at each pilot-point parameter; this process was done for both horizontal and vertical hydraulic conductivity. The result is a set of initial constrained hydraulic conductivity parameters that has mean values, for each vertical group, that are similar to the set of analogous values from previously calibrated models and has grain-size trends consistent with the depositional model but preserves the spatial trends in hydraulic conductivity derived from the logs. The means of the two sets of hydraulic conductivity fields—native and constrained—are similar for groups 1 and 2, representing shallow parts of the aquifer (fig. 30); though contamination does occur in some deep parts of the aquifer, most groundwater flow and plume transport at the JBCC occurs in the shallower parts of the aquifer. The largest difference is for group 4, which has native and constrained means of about 141 and 21 ft/d, respectively. The mean top altitude of group 4 is about −136 ft (NGVD 29), and it is likely that comparatively little flow or transport of contaminants occurs in that part of the aquifer system. The same patterns are seen in comparisons of native and constrained vertical hydraulic conductivity fields. It is assumed that constraining the native values does not adversely affect model calibration because (1) the two sets of values are similar in the upper two vertical groups, where most groundwater flow and transport occurs; (2) the parameters at depth generally are insensitive to pilot-point parameters in the deepest vertical group; (3) the parameters are allowed to vary during the inverse-calibration regression; and (4) the constrained values better represent prior knowledge of the system and result in more reasonable simulated hydrologic conditions.

The final set of prior information used to inform initial hydraulic conductivity fields is the location of water-supply wells. Wells generally are screened in areas with reasonably high hydraulic conductivity, and it was recognized that normalizing native hydraulic conductivity values would lower values, particularly at depth, and that this could cause model cells representing, or near a cell representing, a water-supply well to have hydraulic conductivity values lower than would be likely given the presence of the pumping well. Initial hydraulic conductivity values in pilot-point parameters within 2,000 ft of a water-supply well were assigned

as either 100 ft/d in the upper two vertical groups or 70 ft/d in the lower two vertical groups, if the estimated value was lower than the normalized native value, to minimize the potential inconsistencies.

Hydraulic conductivity parameters were defined as zones of piecewise constancy in four surficial geology zones: the Barnstable and Harwich outwash plains, and the Dennis and Nantucket ice-contact deposits (fig. 29*A*). The same four vertical groups were used for each of the zones for a total of 16 horizontal and 16 vertical hydraulic conductivity parameters. Single horizontal and vertical hydraulic conductivity parameters also were defined for sediments underlying ponds (fig. 29*A*) that represent geologic collapse structures. All hydraulic conductivity parameters were allowed to change during the inverse-calibration regression. Upper and lower constraints were placed on hydraulic parameters to ensure that estimated parameters were within a range of reasonable values, based on prior knowledge of the aquifer system. Upper constraints of 320 and 100 ft/d were placed on horizontal and vertical hydraulic conductivity parameters, respectively; these values generally correspond to coarse sand and gravel. The lower constraint on horizontal hydraulic conductivity decreased with depth: 100, 70, 10, and 1 ft/d for vertical groups 1–4, respectively. The lower constraints on vertical hydraulic conductivity in groups 1, 2, 3, and 4 were 10, 5, 1, and 0.1 ft/d, respectively. A single porosity parameter was defined for all aquifer sediments, representing the primary porosity of the sediments; an initial value of 0.35 was specified, and the parameter was allowed to change during model calibration.

Observations

The data compilation effort, discussed previously in the section "Data Compilation and Analysis," yielded a large set of diverse data on the hydrologic system of western Cape Cod, including water-level and streamflow measurements at 5,626 wells and ponds and 78 streamflow sites, age measurements at 162 groundwater-sampling points, and estimates of the center of mass at 31 plume sections derived from water-quality samples. These data, when combined with a highly parameterized model, can inform a model calibration that can closely match observed conditions and facilitate accurate predictions of advective transport. The data can be used to formulate observations that are either direct (water levels and streamflows), extracted directly from model outputs (gradients), or derived through particle tracking (plume transport paths and groundwater ages). Prior to inclusion of a set of observations that include groups representing different observation types and degrees of reliability, weights that reflect the reliability and importance of the observations need to be determined.

Water Levels

A total of 547 water-level observations were determined to be generally representative of long-term average conditions and suitable for calibration of the steady-state model. The observations were grouped in four categories based on the quality of the observation, as determined by length of record and number of measurements. The four observation groups include (1) long-term index wells near the JBCC, (2) long-term index wells to the east of the JBCC, (3) partial-record wells with data from the USGS, and (4) partial-record wells with data from the JBCC. The 29 long-term wells measured monthly by the Cape Cod Commission (groups 1 and 2) are the most reliable, in terms of frequency and duration of the period of record (fig. 31). Groups 1 and 2 consist of long-term wells in the western and eastern parts of the study area, respectively. Monthly measurements at three wells (MA–SDW 252, MA–SDW 253, MA–BHW 198) began in 1962, covering the period of drought in the late 1960s (figs. 9 and 31); measurements at the remaining wells began in 1975. The long-term wells represent a well-distributed monitoring network throughout the Sagamore flow lens, and these wells are considered to be outside of the influence of nearby pumping. Separating the long-term wells into two groups (east and west) allows wells in the Mashpee Pitted Plain (MPP), where the model will be used predominantly to make predictions for the JBCC, to be more highly weighted. Mean pond stages for four ponds in the MPP (Ashumet, Crocker, Snake, and Spectacle Ponds) are included in group 1.

Mean water levels were measured intermittently by the USGS and the JBCC at partial-record wells, which were included in groups considered to be less reliable than those of the long-term record wells. However, these partial-record wells were determined to be generally reliable as indicators of long-term average water levels and provide near-average water-level observations distributed spatially between the long-term wells, particularly in the area of the JBCC where a detailed head distribution is desired. The 191 USGS sites include wells established and measured regularly as part of the USGS Toxic Substances Hydrology research program and wells historically measured as part of synoptic, regional water-table measurements (group 3). The six remaining intermittently measured pond-stage sites are included in this group (group 3). The 317 sites used by the JBCC to monitor water levels (group 4) include wells in areas of contaminant monitoring and remediation on or near the JBCC and locations of pump-and-treat remedial activities, which could minimally affect the observation. Water levels are directly simulated by the groundwater model, and residuals are calculated as the difference between the observed value and the simulated equivalent. The relative value of the water-level observations is reflected in the weighting used in the inverse calibration; weighted water levels compose about 15 percent of the initial objective function in the inverse model calibration regression. Group 1 water levels were weighted about 6 times greater than the group 2 wells and about 20 times greater than the partial-record wells (groups 3 and 4) (<0.5 percent each of the initial objective function).

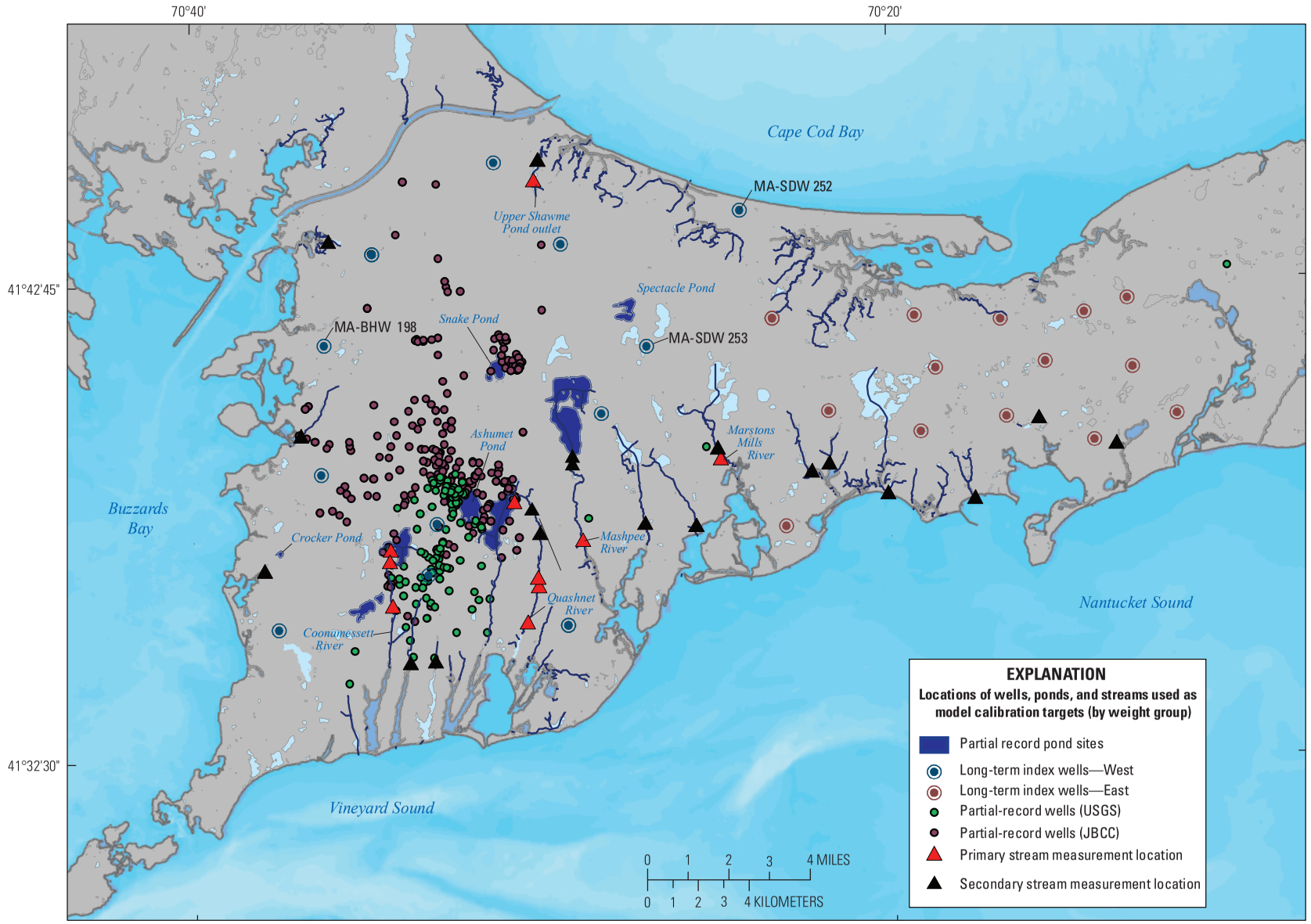

Base from U.S. Geological Survey and Massachusetts Office of Geographic Information digital data
North American Datum of 1983

Figure 31. Locations of wells, ponds, and streamflow measurement sites on Cape Cod, Massachusetts, used as calibration targets (by weight group). JBCC, Joint Base Cape Cod; USGS, U.S. Geological Survey.

Streamflows

Streamflow sites identified as generally representing long-term average hydrologic conditions were classified into two groups that reflect the degree of reliability and importance of the measurements: group "primary" and group "secondary." The primary group includes 10 sites along five surface-water bodies: Quashnet River (4), Coonamessett River (3), Mashpee River (1), Upper Shawme Pond Outlet (1), and Marstons Mills River (1) (fig. 31). These sites have regionally substantial flows (greater than 6 ft^3/s) and have been measured intermittently by the USGS; these observations were assigned a larger weight, reflecting general confidence in the reliability and quality of the measurements. These sites represent, in total, more than 45 percent of all measured streamflows (29 sites) in the study area.

Measurements at an additional 19 partial-record streams (secondary group) were made during times of average conditions or were calculated by using a regression approach to extend the record period, as previously discussed in the "Hydrologic Data" section (fig. 31). These observations were determined to be generally less reliable than those in the primary group, owing to limited site information, limited measurements at an individual site, shifting channel controls at the measurement location, or flows that were reported by other groups (such as MEP and JBCC) and made by using unknown methods.

Streamflows are directly simulated by the groundwater model—the summation of discharge along individual stream reaches—and residuals are calculated as the difference between the observed value and the simulated equivalent. Streamflow measurements from the primary group were weighted at about 8 percent of the initial total objective function for the inverse calibration regression, comparable to the weighting given to the water levels at the "index wells west" group. Observations in the secondary group were given a zero weight in the final calibration because of the limited confidence level in the mean values; however, observed values and simulated equivalents were compared as part of the assessment of model fit.

Tracers of Advective Transport

Contaminant plumes on and near the JBCC determined to be suitable as calibration targets were assigned to two groups ("plumes 1" and "plumes 2") on the basis of confidence in the source location and plume definition along downgradient transverse sections. Group plumes 1 includes observations for which sources could be reasonably defined by a point location (X, Y) and the distribution of contaminants was well mapped. As an example, the Demo-1 plume source area is a small kettle hole where demolition training was conducted from the late 1970s to the mid-1980s (figs. 6 and 32*C*). The downgradient transverse sections define a single connected cross-sectional area of perchlorate contamination. Group plumes 1 includes 22 plume sections and source pairings from well-defined contaminant plumes on the JBCC, including the Demo-1, CS–4, Ashumet Valley plume, FS–1, J–1 and J–2 ranges (fig. 17). By contrast, the source area for the LF–1 plume is a large area where a single point does not adequately define a source, and the CS–10 plume may emanate from multiple sources. Large or multiple-source areas create discontinuous, segmented plumes that are difficult to identify as one continuous cross-sectional area along downgradient transverse sections. Nine additional plume sections and source pairs—group "plumes 2"—were identified as plumes with either large source areas (LF–1 and CS–10) or geochemical sections that proved difficult to estimate as a single center of plume mass (such as FS–12).

Plume observations are referred to as "derived observations" because the simulated equivalents are not directly simulated by the model but rather are derived from postmodeling particle tracking. The particle-tracking program MODPATH simulated advective transport by computing flow paths (defined by sequential particle locations) from defined starting locations either in the direction of groundwater flow or in the reverse direction by using intercell flow terms computed by the groundwater model. The observed (estimated) centers of plume mass in the transverse sections identified in the previous paragraph were used to define the starting location of a particle; the particle was tracked in reverse to the simulated recharge point at the water table, representing the source of the particle (fig. 32*B*) (Pollock, 1994). The X, Y coordinates of the computed recharge location become the simulated equivalent to the observed (estimated) X, Y source location. The distance between the observed X, Y source—the location of source observation—and the simulated equivalent—the ending location of the particle track—is the residual (fig. 32*C*). These residuals are included in the objective function computed during the inverse calibration. Plume observations are important both for their reliability as indicators of long-term hydraulic gradients and advective-transport patterns (Walter and Masterson, 2003) and for the intended use of the model to predict advective transport at the JBCC. Residuals for the two plume groups, in total, compose most of the initial objective function, reflecting the importance of the observations, indicated by the large weights assigned to those observations; residuals for groups 1 and 2 compose about 49.7 and 24 percent, respectively, of the initial objective function.

Groundwater-age measurements and estimated traveltimes to tritium peaks also are derived observations. Particles are started at the midpoint of the 132 sampling intervals and reverse tracked to recharge locations by using MODPATH; the computed time for the particle to travel from the sample point to the water table is the simulated equivalent, and the residual is the departure from the observed value (fig. 33*A*). The observed apparent groundwater ages, as estimated from the ratio of helium 3 to tritium ($^3He/^3H$) and from the concentrations of chlorofluorocarbons (CFCs), were compared directly to the simulated traveltimes produced by MODPATH (fig. 33*B*). Traveltimes associated with the location of peak tritium (^3H) concentrations also were simulated by using reverse particle tracking but were corrected for unsaturated-zone

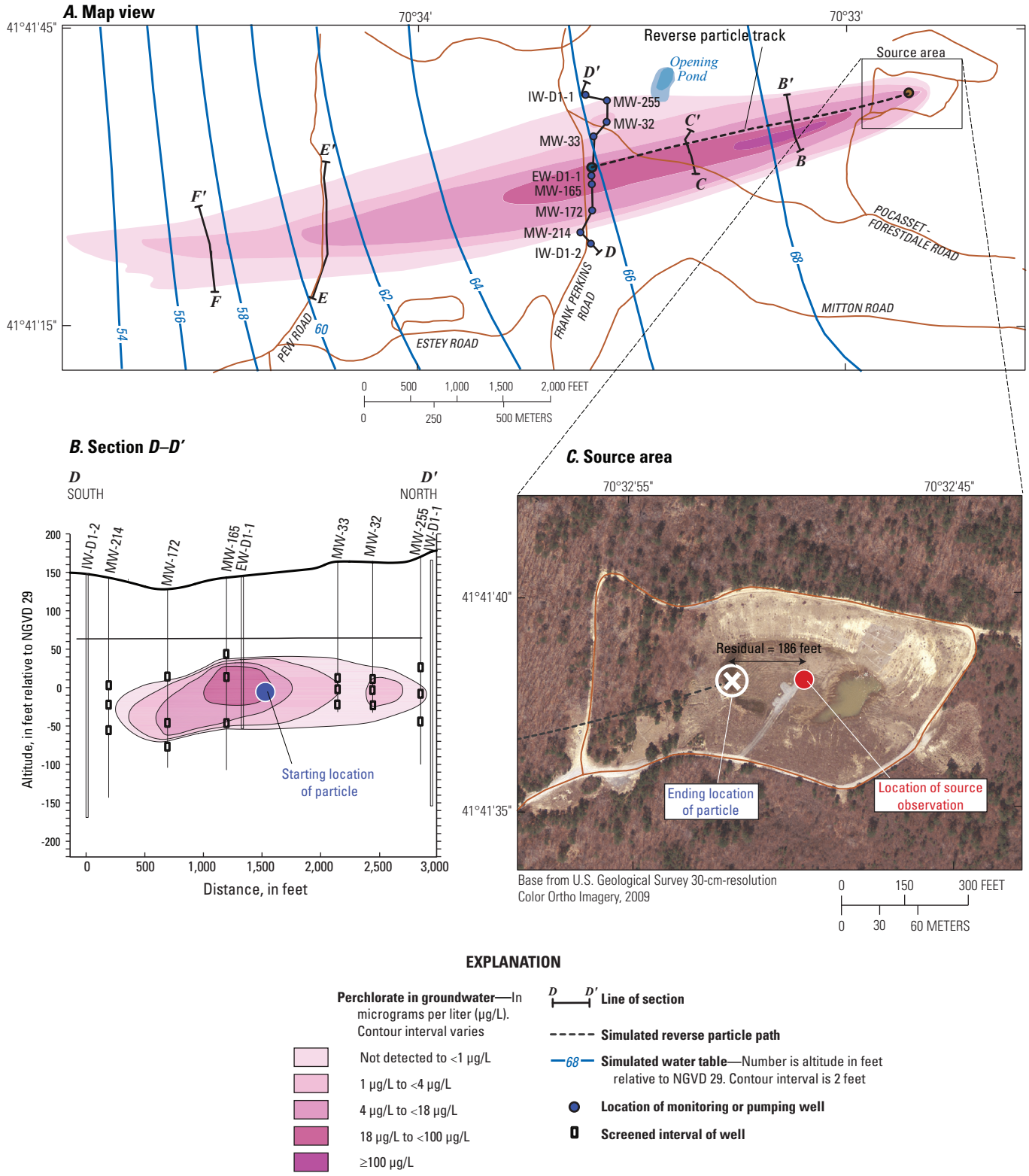

Figure 32. *A*, Demo-1 plume, location of transverse sections, and simulated reverse particle track, *B*, section *D–D'* showing estimated center of plume mass, and *C*, map showing the source area, western Cape Cod, Massachusetts. Figure 32*A* modified from Army National Guard (2005). cm, centimeter; NGVD 29, National Geodetic Vertical Datum of 1929.

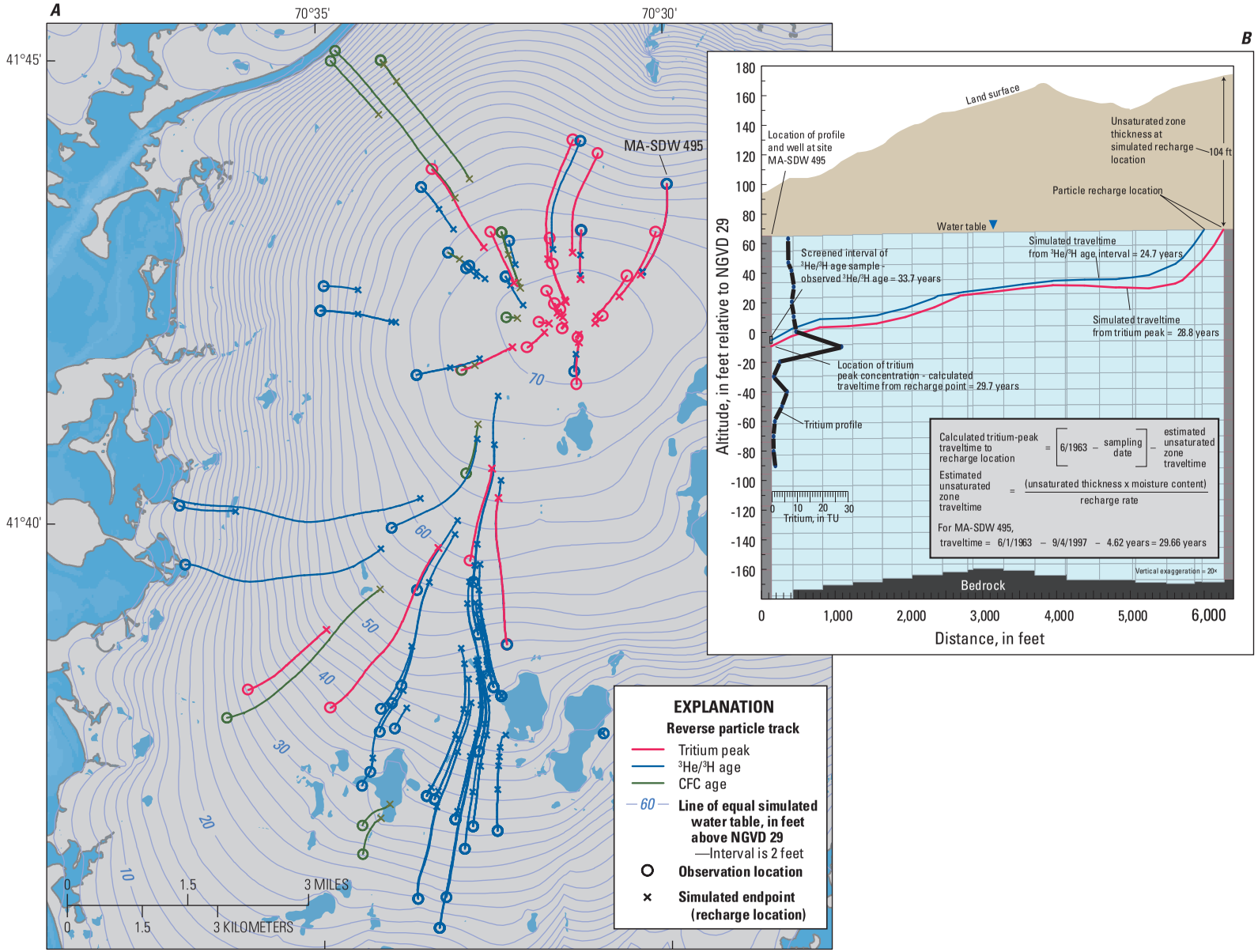

Base from U.S. Geological Survey and
Massachusetts Office of Geographic Information digital data
North American Datum of 1983

Figure 33. *A*, Groundwater-age sites with particle tracks and endpoint recharge locations and *B*, inset of reverse particle tracks from an age observation and a tritium peak with unsaturated zone correction, western Cape Cod, Massachusetts. CFC, chlorofluorocarbon; ft, foot; $^{3}He/^{3}H$, ratio of helium 3 to tritium; NGVD 29, National Geodetic Vertical Datum of 1929; TU, tritium unit.

thickness. Note that apparent groundwater ages do not account for mixing of waters of different ages, which can result from the use of long-screen wells or large pumping rates; groundwater ages used in this analysis are from short-screen wells (less than 5 ft long) sampled at low pumping rates to minimize mixing effects.

The estimated traveltime is inversely proportional to effective porosity; values of effective porosity range from 0.36 to 0.42 on Cape Cod, as estimated from past field studies (Garabedian and others, 1988; LeBlanc and others, 1991; Barlow, 1997; Morin, 2006). Porosity is included in the inverse calibration as an adjustable parameter. Particle tracking represents advective transport only and does not account for hydrodynamic mixing, dispersion, or geochemical reactions, all of which, to some degree, affect concentrations of environmental tracers and estimated apparent ages. Age observations generally are considered less reliable than other observation types, which is reflected in the smaller weights assigned to the age observations in the inverse calibration. Residuals for traveltimes estimated from groundwater ages—$^{3}He/^{3}H$, CFCs, and tritium—and simulated equivalents, in total, account for about 1 percent of the initial objective function. Traveltimes estimated from tritium observations had slightly larger weights than the apparent-age observations owing to the more direct and robust nature of those observations.

Hydraulic Gradients

The magnitude and direction of hydraulic gradients (the change in head with distance) can be determined from water-level measurements or inferred from indicators of advective transport. Two observations of the gradient are included in the inverse-calibration regression: (1) the location of the top of the radial water-table divide in the north-central part of the JBCC as inferred from patterns of advective transport and (2) the transition between upward and downward hydraulic gradients along the western shore of Ashumet Pond (fig. 2) as determined from gradient measurements. These observed gradient locations are relevant to nearby contaminant plumes.

The radial water-table divide, at the top of the water-table mound, is in the north-central part of the JBCC (fig. 2) and represents the highest water-table altitude in the aquifer. The horizontal gradient at that theoretical point is zero, and gradients are small near the divide. Several contaminant plumes emanating from nearby sources define a radial pattern of advective transport (fig. 34*A*) that can be used to infer the approximate "observed" location of the radial divide. The location of the radial divide is particularly important owing to its control on hydraulic gradient directions and transport of the numerous plumes near the divide (fig. 34*A*). The inferred "observed" location of the divide was included in the inverse-calibration regression by using a local X, Y coordinate system with a 1-foot discretization. The residual is the difference, in feet, between the two points defined within the local X, Y coordinate system. The large horizontal discretization (400 ft) and the small horizontal gradients around the divide cause the simulated location of the mound to be a step function with respect to perturbation of the parameters during the inverse-calibration regression, resulting in either false zero values or large overestimates of sensitivities. It was necessary to interpolate the true simulated top of the mound at a fine horizontal scale from a set of the largest simulated water-table altitudes from the regional model. For each perturbation run, the 26 highest water-table altitudes and their X, Y locations were used to produce a local grid with a 1-foot discretization that included the 26 points. The points were used in a polynomial interpolation to determine the location of the highest point within the local grid (fig. 34*B*). The location of the radial water-table divide therefore approximates a continuous function over the small head changes that arise from the parameter perturbation and allows for the observed location to be included in the inverse-calibration regression.

Ashumet Pond is a kettle-hole pond located near and to the south of the JBCC (fig. 2). The pond is downgradient from a former WWTF and part of a plume of treated-wastewater-contaminated groundwater, referred to as the "Ashumet Valley plume," that is discharging into the pond. The pond is near the USGS Toxic Substances Hydrology Cape Cod research site. Data collected as part of ongoing research at that site include the distribution of contaminants discharging to the pond (McCobb and others, 2009) and measurements of pond-bottom hydraulic gradients (Walter and others, 1996). Ashumet Pond is a flow-through pond where, to the north, upward gradients focus groundwater into the pond and, to the south, downward gradients disperse seepage from the pond into the aquifer. There is a point where the vertical gradient is zero between these two flow regimes; this is referred to as the "hinge point." The Ashumet Valley plume discharges along the western shore of the pond to the north of, but close to, the hinge point, and the simulated location of the hinge point has an important effect on the simulated advective transport of the plume. Measured pond-bottom hydraulic gradients indicate that the approximate location of this point is about 200 ft to the south of Fishermans Cove (fig. 35). The location of the hinge point is included in the inverse-calibration regression as a Y (northing) coordinate. The simulated equivalent is computed by linear interpolation between the cells to the north and south of the transition between positive (upward) and negative (downward) gradients, as simulated by the model, weighted by the magnitude of the simulated water levels in the two cells. The residual is the difference, in feet, between the observed and simulated Y coordinate (fig. 35).

Calibration Approach

Gauss-Levenberg-Marquardt nonlinear regression is a gradient-based technique that minimizes the weighted misfit between observations and model-calculated equivalents. The nonlinearity of the system requires an iterative approach to minimization. Observation sensitivities with respect to each parameter are computed by perturbing (by 1 percent) individual parameters and evaluating the change in simulated equivalents for each observation; this process requires a model

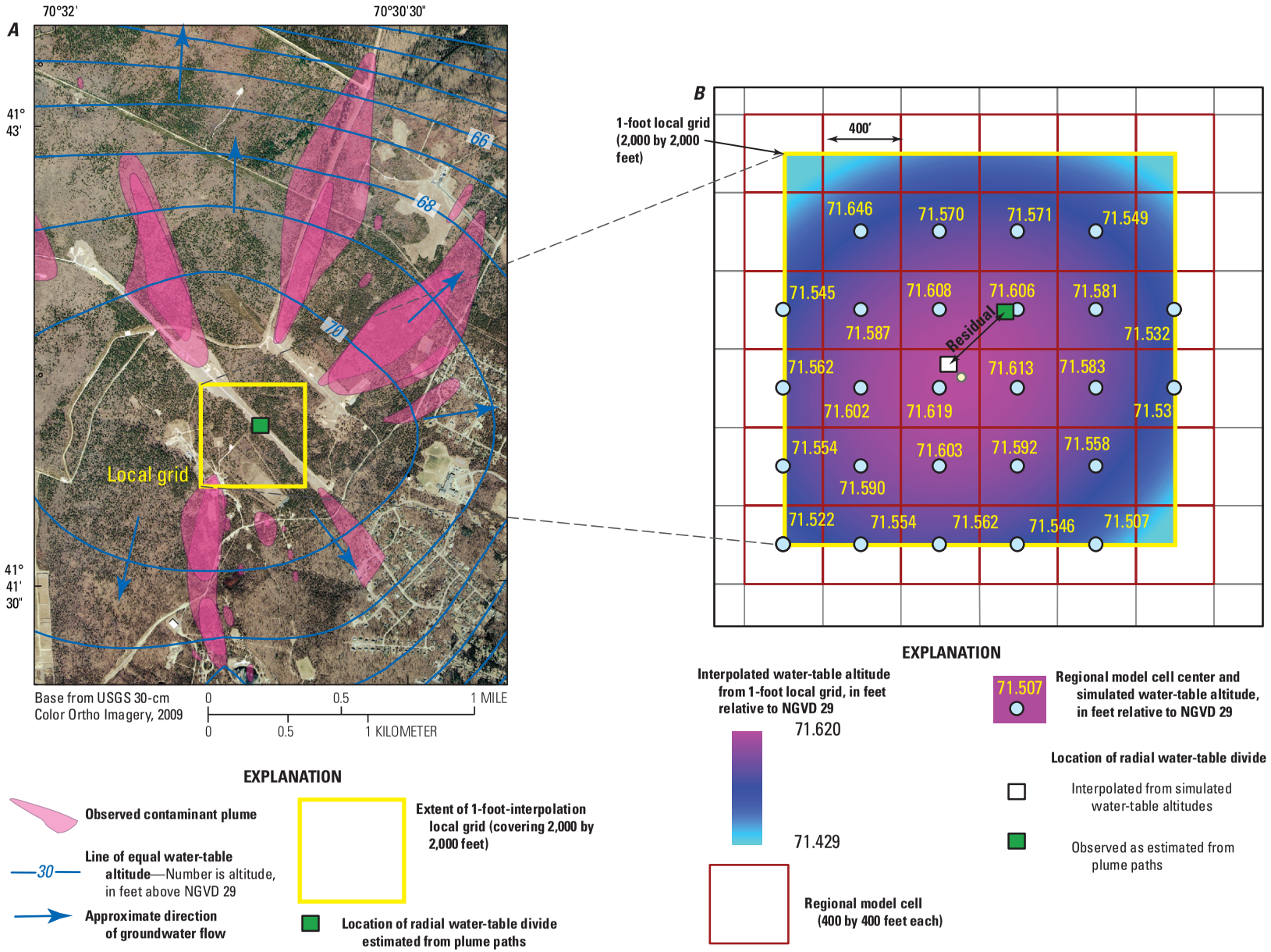

Figure 34. *A*, Location of water-table mound, J-range plumes, and location of interpolation local grid, and *B*, location of simulated heads used for interpolation within the local grid, western Cape Cod, Massachusetts. cm, centimeter; NGVD 29, National Geodetic Vertical Datum of 1929; USGS, U.S. Geological Survey.

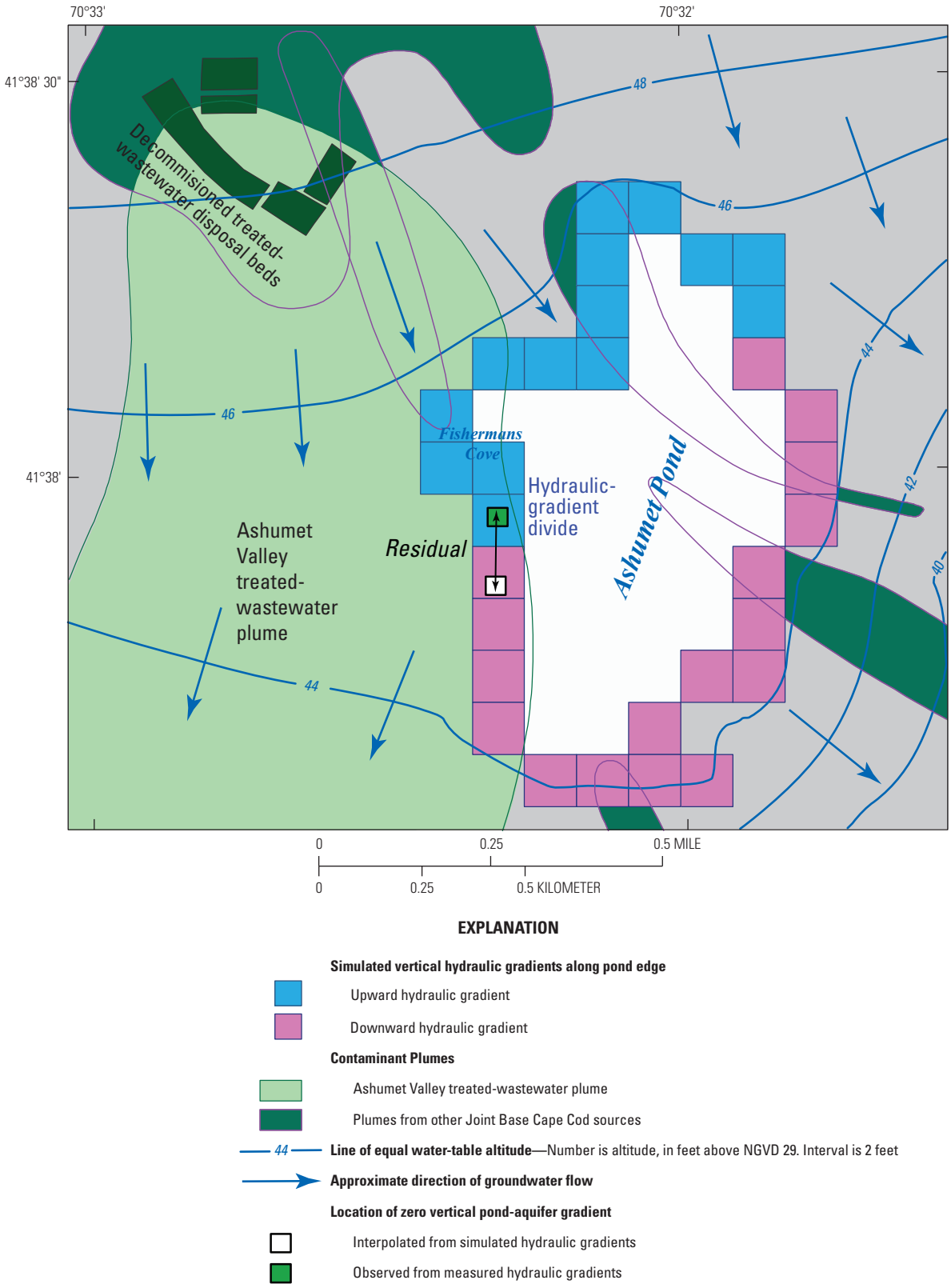

Figure 35. The location of Ashumet Pond hydraulic-gradient divide and pond-edge model cells, western Cape Cod, Massachusetts. NGVD 29, National Geodetic Vertical Datum of 1929.

run for each parameter and results in a matrix of sensitivities, referred to as a "Jacobian matrix." The Jacobian matrix is computed initially and updated between successive iterations to guide the nonlinear regression. Exploratory runs between each iteration are performed to determine the local objective-function gradient and to update parameter values and lower the value of the objective function. This process is repeated until updated parameters change by less than a specified closure criteria (1 percent), at which point the regression is considered to be complete.

The objective function includes individual terms for each observation that are equal to the square of the difference between the observed quantity and the simulated equivalent multiplied by the weight of the observation; the weight is the inverse of an estimate of error associated with the observation. Weighting reflects the confidence in the observation and, to a degree, the importance of the observation. Weighting can represent physically based errors associated with the measurement; however, such estimates are often difficult to quantify. The use of a diverse set of observations with differing units can complicate weighting schemes based strictly on estimates of error. This is further exacerbated by different numbers of observations for different groups because a larger number of observations—even with relatively small values of misfit—can overwhelm the objective function such that groups with more observations or larger units have disproportionate influence on the regression. It is also difficult to quantify the error incurred by modeling assumptions and structure (Doherty and Welter, 2010). An alternative is to use a relative weighting scheme whereby a more qualitative measure of the importance of a set of observations, as indicated by the portion of the objective function a given group of observations contributes to the total value, can be used to order weights to reflect the user's confidence in individual groups. Initial weights are set strictly on the basis of assumption of error, but they can be adjusted to trade off the desired influence of specific groups on the basis of the factors mentioned above. This level of subjectivity importantly improves the results, provided there is disclosure of the assumptions made (Fienen, 2013). The use of relative weighting requires that observations be grouped such that units and confidence in the value of the observations are similar within each weighting group. The inverse-model calibration in this study used a relative weighting scheme owing to the diverse set of observation types and the difficulty of assigning physically based measures of error to inferred observations, such as plume center points and zero-gradient locations. The development of a reasonable weighting scheme is an iterative process; the effectiveness of alternate weighting schemes was evaluated with a sensitivity test.

Singular value decomposition (SVD) is used to improve stability when a large number of parameters is used in the calibration by suppressing variability of insensitive parameters in the regression on the basis of a user-defined range of eigenvalues (analogous to sensitivities) from SVD performed on the weighted Jacobian matrix (Doherty and Hunt, 2010). In addition, SVD Assist (SVDA) (Tonkin and Doherty, 2005) is used to more efficiently manage model run times by reducing the number of parameters to 200 linear combinations of parameters, referred to as "super parameters." Application of SVDA assumes that the model generally is linear and that a full Jacobian matrix does not need to be computed for each successive iteration of the regression. The inverse calibration uses regularization to balance the fit to observations with prior geologic knowledge of the aquifer, primarily in the form of initial hydraulic conductivities. Regularization allows for the inclusion of prior information as a penalty function within the objective function. As the fit to observations improves and that component of the objective function decreases, departure from initial parameter values increases the value of the penalty function and offsets the total decrease. Regularization can enforce either smoothness between parameters or the initial value of the parameter. The latter, referred to as "preferred value regularization," was used in this calibration. The variable that controls the relative importance of the two components is PHIMLIM; a value of 1,000 was used in the calibration, similar to the number of observations (802) used in the regression. This approach assumes that weights assigned to observations reasonable represent actual measurement error (Fienen and others, 2009).

Calibration Results

The inverse-calibration regression discussed here, referred to as the "preferred calibration," is the result of an iterative process whereby different types of observations were included and the associated weights were varied to reflect confidence in the observations and the desire to match observations of importance to the prediction of advective transport at the JBCC. The criteria for a model calibration to be successful include (1) an acceptable fit to observed data, particularly those observations of importance to model predictions and (2) estimates of parameter values, such as recharge and hydraulic conductivity, that adequately reflect prior knowledge of the aquifer system.

The preferred calibration included five broad types of observations: water-level altitudes, streamflow measurements, traveltimes estimated from groundwater ages, advective-transport patterns as indicated by plumes, and the hydraulic-gradient observations. Each of these groups was, in turn, divided into subgroups (for a total of 13 groups) and assigned weights based on relative confidence (table 2). A relative weighting scheme was used whereby groups and subgroups of observations were assigned weights as a percentages of the initial objective-function value; larger weights indicate that observations within that group were desired to have a larger influence on estimated parameters. In the preferred calibration (variant HFPA in table 2), the five observation types—water levels (heads), streamflows, plumes, groundwater ages, and hydraulic gradients—were assigned weights that are equal to percentages of the initial objective-function value. The weights for this calibration were 14.8, 8, 73.7, 1, and 2.5 percent, respectively (table 2).

Table 2. Observation groups, weighting, and calibrated absolute mean residual by group and simulation for alternative calibrations of the Joint Base Cape Cod regional groundwater flow model, western Cape Cod, Massachusetts.

[Simulation code abbreviations: H, heads; F, streamflows; P, plumes; A, ages; CCC, Cape Cod Commission; USGS, U.S. Geological Survey; JBCC, Joint Base Cape Cod; ^{3}H, tritium; ^{3}He/^{3}H, helium-3/tritium ratio; CFC, chlorofluorocarbon; ft^3/d, cubic foot per day]

Observation type	Observation group	Description	Unit	Weighting, as percent contribution to initial total objective function	Final absolute mean residual
Simulation code HFPA (722 non-zero observations)—Preferred calibration					
Heads	CCC west	Long-term water level	Feet	12	0.54
	CCC east	Long-term water level	Feet	2	1.17
	USGS partial	Partial-record water level	Feet	0.4	0.90
	JBCC partial[1]	Partial-record water level	Feet	0.4	1.01
Flows	Primary	Streamflow—multiple measurements	ft^3/d	8	61,129
	Secondary	Streamflow—partial records	ft^3/d	0	186,202
Plumes	Plumes 1	Plume transect—well-defined source	Feet	49.7	382
	Plumes 2	Plume transect—approximate source	Feet	24	338
Ages	^{3}H	Age associated with tritium peak	Years	0.6	7.5
	^{3}He/^{3}H	Groundwater age	Years	0.3	13.4
	CFCs	Groundwater age	Years	0.1	17.9
Gradients	Hinge	Ashumet Pond hinge location—western shore	Feet	1	228
	Mound	Regional water-table mound location	Feet	1.5	453
Simulation code HF (578 non-zero observations)					
Heads	CCC west	Long-term water level	Feet	29	0.11
	CCC east	Long-term water level	Feet	14.5	0.49
	USGS partial	Partial-record water level	Feet	2.5	0.51
	JBCC partial[1]	Partial-record water level	Feet	2.5	0.69
Flows	Primary	Streamflow—multiple measurements	ft^3/d	40	11,701
	Secondary	Streamflow—partial records	ft^3/d	9	105,768
Plumes	Plumes 1	Plume transect—well-defined source	Feet	0	2,564
	Plumes 2	Plume transect—approximate source	Feet	0	2,518
Ages	^{3}H	Age associated with tritium peak	Years	0	14.5
	^{3}He/^{3}H	Groundwater age	Years	0	12.7
	CFCs	Groundwater age	Years	0	47.9
Gradients	Hinge	Ashumet Pond hinge location—western shore	Feet	1	58
	Mound	Regional water-table mound location	Feet	1.5	719
Simulation code HFP (609 non-zero observations)					
Heads	CCC west	Long-term water level	Feet	14.5	0.43
	CCC east	Long-term water level	Feet	7.25	0.79
	USGS partial	Partial-record water level	Feet	1.25	0.67
	JBCC partial[1]	Partial-record water level	Feet	1.25	0.82
Flows	Primary	Streamflow—multiple measurements	ft^3/d	20	25,472
	Secondary	Streamflow—partial records	ft^3/d	4.5	128,969
Plumes	Plumes 1	Plume transect—well-defined source	Feet	34.5	608
	Plumes 2	Plume transect—approximate source	Feet	14.25	535
Ages	^{3}H	Age associated with tritium peak	Years	0	22.9
	^{3}He/^{3}H	Groundwater age	Years	0	16.4
	CFCs	Groundwater age	Years	0	23.1
Gradients	Hinge	Ashumet Pond hinge location—western shore	Feet	1	65
	Mound	Regional water-table mound location	Feet	1.5	583

Table 2. Observation groups, weighting, and calibrated absolute mean residual by group and simulation for alternative calibrations of the Joint Base Cape Cod regional groundwater flow model, western Cape Cod, Massachusetts.—Continued

[Simulation code abbreviations: H, heads; F, streamflows; P, plumes; A, ages; CCC, Cape Cod Commission; USGS, U.S. Geological Survey; JBCC, Joint Base Cape Cod; ^{3}H, tritium; ^{3}He/^{3}H, helium-3/tritium ratio; CFC, chlorofluorocarbon; ft^3/d, cubic foot per day]

Observation type	Observation group	Description	Unit	Weighting, as percent contribution to initial total objective function	Final absolute mean residual
Simulation code P (33 non-zero observations)					
Heads	CCC west	Long-term water level	Feet	0	2.32
	CCC east	Long-term water level	Feet	0	4.87
	USGS partial	Partial-record water level	Feet	0	1.55
	JBCC partial[1]	Partial-record water level	Feet	[1]0.01	1.28
Flows	Primary	Streamflow—multiple measurements	ft^3/d	0	316,109
	Secondary	Streamflow—partial records	ft^3/d	0	298,833
Plumes	Plumes 1	Plume transect—well-defined source	Feet	73	423
	Plumes 2	Plume transect—approximate source	Feet	24.5	432
Ages	^{3}H	Age associated with tritium peak	Years	0	22.5
	^{3}He/^{3}H	Groundwater age	Years	0	16.1
	CFCs	Groundwater age	Years	0	23.7
Gradients	Hinge	Ashumet Pond hinge location—western shore	Feet	1	57
	Mound	Regional water-table mound location	Feet	1.49	181
Simulation code PA (163 non-zero observations)					
Heads	CCC west	Long-term water level	Feet	0	1.96
	CCC east	Long-term water level	Feet	0	5.64
	USGS partial	Partial-record water level	Feet	0	0.92
	JBCC partial[1]	Partial-record water level	Feet	[1]0.01	1.45
Flows	Primary	Streamflow—multiple measurements	ft^3/d	0	345,478
	Secondary	Streamflow—partial records	ft^3/d	0	324,444
Plumes	Plumes 1	Plume transect—well-defined source	Feet	34.5	726
	Plumes 2	Plume transect—approximate source	Feet	14.25	587
Ages	^{3}H	Age associated with tritium peak	Years	28.75	2.4
	^{3}He/^{3}H	Groundwater age	Years	15	9.8
	CFCs	Groundwater age	Years	5	6.3
Gradients	Hinge	Ashumet Pond hinge location—western shore	Feet	1	8
	Mound	Regional water-table mound location	Feet	1.49	484
Simulation code A (134 non-zero observations)					
Heads	CCC west	Long-term water level	Feet	0	2.74
	CCC east	Long-term water level	Feet	0	6.13
	USGS partial	Partial-record water level	Feet	0	1.97
	JBCC partial[1]	Partial-record water level	Feet	[1]0.01	2.75
Flows	Primary	Streamflow—multiple measurements	ft^3/d	0	383,993
	Secondary	Streamflow—partial records	ft^3/d	0	361,627
Plumes	Plumes 1	Plume transect—well-defined source	Feet	0	3,164
	Plumes 2	Plume transect—approximate source	Feet	0	2,512
Ages	^{3}H	Age associated with tritium peak	Years	57.5	2.1
	^{3}He/^{3}H	Groundwater age	Years	30	7.2
	CFCs	Groundwater age	Years	10	5.5
Gradients	Hinge	Ashumet Pond hinge location—western shore	Feet	1	14
	Mound	Regional water-table mound location	Feet	1.49	389

Table 2. Observation groups, weighting, and calibrated absolute mean residual by group and simulation for alternative calibrations of the Joint Base Cape Cod regional groundwater flow model, western Cape Cod, Massachusetts.—Continued

[Simulation code abbreviations: H, heads; F, streamflows; P, plumes; A, ages; CCC, Cape Cod Commission; USGS, U.S. Geological Survey; JBCC, Joint Base Cape Cod; ^{3}H, tritium; ^{3}He/^{3}H, helium-3/tritium ratio; CFC, chlorofluorocarbon; ft^3/d, cubic foot per day]

Observation type	Observation group	Description	Unit	Weighting, as percent contribution to initial total objective function	Final absolute mean residual
Simulation code HFA (710 non-zero observations)					
Heads	CCC west	Long-term water level	Feet	14.5	0.46
	CCC east	Long-term water level	Feet	7.25	0.92
	USGS partial	Partial-record water level	Feet	1.25	0.82
	JBCC partial[1]	Partial-record water level	Feet	1.25	1.30
Flows	Primary	Streamflow—multiple measurements	ft^3/d	20	9,830
	Secondary	Streamflow—partial records	ft^3/d	4.5	189,474
Plumes	Plumes 1	Plume transect—well-defined source	Feet	0	4,037
	Plumes 2	Plume transect—approximate source	Feet	0	2,271
Ages	^{3}H	Age associated with tritium peak	Years	29.25	2.3
	^{3}He/^{3}H	Groundwater age	Years	14.625	7.6
	CFCs	Groundwater age	Years	4.875	8.4
Gradients	Hinge	Ashumet Pond hinge location—western shore	Feet	1	13
	Mound	Regional water-table mound location	Feet	1.5	494
Simulation code H (549 non-zero observations)					
Heads	CCC west	Long-term water level	Feet	58	0.19
	CCC east	Long-term water level	Feet	29	0.53
	USGS partial	Partial-record water level	Feet	5.25	0.50
	JBCC partial[1]	Partial-record water level	Feet	5.25	0.62
Flows	Primary	Streamflow—multiple measurements	ft^3/d	0	231,062
	Secondary	Streamflow—partial records	ft^3/d	0	232,675
Plumes	Plumes 1	Plume transect—well-defined source	Feet	0	3,442
	Plumes 2	Plume transect—approximate source	Feet	0	2,270
Ages	^{3}H	Age associated with tritium peak	Years	0	12.0
	^{3}He/^{3}H	Groundwater age	Years	0	15.0
	CFCs	Groundwater age	Years	0	18.9
Gradients	Hinge	Ashumet Pond hinge location—western shore	Feet	1	20
	Mound	Regional water-table mound location	Feet	1.5	339
Simulation code F (31 non-zero observations)					
Heads	CCC west	Long-term water level	Feet	0	1.26
	CCC east	Long-term water level	Feet	0	3.87
	USGS partial	Partial-record water level	Feet	0	0.97
	JBCC partial[1]	Partial-record water level	Feet	[1]0.01	1.24
Flows	Primary	Streamflow—multiple measurements	ft^3/d	80	11,816
	Secondary	Streamflow—partial records	ft^3/d	17.5	124,067
Plumes	Plumes 1	Plume transect—well-defined source	Feet	0	2,996
	Plumes 2	Plume transect—approximate source	Feet	0	1,678
Ages	^{3}H	Age associated with tritium peak	Years	0	14.0
	^{3}He/^{3}H	Groundwater age	Years	0	14.2
	CFCs	Groundwater age	Years	0	20.0
Gradients	Hinge	Ashumet Pond hinge location—western shore	Feet	1	20
	Mound	Regional water-table mound location	Feet	1.49	339

Table 2. Observation groups, weighting, and calibrated absolute mean residual by group and simulation for alternative calibrations of the Joint Base Cape Cod regional groundwater flow model, western Cape Cod, Massachusetts.—Continued

[Simulation code abbreviations: H, heads; F, streamflows; P, plumes; A, ages; CCC, Cape Cod Commission; USGS, U.S. Geological Survey; JBCC, Joint Base Cape Cod; ^{3}H, tritium; ^{3}He/^{3}H, helium-3/tritium ratio; CFC, chlorofluorocarbon; ft^3/d, cubic foot per day]

Observation type	Observation group	Description	Unit	Weighting, as percent contribution to initial total objective function	Final absolute mean residual
Simulation code sandy (722 non-zero observations)					
Heads	CCC west	Long-term water level	Feet	12	0.83
	CCC east	Long-term water level	Feet	2	3.54
	USGS partial	Partial-record water level	Feet	0.4	1.21
	JBCC partial[1]	Partial-record water level	Feet	0.4	1.04
Flows	Primary	Streamflow—multiple measurements	ft^3/d	8	203,797
	Secondary	Streamflow—partial records	ft^3/d	0	221,535
Plumes	Plumes 1	Plume transect—well-defined source	Feet	49.7	379
	Plumes 2	Plume transect—approximate source	Feet	24	336
Ages	^{3}H	Age associated with tritium peak	Years	0.6	14.7
	^{3}He/^{3}H	Groundwater age	Years	0.3	10.5
	CFCs	Groundwater age	Years	0.1	25.0
Gradients	Hinge	Ashumet Pond hinge location—western shore	Feet	1	46
	Mound	Regional water-table mound location	Feet	1.5	352
Simulation code silty (722 non-zero observations)					
Heads	CCC west	Long-term water level	Feet	12	2.02
	CCC east	Long-term water level	Feet	2	5.10
	USGS partial	Partial-record water level	Feet	0.4	0.91
	JBCC partial[1]	Partial-record water level	Feet	0.4	1.07
Flows	Primary	Streamflow—multiple measurements	ft^3/d	8	313,594
	Secondary	Streamflow—partial records	ft^3/d	0	286,399
Plumes	Plumes 1	Plume transect—well-defined source	Feet	49.7	488
	Plumes 2	Plume transect—approximate source	Feet	24	419
Ages	^{3}H	Age associated with tritium peak	Years	0.6	17.9
	^{3}He/^{3}H	Groundwater age	Years	0.3	15.2
	CFCs	Groundwater age	Years	0.1	33.0
Gradients	Hinge	Ashumet Pond hinge location—western shore	Feet	1	257
	Mound	Regional water-table mound location	Feet	1.5	445

[1]Heads from JBCC partial group were weighted at 0.01 percent to increase number on non-zero-weighted observations.

Observations of advective transport are considered reliable indicators of steady-state hydraulic gradients because plume transport occurs over time scales that are much larger than the time scales over which water levels and streamflow vary (Walter and Masterson, 2003). The large weight placed on plume observations (73.7 percent of the initial objective function) reflects the robustness of the observations as indicators of steady-state conditions. The large weight also reflects the need to match observed plumes given the intended use of the model to simulate advective transport at the JBCC. Different weights were assigned to subgroups within each broad type of observation to reflect differing degrees of confidence in different observations (table 2). Observation subgroups assigned a larger weight within their broader group include water levels in long-term monitoring wells, streamflows in major (primary) streams, and ages obtained from tritium profiles (table 2). Plume observations were divided into two groups based on a subjective evaluation regarding confidence in estimated plume center points along plume sections and determination of likely source areas. The importance of relative weighting and the effect of weighting on model calibration results and prediction are discussed in the section "Factors Affecting Model Calibration and Predictions."

The inverse-calibration regression satisfied the specified closure criteria after 22 iterations of the nonlinear regression. The use of a relative weighting scheme resulted in objective function values with no physical meaning; however, the value of the objective function decreased 25-fold, indicating a large improvement in fit to the observations. The degree of improvement in individual observation groups is a function of the weights assigned to the observations. Absolute mean residuals of water levels in long-term monitoring wells near the JBCC and streamflows in primary streams were substantially weighted in the preferred calibration, and the fit to the observed values for both improved substantially (fig. 36*A*). Absolute mean residuals, defined as the absolute values of the difference between observed values and simulated equivalents, decreased from 2.9 ft to about 0.5 ft for water levels and from about 3.0 to about 0.6 ft^3/s for streamflows. Model fit to observations of advective transport—plumes and groundwater ages—also improved (fig. 36*B*). The absolute mean residual for simulated plume-source locations, as determined from reverse particle tracking from observed plume center points, decreased from about 2,050 ft to about 382 ft, within the 400-ft discretization of the model (fig. 36*B*); the large improvement is a result of the large weight assigned to the observations. Groundwater ages estimated from tritium peaks and reverse particle tracking were considered the most reliable age measurements but were assigned relatively small weights in the preferred calibration (table 2). Absolute mean residual groundwater age from tritium peaks decreased from about 11 to about 7.5 years (fig. 36*B*). The difference between the position of the radial water-table divide and the observed location inferred from water levels and mapped plumes decreased from about 1,951 ft to about 656 ft. The difference in the location of the simulated transition from upward to downward gradients along the western shore of Ashumet Pond and observed location decreased from about 394 ft to about 20 ft.

Estimated Parameters

Native sensitivities are derivatives of simulated equivalents with respect to parameters and, when combined with observation weights, produce composite-scaled sensitivities for each parameter. These can be mapped to identify areas where a given set of observations and associated weights can best inform estimates of parameter values. Composite-scaled sensitivities are largest near plumes in the preferred calibration owing to the large weight assigned to those observations (fig. 37*A*; table 2). The use of water-level and streamflow observations alone typically results in low parameter sensitivities at depth in the aquifer (Walter and LeBlanc, 2008). The addition of observations of advective transport results in larger sensitivities at depth and better informed parameter estimation in deeper parts of the aquifer system (fig. 37*B*). The high parameter sensitivities near plumes also indicate that model predictions of advective transport in those areas are more reliable with inclusion of advective-transport observations.

The final conductivity parameters estimated at pilot points by the inverse calibration were interpolated by using kriging to generate hydraulic conductivity fields for each model layer. The final horizontal hydraulic conductivity of aquifer sediments in layer 7 (vertical group 2), which has a mean bottom altitude of about −40 ft (NGVD 29), ranged from about 10 ft/d to about 320 ft/d; the largest values were in the north-central part of the MPP and in the southwestern part of the aquifer, near the Falmouth ice-contact deposits and the southern part of the Buzzards Bay Moraine (figs. 3 and 38*A*). The final vertical hydraulic conductivities in layer 7 ranged from about 1 ft/d to about 100 ft/d and showed a spatial pattern generally similar to horizontal hydraulic conductivity (fig. 38*B*). The initial (precalibration) hydraulic conductivity generally decreased with depth (fig. 26*A*), which is consistent with the depositional model of the system, and the final hydraulic conductivities preserve that vertical trend. Mean horizontal hydraulic conductivities for vertical groups 1, 2, 3, and 4 were about 185, 125, 70, and 33 ft/d, respectively; the mean vertical hydraulic conductivities for the four groups were about 49, 23, 9, and 4 ft/d.

The use of regularization in the inverse calibration incorporates changes in estimated hydraulic conductivity from initial values as penalty terms in the objective function. Calibrated hydraulic conductivity values were within a range of values considered reasonable for the aquifer (between about 10 and 350 ft/d). The mean calibrated horizontal hydraulic conductivities of the four vertical groups were within 10 percent of mean initial values, indicating that the total transmissivity of the system was similar before and after calibration. However, the final estimated horizontal hydraulic conductivity values in vertical groups 1, 2, and 3 were within 10 percent of the initial values in less than about 17 percent of model cells and less than 30 percent of model cells in vertical group 4,

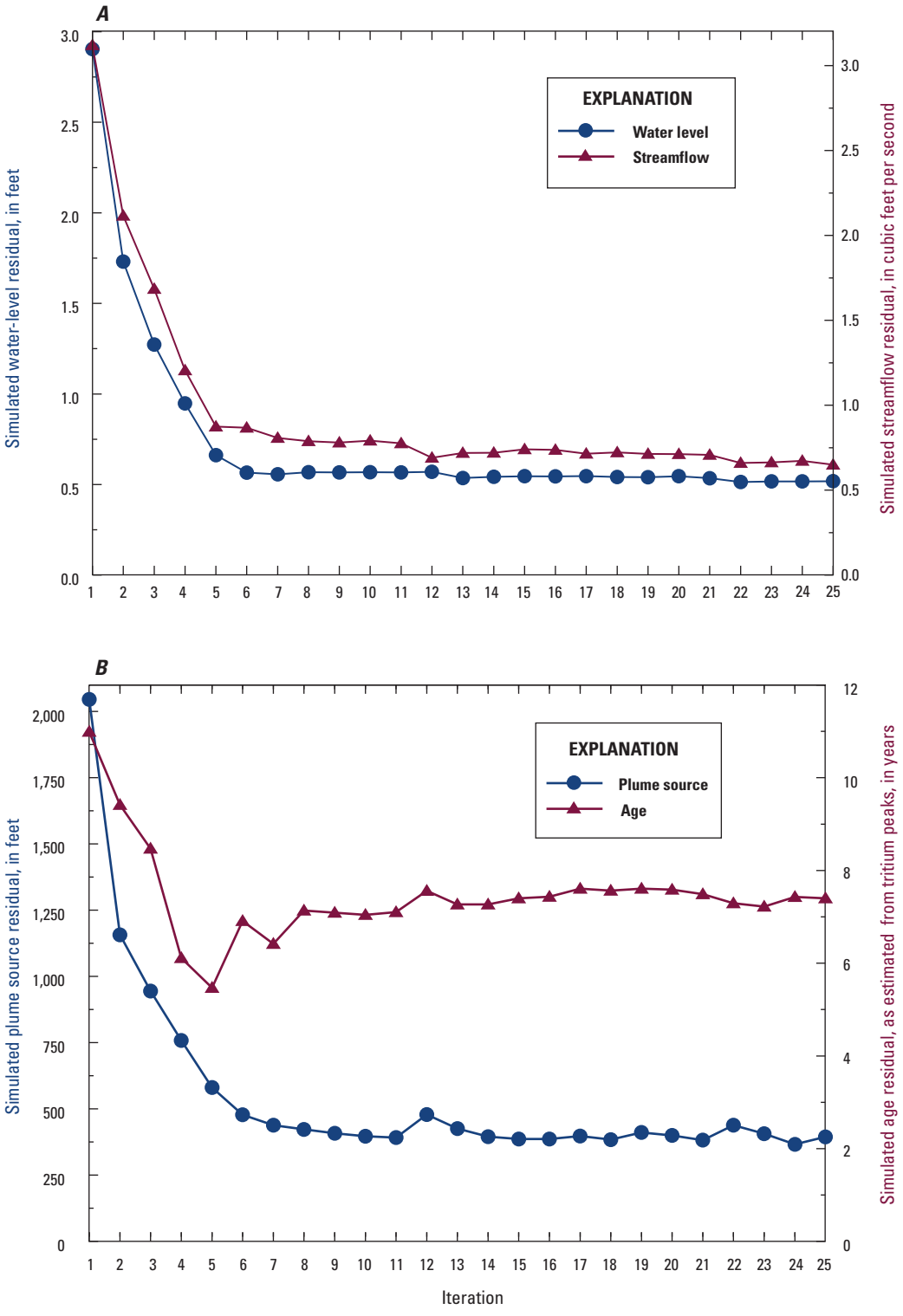

Figure 36. Change in absolute mean residuals with inverse-modeling iteration for the preferred calibration for *A*, long-term water levels and primary streamflows and *B*, plume sources and groundwater ages derived from tritium peaks.

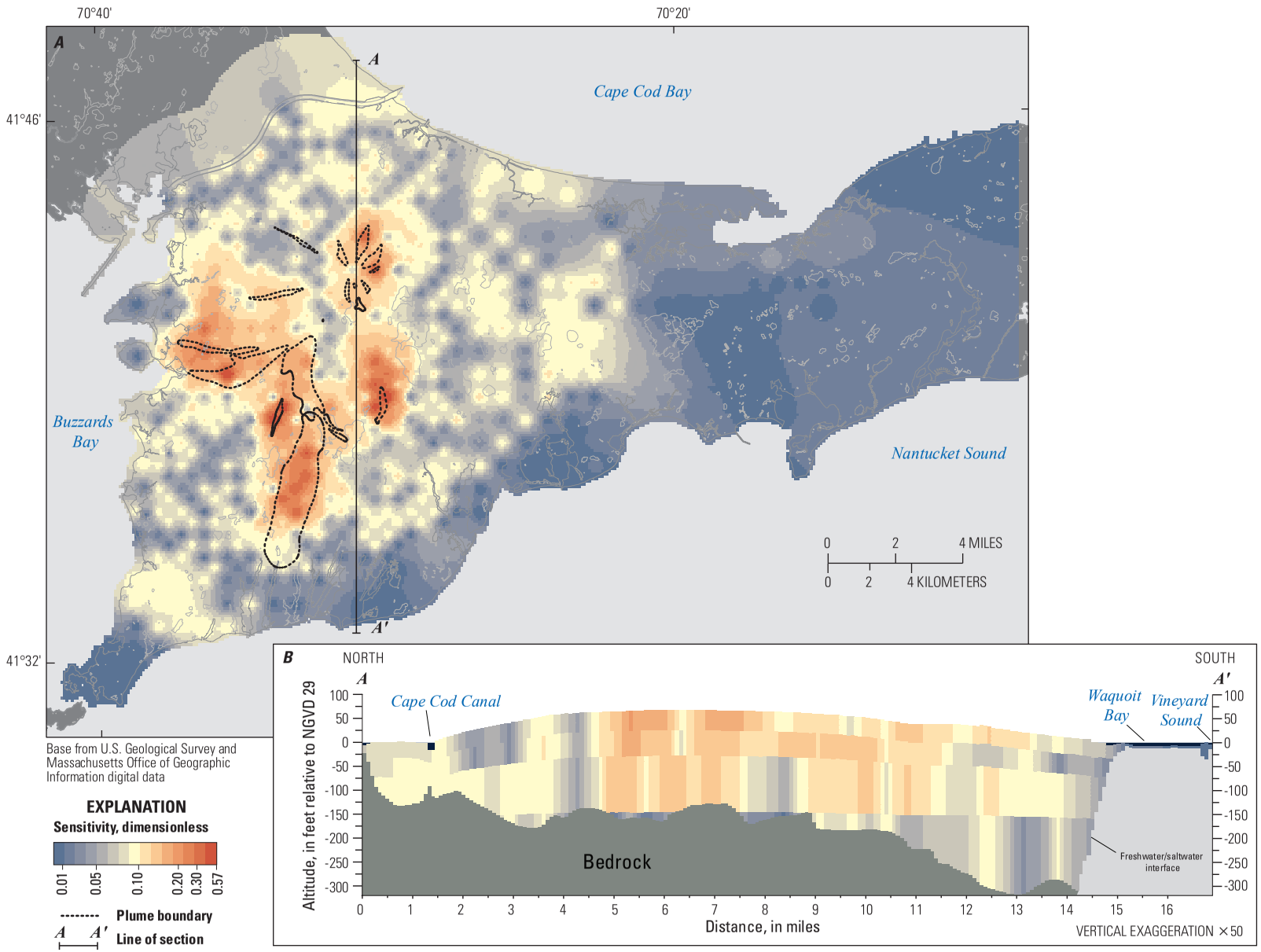

Figure 37. *A*, Parameter (horizontal hydraulic conductivity) sensitivity for layer 7 of the Joint Base Cape Cod regional groundwater flow model and *B*, sensitivities along a section through the Mashpee Pitted Plain, western Cape Cod, Massachusetts. NGVD 29, National Geodetic Vertical Datum of 1929.

***A.* Final horizontal hydraulic conductivity of layer 7**

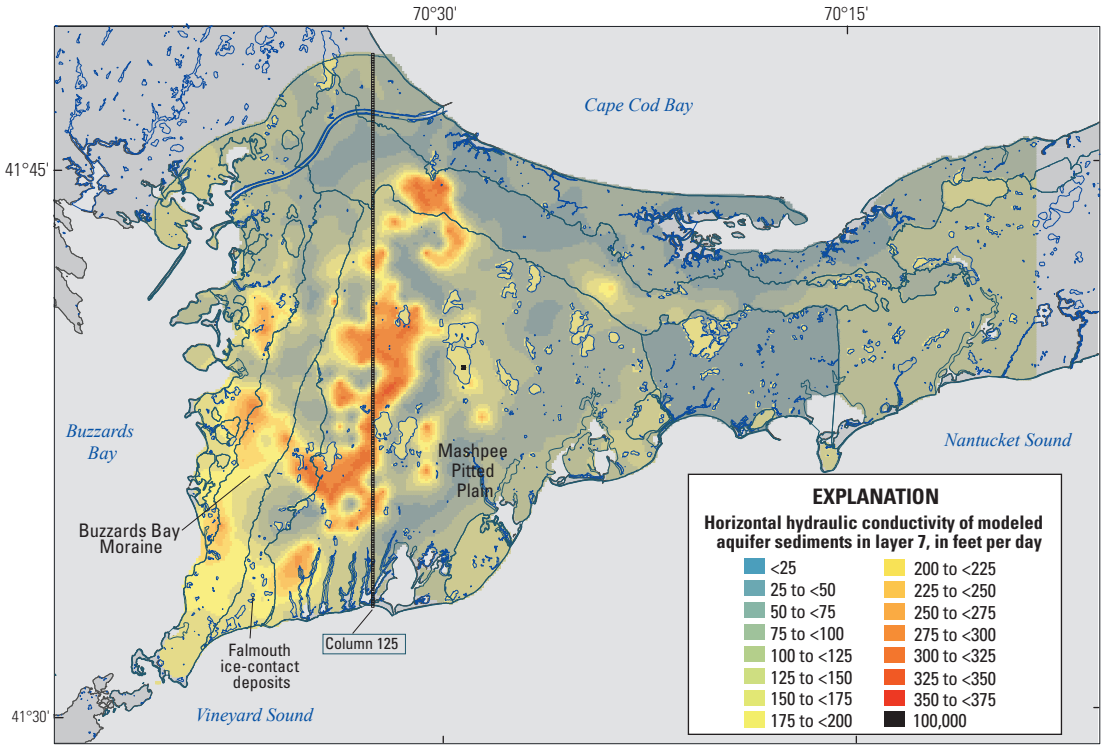

***B.* Final vertical hydraulic conductivity of layer 7**

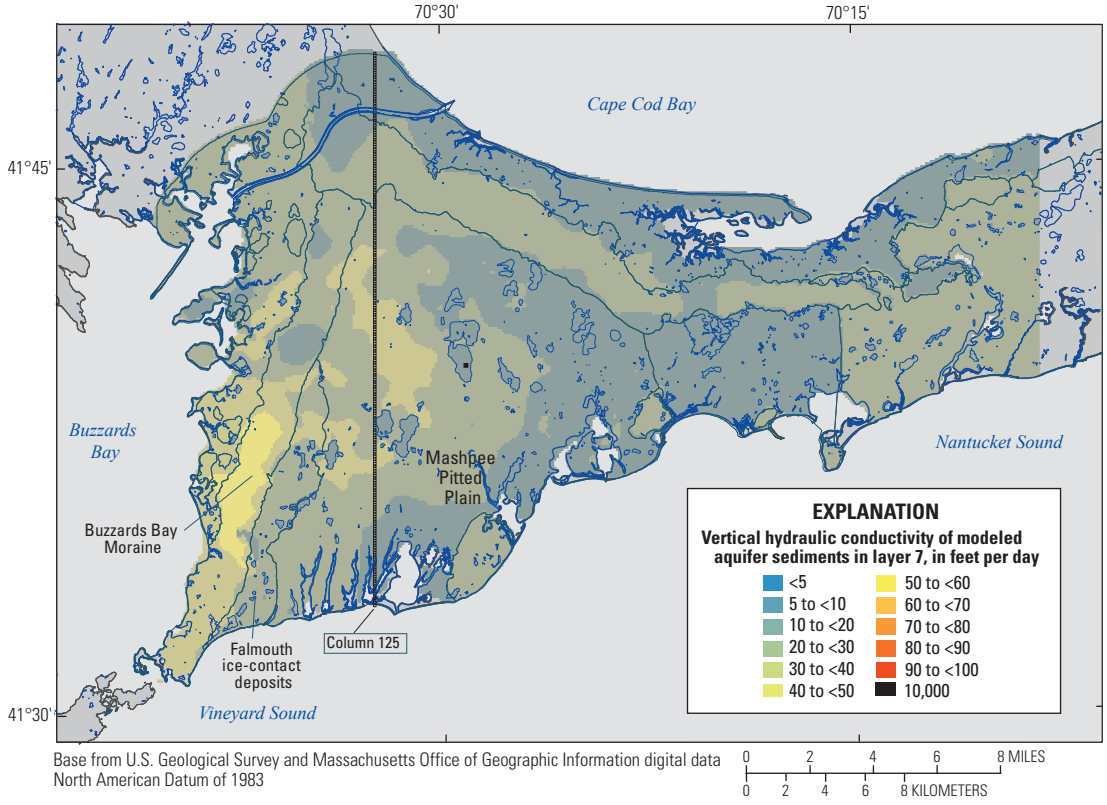

Figure 38. Final *A*, horizontal and *B*, vertical hydraulic conductivity fields for layer 7 of the Joint Base Cape Cod regional groundwater flow model, western Cape Cod, Massachusetts.

indicating that the distribution of hydraulic conductivity did change substantially. Initial and final vertical hydraulic conductivity values were within 10 percent in more than 70 percent of the modeled area in groups 1, 2, and 3 and in all of the modeled area in group 4. This is consistent with the generally smaller sensitivities of observations with respect to vertical hydraulic conductivity.

The largest change in hydraulic conductivity between initial and calibrated values was in vertical group 2, with about a 10-percent increase in mean horizontal hydraulic conductivity. The change in model layer 7, which is within that group, ranged from increases of more than 150 ft/d to decreases of more than 100 ft/d (fig. 39*A*). Areas where initial and final hydraulic conductivities were within 10 percent encompassed about 17 percent of the total model area in layer 7 (fig. 39*A*). The largest degree of variability generally was in the area around the JBCC where most observations were located, indicating the large effect that observations had on the estimated hydraulic conductivity field. Changes in vertical hydraulic conductivity were smaller, ranging from increases of more than 15 ft/d to decreases of more than 15 ft/d (fig. 39*B*). Differences between initial and final vertical hydraulic conductivities were within 10 percent in about 76 percent of the total modeled area in layer 7 (fig. 39*B*).

The inverse calibration produced hydraulic conductivity values that, while similar in mean value, generally were more spatially variable than initial values. The coefficients of variation (COVs) for initial horizontal hydraulic conductivity in vertical groups 1, 2, 3, and 4 were 3.7, 4.4, 2.3, and 3.0, respectively. The COVs for the calibrated values were substantially higher—37.8, 52.4, 76.1, and 34.5, respectively. The higher variability of the calibrated hydraulic conductivity fields indicates more simulated heterogeneity in the aquifer; this likely is the result of the highly weighted advective-transport observations near the JBCC and the associated large parameter sensitivities (fig. 37*A*). Coefficients of variation for the final vertical hydraulic conductivities also were higher—4.6, 2.5, 2.2, and 0.8 for vertical groups 1, 2, 3, and 4, respectively—than COVs for the initial values—3.8, 1.6, 0.04, and 0.04 for vertical groups 1, 2, 3, and 4, respectively—indicating more spatial variability in the final values than in the initial values. These differences in the COVs for vertical hydraulic conductivities were smaller because of the smaller sensitivities and lesser amounts of change observed than for the COVs of horizontal hydraulic conductivities. The largest increase in variability, as indicated by coefficients of variation, was in vertical group 3 (fig. 40*A*); the coefficient of variation increased from 2.3 to 76.1 for horizontal hydraulic conductivity and from 0.04 to 2.2 for vertical hydraulic conductivity. Mean values of initial and final hydraulic conductivity were similar, 61 and 71 ft/d, respectively; however, the values were more variable. The vertical heterogeneity near the JBCC (column 125) also was much larger in final values (fig. 40*A*) than in initial values (fig. 26*A*) owing to the advective-transport observations and the larger associated sensitivities (fig. 37*B*). The largest changes between initial and final values (increases greater than 250 ft/d) also were within group 3 (layers 10–20) (fig. 40*B*). The large changes within the group were a result of the highly weighted advective-transport observations; parameter sensitivities associated with the observations generally were large in vertical group 3 (fig. 37*A*). Inverse calibrations using water levels and streamflows generally resulted in low parameter sensitivities in deeper parts of the aquifer and little change during calibration because most groundwater flow occurred in shallower parts of the aquifer (Walter and LeBlanc, 2008). The results indicate that inclusion of highly weighted advective-transport observations increases parameter sensitivities at depth and provides information allowing for the estimation of hydraulic conductivity at depth.

Prior information was included in the inverse calibration as weights on initial values, formally as regularization, and as constraints on the estimated parameters. These constraints on parameters were included to ensure that estimated parameters are reasonable based on general knowledge of the aquifer system from aquifer tests, previously calibrated models, and conceptual models of the hydrogeologic framework. Constraining parameters can result in a degraded fit to observations but is necessary to avoid estimated hydraulic conductivity fields that violate that prior knowledge. Upper constraints of 300 and 100 ft/d were placed on horizontal and vertical hydraulic conductivity parameters, respectively, in all four vertical groups. These values are typical of coarse sand and allow for the presence of coarse sediments at depth in the aquifer, such as have been observed near some contaminant plumes. Lower constraints on horizontal hydraulic conductivity in vertical groups 1, 2, 3, and 4 were 100, 70, 30, and 10 ft/d, respectively; vertical hydraulic conductivity had lower constraints of 10, 5, 2, and 1 ft/d, respectively. These values generally are based on the depositional model of western Cape Cod (Masterson and others, 1997a). The lower constraints were increased for parameters—100 ft/d for vertical groups 1 and 2 and 70 ft/d for vertical groups 3 and 4—located within 2,000 ft of a water-supply well; it was assumed that local aquifer sediments are suitably coarse to allow pumping of the water-supply well. The upper and lower constraints on horizontal hydraulic conductivity were reached at 546 and 610 out of 2,286 parameters, respectively. Upper constraints on vertical hydraulic conductivity were reached at 7 parameters and lower constraints at 6 parameters, which is consistent with the smaller sensitivities and relatively small changes in those parameters.

Estimated parameters also included leakances at stream boundaries and ponds, porosity, and recharge. The estimated vertical hydraulic conductivity of stream-bottom sediments was about 1.0 ft/d, a change of about 1 percent from the initial value. Likewise, the estimated horizontal hydraulic conductivity of pond-bottom sediments was about 97 ft/d, similar to the initial value of 100 ft/d. The estimated porosity was about 0.29, similar to the initial value and consistent with field observations (Garabedian and others, 1988). Estimated recharge reached its upper constraint of 30.0 in/yr; a constraint on the recharge parameter was necessary owing to its large

***A*. Difference between initial and final horizontal hydraulic conductivity**

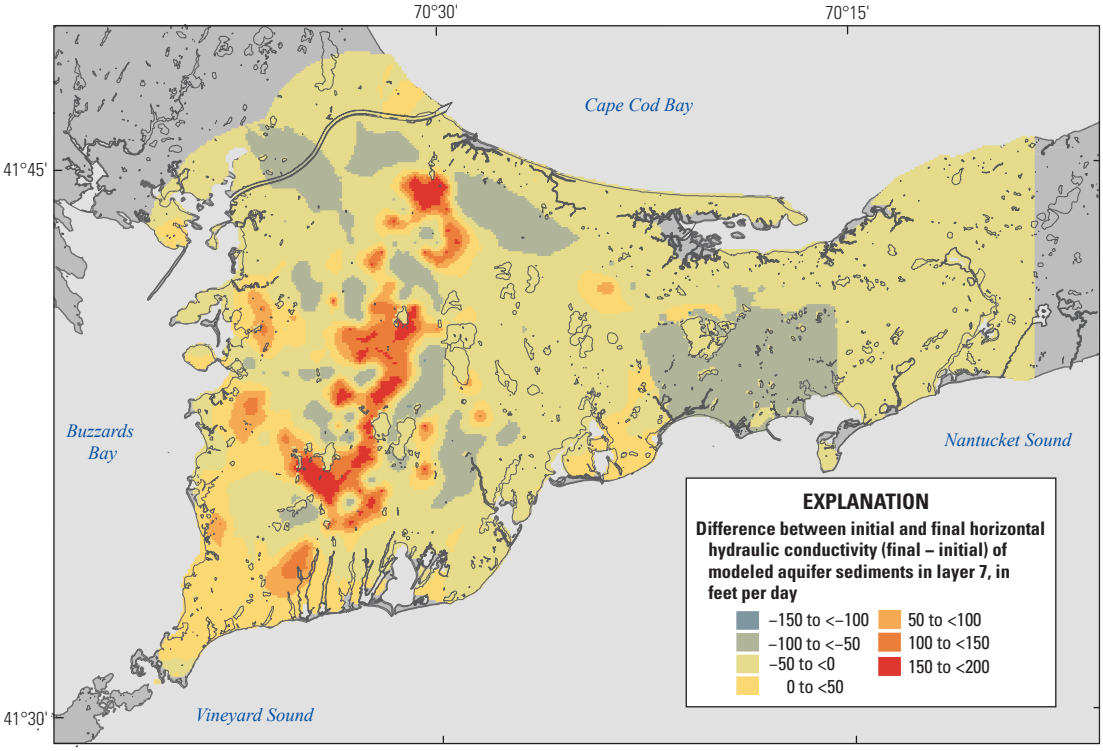

***B*. Difference between initial and final vertical hydraulic conductivity**

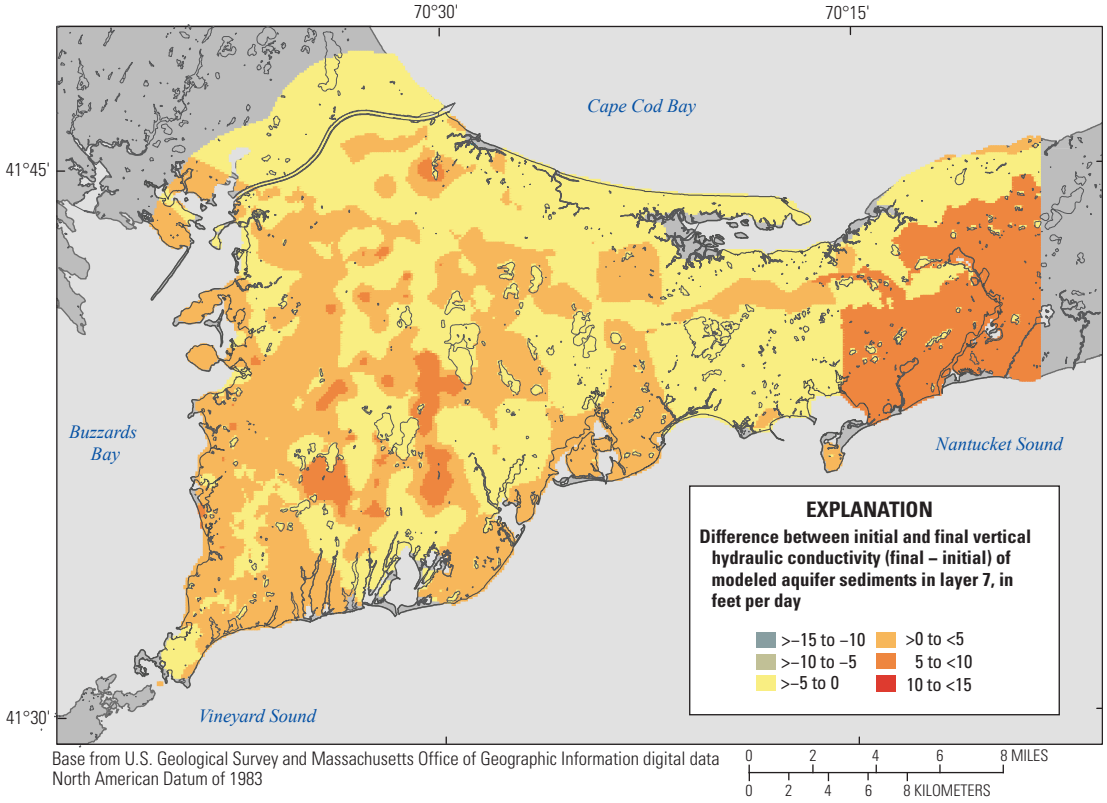

Figure 39. Differences between initial and final *A*, horizontal and *B*, vertical hydraulic conductivity fields for layer 7, western Cape Cod, Massachusetts.

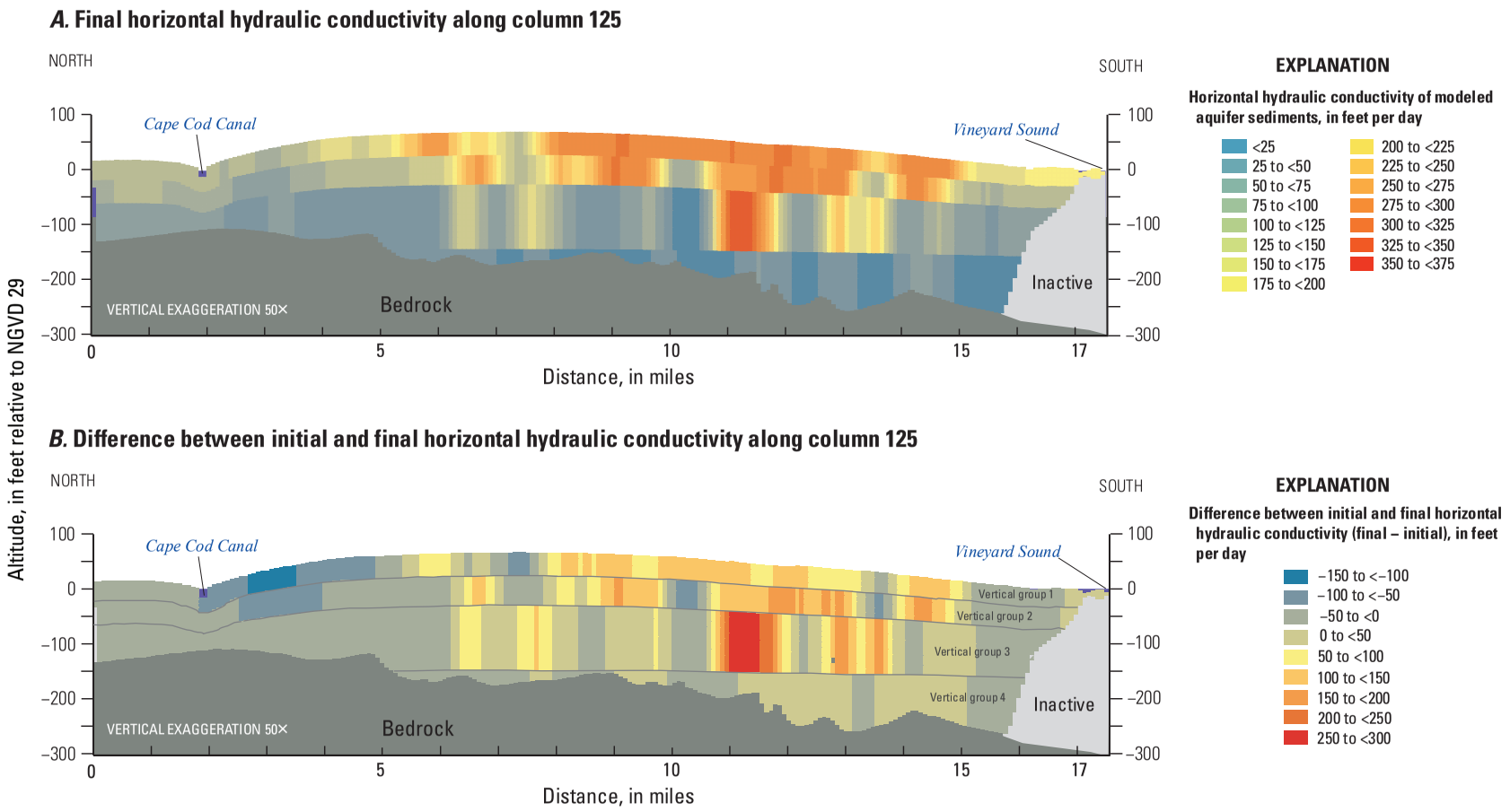

Figure 40. *A*, Final horizontal hydraulic conductivity field and *B*, differences between the initial and final horizontal hydraulic conductivity fields (section oriented north to south through the Mashpee Pitted Plain), for the model layers in vertical groups 1–4 (assigned number increases stratigraphically from top to bottom), western Cape Cod, Massachusetts. Section location shown on figure 38. NGVD 29, National Geodetic Vertical Datum of 1929.

sensitivity and potential correlation with other parameters. The estimated recharge rate was about 2.75 in/yr higher than in previously calibrated models.

Comparison of Observations and Simulated Equivalents

The model fit refers to the agreement between observed hydrologic conditions, either measured or derived, and the simulated equivalents obtained from model output files or derived from model outputs and particle tracking. The goodness of fit is an indicator of the suitability of a model to make reasonable predictions. Five types of observations, as discussed previously in the "Calibration Results" section, were used to calibrate the regional model: measured water levels, streamflows, traveltimes as estimated from groundwater ages, contaminant source location as estimated from plume sections and reverse particle tracking, and location of hydraulic-gradient divides as estimated from field measurements and plume paths.

Four different groups of water-level measurements in wells were used in the calibration: long-term measurements near the JBCC and to the east of the JBCC, and intermittent (partial-record) measurements made by the USGS and the JBCC. The groups were assigned weights based on the confidence in their representation of steady-state conditions and the desire for a close fit to observations near the JBCC; the largest weight was placed on long-term wells near the JBCC (table 2). Observed and simulated water levels generally were in close agreement (fig. 41*A*). Absolute mean residuals were lowest, 0.54 ft, for the long-term wells near the JBCC. The absolute mean residuals for the remaining groups—long-term wells to the east of the JBCC and wells intermittently measured by the USGS and the JBCC—were 1.17, 0.90 and 1.01 ft, respectively. The residuals had a mean of about −0.2 ft and were normally distributed. There were no discernible trends in the residuals with respect to simulated values, indicating little spatial bias (fig. 41*B*). The residuals show some clustering of over- and under-predicted water levels, particularly near plume observations (fig. 42), indicating some small amount of spatial bias or an effect on the fit to water-level observations from the large weight placed on plume observations.

Measurements of streamflow at 10 locations were included in the inverse calibration, including long-term average flow at a USGS-operated streamgage on the Quashnet River (fig. 8). The absolute mean residual between observed streamflow and simulated equivalents is 0.707 ft^3/s (61,129 cubic feet per day [ft^3/d]), indicating a good fit between observations and simulated equivalents (fig. 43). Measurements were made at 15 additional sites but were not included in the inverse calibration owing to the limited period of record, anomalous streamflow values, or the possible effects of unknown pond outflows on the measurements. The absolute mean residual of streamflows not included in the calibration was about 2.16 ft^3/s (186,202 ft^3/d). There was no discernible pattern in the spatial distribution of the streamflow residuals (fig. 42).

Two groups of plume observations were included in the inverse calibration: 23 observations estimated from plume sections that were determined to be reliable (Plumes 1 in table 2) and 9 observations with less confidence and smaller assigned weights (Plumes 2 in table 2). The observations are in the approximate centers of the source areas for the plumes. The simulated equivalents were determined by reverse particle tracking from the approximate center of mass along the plume sections to the point of recharge, as estimated as the center point of mapped source area for each plume. The residual is the distance, in feet, between the two points. The absolute mean residual was 382 ft for the higher weighted plume group and 338 ft for the lower weighted group. Both are less than the horizontal discretization of the model (400 ft). The largest residual was 1,117 ft for an observation in the Ashumet Valley plume. The effect of these residuals on predictions of advective transport, an intended use of the model, can be evaluated by comparing forward particle tracks from the observed source locations to plume geometries, as indicated by mapped plume boundaries and sections (fig. 17). The forward particle tracks from simulated recharge points (to discharge points) generally are in good agreement with the mapped plumes (fig. 44). The use of particle tracking allows for a good fit to vertical plume geometries. The predicted paths of the Demo-1 plume (fig. 45*A*) and the Ashumet Valley plume (fig. 45*B*) are within and close to the delineated plume centers along the lengths of the plumes. The absolute mean residual for observed tritium peaks—the most highly weighted groundwater-age observations—was about 7.5 years. Residuals for ages estimated from $^3He/^3H$ and CFCs were 13.4 and 17.9 years, respectively.

The highly weighted plume observations have a strong effect on the estimated hydraulic conductivities of aquifer sediments. The downgradient part of the Demo-1 plume, as indicated by perchlorate concentrations, stays in the shallow part of the aquifer and may rise in the aquifer near its downgradient extent (fig. 45*A*). The effect of a highly weighted observation in that part of the plume results in lower hydraulic conductivity with depth, which causes increased groundwater flow in the shallow part of the aquifer and a rise in the predicted plume path (fig. 45*A*). The Ashumet Valley plume also is in the shallow part of the aquifer, and estimated hydraulic conductivity is lower at depth, keeping flow paths shallow and similar to those indicated by the observed plume (fig. 45*B*). The downgradient part of the Demo-1 plume may be shallower in the system owing to local silt lenses that cause local upward flow paths (fig. 45*A*). Silt lenses within coarser parts of the aquifer, referred to as "hanging silts," are part of the lithologic data used in the estimation of initial hydraulic conductivity; however, they are not explicitly represented in the regional model. The simulated upward flow path near or above the silts is matched by the model, primarily by lowering hydraulic conductivity at depth rather than by representing the local-scale silt lenses. The effect of local-scale heterogeneity on model calibration is discussed in "Factors Affecting Model Calibration and Predictions."

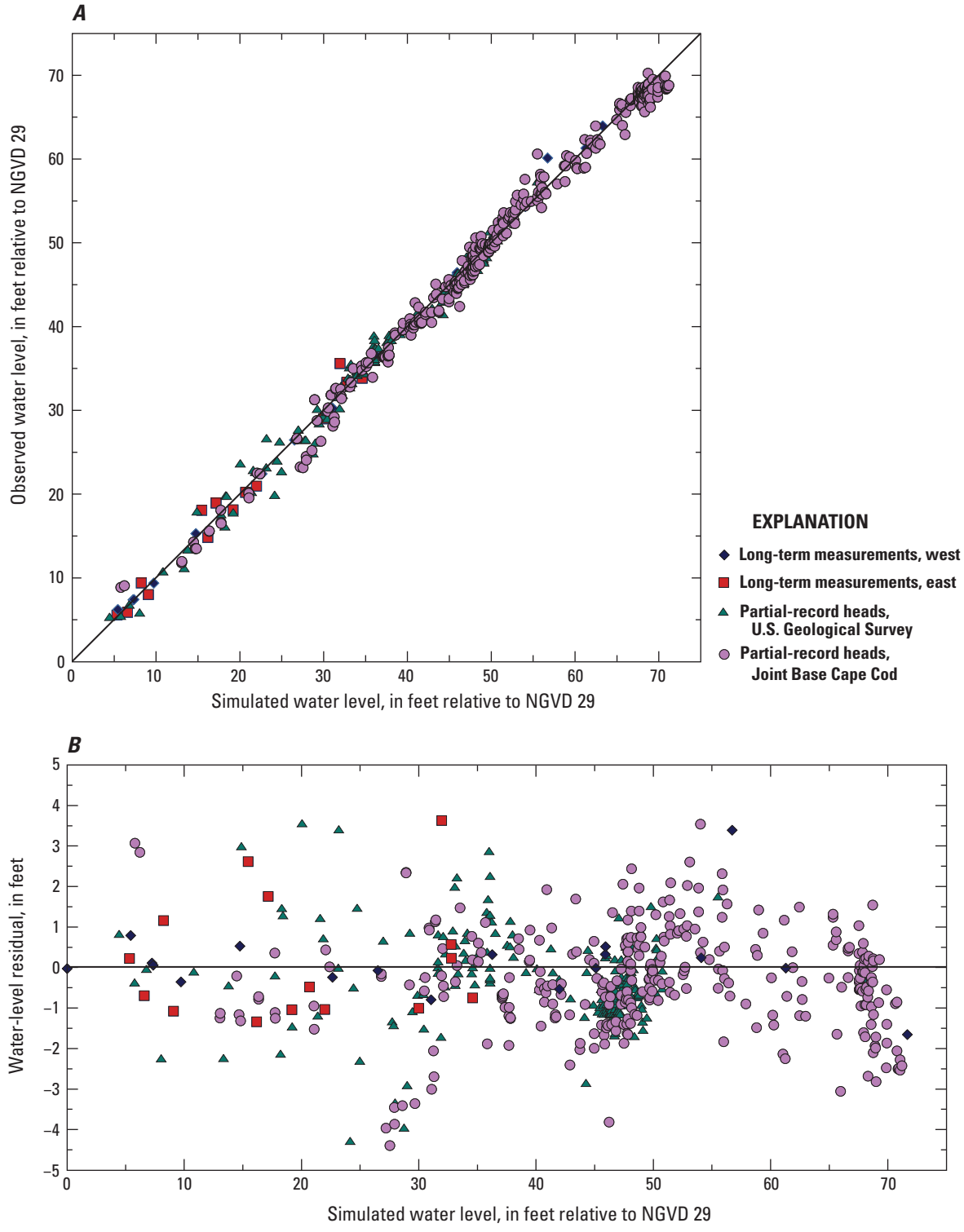

Figure 41. *A*, Observed water levels and simulated equivalents and *B*, distribution of hydraulic-head residuals with respect to simulated equivalents. NGVD 29, National Geodetic Vertical Datum of 1929.

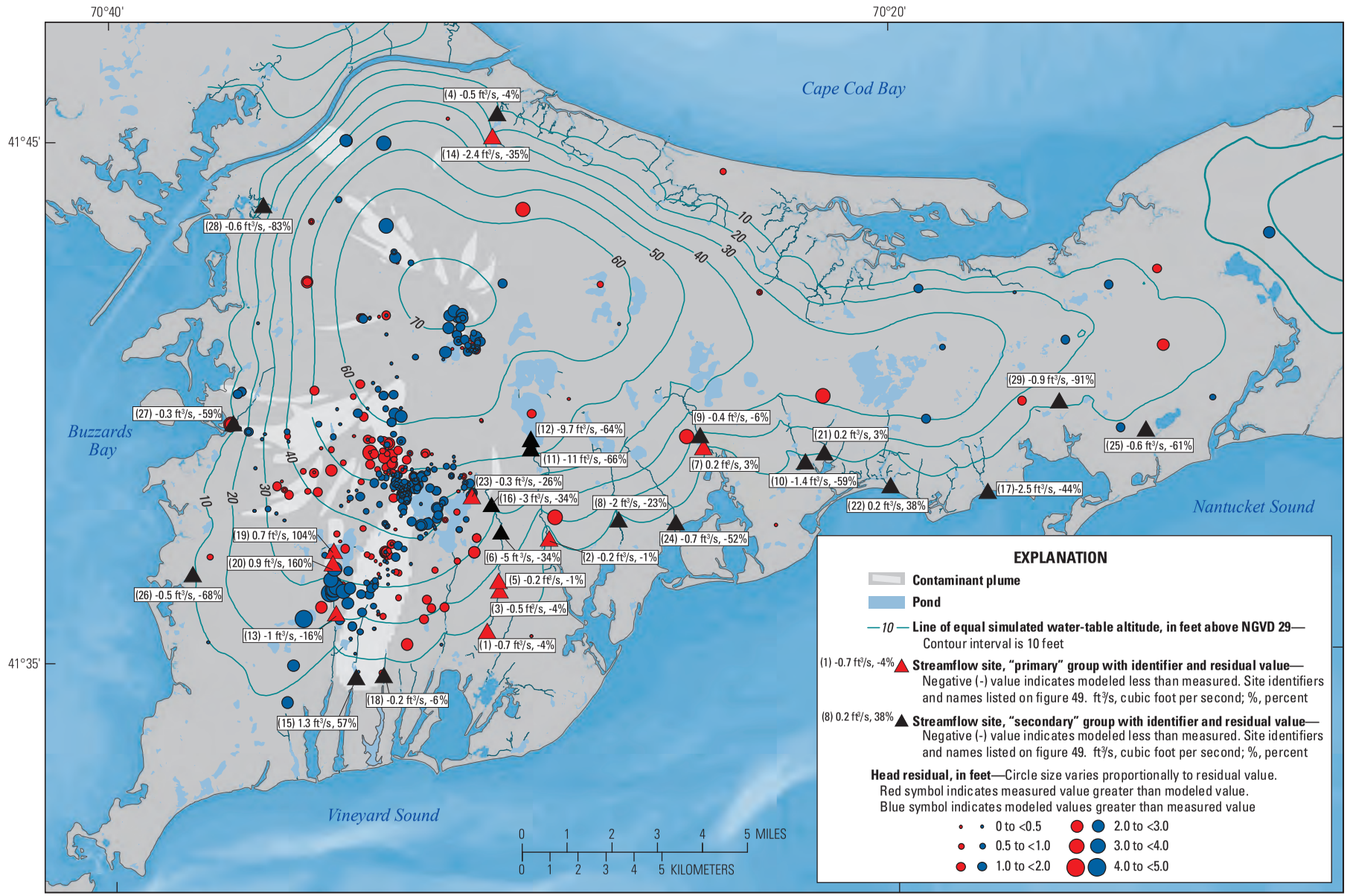

Base from U.S. Geological Survey and Massachusetts Office of Geographic Information digital data
North American Datum of 1983

Figure 42. Water-level and streamflow residuals for the calibrated Joint Base Cape Cod regional groundwater flow model of western Cape Cod, Massachusetts. NGVD 29, National Geodetic Vertical Datum of 1929.

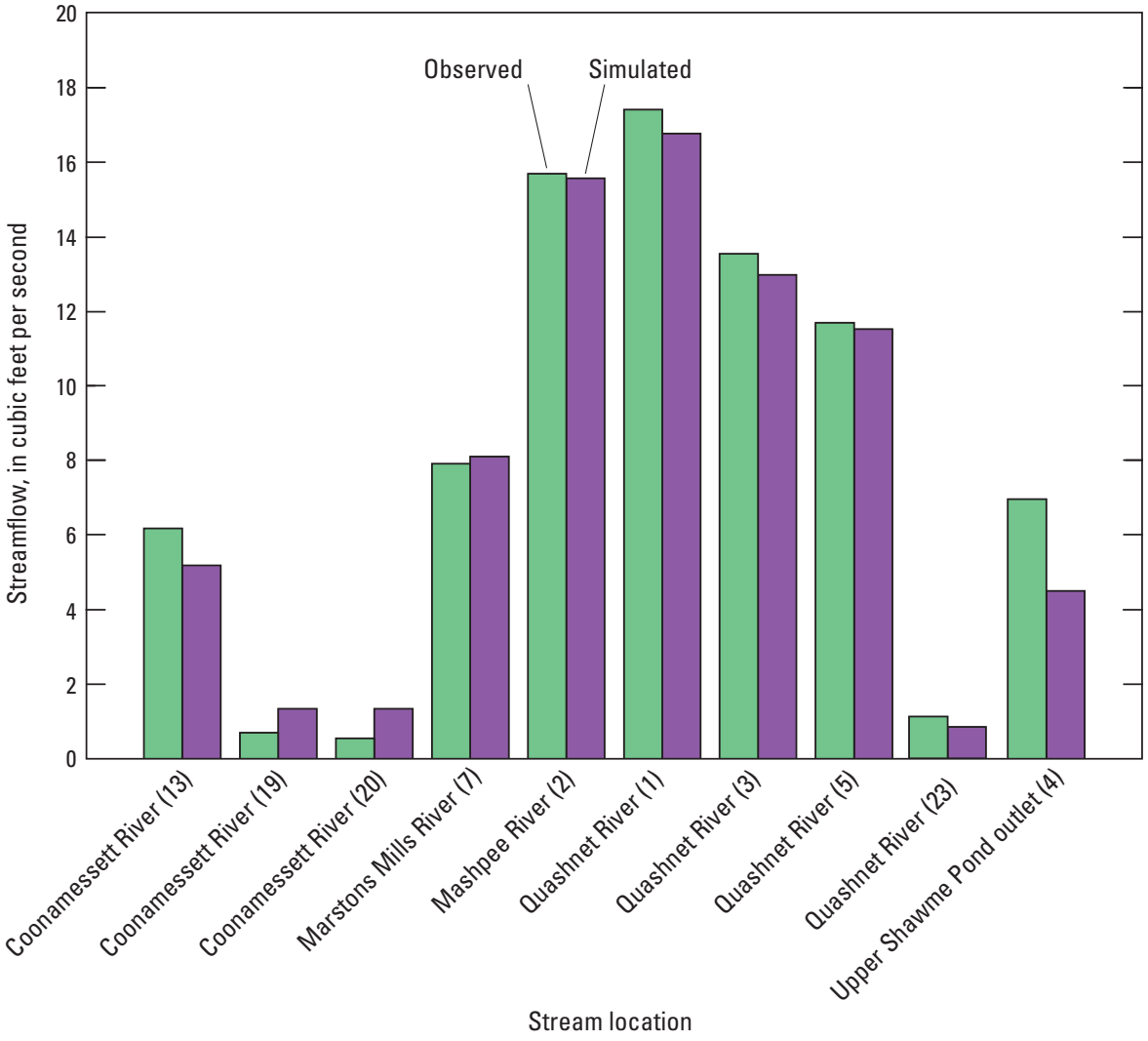

Figure 43. Observed and simulated streamflows for highly weighted streams, western Cape Cod, Massachusetts. Numbers in parentheses refer to site identifiers in figure 49.

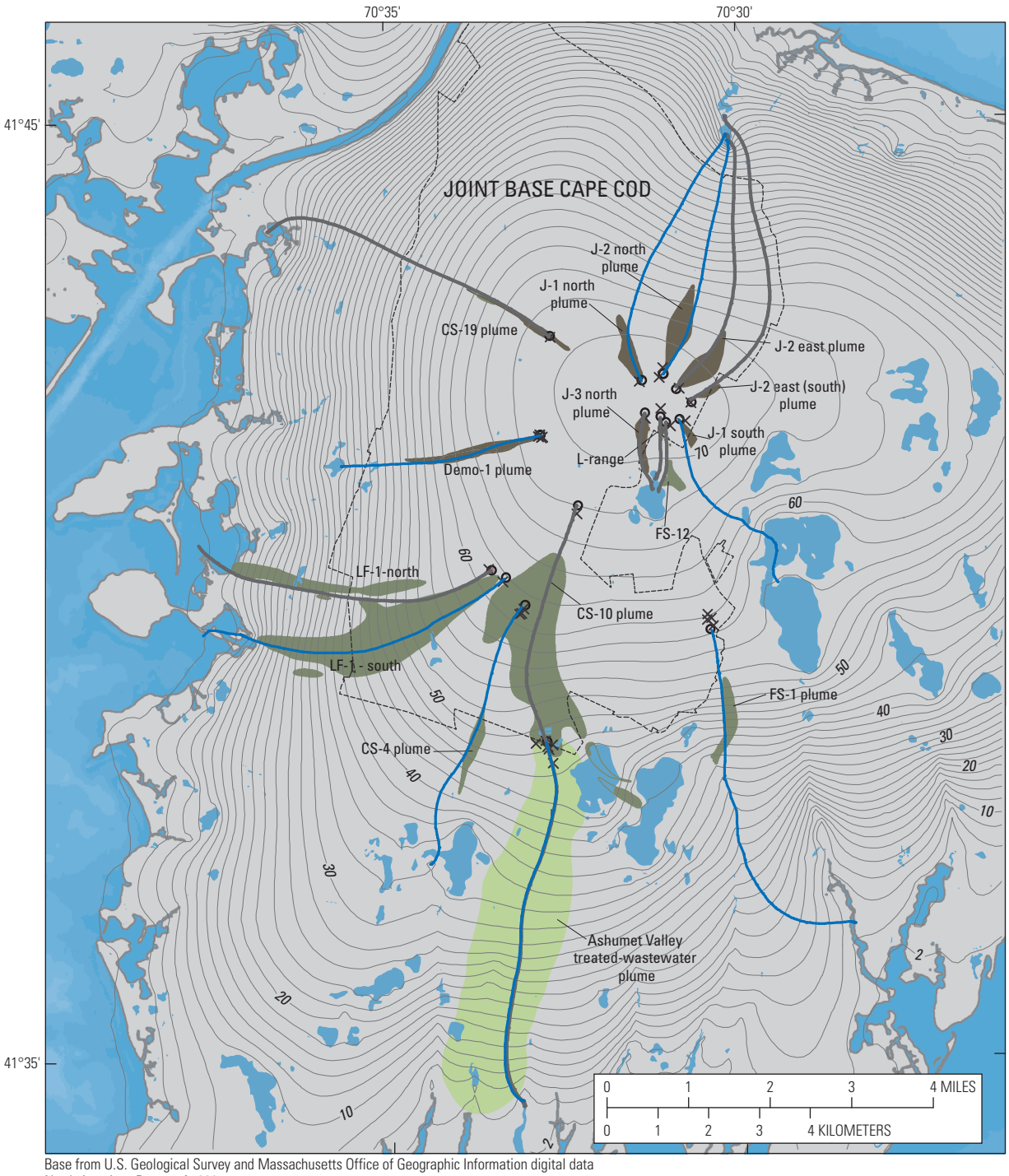

Base from U.S. Geological Survey and Massachusetts Office of Geographic Information digital data
North American Datum of 1983

EXPLANATION

- **Contaminant plume**—Army National Guard (2007a, b)
- **Contaminant plume**—Air Force Civil Engineer Center (2007)
- **Ashumet Valley treated-wastewater plume**—Barbaro and others (2013)
- —10— **Line of equal simulated water-table altitude (layer 4), in feet above NGVD 29**—Contour interval is 2 feet
- **Simulated forward particle track from source**—Plumes 1 group
- **Simulated forward particle track from source**—Plumes 2 group
- **Observed source area**
- **Simulated source area indicated by reverse particle tracking**

Figure 44. Plume locations, simulated forward particle tracks from observed sources, and final locations of simulated source areas obtained by reverse particle tracking from approximate observed plume centers of mass, western Cape Cod, Massachusetts. NGVD 29, National Geodetic Vertical Datum of 1929.

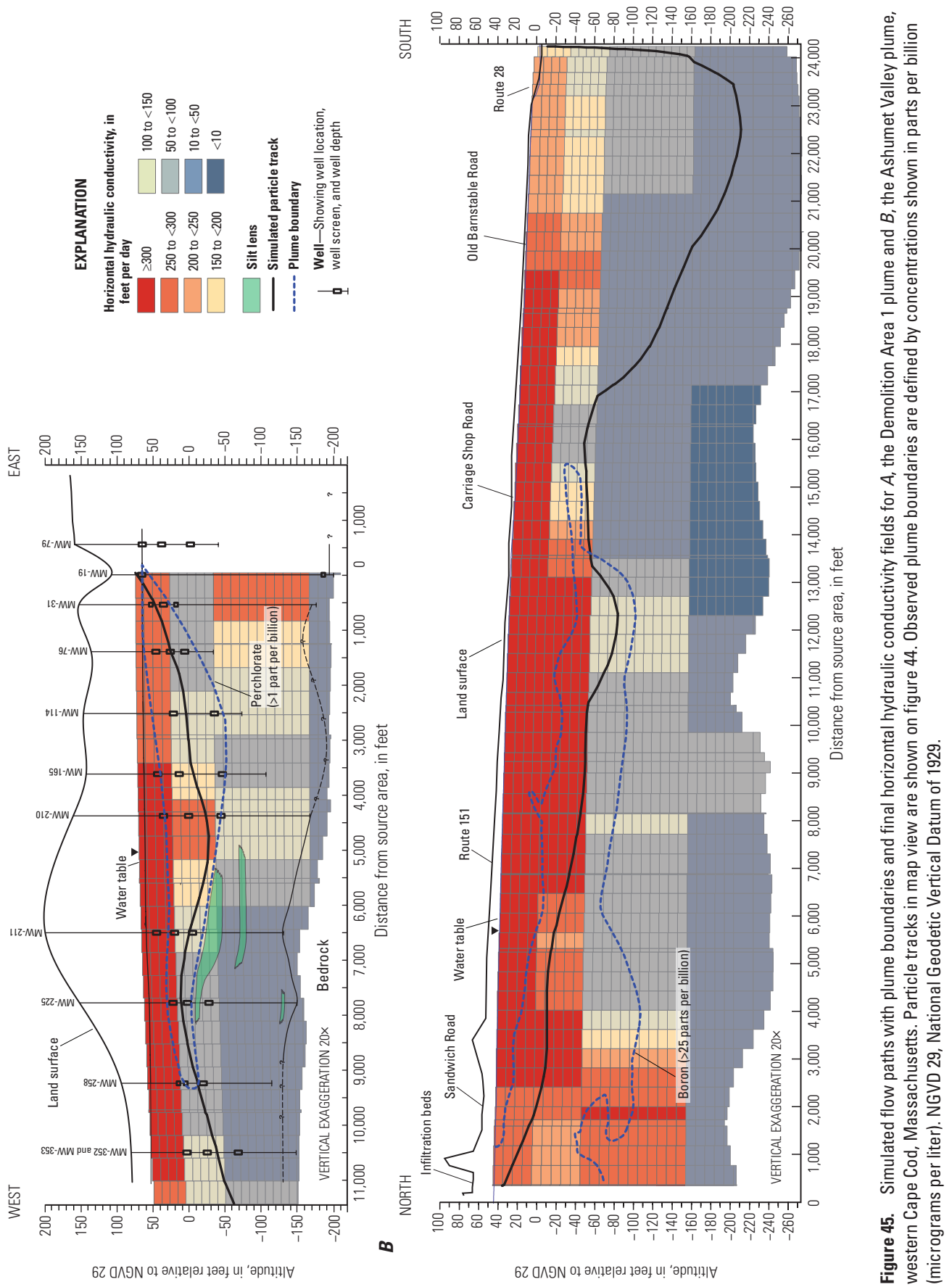

Figure 45. Simulated flow paths with plume boundaries and final horizontal hydraulic conductivity fields for *A*, the Demolition Area 1 plume and *B*, the Ashumet Valley plume, western Cape Cod, Massachusetts. Particle tracks in map view are shown on figure 44. Observed plume boundaries are defined by concentrations shown in parts per billion (micrograms per liter). NGVD 29, National Geodetic Vertical Datum of 1929.

Simulated Current (2010) Hydrologic System and Effects of Future (2030) Water-Supply Withdrawals and Wastewater Disposal

The calibrated steady-state model produces simulated heads and cell-by-cell water budgets that can improve understanding of the flow system under which contaminants are transported from sources on the JBCC. Hydraulic stresses representing current steady-state (2010) pumping and wastewater return-flow stresses (fig. 18) were simulated by the model to improve understanding of the hydrologic system and the physical transport of contaminants in the aquifer. Future (2030) pumping and return-flow stresses were simulated by the model to determine the effects of future pumping and return flow on the aquifer system, including changes in water levels, streamflows, hydraulic gradients, and advective-transport patterns within and near the JBCC.

Current (2010) Hydrologic Conditions

Currently (2010), about 332 Mgal/d of water recharges the simulated aquifer, which includes the Sagamore flow lens, parts of the adjacent Monomoy flow lens, and parts of Plymouth-Carver aquifer. About 52 and 43 percent of the recharged water discharges to coastal waters and streams, respectively. About 5 percent is withdrawn for public supply; most (about 85 percent) of the withdrawn water re-enters the aquifer as wastewater return flow, resulting in a total consumptive loss of less than 1 percent.

The current (2010) water table, as simulated in the model, has a maximum altitude of about 71 ft above NGVD 29 in the northwestern part of the flow lens (fig. 46). The location of the maximum water-table altitude represents a radial groundwater flow divide. Flow is radially downgradient from the divide, and all possible gradient directions occur in the aquifer. Horizontal hydraulic gradients near the radial water-table divide are small (less than 0.001) and increase in magnitude—to more than 0.01—near coastal boundaries, ponds, and streams. Horizontal gradients explain patterns of advective transport observed in the aquifer, including the radial pattern of mapped plumes around the water-table divide in the northern part of the JBCC (fig. 2*B*).

Vertical hydraulic gradients generally are upward near streams, ponds, and the coast where groundwater discharges and downward away from boundaries owing to recharge at the water table and at the downgradient sides of ponds (fig. 47*A*). Groundwater fluxes generally decrease and travel times increase exponentially with depth in an unconsolidated, porous, homogenous aquifer (Vogel, 1967). In addition, most groundwater flow in the aquifer underlying Cape Cod occurs in shallower parts of the aquifer where aquifer sediments generally are coarser.

Patterns of flow through the aquifer near the downgradient extent of the Ashumet Valley plume reflect this regional trend in the vertical distribution of groundwater flux, as well as the local effects of surface-water features (fig. 47*B*). The cumulative flow through the aquifer, expressed as a percentage of total flow through the saturated thickness, defined as flow perpendicular to a section generally transverse to groundwater flow, generally exceeds 50 percent within about the upper 20 percent of the aquifer, indicating that the amount of groundwater flux in the upper 20 percent of the aquifer is about the same as the flux in the bottom 80 percent. Groundwater flux generally is greater through the shallowest parts of the aquifer near surface-water features such as streams than elsewhere in the aquifer because flow is focused near discharge boundaries (fig. 47*B*). Ponds, which are flow-through features, have the largest effect on the vertical distribution of groundwater flux. Groundwater flux is focused through ponds, resulting in a region of small fluxes beneath them; for example, about 86 percent of total groundwater flux occurs within the upper 5 percent of the saturated thickness near Jenkins Pond to the south of the JBCC (fig. 47*B*). Groundwater flux is proportional to velocity and, therefore, inversely proportional to groundwater age (the proportionality constant is porosity). Groundwater traveltimes and associated ages in the aquifer can exceed several hundred years (Walter and others, 2004). Young groundwater, defined here as less than 50 years old (the approximate age of observed tritium peaks in groundwater), generally is within the shallow upper half of the saturated thickness (fig. 47*B*). The depth of young water shows spatial trends similar to trends in the vertical distribution of groundwater fluxes. Young water generally is shallower near surface-water features where groundwater fluxes are higher and extends deeper in the aquifer away from surface-water features. The depth to which young groundwater extends into the aquifer also is a function of the depth to bedrock and the saturated thickness of the aquifer. Young groundwater extends to near bedrock in some areas to the west of Jenkins Pond where the altitude of the bedrock surface is shallow (about −150 ft relative to NGVD 29), whereas young groundwater to the east where the bedrock surface is deeper than −330 ft relative to NGVD 29 is present only in the upper 25 percent of the saturated thickness of the aquifer (fig. 47*B*). The distribution of groundwater flux in the aquifer explains patterns of advective transport observed in the aquifer, including observations that contaminant plumes often are within the shallow parts of the aquifer (fig. 45).

Effects of Future (2030) Pumping on Water Levels and Streamflows

Groundwater withdrawals from the Sagamore flow lens are projected to increase by about 6.1 Mgal/d by 2030, which represents an increase of about 30 percent; the largest projected increase for a town, about 2.05 Mgal/d, is in Barnstable to the east of the JBCC (fig. 19). Projected increases in the

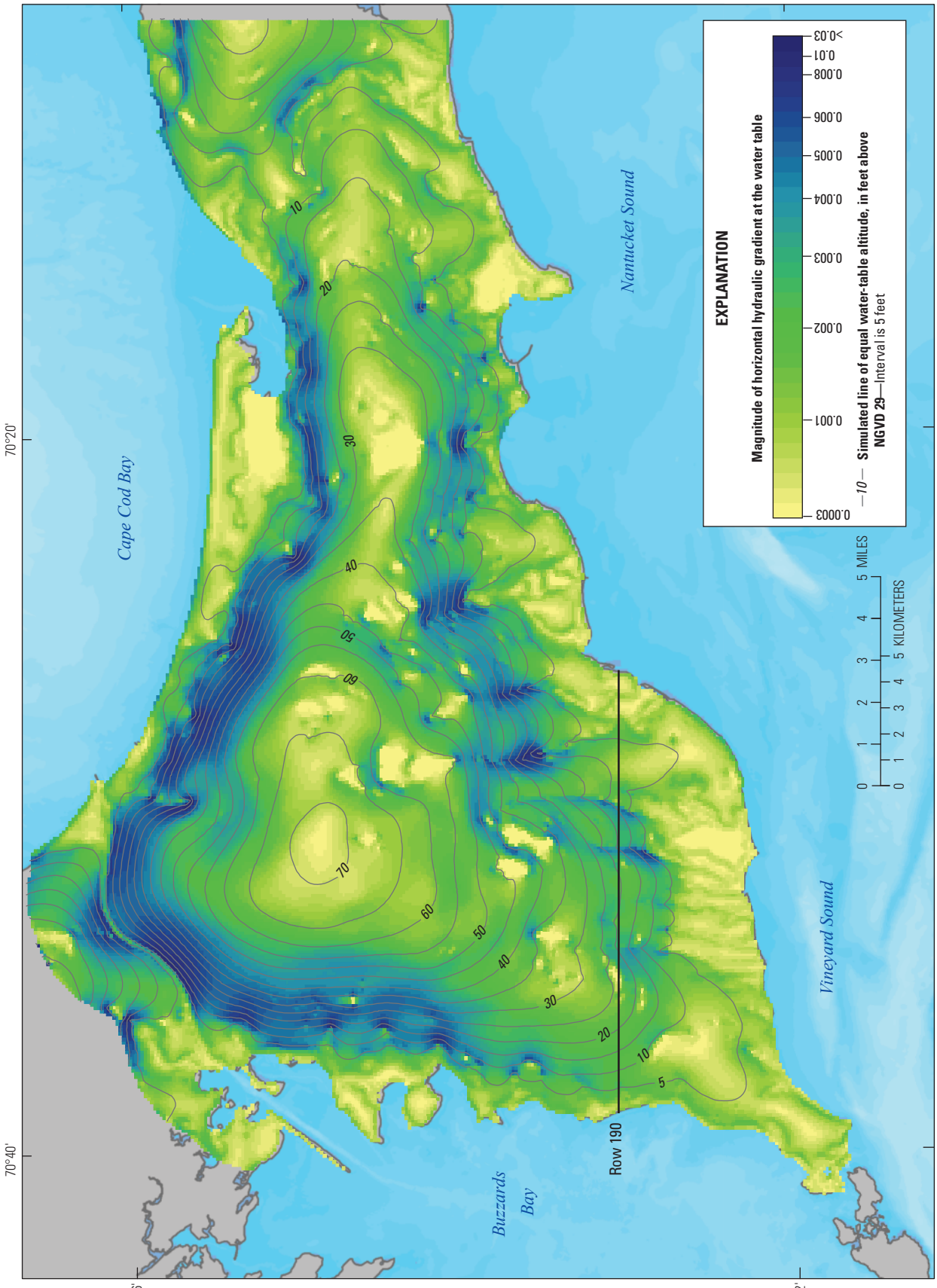

Figure 46. Simulated current (2010) water table and magnitude of the horizontal hydraulic gradient, western Cape Cod, Massachusetts. NGVD 29, National Geodetic Vertical Datum of 1929.

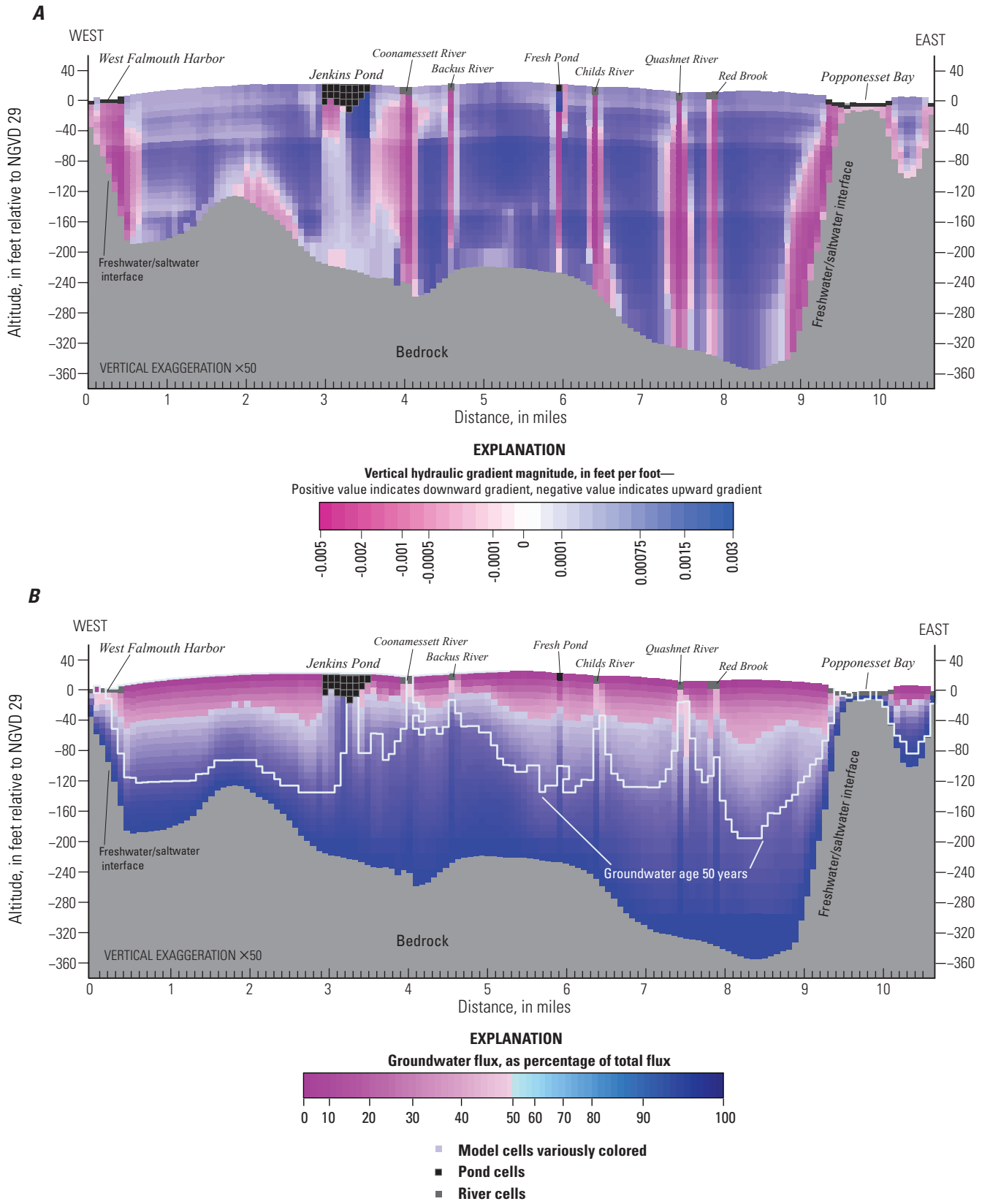

Figure 47. Model row 190 *A*, vertical hydraulic gradients and *B*, depth of 50-year-old groundwater and groundwater flux as percentage of total flow through a section of the aquifer generally transverse to groundwater flow, for 2010 pumping conditions, western Cape Cod, Massachusetts. Section location is shown on figure 46. NGVD 29, National Geodetic Vertical Datum of 1929.

four towns near the JBCC range from about 0.46 Mgal/d in Bourne to 1.37 Mgal/d in Falmouth (data from the Massachusetts Department of Conservation and Recreation, reported in Upper Cape Regional Water Supply Cooperative, 2015). Projected pumping represents about 7 percent of the total hydrologic budget of the simulated aquifer. These hydraulic stresses, as well as internally consistent estimates of return flow, were included in the model to help evaluate the effects of the projected increase in pumping on water levels and streamflows. Note that (1) these projections are estimates, by town, with a significant degree of uncertainty; (2) the simulated pumping rates assume that the current (2010) distribution of pumping, by well, will be the same proportion of the total withdrawals, by town, in 2030; (3) new sources, currently unknown, are not included in the simulation; and (4) substantial changes in the distribution of return flow, not included here, are likely to occur by 2030 as communities implement wastewater-management plans to reduce nutrient-loading to coastal waters.

The projected increases in pumping and associated return flow would affect water levels and groundwater flow direction in several areas on the Sagamore flow lens (fig. 48). Declines in water levels, referred to as "drawdown," would occur generally near water withdrawals; the largest declines near the JBCC (about 1.2 to 1.8 ft of drawdown) are near the only surface-water withdrawal at Long Pond in Falmouth and a broad area around the Upper Cape Cooperative wells in the northern part of the JBCC (fig. 48). Projected drawdown exceeds 0.4 ft locally in several areas around pumped wells near the JBCC. The effects of projected increases in pumping and associated return flow in Barnstable, to the east of the JBCC, are significant, and projected drawdowns exceed 1.6 ft near pumped wells. The increased rates of wastewater disposal projected at the Barnstable WWTF associated with the pumping would result in an increase in water levels, referred to as "mounding," near the facility (fig. 48); the increase in water levels would be about 1.2 ft.

The effects of projected (2030) groundwater withdrawals and return flow on streamflow generally are small owing to the hydrologic near balance between pumping and return flow (fig. 49). The mean projected decrease at locations where there are streamflow observations (fig. 31) is about 0.14 ft^3/s, or about 6 percent. The largest projected decrease in flow (0.56 ft^3/s) is at the outlet of Upper Shawme Pond, which is north of the JBCC in Sandwich (site 14, fig. 42). The site is located near a broad area of drawdown, and the projected streamflow depletion likely is due to increased simulated pumping from the Upper Cape Cooperative wells (fig. 2*A*). Flow at the USGS streamgage on the Quashnet River (fig. 8 and site 1, fig. 42) is projected to decrease by about 0.04 ft^3/s (fig. 49). Total depletion for all sites is about 1 percent from current (2010) flows and is proportionally larger in smaller streams. The average projected depletions, in percent of current (2010) flows, for streams with flows greater and less than 1 ft^3/s, are about 2 and 12 percent, respectively. Streamflow is projected to increase slightly at five of the sites: Bumps River (site 21, fig. 42) in Barnstable, Backus River (site 15, fig. 42) and Bourne River (site 18, fig. 42) in Falmouth, and Quashnet River in Mashpee (sites 16 and 23, fig. 42; fig. 49). Bumps River is near an area where water levels have increased in response to wastewater disposal at the Barnstable WWTF. The Backus River and Bourne River are in southern Falmouth in an area with dense residential development and septic-system return flow (fig. 18*B*), and the projected increase in streamflow likely results from the projected increase in return flow. Note that the analysis does not account for changes in the actual spatial distribution of return flow arising from future development and sewering.

Effects of Future (2030) Pumping on Hydraulic Gradients

In the projected future (2030) pumping scenario, changes in water levels result in changes in hydraulic-gradient magnitude and direction; gradient direction affects advective-transport patterns in the aquifer. Groundwater flow is outward from the radial water-table divide (fig. 46), and all possible hydraulic-gradient directions occur in the aquifer. The projected (2030) pumping and return flow shifts the position of the radial water-table divide, as determined by interpolation of simulated water levels, by about 249 ft to the southwest of the simulated current (2010) location. Gradient directions at the water table change by less than 1 degree in most (about 87 percent) of the aquifer (fig. 48), and areas where the change in direction exceeds 1 degree generally occur near pumped wells, the Barnstable WWTF (fig. 18), and the regional groundwater divide that extends eastward from the northern part of the JBCC (fig. 48). Gradient magnitudes generally are small near groundwater divides (fig. 46) and, as a result, changing pumping and return-flow stresses have a larger effect in those areas (Walter, 2008). The largest change in gradient direction is about 45 degrees, adjacent to Long Pond in Falmouth, reflecting the large projected increase in withdrawals from the pond and the effect of the pond on adjacent gradients. The largest changes in gradient direction in the JBCC are in the northernmost part of the facility (fig. 48), near pumped wells and generally away from contaminant plumes (fig. 2). Gradient-direction changes at the water table exceed 10 degrees in only about 0.5 percent of the aquifer. The mean gradient-direction change is about 0.6 degree and, within the JBCC, generally is small (about 0.5 degree), indicating that projected (2030) increases in pumping likely will not affect the gradient conditions under which contaminants are transported near the JBCC.

Predictions of advective transport from a set of random source locations at the water table in and near the JBCC were essentially identical for current (2010) and future (2030) pumping and return-flow stresses (fig. 50). Predictions of advective transport are a function of hydraulic gradients, and the close agreement between advective-transport predictions for the two sets of stresses is consistent with the fact that areas where gradient-direction changes at the water table exceeded

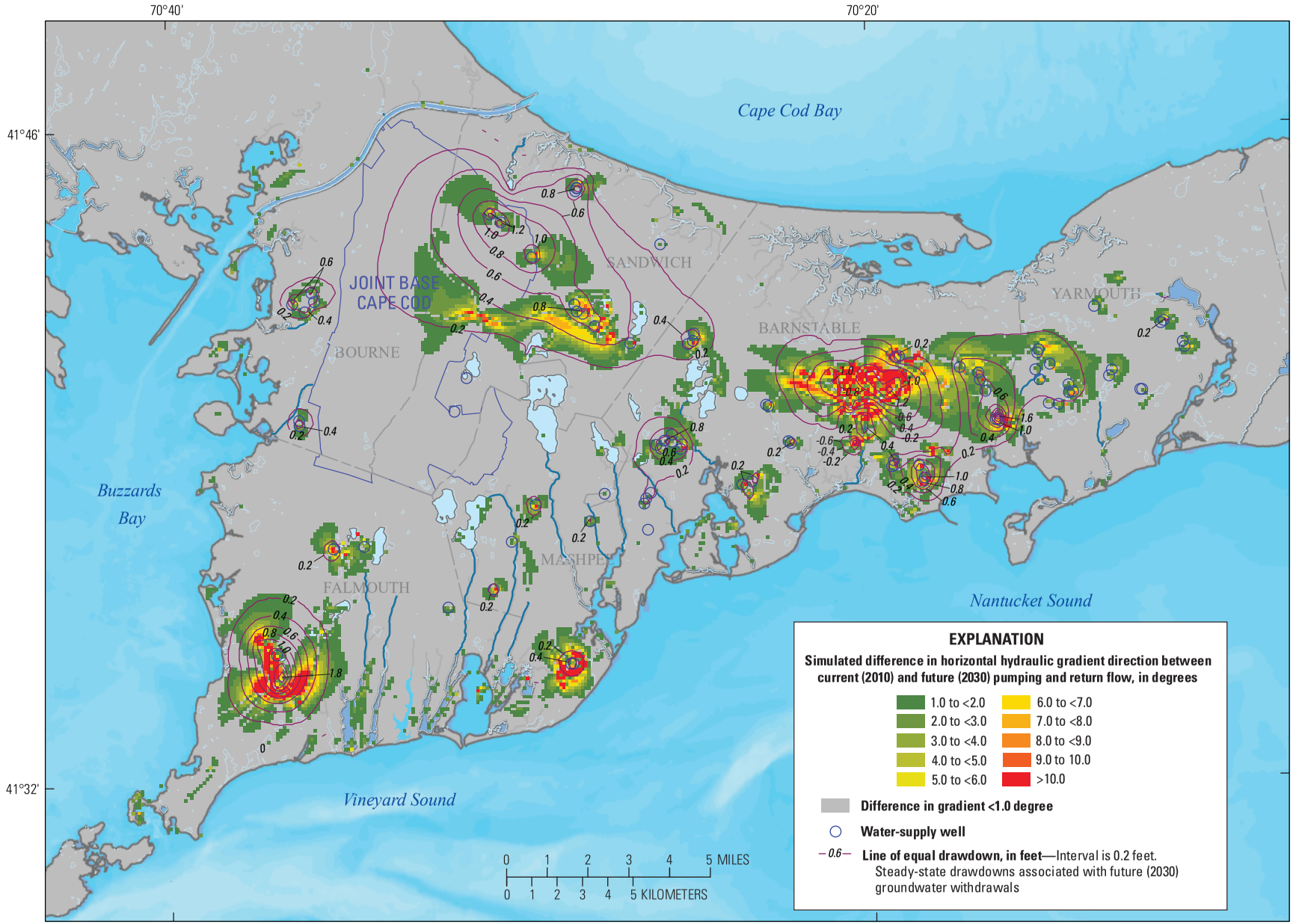

Base from U.S. Geological Survey and Massachusetts Office of Geographic Information digital data
North American Datum of 1983

Figure 48. Simulated difference in horizontal hydraulic gradient direction between current (2010) and future (2030) pumping and return flow, and associated steady-state drawdown, western Cape Cod, Massachusetts.

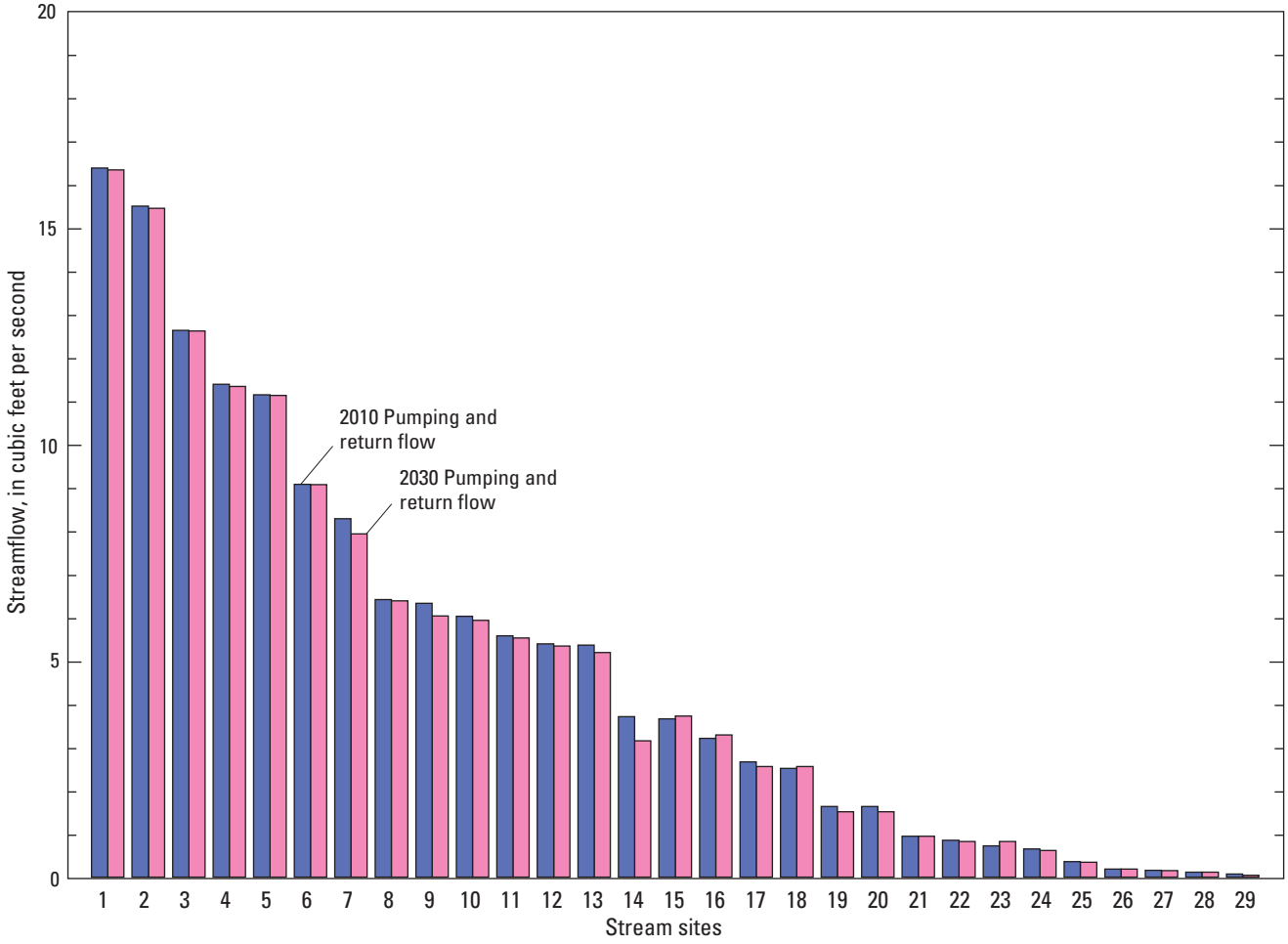

1. Quashnet River (011058837)
2. Mashpee River at Route 28
3. Quashnet River downstream of Route 151
4. Mill Creek
5. Quashnet River at fish ladder
6. Quashnet River at Route 151
7. Marstons Mills River
8. Santuit River at Old Kings Road
9. Marstons Mills River (MEP)
10. Skunk River (MEP)
11. Mashpee River at Route 130
12. Mashpee River at pond outlet
13. Coonamessett River
14. Upper Shawme Pond outlet
15. Backus River
16. Quashnet River 0.6 mile downstream of outlet
17. Stewarts Creek (MEP)
18. Bourne River
19. Coonamessett River 2,500 feet north of Hatchville Road
20. Coonamessett River 800 feet north of Hatchville Road
21. Bumps River (MEP)
22. Stream from Lake Elizabeth (MEP)
23. Quashnet River at pond outlet
24. Little River (MEP)
25. Phlashes Creek
26. Mashapaquit Creek (MEP)
27. Stream into Squeteague Harbor (MEP)
28. Back River (MEP)
29. Hawes Run (MEP)

Figure 49. Simulated streamflows for current (2010) and future (2030) pumping and return flow, by stream site, western Cape Cod, Massachusetts. Locations are shown by site identifiers (numbers in parentheses) on figure 42. MEP, Massachusetts Estuaries Project.

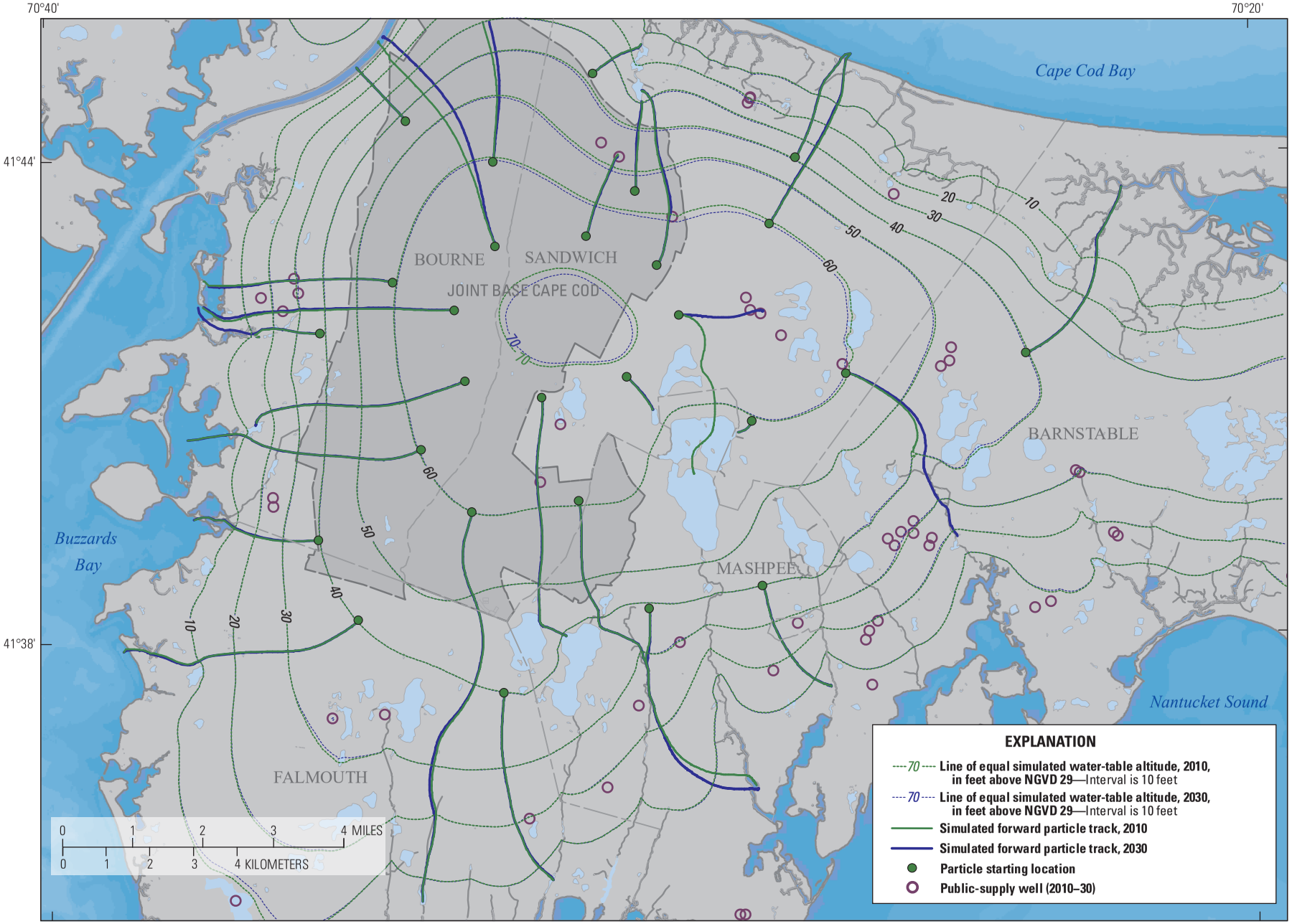

Base from U.S. Geological Survey and Massachusetts Office of Geographic Information digital data
North American Datum of 1983

Figure 50. Forward particle tracks starting at selected locations along the 65-, 60-, and 40-foot water-table contours for current (2010) and future (2030) pumping and return flow, western Cape Cod, Massachusetts. NGVD 29, National Geodetic Vertical Datum of 1929.

1 degree are limited to a small part of the aquifer, primarily along the groundwater divide and near pumped wells (fig. 48). Results of the analysis indicate that future hydraulic stresses, if similar in location and relative magnitude to those in the 2030 scenario, likely will not affect the advective transport of existing contaminant plumes emanating from sources on the JBCC.

Factors Affecting Model Calibration and Predictions

Groundwater-model parameter values are nonunique, and several factors can affect the outcome of a model calibration, including the types of observations, associated weights, and the conceptualization of the aquifer; model predictions also are affected by the same factors. Observations and model parameterization affect the estimated parameters and the precision of the model, as indicated by model fit. The set of observations and weights used in the preferred calibration (simulation HFPA, table 2) represent, to a degree, the results of a trial-and-error process in which different combinations of observations and associated weights are specified that reflect relative confidence in the observations, their suitability to represent steady-state conditions, and their ability to inform model predictions. Likewise, model parameterization reflects both the confidence in prior information about aquifer characteristics and the need to match observed conditions in areas where the model likely will be used for predictions, particularly of advective transport. Parameterization, like observation weight, can be changed during the calibration until a reasonable model is produced. The conceptualization of the aquifer also includes inherent assumptions that affect model calibration. Two assumptions underlying this calibration are that the silt lenses can be represented implicitly rather than as specific units, and that the freshwater/saltwater interface obtained from the interface model is correct. These assumptions, as well as final model parameterization and the set of observations and associated weights, were judged to be the most appropriate for the analysis; however, an evaluation of different sets of observations and associated weights, and alternative conceptual models, can provide insight into the magnitude of those assumptions on model calibration results and predictions.

Observations and Weights

The preferred calibration was judged to have the best overall fit to the observations and includes all five observation types: water levels, streamflows, hydraulic gradients, plume paths estimated from water-quality sections, and traveltimes estimated from groundwater ages. The largest weights were assigned to plume observations, followed in decreasing order by water levels and hydraulic gradients (the weighting of hydraulic gradients was held constant for all calibrations), streamflow, and groundwater ages (table 2). Plumes are important observations because they likely are good indicators of long-term hydraulic gradients and provide more information for estimation of hydraulic conductivity parameters than heads and flows. The weighting scheme also reflects, in part, the intended use of the model to predict patterns of advective transport near existing contaminant plumes, and the estimated hydraulic conductivity fields are a result of the weighting scheme. Varying the types of observations to include in the inverse-calibration regression and the associated weights (table 2) in eight alternative weighting schemes results in different model fits, as indicated by the absolute mean residuals for four observation types: water levels (H), streamflows (F), plumes (P), and groundwater ages (A) (fig. 51). The preferred calibration (simulation HFPA)—with all observation types included—generally best fits the observed data (fig. 51).

Absolute mean residuals for individual observation types generally were lower in inverse-calibration runs in which those observations had larger weights or in which fewer types of observations were included. As an example, the absolute mean residuals for water levels were lower in simulations H (including essentially only water-level observations) and HF (including essentially only water-level and streamflow observations) than in the preferred calibration; however, the absolute mean residuals for plumes were much larger (fig. 51). Likewise, the absolute mean residuals for streamflows generally were lower than in the preferred calibration for inverse-calibration regressions in which streamflows had higher weights and fewer observation types were included, such as simulations HF and F (which included essentially only streamflow observations) (fig. 51). Similarly, the absolute mean residual for ages was lowest in the inverse-calibration regression that included age observations only (simulation A). Absolute mean residuals for ages generally were lower in regressions in which ages had higher weights and fewer observation types were included (simulations HFA and PA) than in the preferred calibration; however, absolute mean residuals for heads, streamflows, and plumes were much larger in those weighting schemes. Absolute mean residuals for plume observations were lower in the preferred calibrated model than in all the alternative inverse calibrations, including inverse-calibration regressions in which plumes had larger weights (fig. 51). This indicates that in addition to increasing observation weights, the inclusion of a diverse set of observations also improves the fit to plume observations. The fit to plume observations is of particular importance to model predictions of advective transport, and the results indicate that the preferred calibration with all observations types included represents the most reasonable weighting scheme, of those evaluated, for the intended analysis.

The use of alternative sets of observations results in different estimated parameters and model predictions. Previous regional models typically used observations of heads and streamflows because observations of advective transport generally are sparse or unavailable. Most groundwater flow occurs in the upper part of the aquifer (fig. 47*B*), and parameter sensitivities generally are low in deeper parts of the aquifer

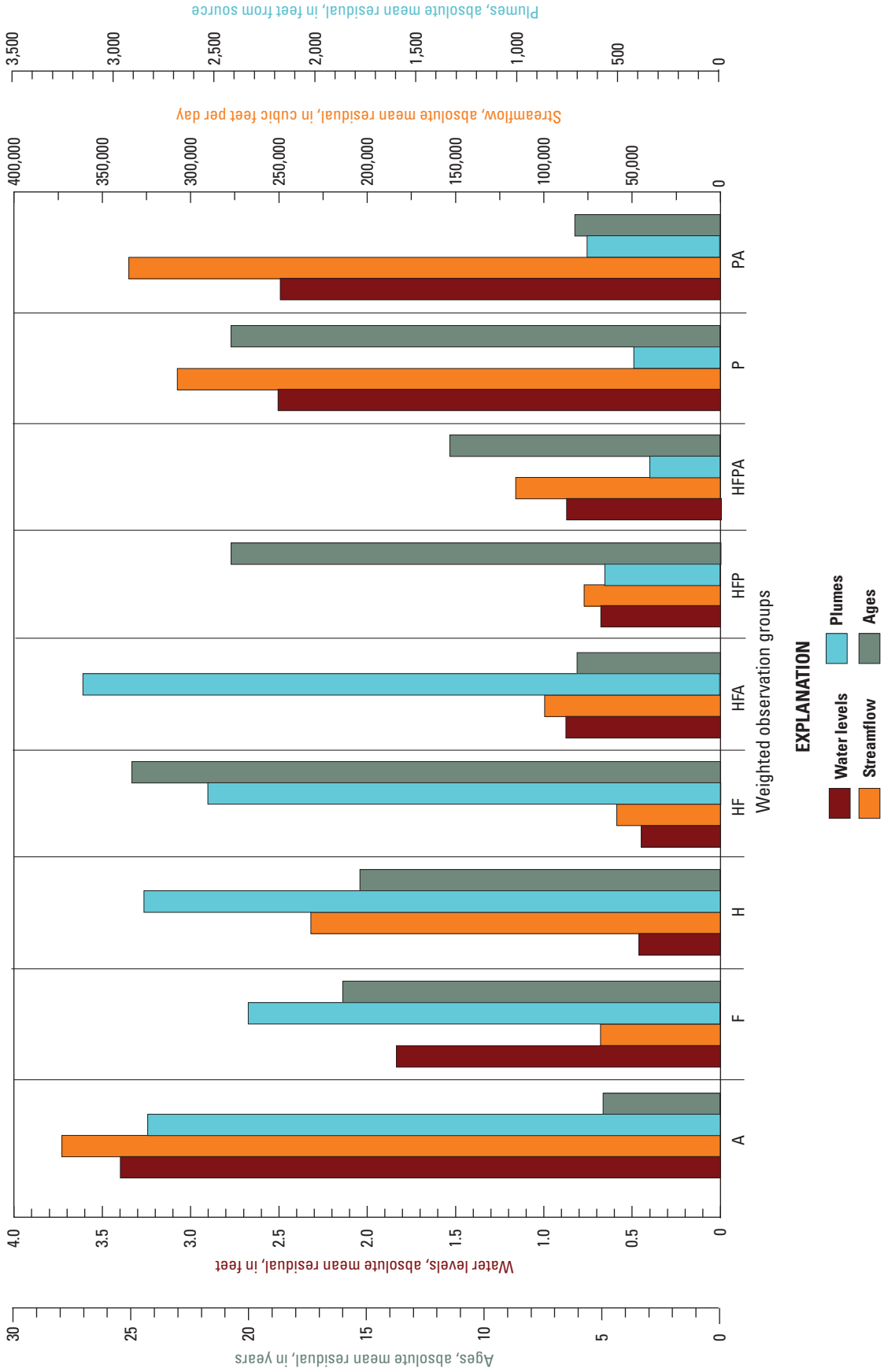

Figure 51. Absolute mean residuals for the preferred model calibration (HFPA) and alternative calibrations that used different weighting combinations of observations of heads (H), streamflows (F), and advective-transport plume paths (P) and ages (A).

when inverse-model calibrations use only observations of heads and flows (Walter and LeBlanc, 2008). The inclusion of advective-transport observations from plumes and groundwater age increases parameter sensitivities at depth in the aquifer (fig. 37) and likely provides more information for the estimation of hydraulic conductivity parameters at depth. Alternative calibrations in which horizontal hydraulic conductivity parameters were estimated by using only observations of heads and streamflows (HF) and those estimated by using heads, flows, and advective-transport observations (HFPA) matched well in the observed heads and flows (fig. 51). The two sets of observations result in regionally similar estimated hydraulic conductivities (within about 5 percent). However, hydraulic conductivities estimated from the two sets of observations can differ substantially at a local scale (fig. 52). The initial hydraulic conductivity generally decreased with depth, reflecting the depositional model (fig. 52*A*). An inverse calibration using head and flow observations results in the same general pattern of hydraulic conductivity but with more spatial variability than the initial values (fig. 52*B*). The inclusion of advective-transport observations results in hydraulic conductivities that generally are more variable at depth (vertical groups 3 and 4) in areas proximal to advective-transport observations than in other areas (fig. 52*C*). The advective-transport observations locally increase parameter sensitivities and provide more information for the estimation of parameters at depth, resulting in more simulated heterogeneity.

Representation of Local-Scale Heterogeneity

Fine-grained, silty sediments are present within the Cape Cod aquifer—regionally at depth, referred to as "basal silts," and locally in shallow parts of the aquifer, referred to as "hanging silts." Hanging silts are present as lenses of silty sediments within coarser, sandy deposits and affect local-scale hydraulic gradients and advective-transport patterns. There is evidence that the presence of local-scale silt lenses can affect the distribution of contaminants (fig. 6) and groundwater ages (fig. 7) in the aquifer. The representation of local-scale hydrogeologic units in a numerical model presents challenges because information often is limited to observations of silt layers in individual lithologic logs (fig. 4) with little or no information regarding the spatial extent of the silt deposits or possible correlations with silt layers from other logs. Extending silt observations between lithologic logs may overestimate the extent of a silt lens and its effect on local-scale hydraulic gradients, whereas limiting silts to single model cells may underestimate the effect of a silt lens. Also, representation of local-scale silt lenses in a regional model can be difficult owing to the discretization of the model (400 ft), as compared to the possible extent of the silt deposits. Silt layers are not explicitly represented in the regional model; however, the contribution of silt layers was included in the estimate of initial vertical and horizontal hydraulic conductivity values that were averaged from lithologic logs and assigned to corresponding model cells (fig. 14). This approach implicitly incorporates the silts into the hydraulic conductivity field but may have underestimated the potential effect of the silts on advective-transport predictions.

The potential effect of silt layers on the results of the inverse calibration can be inferred by developing alternative model parameterizations in which silt layers are explicitly represented, and evaluating the resulting absolute mean residuals for different types of observations; a larger difference in absolute mean residuals between the calibrated model and the alternative model indicates a larger potential effect on the model calibration. Lithologic data were used to inform the analysis by developing a set of silt seeds, representing locations within the aquifer of silt layers with a thickness of 5 ft or greater, as observed in a lithologic log; a total of 897 silt seeds that met the criteria were identified (fig. 13). The potential effect of a silt layer on advective-transport patterns is a function of the horizontal and vertical hydraulic conductivities of the silty sediments and the lateral extent of the silt layer; however, only the presence of the silt layers is known, and little or no information on those characteristics is available. Alternative aquifer realizations were developed to explicitly represent the observed silt seeds over a range of correlation distances from 200 to 2,200 ft; the correlation distance refers to the distance the silt layer extends laterally from the silt seed. Hydraulic conductivity values estimated from the preferred inverse calibration are represented as background aquifer hydraulic conductivities (fig. 53*A*) onto which explicit zones representing silt layers are superimposed (figs. 53*B*–*E*). A correlation distance of 200 indicates the silt seed is represented in a single model cell (fig. 53*B*), and a correlation distance of 1,400 ft indicates representation in 49 model cells (7 rows by 7 columns) (fig. 53*E*). Larger correlation distances increase the part of the aquifer represented as a silt layer, and silt layers coalesce at large correlation distances to represent more regional features. A range of horizontal hydraulic conductivities of the silts—1, 2, 5 and 10 ft/d—and a range of vertical hydraulic conductivities—0.1, 0.2, 0.5, and 1 ft/d—were evaluated for each correlation distance. The largest effects on residuals would be expected for large correlation distances and small hydraulic conductivity values.

Absolute mean residuals for heads, streamflows, and plume sources increased for all combinations of correlation distance and hydraulic conductivity (fig. 54*A*), indicating that explicitly representing silt layers in the regional model likely would affect model-calibration results. The largest increases were for combinations of large correlation distances and small values of hydraulic conductivity (fig. 54A). The absolute mean residuals for heads and streamflows, assuming a correlation distance of 200 ft, were similar to calibrated values, indicating that representation of silts as local-scale lenses likely would not greatly affect calibration if only head and streamflow observations were used. The largest absolute mean residual for streamflow was about 1.6 ft^3/s and for head about 3.0 ft (about 4 percent of the total water-table gradient), indicating that head and streamflow generally were reasonable and could be considered calibrated for the ranges of silt hydraulic conductivity and correlation distances evaluated.

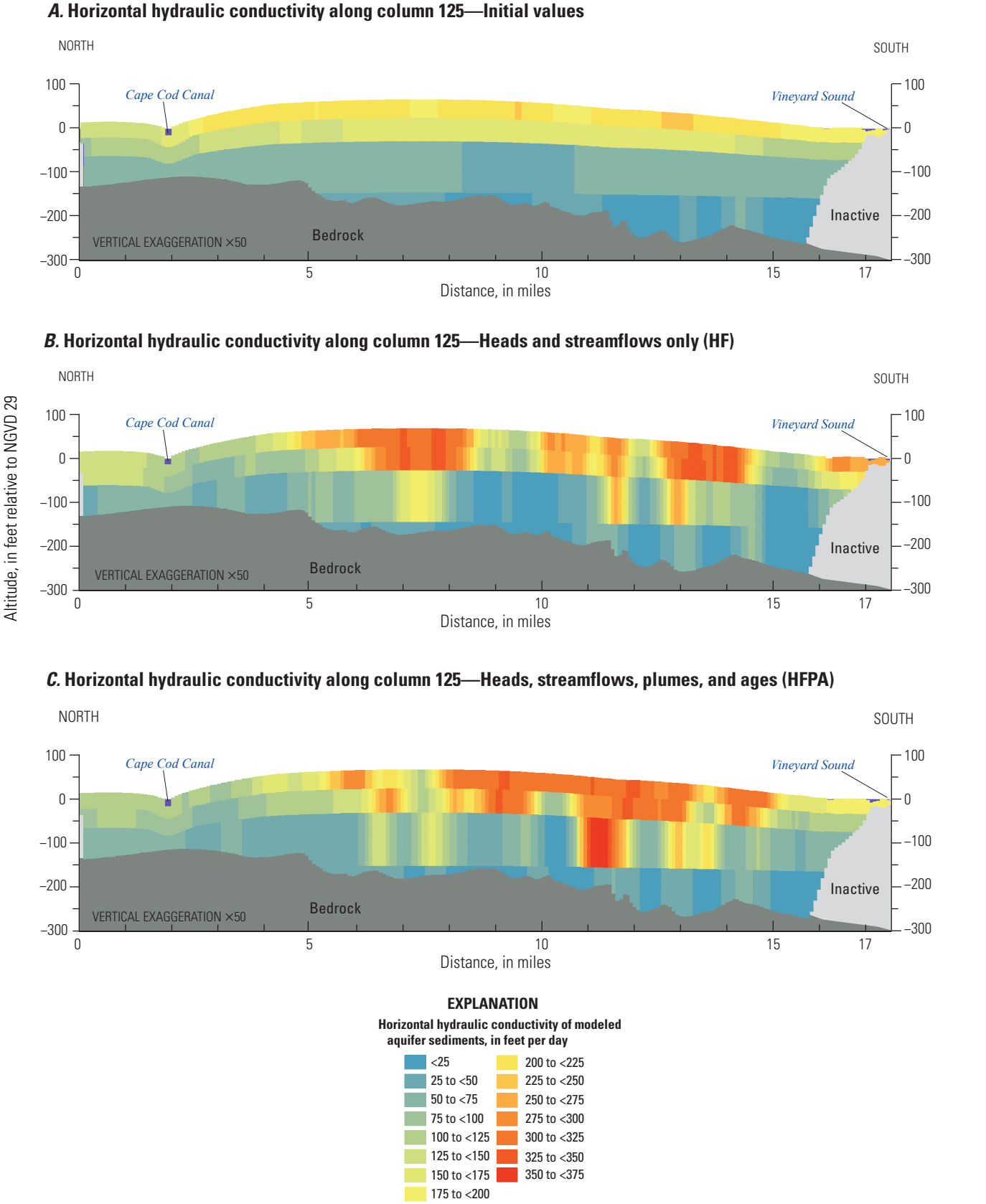

Figure 52. *A*, Initial horizontal hydraulic conductivity field, *B*, horizontal hydraulic conductivity field from model calibrated by using heads and flows only, and *C*, horizontal hydraulic conductivity field from model calibrated by using heads, flows, plumes, and ages, western Cape Cod, Massachusetts. Section location along model column 125 is shown on figure 25. NGVD 29, National Geodetic Vertical Datum of 1929.

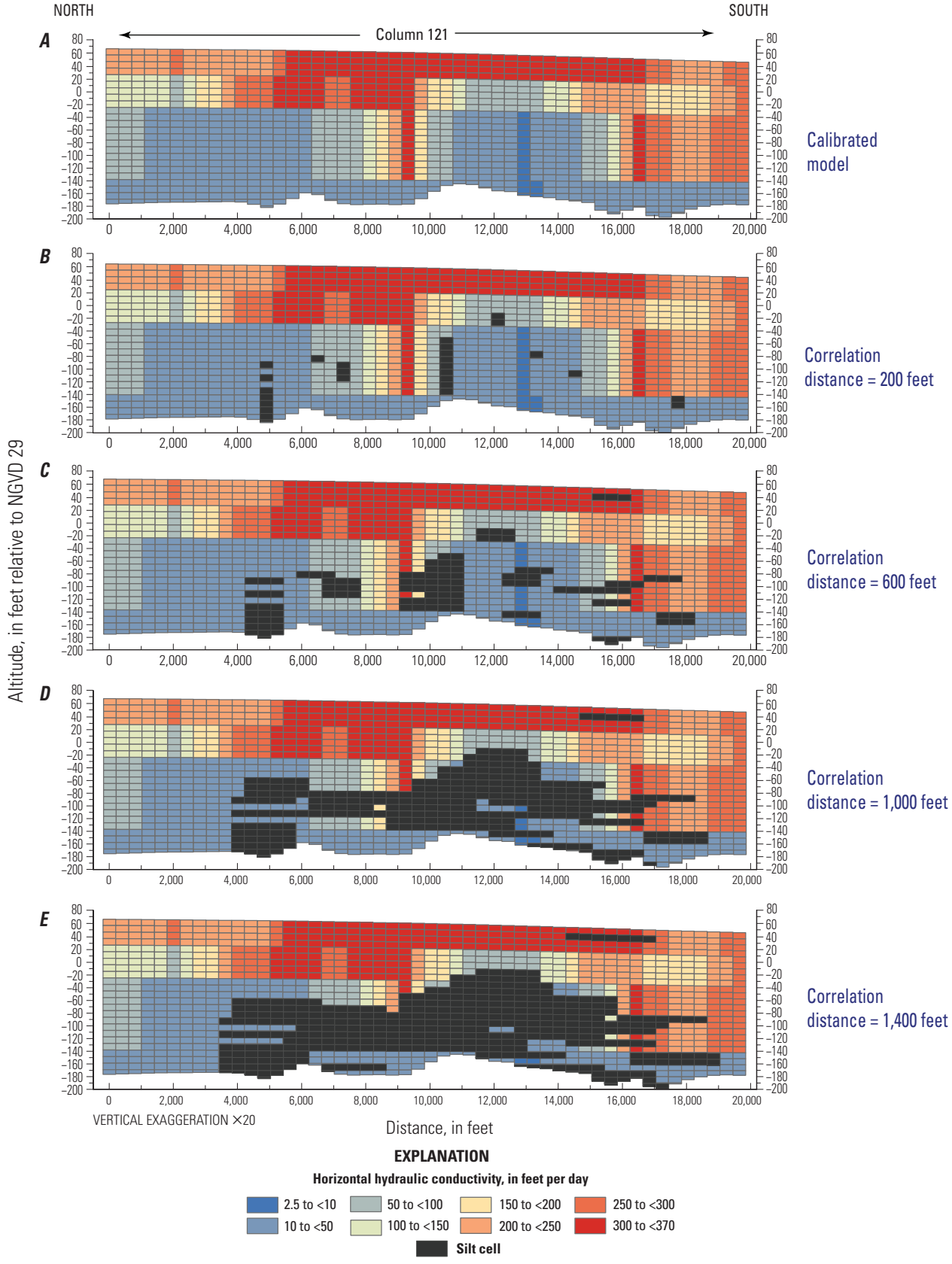

Figure 53. *A*, Estimated horizontal hydraulic conductivity values upon which simulated silt layers are imposed with correlation distances of *B*, 200, *C*, 600, *D*, 1,000, and *E*, 1,400 feet for selected points northwest of Ashumet Pond, western Cape Cod, Massachusetts. Section location along model column 121 is shown on figure 25*A*. NGVD 29, National Geodetic Vertical Datum of 1929.

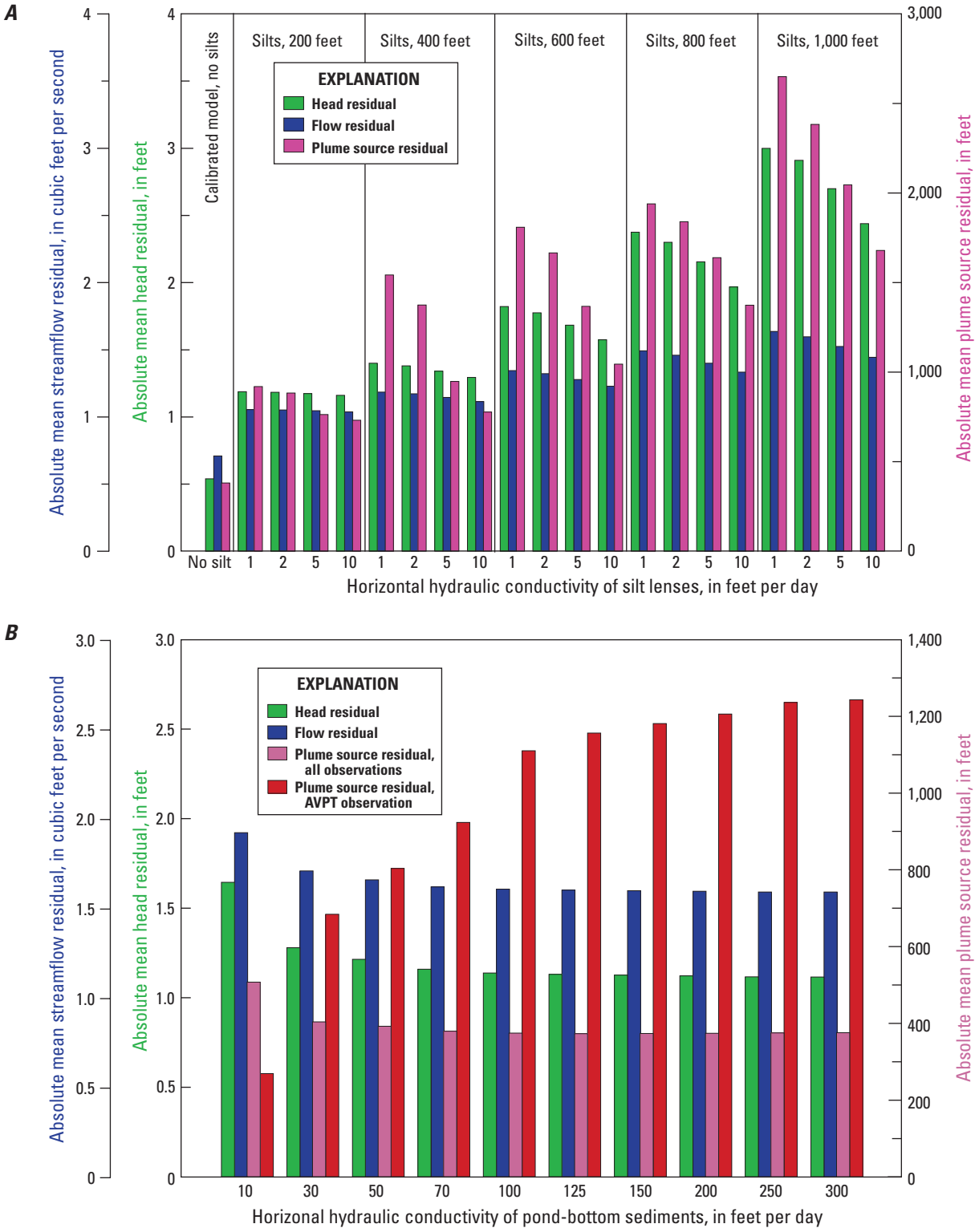

Figure 54. Changes in absolute mean residuals for heads, streamflows, and plume sources as a function of horizontal hydraulic conductivity, of *A*, silt lenses with correlation distances of 200, 400, 600, 800, and 1,000 feet, and *B*, pond-bottom sediments, western Cape Cod, Massachusetts. AVPT, an Ashumet Valley plume observation point.

The absolute mean residual for plume sources, defined as the distances between the simulated recharge points of the observed plume centers and the estimated locations of the plume sources, was about 381 ft for the calibrated model. The representation of silt layers as individual model cells and a hydraulic conductivity of 5 ft/d more than doubled the absolute mean residual (fig. 54*A*). The absolute mean residual ranged from 731 ft for the largest silt hydraulic conductivity (10 ft/d) and the smallest correlation distance (200 ft) to 2,649 ft for a hydraulic conductivity of 1 ft/d and a correlation distance of 1,000 ft (fig. 54*A*). The large increase in plume source residual with larger correlation distance and smaller hydraulic conductivity indicates that the explicit inclusion of silt layers could greatly affect the model calibration, including representation of silts as single regional model cells. Note that absolute mean residuals for all observation types generally are less similar for larger correlation distances than for smaller distances, indicating that the relative effects increase for larger correlation distances because silt layers coalesce into more regional features. The results indicate that inclusion of explicit silt lenses could affect calibration, but the calibration results would, in part, depend on assumptions about correlation distances, which are poorly understood.

The potential effect of the explicit representation of silt lenses on predictions of advective transport made by using this model can be evaluated by forward particle tracking from selected locations for different silt realizations. The simulation of silt layers affects predictions of advective transport; however, the predictions generally can be considered to be similar at the regional scale (fig. 55). Local-scale predictions of advective transport, such as those that might be needed for designing and evaluating remedial systems, likely would be affected by a given representation of silts; however, the results indicate that the calibrated regional model produces similar regional hydraulic gradients and advective-transport patterns at the regional scale and that the model can provide the necessary boundary conditions for subregional models capable of representing local-scale heterogeneity.

Silty sediments also can be present beneath kettle-hole ponds as a result of postglacial lacustrine deposition within the ponds. Ponds can affect local hydraulic gradients and advective-transport patterns; the degree to which a pond affects hydraulic gradients is partly a function of the permeability of the pond-bottom sediments (Walter and Masterson, 2003). Several plumes emanating from source areas on the JBCC are near ponds, and the simulated hydraulic connection between the ponds and the aquifer could affect simulated plume paths and calibration results, as represented by absolute mean residuals of different observation types. Absolute mean head residuals were similar over a range of pond-bottom hydraulic conductivity (10 to 300 ft/d for the horizontal component and 0.1 to 100 ft/d for the corresponding vertical component); absolute mean head residuals ranged from 1.6 to 1.1 ft for horizontal hydraulic conductivity values between 10 and 300 ft/d (fig. 54*B*). Absolute mean streamflow residuals ranged from 1.9 to 1.6 ft^3/s over the range of simulated pond-bottom hydraulic conductivities (fig. 54*B*). Note that the simulated value of pond-bottom horizontal hydraulic conductivity in the calibrated model was about 100 ft/d.

Excluding the lowest value in the pond-bottom hydraulic conductivity range, absolute mean residuals including all plume observations were similar (between 376 and 404 ft) (fig. 54*B*). The results indicate that plume residuals, including all observations, generally were not substantially affected by simulated pond-bottom hydraulic conductivity; this is consistent with the location of many plumes in areas away from ponds (fig. 2*B*). The simulated pond-bottom hydraulic conductivity does affect plume observations from within the Ashumet Valley plume, which is located near Ashumet Pond (fig. 2). The residual for observation AVPT near Ashumet Pond (fig. 17) increased from 269 to 1,242 ft with increasing pond-bottom horizontal hydraulic conductivity (fig. 54*B*). Residuals for most plume observations within the Ashumet Valley plume changed by more than a factor 2 over the range of simulated values. The results indicate that although simulated pond-bottom hydraulic conductivity does not have a substantial effect regionally, the parameters could affect model calibration and predictions of advective transport in areas near the ponds.

Freshwater/Saltwater Interface Position

The steady-state, regional groundwater model represents the coastal boundary as a head-dependent-flux boundary condition at the seabed that is underlain by a freshwater/saltwater interface represented as a static no-flow boundary. The assumed interface position is calculated from the FW/SW interface model (as described in the "Numerical Model Design" section) (fig. 21). Coastal leakances were varied in that model by trial and error until a reasonable fit to the observed interface position at 17 locations was achieved; the simulated coastal leakance that produced a simulated interface that best matched the observed positions was 0.4 ft/d (fig. 23) (Walter and others, 2016). The general-head boundary leakances and the internally consistent interface position were not varied during model calibration, and the potential exists that the assumed specified coastal leakances and assumed interface position could affect model calibration and predictions.

The potential effects of the coastal boundary condition and the assumed interface position were evaluated for two alternative coastal leakances, 0.2 ft/d and 20 ft/d, referred to as "silty" and "sandy" coastal-boundary conditions. Alternative freshwater/saltwater positions were determined for the alternative coastal-boundary conditions by using the FW/SW interface model (fig. 21) and were incorporated into the regional groundwater flow model as a static no-flow boundary (fig. 56). The change in aquifer geometry occurs near the coast because most of the aquifer is underlain by bedrock (fig. 56*A*). Interface positions are deeper for smaller (silty) coastal leakances than for sandy leakances, for which the interface forms laterally isolated freshwater lenses to the south of the JBCC in Falmouth (figs. 24 and 56*B*). Most groundwater discharge in the calibrated model (278.7 ft^3/s, or about 52 percent of the total) occurs at the coast; about

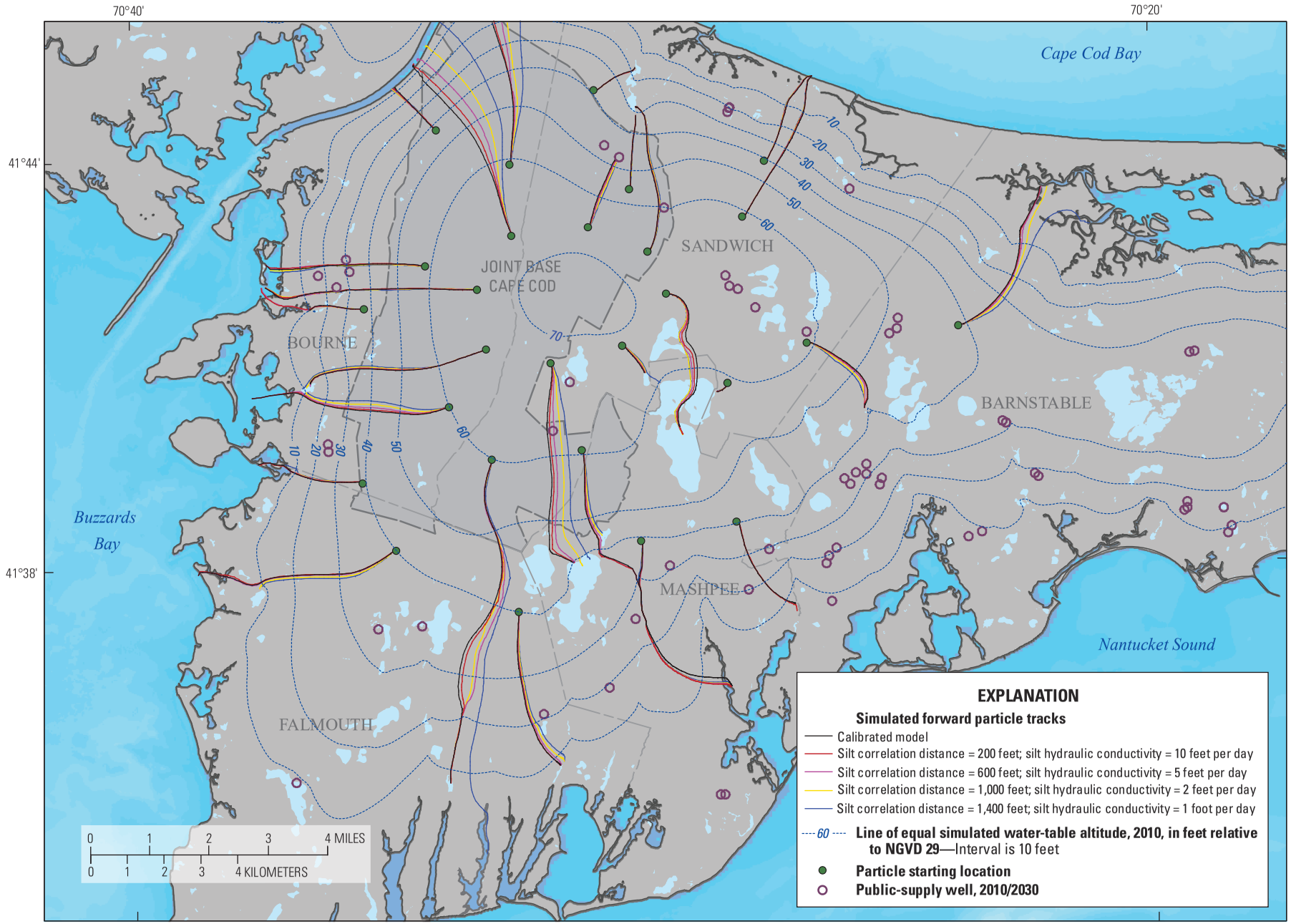

Base from U.S. Geological Survey and Massachusetts Office of Geographic Information digital data
North American Datum of 1983

Figure 55. Forward particle tracks starting at selected locations along the 65-, 60-, and 40-foot water-table contours for alternative realizations of silt layers, western Cape Cod, Massachusetts. NGVD 29, National Geodetic Vertical Datum of 1929.

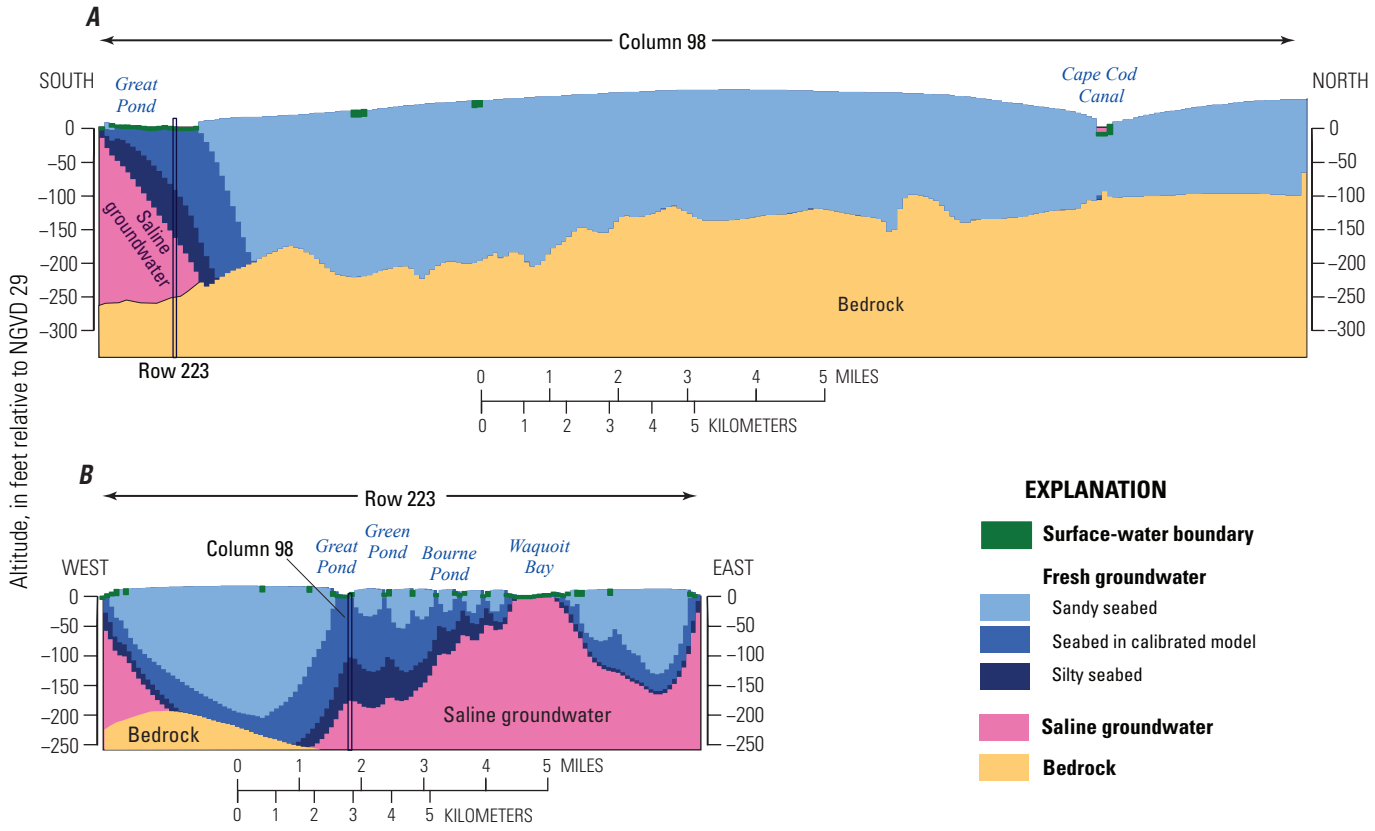

Figure 56. The simulated position of the freshwater/saltwater interface for three coastal seabed leakance values, Cape Cod, Massachusetts. Locations of *A*, column 98 and *B*, row 223, are shown on figure 24. NGVD 29, National Geodetic Vertical Datum of 1929.

236.9 ft^3/s (or about 43 percent of the total) occurs at freshwater streams. Groundwater discharges naturally to either streams or the coast; decreasing coastal leakances (resistance to groundwater discharge) decreases discharge at the coast and increases streamflow. Discharge to streams for the alternative silty and sandy coastal leakances were 302.4 ft^3/s (about 59 percent of the total discharge) and 243.2 ft^3/s (about 47 percent of the total), respectively. Discharge to small coastal streams generally is more affected by coastal leakances than discharge into larger streams.

Absolute mean residuals for the preferred calibrated model and the alternative models with silty and sandy coastal leakances differed for heads and streamflows but were similar for plume sources (fig. 57; table 2). The absolute mean residuals for heads for silty and sandy coastal leakances, including all observation wells, were 2.25 and 1.67 ft, respectively, which are larger than the residual of about 0.9 ft for the intermediate leakance used in the calibrated model. Likewise, mean residuals for flow, 2.3 and 1.65 ft^3/s, were larger than the residual of about 0.95 ft^3/s for the calibrated model. The results indicate that the assumption of a sandy seabed could affect calibrations, results, and predictions. Residuals for all plume observations (groups "plumes 1" and "plumes 2") were about 454 and 357 ft, respectively, for the alternative models with silty and sandy coastal leakances; the residual for the calibrated model was about 360 ft. Note that the seabed characteristics likely are spatially variable and that the assumption of a sandy seabed best matched observed freshwater/saltwater interface positions in some areas, particularly where the interface is shallow.

Predictions of advective transport from randomly selected locations at the water table generally were similar among the three representations of seabed leakance, particularly away from the coast (fig. 58), though differences were larger for some locations near Buzzards Bay. Predicted discharge locations did differ substantially in some areas (fig. 58). Different interface positions, as well as a different balance between stream and coastal discharge, would affect hydraulic gradients near the coast. The effect of representation of the coastal boundary generally is larger in areas with complex coastal morphologies, such as southern Falmouth where there are numerous estuaries extending inland to streams (fig. 5). A particle recharging the water table to the northeast of Johns Pond discharges to a different coastal water body for each of the three assumed coastal boundaries—the preferred calibrated model, the silty seabed alternative, and the sandy seabed alternative. A particle recharging in the south-central part of the JBCC discharges to Coonamessett Pond for the calibrated and sandy coastal boundaries but discharges to Green Pond to the southeast for the silty coastal boundary. Discharge locations generally are similar in areas with simpler coastal morphologies, such as Cape Cod Bay (fig. 58).

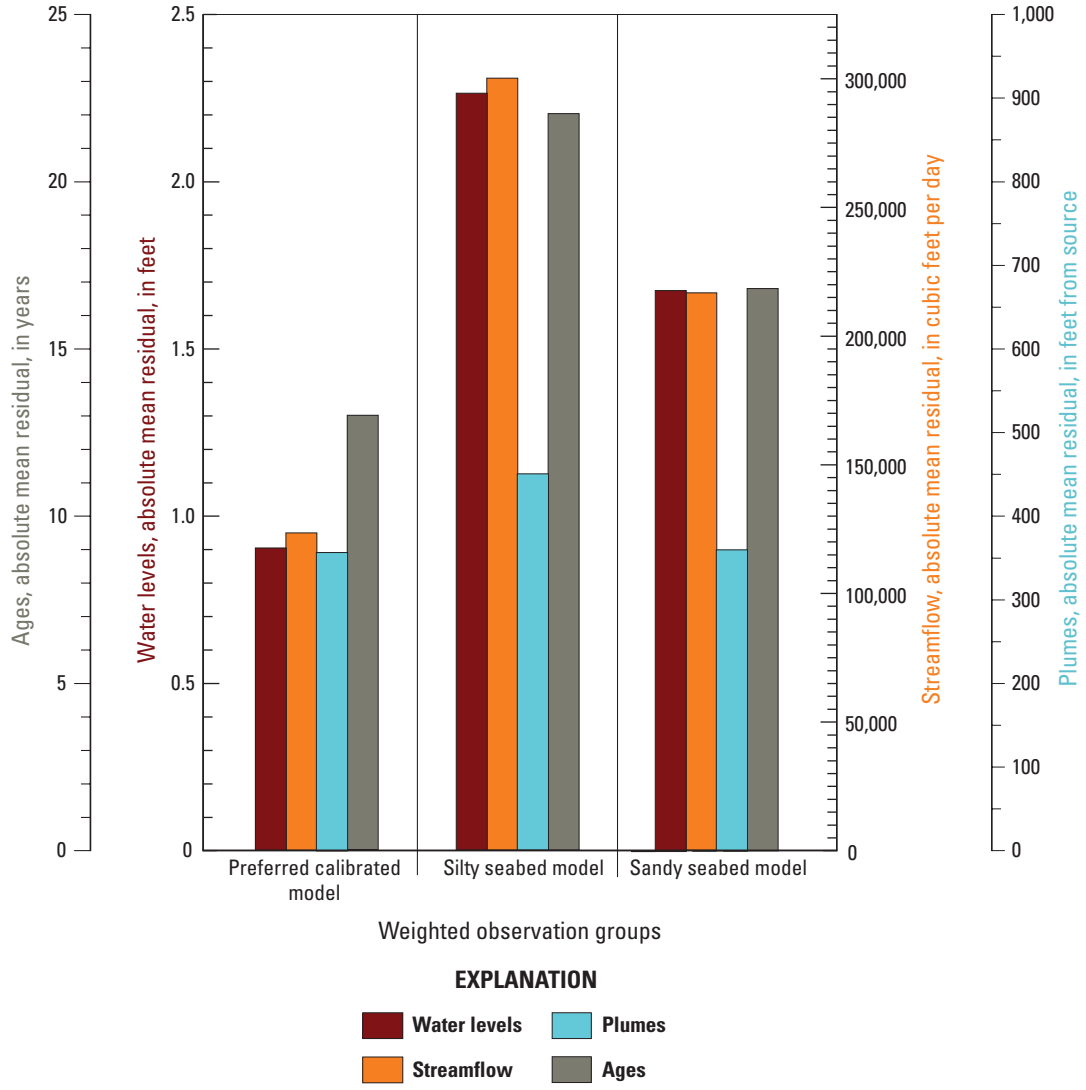

Figure 57. Absolute mean residuals for heads, streamflows, plume sources, and ages for three freshwater/saltwater realizations obtained by adjusted seabed leakances.

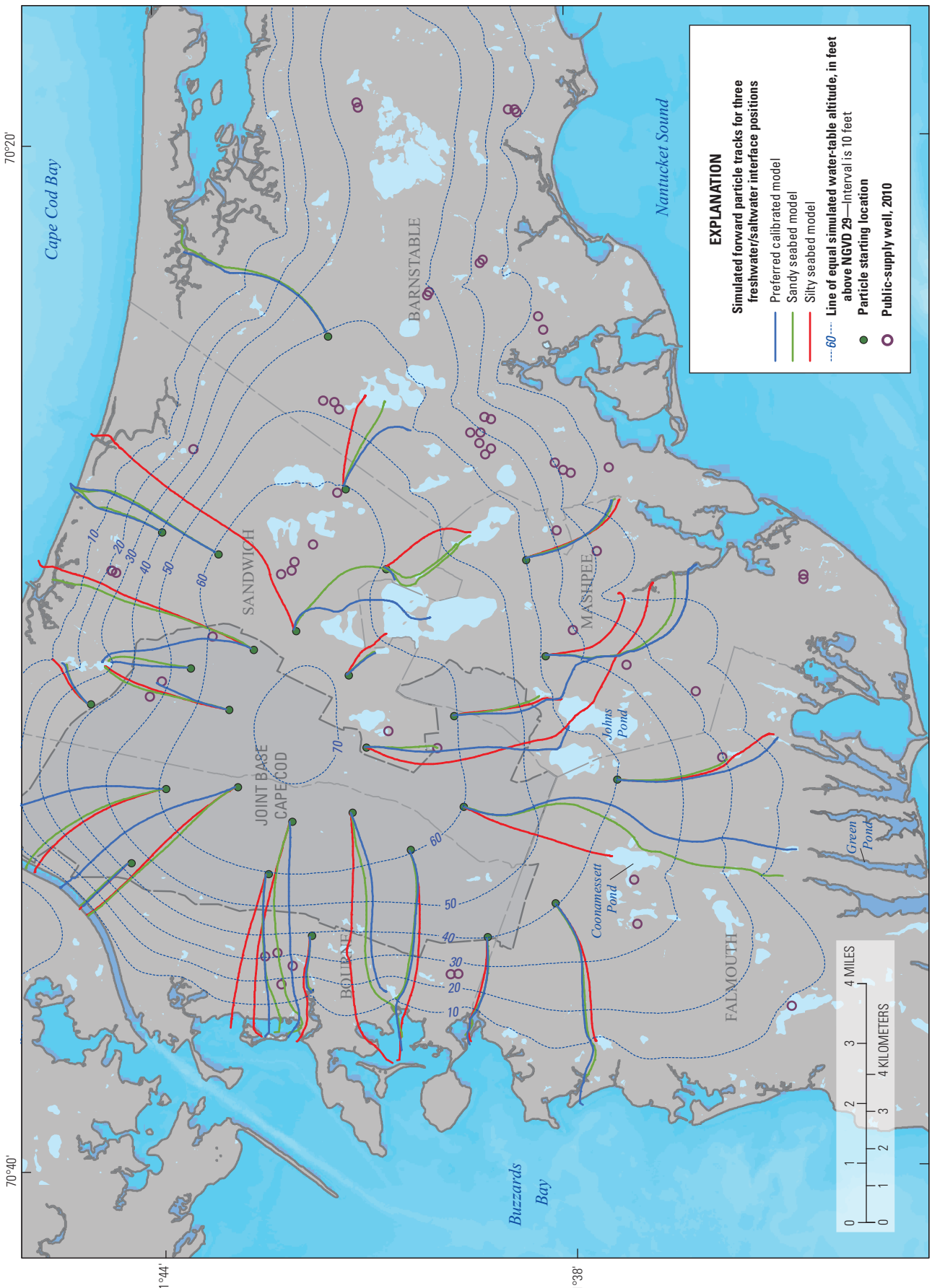

Figure 58. Forward particle tracks from selected locations for the different positions of the freshwater/saltwater interface in the preferred calibrated model and alternative models with silty and sandy seabeds, western Cape Cod, Massachusetts. NGVD 29, National Geodetic Vertical Datum of 1929.

Summary and Conclusions

Joint Base Cape Cod (JBCC), formerly known as the Massachusetts Military Reservation, is a 22,000-acre, multiuse military facility on western Cape Cod, Massachusetts. The facility has been in operation since the early 20th century and has been used by various military branches, including the U.S. Army, U.S. Air Force, Army and Air National Guards, and the U.S. Coast Guard. The northern part of the facility generally is undeveloped and used for training, whereas the southern part is developed with large installations. The facility is underlain by a sand and gravel aquifer, and historical training and operational activities at the facility have resulted in the release of anthropogenic contaminants into the aquifer. Subsurface plumes extend more than 7 miles downgradient from sources on the JBCC, and two ongoing programs have been tasked with remediating groundwater contamination at the site. The Air Force Civil Engineer Center Installation Restoration Program has been conducting remedial investigations in the southern part of the facility, where the contaminants of concern include volatile organic compounds, fuel additives, and nutrients, and the Army National Guard Impact Area Groundwater Study Program has been conducting remedial investigations in the northern part of the facility, where the contaminants are primarily explosives (RDX) and perchlorate. The underlying aquifer is the sole source of drinking water to the surrounding communities, and demand for potable water is projected to increase as the region continues to be developed.

Remedial investigations include the collection of large and diverse sets of data and the application of numerical models to improve understanding of the groundwater flow system at regional and local scales. Types of data collected include lithologic data (aquifer lithology and bedrock), hydrologic data (water levels and streamflows), water-use data, water-quality data, and groundwater ages. Regional-scale models are used to improve understanding of regional hydraulic gradients and to provide boundary conditions for local-scale models; these simulate local-scale hydrologic conditions and are used to guide data collection, design remedial systems, and evaluate system performance. A large amount of diverse data of potential use in updating and calibrating regional models of the aquifer was collected since the most recent (2002) comprehensive update of a regional model.

The U.S. Geological Survey, in cooperation with the Air Force Civil Engineer Center, recently (since 2010) developed and calibrated a steady-state regional model of western Cape Cod, with particular emphasis in the area around the JBCC, that uses the large amount of data collected as part of remedial investigations at the site since 2002. The multipurpose regional model can be used to inform development of local-scale models to evaluate the effect of future water-supply withdrawals on the advective transport of contaminants at the JBCC, as well as to improve understanding of several aspects of the regional aquifer system. This investigation included (1) the compilation and analysis of data relevant to the hydrologic system of western Cape Cod and the transport of contaminants near the JBCC; (2) the use of that data to develop and calibrate a new regional groundwater flow model of the Sagamore flow lens (a hydraulically distinct groundwater flow system within the Cape Cod aquifer), with particular emphasis on the area around the JBCC; (3) the use of the model to characterize current (2010) hydrologic conditions and to evaluate the potential effects of future (2030) water-supply withdrawals and return flow on the hydrologic system; and (4) limitations and technical considerations relevant to the use of the calibrated model to make predictions of advective transport from sources on the JBCC.

Hydrologic, lithologic, climatic, and water-quality data have been collected as part of remedial investigations at the JBCC to inform the design of remedial systems for contaminant plumes; these data also provide information about the hydrogeology of western Cape Cod. These data informed the development and calibration of the numerical model. Principal points are summarized as follows.

- A total of 5,626 water-level measurements from 2,478 sites with records exceeding 10 years, including 10 ponds, were compiled from various sources, including 38 long-term monitoring wells that have been measured monthly for 30 to more than 50 years. Partial-record wells with intermittent measurements for at least 10 years were evaluated for their suitability as observations of near-average (steady-state) conditions; the mean water level in the long-term wells for the period overlapping with the partial record was compared with the mean of the entire record. If the two means were similar, as indicated by the standard deviation of the long-term record, the mean from the partial-record site was assumed to represent a near-average water level. Streamflow measurements from a continuous streamgage (Quashnet River) and 79 partial-record sites were compiled and evaluated for their suitability as steady-state observations of streamflow. Thirteen sites had more than five measurements; a statistical technique was used to extend data for 10 of the 13 sites.

- Daily precipitation and temperature for 1949–2012 from the National Oceanic and Atmospheric Administration monitoring site at Hyannis, Mass., and geographic information system (GIS) data layers of the distribution of soil types (from the Natural Resources Conservation Service) and land use (from the Massachusetts Office of Geographic Information) were compiled and used to estimate the spatial distribution of recharge by using the Soil-Water-Balance model. The positions of the freshwater/saltwater interface were estimated from salinity profiles at 17 locations.

- Recently (2009) mapped geologic quadrangles of western Cape Cod were converted to a spatial data layer to define zonation of the aquifer based on the surficial geology. Lithologic logs from 973 boreholes were

compiled, primarily from sources at the JBCC. The unconsolidated glacial sediments were grouped into eight general lithologic types, and hydraulic conductivity values were assigned to each identified interval on the basis of previous knowledge of the aquifer. Thickness-weighted values within regular 10-foot intervals over the depth of the borehole (from land surface to bedrock) were used to generate point values of hydraulic conductivity for each 10-foot interval. Kriging was used to interpolate these values into a series of stacked, regular grids to estimate a quasi-three-dimensional horizontal and vertical hydraulic conductivity field. Measurement of the bedrock-surface altitude by using ambient-noise seismic techniques was combined with direct observations from deep boreholes to develop an interpolated bedrock surface for western Cape Cod.

- Water-quality sections defining the distribution of subsurface contamination were compiled for several plumes at the JBCC and used to estimate the approximate centers of mass along suitable sections. A total of 31 estimated centers of mass, with associated source locations, were identified as reliable indicators of long-term average hydraulic-gradient and advective-transport patterns. Measurements of environmental tracers—24 profiles of tritium concentrations, 93 helium-3/tritium ratios, and 15 chlorofluorocarbon concentrations—were compiled and used to estimate traveltimes from the water table to the sampling points.

- Current (2010) and projected (2030) groundwater withdrawals from public and private wells were compiled from the Massachusetts Department of Conservation and Recreation and local sources. Current (2010) and future (2030) discharge rates at wastewater-treatment facilities were compiled from the Massachusetts Department of Conservation and Recreation, and the current (2010) locations of private septic-system return flows, at the parcel scale, were compiled from the Cape Cod Commission.

The compiled data were used to inform the development and calibration of a steady-state regional model of the Sagamore flow lens; the model described in this report is based on existing regional models of the Sagamore and adjacent flow lenses. Two models were used in the analysis: a two-dimensional model of the Sagamore and Monomoy flow lenses that can be used to simulate a dynamic freshwater/saltwater interface (the FW/SW interface model) and a three-dimensional groundwater flow model of the Sagamore flow lens that is capable of predicting advective transport (the JBCC regional model). Principal points are summarized as follows.

- The two-dimensional FW/SW interface model was used to simulate the position of the freshwater/saltwater interface beneath western and central Cape Cod. The model uses average transmissivity and recharge from existing regional models of the region. Coastal leakances were adjusted to produce a simulated interface position that reasonably matches the observed interface at 17 locations. The simulated interface position and a bedrock surface interpolated from observed altitudes were used to define a no-flow boundary at the lower boundary of the aquifer.

- The steady-state, three-dimensional groundwater flow model was used to simulate the effect of pumping stresses on the advective transport of contaminants at the JBCC. A series of vertically stacked grids of hydraulic conductivities determined for 10-foot intervals by interpolation from estimated values from lithologic logs was used to assign initial hydraulic conductivity values to the three-dimensional model grid. The initial values were further constrained to better match grain-size patterns consistent with existing depositional models of the aquifer and general hydrologic conditions in the region. Spatial patterns of recharge estimated from climate and landscape data were used to define simulated recharge; the values were adjusted so that mean values were similar to values from previous investigations. Hydrologic boundaries—streams, wetlands, ponds, estuaries, and coastal waters—were updated by using aerial photos and 10-meter digital elevation model data.

- Inputs were represented in the groundwater flow model as adjustable parameters to facilitate inverse calibration of the model to achieve a best fit to observed hydrologic conditions. A total of 4,568 parameters were included as model inputs. Horizontal and vertical hydraulic conductivity were represented as zoned pilot points in areas where sufficient data were available and in other areas were represented more simply as zones of piecewise constancy. Ponds were represented as areas of essentially infinite hydraulic conductivity. Natural recharge was represented as a single parameter that was applied to multipliers obtained from spatially variable recharge from the Soil-Water-Balance model. Leakances into freshwater streams and into ponds were represented as parameters, as was aquifer porosity. Leakances into coastal boundaries—estuaries and streams—were fixed to maintain consistency with the no-flow boundary obtained from the interface position, as simulated in the two-dimensional FW/SW interface model of the Sagamore and Monomoy flow lenses.

- Water-level and streamflow measurements determined to be representative of near-average hydrologic conditions were used as hydraulic head and streamflow observations in the inverse-model calibration. A total 547 water-level observations and 10 streamflow observations were determined to be suitable for inclusion in the calibration. Estimates of the centers of mass of contaminant plumes along 31 cross sections, and the associated source areas, were determined to be suitable

for inclusion in the calibration as observations of long-term hydraulic gradients and advective transport. The observations were represented in the model calibration as locations of the specified source areas; the simulated equivalents are the locations of the source areas predicted by using reverse particle tracking from the specified centers of mass. A total of 132 observations of groundwater age were included in the calibration; the ages were included in the regression as the estimated traveltime of a particle of water from the water table to the sampling point. Simulated equivalents are the model-predicted traveltimes based on reverse particle tracking from the sampling points to the water table. Traveltimes of peak tritium concentrations to the water table were corrected for unsaturated-zone thickness.

- The inverse modeling software package PEST was used to automate the inverse calibration of the model. The sets of parameters and steady-state observations were used in the inverse calibration to estimate parameters that optimally fit the observations. Regularization was used to formally incorporate prior information on the parameters into the calibration. A relative weighting scheme was used in which weights for different types of observations were defined based on their contributions to the initial objective function. The largest weights were assigned to plume observations—about 74 percent of the initial objective function—because they were considered to be the most robust observations for representing long-term hydraulic gradients and were the most relevant to the intended use of the model to simulate advective transport near the JBCC. Mean water levels at long-term index wells and streamflow in primary streams also were substantially weighted at 15 and 8 percent, respectively, of the initial objective function. Water levels from partial-record wells and groundwater ages were assigned lower weights—1 percent or less for each group. The inverse calibration resulted in an improved match to observations from the initial parameter values. Absolute mean residuals for long-term water levels decreased during calibration from 2.9 to 0.5 feet (ft) and for streamflows decreased from 3.0 to 0.6 cubic feet per second. The absolute mean residuals for plume observations, which had the largest weights, decreased from 2,050 to 382 ft. Groundwater ages were assigned small weights; however, absolute mean residual traveltime from peak tritium concentrations decreased from about 11 to 7.5 years.

- Estimated hydraulic conductivity generally was similar to initial values over the extent of the aquifer but did change substantially in some areas. The mean estimated horizontal hydraulic conductivity was within 10 percent of the initial mean value in all four vertical groups of estimated parameters; however, the change in horizontal hydraulic conductivity exceeded 10 percent in most (more than 70 percent of) individual cells. Areas with the large simulated heterogeneity are near plume observations. Inclusion of highly weighted observations of advective transport, such as plume paths, increases parameter sensitivities, particularly at depth where sensitivities generally are low when only heads and flow observations are included in the calibration.

The calibrated model was used to characterize groundwater flow, hydraulic gradients, and advective transport near the JBCC. Current (2010) pumping rates and wastewater return flow were used in the simulation of water levels, streamflows, and hydraulic gradients. Future (2030) pumping rates and return flow were used to evaluate the effects of projected increases on the groundwater flow system and advective transport of contaminants at the JBCC. Principal findings are summarized as follows.

- Advective transport is a function of hydraulic gradients, which are radially outward from the top of a water-table mound in the northern part of the JBCC. Horizontal gradients are smallest near groundwater divides and largest near the coast. Large gradients also generally occur near discharge locations at streams and ponds. Vertical gradients generally are upward near discharge locations—pond and streams—and downward at locations not near discharge boundaries owing to areal recharge. Gradients are also downward at the downgradient sides of groundwater flow-through ponds. Most groundwater flow and, as a result, contaminant transport are within shallow parts of the aquifer. On average, about one-half of the groundwater flux occurs in the upper 20 percent of the saturated aquifer. Groundwater fluxes generally are large in shallow parts of the aquifer and near streams and ponds.

- The projected (2030) increase in groundwater withdrawals (about 30 percent above current [2010] withdrawals) results in local decreases in water levels. The largest projected decreases (between 1 and 2 ft) are near the largest increases in withdrawals, including near the region's only surface-water withdrawal at Long Pond to the southwest of the JBCC and in the northern part of the JBCC near the supply wells installed as an ancillary water supply for the surrounding communities. Projected groundwater withdrawals are regionally balanced by wastewater return flows. Streamflows generally are unaffected by the projected increase in pumping; the average decrease is about 6 percent of current (2010) flows. The largest projected decrease in streamflow is at the outlet of Upper Shawme Pond to the north of the JBCC near the areas of substantial drawdown near the ancillary supply wells.

- Differences in hydraulic-gradient directions at the water table between current (2010) and future (2030)

scenarios generally are largest near groundwater divides where gradient magnitudes are small and near locations of large increases in pumping. Areas where changes in gradient directions exceed 1 degree compose only about 13 percent of the aquifer. Particle paths from various randomly selected points at the water table, which are indicators of advective transport, were similar for current (2010) and future (2030) groundwater withdrawals. The results indicate that future hydraulic stresses, if similar in location and magnitude to those in the 2030 scenario, likely will not affect the advective transport of existing contaminant plumes emanating from sources on the JBCC.

Several simplifying assumptions inherent in the model design, parameterization, and calibration can affect simulated hydrologic conditions and predictions made by the model. Assumptions that are relevant to this analysis include the choice of observations and associated weights used in the calibration, the effects of local-scale heterogeneity, and the representation of the freshwater/saltwater interface. Principal findings are summarized as follows.

- A diverse set of data—water levels, streamflows, plumes, hydraulic gradients, and groundwater ages—was used in the calibration of the steady-state model. The largest weights were assigned to plume observations, moderate weights were assigned to water levels from long-term wells and streamflows from primary streams, and the smallest weights were assigned to partial-record wells and groundwater ages. Calibrations using eight alternative sets of observations and weights were performed. All eight alternative calibrations can be considered reasonably calibrated, though the preferred calibrated steady-state model best fit the complete observation dataset and was determined to be most suitable for the desired model predictions. Alternative calibrations in which fewer types of observations with larger weights were used generally had a slightly better fit to those observation types than did the preferred calibrated model, as was expected, but the overall fit to all observations types was substantially inferior than for the preferred model. The preferred calibrated model had a better fit to plume observations, which are of particular importance to the modeling analysis, than all the alternative calibrations, including a calibration in which plume observations had a larger weight than in the preferred model. The results indicate that any given set of observations affects model calibration but that inclusion of a diverse set of observations, such as those used in the preferred calibrated model, results in a better representation of the groundwater flow system.

- Silt deposits exceeding 5 ft in thickness were identified in lithologic logs at 897 points in the aquifer but are not explicitly represented in the model owing to the regional scale of the model and the lack of information about the extent of silt deposits. The silt locations were used to generate alternative aquifer zonation that explicitly represents the 897 silt zones with different correlation distances (200–2,200 ft) and horizontal hydraulic conductivities (1–10 feet per day). Absolute mean residuals generally increased substantially with increasing correlation distance and decreasing hydraulic conductivity. The results indicate that explicitly representing silts in the model would result in different estimated parameters. However, model predictions of advective transport from randomly selected locations at the water table for different silt realizations were similar to those made with the calibrated model; this indicates that not explicitly representing local-scale silts in the model does not affect representation of hydraulic gradients and advective-transport patterns at the regional scale. Silts also are present beneath kettle-hole ponds, which can locally affect hydraulic gradients and contaminant plumes near ponds. A range of pond-bottom hydraulic conductivities resulted in similar overall absolute mean residuals for plume observations, but residuals for individual observations did change substantially, indicating that pond-bottom hydraulic conductivity could locally affect model calibration.

- Alternative coastal seabed leakances representing sandy and silty sediment end members and the resulting freshwater/saltwater interface were incorporated into the regional model. Absolute mean residuals generally were similar to the residuals when the alternative coastal leakances and interface positions were used. Predictions of advective transport from randomly selected locations at the water table generally were similar for the preferred calibrated model and the alternative seabed leakances and interface, particularly near the JBCC. Change in the representation of coastal boundaries changes the balance between discharge to coastal waters and to freshwater streams; simulated streamflow increases as simulated coastal leakances are decreased. As a result, predictions of advective transport and discharge locations can vary substantially in some areas near the coast.

References Cited

Air Force Civil Engineer Center [AFCEC], 1996, Plume containment design data gap field work technical memorandum, Massachusetts Military Reservation, Installation Restoration Program: Prepared for the Air Force Civil Engineer Center by Operational Technologies Corp., December 1996 [variously paged].

Air Force Civil Engineer Center [AFCEC], 2000, Final CS–10 in-plume remedial system design ground-water modeling report: Prepared for the Air Force Civil Engineer Center by Jacobs Engineering Group [variously paged].

Air Force Civil Engineer Center [AFCEC], 2001, Final Fuel Spill-1 wellfield design report: Prepared for the Air Force Civil Engineer Center by Jacobs Engineering Group [variously paged].

Air Force Civil Engineer Center [AFCEC], 2003, Draft Chemical Spill-4, Chemical Spill-20, Chemical Spill-21, and Chemical Spill-29 pre-design investigation report: Prepared for the Air Force Civil Engineer Center by Jacobs Engineering Group [variously paged].

Air Force Civil Engineer Center [AFCEC], 2007, Groundwater plume maps and information booklet, Massachusetts Military Reservation, Cape Cod, Massachusetts: Air Force Civil Engineer Center, 36 p.

Air Force Civil Engineer Center [AFCEC], 2013, Final Chemical Spill-10 2012 data gap investigation technical memorandum: Prepared for the Air Force Civil Engineer Center by CH2M Hill, Inc., [variously paged].

Air Force Civil Engineer Center [AFCEC], 2019, U.S. Air Force Civil Engineer Center administrative record search: Air Force Civil Engineer Center web page, accessed January 29, 2019, at http://afcec.publicadmin-record.us.af.mil/.

American Society for Testing and Materials [ASTM], 1985, Classification of soils for engineering purposes: American Society for Testing and Materials Annual Book of ASTM Standards D 2487–83, v. 04.08, p. 395–408.

Army National Guard [ARNG], 2005, System performance and ecological impact monitoring (SPEIM) report, rapid response action systems Demo 1 groundwater operable unit: Prepared for the National Guard Bureau Impact Area Groundwater Study Program by AMEC Earth & Environmental, Inc., Report MMR–9300, 164 p.

Army National Guard [ARNG], 2007a, Draft J–2 range groundwater remedial investigation and feasibility study: Prepared for the Army National Guard Impact Area Groundwater Study Program by Environmental Chemical Corporation [variously paged].

Army National Guard [ARNG], 2007b, Impact Area Groundwater Study Program investigation and cleanup update, Camp Edwards, Massachusetts: Army National Guard, 32 p.

Army National Guard [ARNG], 2009, Final Demolition Area 1 source area completion work report: Prepared for the Army National Guard Impact Area Groundwater Study Program by Environmental Chemical Corporation [variously paged].

Army National Guard [ARNG], 2010a, Final L Range remedial investigation/feasibility study: Prepared for the Army National Guard Impact Area Groundwater Study Program by Environmental Chemical Corporation [variously paged].

Army National Guard [ARNG], 2010b, J–1 Range remedial investigation/feasibility study: Prepared for the Army National Guard Impact Area Groundwater Study Program by Environmental Chemical Corporation [variously paged].

Army National Guard [ARNG], 2013, Joint Base Cape Cod cleanup update: Army National Guard, 11 p., accessed January 28, 2019, at http://jbcc-iagwsp.org/whats_new/jbcc_cleanup_update.pdf.

Army National Guard [ARNG], 2019, Joint Base Cape Cod environmental data management system portal: Army National Guard database, accessed January 28, 2019, at http://jbcc-edms.org.

Association to Preserve Cape Cod, 2018, Science programs: Association to Preserve Cape Cod, Dennis, Mass., accessed October 18, 2018, at http://www.apcc.org/science/index.html.

Bakker, M., Schaars, F., Hughes, J.D., Langevin, C.D., and Dausman, A.M., 2013, Documentation of the seawater intrusion (SWI2) package for MODFLOW: U.S. Geological Survey Techniques and Methods, book 6, chap. A46, 47 p., accessed May 12, 2013, at https://pubs.usgs.gov/tm/6a46/.

Barbaro, J.R., Walter, D.A., and LeBlanc, D.R., 2013, Transport of nitrogen in a treated-wastewater plume to coastal discharge areas, Ashumet Valley, Cape Cod, Massachusetts: U.S. Geological Survey Scientific Investigations Report 2013–5061, 37 p.

Barlow, P.M., 1997, Particle-tracking analysis of contributing areas of public-supply wells in simple and complex flow systems, Cape Cod, Massachusetts: U.S. Geological Survey Water-Supply Paper 2434, 66 p.

Barlow, P.M., and Hess, K.M., 1993, Simulated hydrologic responses of the Quashnet River stream-aquifer system to proposed ground-water withdrawals, Cape Cod, Massachusetts: U.S. Geological Survey Water-Resources Investigations Report 93–4064, 52 p.

Cape Cod Commission, 2018, Resource center, water resources: Cape Cod Commission, Barnstable, Mass., accessed October 18, 2018, at http://www.capecodcommission.org/index.php?id=62&a=dept&cat=Water%20Resources

Cronshey, R., McCuen, R.H., Miller, N., Rawls, W., Robbins, S., and Woodward, D., 1986, Urban hydrology for small watersheds (2d ed.): U.S. Department of Agriculture Technical Release 55 [variously paged].

DeSimone, L.A., Walter, D.A., Eggleston, J.R., and Nimiroski, M.T., 2002, Simulation of ground-water flow and evaluation of water-management alternatives in the upper Charles River Basin, eastern Massachusetts: U.S. Geological Survey Water-Resources Investigations Report 02–4234, 94 p.

Doherty, J., 2003, Groundwater model calibration using pilot points and regularization: Ground Water, v. 41, no. 2, p. 170–177.

Doherty, J., 2010, PEST–Model-independent parameter estimation–User manual (5th ed., with slight additions): Brisbane, Australia, Watermark Numerical Computing, 336 p.

Doherty, J.E., and Hunt, R.J., 2010, Approaches to highly parameterized inversion—A guide to using PEST for groundwater-model calibration: U.S. Geological Survey Scientific Investigations Report 2010–5169, 59 p.

Doherty, J., and Welter, D., 2010, A short exploration of structural noise: Water Resources Research, v. 46, p. 1–14.

Esri, 2014, Kriging in Geostatistical Analyst: Esri ArcGIS Help 10.1 web page, accessed November 4, 2012, at http://resources.arcgis.com/en/help/main/10.1/index.html#//003100000032000000/.

Fairchild, G.M., Lane, J.W., Jr., Voytek, E.B., and LeBlanc, D.R., 2013, Bedrock topography of western Cape Cod, Massachusetts, based on bedrock altitudes from geologic borings and analysis of ambient seismic noise by the horizontal-to-vertical spectral-ratio method: U.S. Geological Survey Scientific Investigations Map 3233, 1 sheet, maps variously scaled, 17-p. pamphlet, on one CD–ROM.

Fienen, M.N., 2013, We speak for the data: Groundwater, v. 51, no. 2, p. 157–157.

Fienen, M.N., Muffels, C.T., and Hunt, R.J., 2009, On constraining pilot-point calibration with regularization in PEST: Groundwater, v. 47, no. 6, p. 835–844.

Garabedian, S.P., Gelhar, L.W., and Celia, M.A., 1988, Large-scale dispersive transport in aquifers—Field experiments and reactive transport theory: Cambridge, Mass., Massachusetts Institute of Technology, Department of Civil Engineering, Ralph M. Parsons Laboratory Report 315, 290 p. [Also available at https://www.nrc.gov/docs/ML0331/ML033160542.pdf.]

Granato, G.E., 2009, Computer programs for obtaining and analyzing daily mean streamflow data from the U.S. Geological Survey National Water Information System Web site: U.S. Geological Survey Open-File Report 2008–1362, 123 p. on CD–ROM, 5 app.

Harbaugh, A.W., 2005, MODFLOW–2005, The U.S. Geological Survey modular ground-water model—the ground-water flow process: U.S. Geological Survey Techniques and Methods, book 6, chap. A16 [variously paged].

Hirsch, R.M., 1982, A comparison of four streamflow record extension techniques: Water Resources Research, v. 18, no. 4, p. 1081–1088.

Hsieh, P.A., and Freckleton, J.R., 1993, Documentation of a computer program to simulate horizontal-flow barriers using the U.S. Geological Survey's modular three-dimensional finite-difference ground-water flow model: U.S. Geological Survey Open-File Report 92–477, 32 p.

LeBlanc, D.R., 1984, Sewage plume in a sand and gravel aquifer, Cape Cod, Massachusetts: U.S. Geological Survey Water-Supply Paper 2218, 28 p.

LeBlanc, D.R., Garabedian, S.P., Hess, K.M., Gelhar, L.W., Quadri, R.D., Stollenwerk, K.G., and Wood, W.W., 1991, Large-scale natural-gradient tracer test in sand and gravel, Cape Cod, Massachusetts—1. Experimental design and observed tracer movement: Water Resources Research, v. 27, no. 5, p. 895–910.

LeBlanc, D.R., Guswa, J.H., Frimpter, M.H., and Londquist, C.J., 1986, Ground-water resources of Cape Cod, Massachusetts: U.S. Geological Survey Hydrologic Investigations Atlas HA–692, 4 sheets, scale 1:24,000.

Levenberg, K., 1944, A method for the solution of certain non-linear problems in least squares: Quarterly of Applied Mathematics, v. 2, no. 2, p. 164–168.

Marquardt, D.W., 1963, An algorithm for least-squares estimation of nonlinear parameters: Journal of the Society of Industrial Allied Mathematics, v. 11, no. 2, p. 431–441.

Massachusetts Department of Environmental Protection [MassDEP], 2019, Energy and environmental affairs data portal: Commonwealth of Massachusetts database, accessed January 29, 2019, at https://eeaonline.eea.state.ma.us/portal#!/search/welldrilling.

Massachusetts Estuaries Project [MEP], 2019, The Massachusetts Estuaries Project and reports: Commonwealth of Massachusetts web page, accessed January 29, 2019, at https://www.mass.gov/guides/the-massachusetts-estuaries-project-and-reports#cape-cod-mep-reports.

Massachusetts Office of Geographic Information [MassGIS], 2012a, MassGIS data: USGS Color Ortho Imagery (2008/2009): Commonwealth of Massachusetts dataset, accessed June 15, 2012, at https://docs.digital.mass.gov/dataset/massgis-data-usgs-color-ortho-imagery-20082009.

Massachusetts Office of Geographic Information [MassGIS], 2012b, Office of Geographic Information (MassGIS): Commonwealth of Massachusetts web page, accessed June 15, 2012, at http://www.mass.gov/anf/research-and-tech/it-serv-and-support/application-serv/office-of-geographic-information-massgis/.

Massey, A.J., Carlson, C.S., and LeBlanc, D.R., 2006, Groundwater levels near the top of the water-table mound, western Cape Cod, Massachusetts, 2002–04: U.S. Geological Survey Scientific Investigations Report 2006–5054, 13 p.

Masterson, J.P., 2004, Simulated interaction between freshwater and saltwater and effects of ground-water pumping and sea-level change, Lower Cape Cod aquifer system, Massachusetts: U.S. Geological Survey Scientific Investigations Report 2004–5014, 72 p.

Masterson, J.P., and Barlow, P.M., 1997, Effects of simulated ground-water pumping and recharge on ground-water flow in Cape Cod, Martha's Vineyard, and Nantucket Island Basins, Massachusetts: U.S. Geological Survey Water-Supply Paper 2447, 79 p.

Masterson, J.P., Carlson, C.S., and Walter, D.A., 2009, Hydrogeology and simulation of groundwater flow in the Plymouth-Carver-Kingston-Duxbury aquifer system, southeastern Massachusetts: U.S. Geological Survey Scientific Investigations Report 2009–5063, 110 p.

Masterson, J.P., Sorenson, J.R., Stone, J.R., Moran, S.B., and Hougham, A., 2007, Hydrogeology and simulated groundwater flow in the Salt Pond region of southern Rhode Island: U.S. Geological Survey Scientific Investigations Report 2006–5271, 56 p.

Masterson, J.P., Stone, B.D., Walter, D.A., and Savoie, J.G., 1997a, Hydrogeologic framework of western Cape Cod, Massachusetts: U.S. Geological Survey Hydrologic Investigations Atlas HA–741, 1 sheet, scale 1:25,000.

Masterson, J.P., Walter, D.A., and Savoie, J.G., 1997b, Use of particle tracking to improve numerical model calibration and to analyze ground-water flow and contaminant migration, Massachusetts Military Reservation, western Cape Cod, Massachusetts: U.S. Geological Survey Water-Supply Paper 2482, 50 p.

McCobb, T.D., LeBlanc, D.R., Parsons, L.A., and Blount, J.G., 2009, Distribution of treated-wastewater constituents in pore water at a pond-bottom reactive barrier, Cape Cod, Massachusetts: U.S. Geological Survey Scientific Investigations Map 3078, 1 sheet.

McDonald, M.G., and Harbaugh, A.W., 1988, A modular three-dimensional finite-difference ground-water flow model: U.S. Geological Survey Techniques of Water-Resources Investigations, book 6, chap. A1, 586 p.

Morin, R.H., 2006, Negative correlation between porosity and hydraulic conductivity in sand-and-gravel aquifers at Cape Cod, Massachusetts, USA: Journal of Hydrology, v. 316, p. 43–52.

National Oceanic and Atmospheric Administration [NOAA] National Climatic Data Center, 2012, NOAA National Centers for Environmental Information: NOAA website, accessed September 1, 2012, at http://www.ncdc.noaa.gov/.

Oldale, R.N., 1992, Cape Cod and the Islands—The geologic story: East Orleans, Mass., Parnassus Imprints, 205 p.

Oldale, R.N., and Barlow, R.A., 1986, Geologic map of Cape Cod and the Islands, Massachusetts: U.S. Geological Survey Miscellaneous Investigations Series Map I–1763, 1 sheet.

Oliver, M.A., and Webster, R., 1990, Kriging—A method of interpolation for geographical information systems: International Journal of Geographic Information Systems, v. 4, no. 3, p. 313–332.

Peel, M.C., Finlayson, B.L., and McMahon, T.A., 2007, Updated world map of the Köppen-Geiger climate classification: Hydrology and Earth System Sciences, v. 11, p. 1633–1644.

Plummer, L.N., Michel, R.L., Thurman, E.M., and Glynn, P.D., 1993, Environmental tracers for age dating young ground water, chap. 11 *of* Alley, W.M., ed., Regional ground-water quality: New York, Van Nostrand Reinhold, p. 255–294.

Pollock, D.W., 1994, User's guide for MODPATH/MODPATH–PLOT, version 3—A particle tracking post-processing package for MODFLOW, the U.S. Geological Survey finite-difference ground-water flow model: U.S. Geological Survey Open-File Report 94–464 [variously paged].

Solomon, D.K., Poreda, R.J., Cook, P.G., and Hunt, D.A., 1995, Site characterization using $^{3}H/^{3}He$ ground-water ages, Cape Cod, MA: Groundwater, v. 33, no. 6, p. 988–996.

Stone, B.D., and DiGiacomo-Cohen, M.L., compilers, 2009, Surficial geologic map of the Pocasset-Provincetown-Cuttyhunk-Nantucket 24-quadrangle area of Cape Cod and islands, southeast Massachusetts: U.S. Geological Survey Open-File Report 2006–1260–E, 19 sheets, 19-p. pamphlet, scale 1:24,000. [Also available at https://pubs.er.usgs.gov/publication/ofr20061260E.]

Thornthwaite, C.W., and Mather, J.R., 1957, Instructions and tables for computing potential evapotranspiration and the water balance: Centerton, N.J., Drexel Institute of Technology, Publications in Climatology, v. 10, no. 3, p. 185–311.

Tonkin, M., and Doherty, J., 2005, A hybrid regularized inversion methodology for highly parameterized models: Water Resources Research, v. 41, no. 10, p. 1–16.

Uchupi, E., Giese, G.S., Aubrey, D.G., and Kim, D.J., 1996, The late Quaternary construction of Cape Cod, Massachusetts—A reconsideration of the W.M. Davis Model: Geological Society of America Special Paper 309, 69 p.

Upper Cape Regional Water Supply Cooperative, 2015, Sagamore lens sustainable management of water resources plan: Prepared for the Upper Cape Regional Water Supply Cooperative by Tata and Howard, Inc. [variously paged].

U.S. Department of Agriculture [USDA], 1998, Soil quality resource concerns—Available water capacity: U.S. Department of Agriculture Soil Quality Information Sheet, 2 p.

U.S. Department of Agriculture [USDA] National Resource Conservation Service (NRCS), 2012, Web soil survey: NRCS database, accessed September 15, 2012, at http://websoilsurvey.sc.egov.usda.gov/App/HomePage.htm.

U.S. Geological Survey [USGS], 2017, USGS 011058837 Quashnet River at Waquoit Village, MA, *in* USGS water data for the Nation: U.S. Geological Survey National Water Information System database, accessed March 23, 2017, at https://doi.org/10.5066/F7P55KJN. [Site information directly accessible at https://waterdata.usgs.gov/ma/nwis/uv?site_no=011058837.]

U.S. Geological Survey [USGS], 2018a, The Menlo Park tritium laboratory: U.S. Geological Survey, accessed October 18, 2018, at https://water.usgs.gov/nrp/menlo-park-tritium-laboratory/.

U.S. Geological Survey [USGS], 2018b, The Reston groundwater dating laboratory: U.S. Geological Survey, accessed October 18, 2018, at https://water.usgs.gov/lab/.

U.S. Geological Survey [USGS], 2018c, USGS water data for the Nation: U.S. Geological Survey National Water Information System database, accessed October 18, 2018, at https://doi.org/10.5066/F7P55KJN.

U.S. Geological Survey [USGS], 2019, USGS water-data site information for Massachusetts: U.S. Geological Survey National Water Information System database, accessed January 29, 2019, at https://waterdata.usgs.gov/ma/nwis/si.

Varni, M., and Carrera, J., 1998, Simulation of groundwater age distributions: Water Resources Research, v. 34, no. 12, p. 3271–3281.

Vogel, J.C., 1967, Investigation of groundwater flow with radiocarbon, *in* Isotopes in hydrology [proceedings of a symposium]: Vienna, International Atomic Energy Agency, p. 355–369.

Vogel, R.M., and Stedinger, J.R., 1985, Minimum variance streamflow record augmentation procedures: Water Resources Research, v. 21, no. 5, p. 715–723.

Walter, D.A., 2008, Use of numerical models to simulate transport of sewage-derived nitrate in a coastal aquifer, central and western Cape Cod, Massachusetts: U.S. Geological Survey Scientific Investigations Report 2007–5259, 41 p.

Walter, D.A., 2013, The simulated effects of wastewater-management actions on the hydrologic system and nitrogen-loading rates to wells and ecological receptors, Popponesset Bay watershed, Cape Cod, Massachusetts: U.S. Geological Survey Scientific Investigations Report 2013–5060, 62 p.

Walter, D.A., and LeBlanc, D.R., 2008, Use of inverse-modeling methods to improve ground-water-model calibration and evaluate model-prediction uncertainty, Camp Edwards, Cape Cod, Massachusetts: U.S. Geological Survey Scientific Investigations Report 2007–5257, 57 p.

Walter, D.A., and Masterson, J.P., 2003, Simulation of advective flow under steady-state and transient recharge conditions, Camp Edwards, Massachusetts Military Reservation, Cape Cod, Massachusetts: U.S. Geological Survey Water-Resources Investigations Report 03–4053, 51 p.

Walter, D.A., Masterson, J.P., and Hess, K.M., 2004, Groundwater recharge areas and traveltimes to pumped wells, ponds, streams, and coastal water bodies, Cape Cod, Massachusetts: U.S. Geological Survey Scientific Investigations Map I–2857, 1 sheet, scale 1:25,000.

Walter, D.A., Masterson, J.P., and LeBlanc, D.R., 2002, Simulated pond-aquifer interactions under natural and stressed conditions near Snake Pond, Cape Cod, Massachusetts: U.S. Geological Survey Water-Resources Investigations Report 99–4174, 35 p.

Walter, D.A., McCobb, T.D., Fienen, M.N., and Watt, M.K., 2019, MODFLOW–2005 and MODPATH used to simulate the hydrologic system and transport of contaminants near Joint Base Cape Cod, Western Cape Cod, Massachusetts: U.S. Geological Survey data release, https://doi.org/10.5066/F77P8XCT.

Walter, D.A., McCobb, T.D., Masterson, J.P., and Fienen, M.N., 2016, Potential effects of sea-level rise on the depth to saturated sediments of the Sagamore and Monomoy flow lenses on Cape Cod, Massachusetts (ver. 1.1, October 18, 2016): U.S. Geological Survey Scientific Investigations Report 2016–5058, 55 p., accessed November 1, 2016, at https://doi.org/10.3133/sir20165058.

Walter, D.A., Rea, B.A., Stollenwerk, K.G., and Savoie, J.G., 1996, Geochemical and hydrologic controls on phosphorus transport in a sewage-contaminated sand and gravel aquifer near Ashumet Pond, Cape Cod, Massachusetts: U.S. Geological Survey Water-Supply Paper 2463, 89 p.

Walter, D.A., and Whealan, A.T., 2005, Simulated water sources and effects of pumping on surface and ground water, Sagamore and Monomoy flow lenses, Cape Cod, Massachusetts: U.S. Geological Survey Scientific Investigations Report 2004–5181, 85 p.

Weissmann, G.S., Zhang, Y., LaBolle, E.M., and Fogg, G.E., 2002, Dispersion of groundwater age in an alluvial aquifer system: Water Resources Research, v. 38, no. 10, p. 1198–1211.

Westenbroek, S.M., Kelson, V.A., Dripps, W.R., Hunt, R.J., and Bradbury, K.R., 2010, SWB—A modified Thornthwaite-Mather soil-water-balance code for estimating groundwater recharge: U.S. Geological Survey Techniques and Methods, book 6, chap. A31, 59 p.

Winter, T.C., Harvey, J.W., Franke, O.L., and Alley, W.M., 1998, Ground water and surface water—A single resource: U.S. Geological Survey Circular 1139, 79 p.

For more information about this report, contact:
Director, New England Water Science Center
U.S. Geological Survey
331 Commerce Way, Suite 2
Pembroke, NH 03275
dc_nweng@usgs.gov
or visit our website at
https://newengland.water.usgs.gov

Publishing support provided by the
Pembroke and West Trenton Publishing Service Centers

ISSN 2328-0328 (online)
https://doi.org/10.3133/sir20185139